

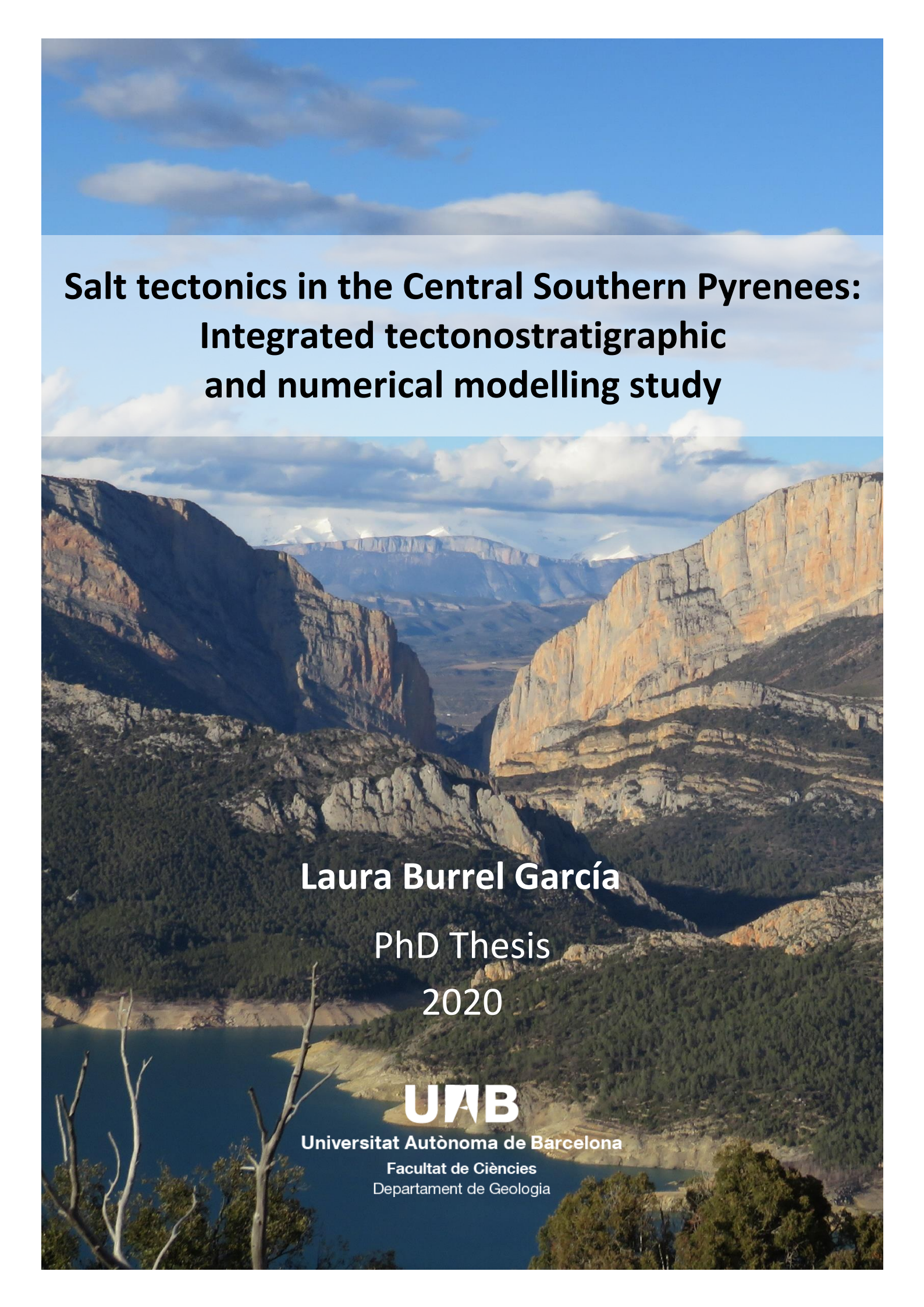


Universitat Autònoma de Barcelona

ADVERTIMENT. L'accés als continguts d'aquesta tesi queda condicionat a l'acceptació de les condicions d'ús establertes per la següent llicència Creative Commons:  http://cat.creativecommons.org/?page_id=184

ADVERTENCIA. El acceso a los contenidos de esta tesis queda condicionado a la aceptación de las condiciones de uso establecidas por la siguiente licencia Creative Commons:  <http://es.creativecommons.org/blog/licencias/>

WARNING. The access to the contents of this doctoral thesis it is limited to the acceptance of the use conditions set by the following Creative Commons license:  <https://creativecommons.org/licenses/?lang=en>



Salt tectonics in the Central Southern Pyrenees: Integrated tectonostratigraphic and numerical modelling study

Laura Burrel García

PhD Thesis

2020

UAB

Universitat Autònoma de Barcelona

Facultat de Ciències

Departament de Geologia



Universitat Autònoma de Barcelona

Facultat de Ciències

Departament de Geologia

Salt tectonics in the Central Southern Pyrenees: Integrated tectonostratigraphic and numerical modelling study

Memòria presentada per Laura Burrel García per
l'obtenció del títol de Doctora en Geologia

Juliol 2020

Tesi doctoral dirigida pel Dr. Antoni Teixell Cácharo del Departament de
Geologia de la Universitat Autònoma de Barcelona

Antoni Teixell Cácharo

Laura Burrel García

Cover image: the Noguera Ribagorçana river, the Àger basin and the Montsec ridge. Further away, the Tremp-Graus basin and the Sant Gervàs megaflap.

This research was supported by a predoctoral FPI grant BES-2015-071786 from the Spanish Ministerio de Economía y Competitividad (MINECO) and projects CGL2014-54180-P and PGC2018-093903-B-C21 of MINECO and MICIU. This PhD project was part of the Orogen project community.

A mis abuelos y a mis padres.

Ai, si el recordés, el cop.

Si fes l'esforç d'evocar el cruixit eixordador. La fondària incandescent, roja i incontrolable.

Tones i tones de roca i de terra, de granit, de gneis i de calcita. Cap al cel ens aixecàrem, des de les profunditats. Amb tota la tenacitat, amb tota la paciència, amb tota la destrossa. La puixança fosca ens enlairava, la força bruta ens enviava Amunt, la roca es cargolava, la terra es sobreposava, s'amuntegava, es plegava, esclatava.

Irene Solà, Canto jo i la muntanya balla

Index

Abstract	6
Resum	7
Chapter 1: Introduction	
1.1. Salt tectonics in fold-and-thrust belts	9
1.2. Geological setting	12
1.2.1. Diapirism in the Pyrenees	12
1.2.2. The Central South-Pyrenean Unit	16
1.3. Motivation and aims of this study.....	19
1.4. Methods	22
1.5. Thesis structure	23
Chapter 2: Compressional salt tectonics, foreland evolution and role of pre-existing diapiric structures in the southern Pyrenees (Montsec and Serres Marginals)	
Abstract	28
2.1. Introduction	29
2.2. Methods	30
2.3. Structure and stratigraphy of Montsec and Serres Marginals.....	34
2.4. Field observations in Montsec and Serres Marginals	37
The Montsec hanging wall	37
Montsec footwall, the Àger syncline and Pasarel·la minibasin	38
The Sant Mamet dome	40
The oblique synclines of Sant Jordi, Boada, Rubió and Montsonís	40
The Montroig unit and adjacent synclines of Monteró and Sant Salvador	41
The Avellanes diapir.....	42
The Garriga unit	42
The Os de Balaguer and Tragó synclines	43
The salt-cored anticlines and imbricated synclines of the Ribagorçana valley	44
2.5. Salt Tectonics interpretation.....	45
2.6. Discussion.....	47

2.6.1.	Reinterpretation of the Montsec footwall structure	47
2.6.2.	Rationale and uncertainties in cross-section construction	49
2.6.3.	Salt tectonics and evolution of the central southern Pyrenees from extension to contraction.....	50
	Jurassic.....	53
	Cretaceous rifting and Late Cretaceous post-rift	53
	Late Santonian to mid Maastrichtian	54
	Early Palaeocene.....	54
	Ypresian	55
	Middle Eocene to Oligocene	56
2.6.4.	Role of key parameters in structural evolution.....	57
	Pre-compressional salt structures	57
	Shortening distribution.....	59
	Role of syncompressional sedimentation and erosion	61
2.7.	Conclusions.....	63
	Supplementary material.....	65

Chapter 3: Basement-involved thrusting, salt migration and intramontane conglomerates: a case from the Southern Pyrenees

	Abstract	67
	Résumé.....	68
3.1.	Introduction	69
3.2.	Geological setting and previous studies.....	72
3.3.	Methods	78
3.4.	Tectonostratigraphy of the La Pobla, Gulp and Senterada conglomeratic basins	79
	The substratum of the northern margin of the Organyà basin	79
	The Espills allogroup (Middle Lutetian)	81
	The Gulp allogroup (Upper Lutetian)	81
	The Pessonada allogroup (Late Lutetian)	83
	The Ermita allogroup (Uppermost Lutetian to Bartonian)	83
	The Pallaresa allogroup (Bartonian to Rupelian)	84
	The Senterada allogroup (Rupelian to Chattian)	85
	The Antist allogroup (Chattian).....	87

3.5.	Clast-counting lithology results.....	88
3.6.	Evolution of alluvial fan catchment areas.....	92
3.7.	Role of salt tectonics and basement thrusting in the evolution of the synorogenic conglomeratic basins	97
3.8.	Conclusions	101
	Supplementary material.....	104

Chapter 4: 2D numerical study on folding in a salt-detached basin

4.1.	Introduction	107
4.2.	Method.....	109
4.2.1.	Governing equations and numerical method	109
4.2.2.	Numerical setup and boundary conditions.....	111
4.2.3.	Material properties	112
4.2.4.	Erosion and sedimentation	112
4.2.4.1.	Aggrading reference level	112
4.2.4.2.	Hillslope diffusion.....	113
4.2.5.	Model setup geometries	114
4.2.5.1.	Target and model setup	114
4.2.5.2.	Single diapir setup.....	115
4.2.6.	Model runs	116
4.3.	Preliminary experiments to develop a functional setup.....	116
4.3.1.	Diapirs with roof: the effect of diapir width	116
4.3.1.1.	<i>Deformation of narrow diapirs (2km)</i>	116
4.3.1.2.	Setups with wide diapirs	117
4.3.1.3.	Diapirs without roof	118
4.3.2.	Adding syntectonic sedimentation.....	119
4.3.3.	Lessons learned from the preliminary experimental attempts	123
4.4.	Systematic studies.....	124
4.4.1.	Effects of syntectonic sedimentation vs pre-shortening cover thickness.....	124
4.4.1.1.	The effect of sedimentation rate	124
4.4.1.2.	The effect of the overburden to salt ratio	125
4.4.1.3.	Lessons learned from the study on syntectonic sedimentation	126

4.4.2.	Study with syntectonic erosion	127
4.4.2.1.	Number and geometry of folds	128
4.4.2.2.	Effect of salt evacuation rate	132
4.4.2.3.	Lessons learned from the systematic study with syntectonic erosion	134
4.4.3.	Study of thrusting through a single diapir	136
4.4.	Discussion of modelling results	138
4.5.	Conclusions	142
	Supplementary material.....	144
 Chapter 5: Conclusions		
5.1.	Structural reinterpretation.....	149
5.2.	Tectonostratigraphy and alluvial systems provenance.....	149
5.3.	Salt tectonics evolution in the Southern Pyrenees	150
5.3.1.	Pre-compressional stage	150
5.3.2.	Pyrenean orogeny	151
5.4.	Folding mechanisms in a salt-detached foreland basin	152
	 References	155
	 Acknowledgements	171
	 Appendix 1	172
	 Appendix 2	172

Abstract/Resum

Abstract

The Triassic Keuper evaporites have long been recognized as the main detachment level of the Pyrenean foreland thrust belts and basins. The Cretaceous to Oligocene deformation of the forelands presents evidences of diapirism, comparatively less studied due to the most visible imprint of thrust and fault-related folds.

This thesis presents a multidisciplinary study that explores the role of salt in the tectonic style of two classical areas of the southern Pyrenees, as are 1) the Montsec and Serres Marginals, and 2) the northern margin of the Organyà basin and the adjacent Nogueres Zone. The study which emphasizes the role of halokinesis in the structural and sedimentary evolution of the central-southern Pyrenees. Addressing the role of salt diapirism during the orogeny provides new interpretations with strong implications for the kinematics of compressional deformation and the amount of orogenic shortening.

In the Serres Marginals, early salt structures developed during the Mesozoic pre-compressional stage into a system of diapirs, anticlines and intervening synclines that were filled. During the Pyrenean compressive stage, the folding mechanisms evolved from predominantly vertical (bending) movements triggered by the sedimentary loading to buckling by horizontal forces. The unroofing of the crests of the structure enhanced salt withdrawal, leading to primary and secondary welding and subsequent syncline imbrication. In the north margin of the Organyà basin, salt migration enabled the northward tilting of the basin during the Eocene and Oligocene, which is reflected in the progressive unconformity and onlap of the La Pobla and Gurp intramontane basins. At the same time, sedimentary load accelerated salt migration, enabling the rotation and overturning of the unrooted leading edge of the Nogueres thrust sheet (têtes plongeantes) into the Keuper evaporites.

From the field case studies and numerical modelling, this thesis explores essential questions on salt tectonics, regarding the transition from load-induced bending to compressional buckling, the role of syn-compressional sedimentation and erosion or the effect of pre-existing diapir structures in the structural development of foreland basins.

Resum

Les evaporites Triàsiques del Keuper han estat reconegudes des de fa temps com el principal nivell de desenganxament de plecs i encavalcaments a les conques d'avantpaís pirinenques. La deformació de les conques entre el Cretaci superior i l'Oligocè mostra evidències de diapirisme, poc estudiat degut a l'empremta més visible que deixen els encavalcaments i plecs de falla.

Aquesta tesi presenta un estudi multidisciplinari en el que s'explora el rol de la tectònica salina en el desenvolupament estructural i dels sistemes sedimentaris de la unitat Sudpirinenca central. El treball està centrat en dues zones d'estudi clàssiques dels Pirineus sud, com son 1) el Montsec i les Serres Marginals, i 2) el marge nord de la conca d'Organyà en contacte amb la zona de les Nogueres. Posar en valor el paper de l'halocinesi durant l'orogènia proporciona noves interpretacions amb fortes implicacions per a l'evolució cinemàtica de la compressió i la quantitat d'escurçament orogènic.

A les Serres Marginals estructures salines primerenques evolucionaren durant l'etapa precompressiva mesozoica cap a un sistema de diapirs, anticlinals salins i sinclinals. Durant la compressió, els mecanismes de plegament van passar de moviments verticals produïts per la càrrega sedimentaria (bending) a plegament per buckling produït per esforços horitzontals. L'erosió de les crestes de les estructures va dur a l'expulsió de la sal i l'evolució de les estructures salines en encavalcaments. Al marge nord de la conca d'Organyà, durant l'Eocè i Oligocè la migració salina va causar el progressiu cabussament cap al nord de la conca, resultant en l'onlap i la discordança progressiva dels conglomerats de la Pobla i Gurp. Al mateix temps, la migració salina accelerada pel pes de la càrrega sedimentaria va permetre la rotació i enfonsament de les làmines desarrelades de les Nogueres en les evaporites del Keuper.

A partir dels estudis de camp i la modelització numèrica, aquesta tesi explora qüestions essencials de la tectònica salina respecte la transició del plegament induït per càrrega sedimentaria al plegament degut als esforços compressius, el rol de la sedimentació i l'erosió sinorogèniques o l'efecte d'estructures diapíriques preexistents en les geometries de deformació dels avantpaïsos.

Chapter 1

Introduction

1.1. Salt tectonics in fold-and-thrust belts

The particularity of salt tectonics arises from the rheological properties of evaporites, substantially less dense and incompressible than most sedimentary rocks. Due to its low viscosity, processes controlling salt mechanics mostly depend on pressure (on the salt column and in friction with overburden rocks) and independent parameters such as shortening and extension rates or sediment progradation (Jackson et al., 1994).

Thin-skinned fold-and-thrust belts are, together with deep-water passive margin fold belts, two main settings for detached shortening and compressional salt tectonics. Thick-skinned thrusting can occur during the inversion of basement-involved, extensional salt-bearing basins. Evaporitic levels whenever present are a key element in conditioning the structural style of the different kinds of fold-and-thrust belts. If the salt unit is continuous, not only it can act as a décollement level for the stratigraphic succession above, it can also accelerate the propagation of the deformation front and determine the fold geometry, given that the coupling with the underlying rock units is reduced (Davis and Engelder, 1985), in addition to promote diapirism.

In detached settings, compressional salt tectonics enhance buckling, thrusting, diapir squeezing and salt sheet advance, usually in a structural style that combines more than one of these processes (Jackson and Hudec, 2017). Important factors conditioning the style of salt-detached fold-and-thrust belts include the relative thickness between the salt layer and the sedimentary cover, the position of the salt pinchout, the sedimentation rates and the direction of progradation of the sedimentary systems (Jackson et al., 1994; Letouzey et al., 1995; Koyi, 1998; Costa and Vendeville, 2002; Hudec and Jackson, 2006; Rowan and Vendeville, 2006). These factors will impact the wavelength and amplitude of folds, as well as the timing of thrusting. On the other hand, pre-existing diapiric structures, usually inherited from rifting stages, will condition fold geometry at a smaller scale and impact the sedimentation patterns and the geometry of subbasins (“minibasins”) within the foreland basin (Hudec and Jackson, 2007; Callot et al., 2012). As orogenic deformation progresses, salt can extrude and enhance the upturning of diapir flanks, forming progressive unconformities and overturned flaps in the adjacent sedimentary units (Brun and Fort, 2004; Rowan and Vendeville, 2006).

When the basal evaporite layer is depleted or secondary feeders are squeezed and shut, thrusts can reactivate or cross-cut the resulting welds (Jackson et al., 1994). The degree of closure of the diapirs will strongly depend on the compressional strain rates. The amount of salt extruded to the surface through diapiric structures under compression will depend on the thickness of the roof covering the salt structures, that if thin enough, it can be breached by the rising salt (Duffy et al., 2018) (Figure 1.1).

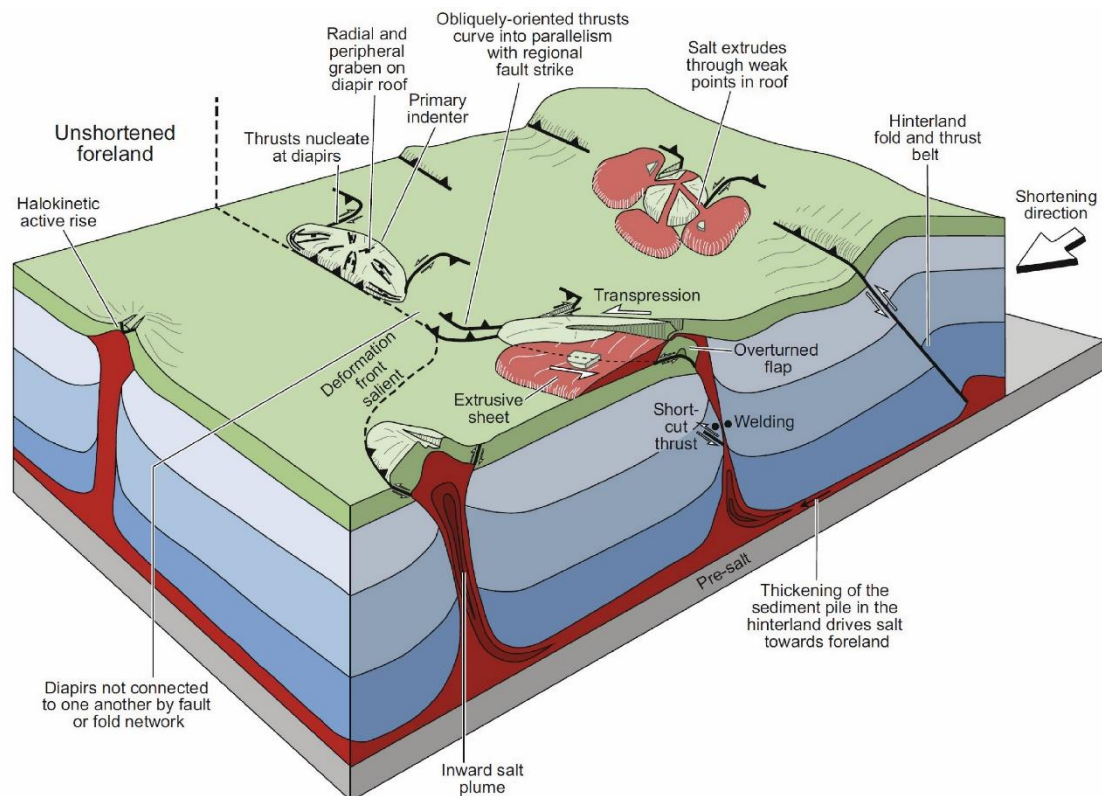


Figure 1.1. Conceptual model showing the evolution of structural styles in a province of thin-roofed diapirs at a low strain. Duffy et al. 2018.

The presence of Triassic evaporitic levels has conditioned the structural evolution of the Jurassic and Cretaceous extensional basins in south-west Europe and north Africa (Masclé and Puigdefábregas, 1998; Alves et al., 2003; McClay et al., 2004; Decarlis et al., 2014; Saura et al., 2014; Soto et al., 2017). The Middle-Upper Triassic evaporites deposited under warm and arid to semi-arid conditions in the Tethys shallow seas, and are distributed in rift basins developed during the extensional break-up of Pangea (Ziegler, 1990; Scotese and Schettino, 2017)(Figure 1.2a). In Iberia, the interaction of several rift systems led to the compartmentalisation of smaller rift basins such as the Prebetic-Subbetic, Iberian, Catalan, Ebro, Basque-Cantabrian and Pyrenean basins

(Arche and López-Gómez, 1996)(Figure 1.2b). During the Alpine orogeny, the Triassic evaporites acted as a detachment level, and were remobilized from pre-existing extensional halokinetic structures, key in the development of fold-and-thrust belts in the Alps (Graham et al., 2012; Decarlis et al., 2014), the Atlas Mountains (Saura et al., 2014; Moragas et al., 2016; Teixell et al., 2017), the Betic Cordillera (Flinch and Casas, 1996; Roca et al., 2006; Pedrera et al., 2020) and the Pyrenees (Séguret, 1972; Sans and Vergés, 1995; McClay et al., 2004; Canérot et al., 2005; Saura et al., 2016; Cámara and Flinch, 2017; Labaume and Teixell, 2020).

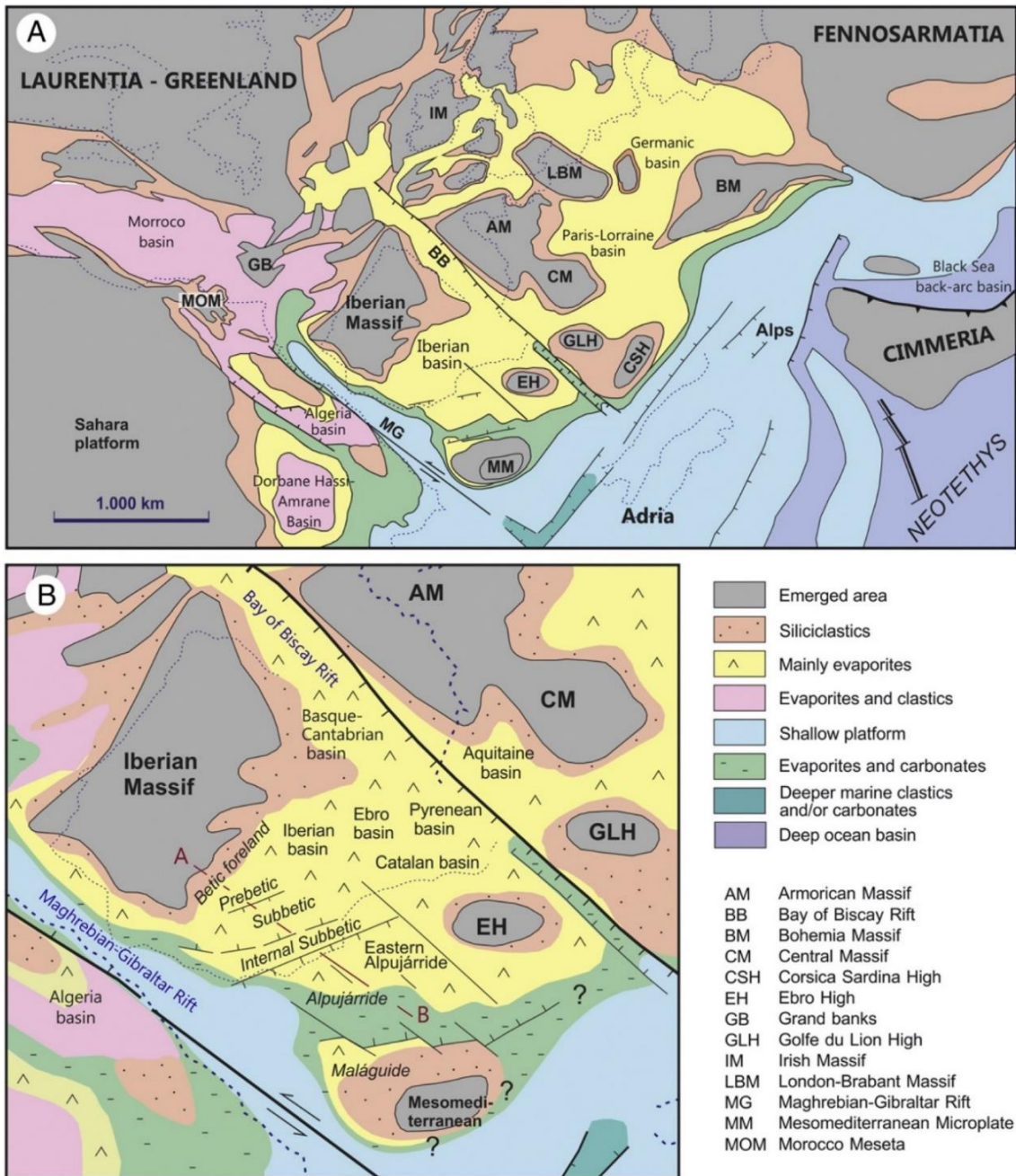


Figure 1.2. Palaeogeographic reconstruction of the westernmost Neotethys and Iberia area for the Late Triassic. Orti et al. 2017.

1.2. Geological setting

1.2.1. *Diapirism in the Pyrenees*

Diapirism in relation to the Triassic evaporite facies has long been recognized all along the Pyrenean orogen (Dalloni, 1930; Selzer, 1934; Almela and Rios, 1943; Dupuoy-Camet, 1953; Serrano et al., 1989). Recent studies have reported halokinesis related to the Mesozoic extension in the Basque-Cantabrian and Parentis domains (Ferrer et al., 2012; Cámara and Flinch, 2017; Bodego et al., 2018)(Figure 1.3), as well as in the North-Pyrenean zone (Canérot, 1988; James and Canérot, 1999; Canérot et al., 2005; Labaume and Teixell, 2020). In the Southern Pyrenees (Figure 1.3) studies have focused on the evolution of the Cretaceous extensional salt basins in the proximal Iberian margin, including the Cotiella thrust sheet (McClay et al., 2004; Lopez-Mir et al., 2014) and the Ribagorça minibasins (Saura et al., 2016), to the north of the Bóixols thrust (Figure 1.3), which show marked changes in stratigraphic thickness due to salt migration associated with listric faulting. Most recent studies on compressional diapirism have focused on specific diapiric structures as the Clamosa dome, the Canelles anticline and the Naval diapir (Teixell and Barnolas, 1995; Salvany, 1999; Muñoz et al., 2013; Santolaria et al., 2014) (Figure 1.3) that are often preserved as exposed diapirs, salt walls, or salt-cored anticlines.

Pyrenean diapirism is generally attributed to the Upper Triassic Keuper facies, although the common existence of Middle Triassic Muschelkalk limestone inliers in diapirs suggest that the basal evaporite detachment level must stratigraphically underlie the limestones. Such evaporite level has never been identified at the surface in the Pyrenees (Ortí et al., 2017), but sub-limestone evaporites (including halite) have been reported from the subsurface of the Ebro basin (“middle Muschelkalk” evaporites, Jurado, 1990). Hence, the disrupted Muschelkalk carbonates observed in the Pyrenean diapirs may have been originally interbedded in shale/evaporite deposits which, for convenience, we will jointly refer as the Triassic evaporite unit or just Keuper.

The Keuper of the Central South Pyrenean unit crops out mainly in the Serres Marginals thrust sheet and in the boundary zone between the Organyà basin and the Paleozoic thrust sheets of the Nogueres Zone (Figure 1.3). In the Nogueres area, the succession of

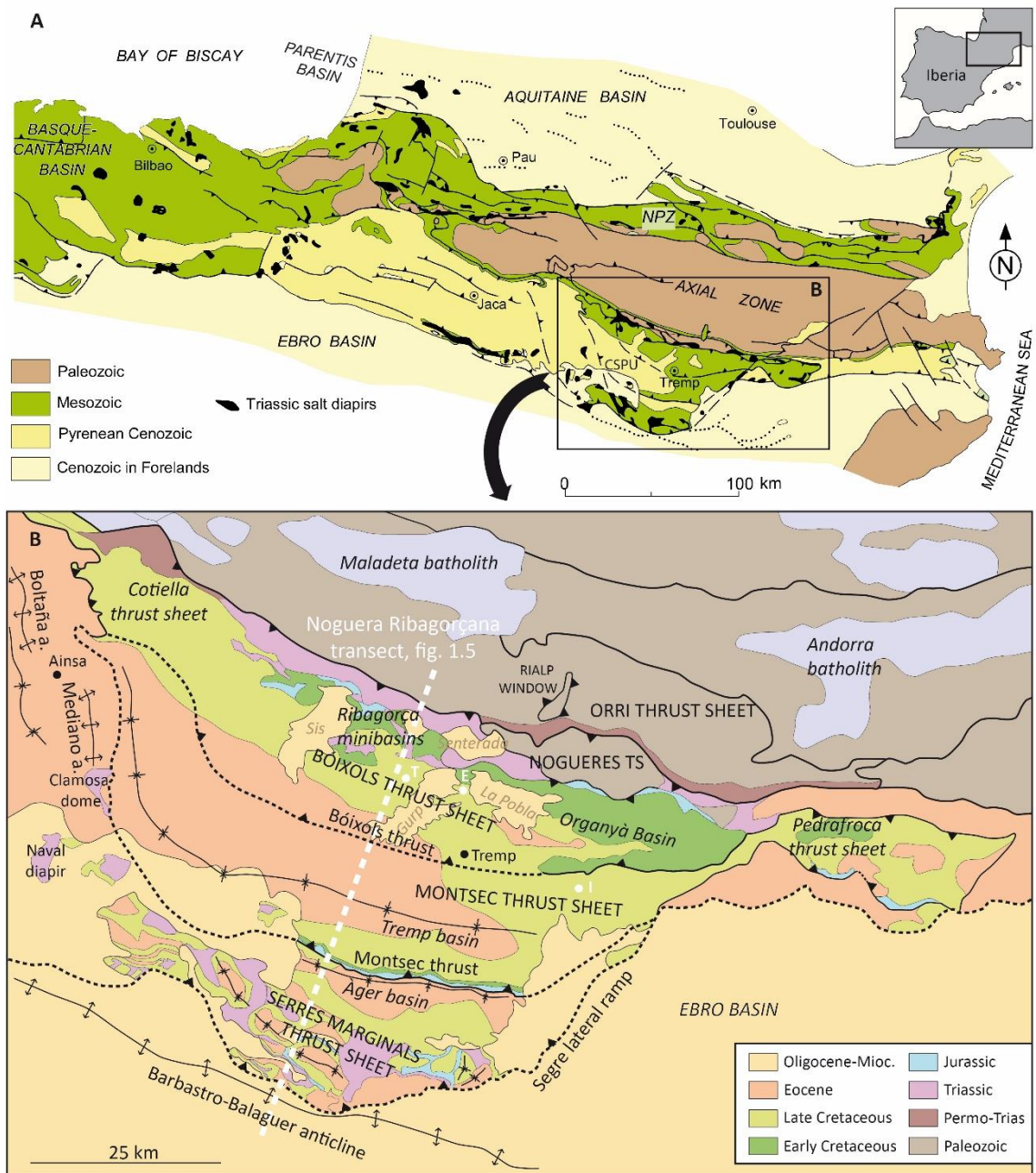


Figure 1.3. (a) Location map of the Pyrenean mountain belt, including the main Triassic salt structures (after Saura et al., 2016). NPZ: North Pyrenean Zone; CSPU: Central South Pyrenean Unit. **(b)** Simplified geological map of the Central South Pyrenean unit, modified from the ICGC 1:250000 structural map. TS, Thrust sheet; a, anticline. I, Isona-1bis well; E, Erinyà-1 well; T, Tamúrcia well.

Keuper cropping out at present day is about 250m thick, while in Serres Marginals it can reach up to 540m. However, these thickness are likely to have been significantly affected by deformation and/or salt dissolution. In fact, several authors have envisaged originally thousands of meters of evaporites to account for observed diapir-and-minibasin structures (López-Mir et al., 2015; Saura et al., 2016; Espurt et al., 2019b; Labaume and Teixell, 2020). Of the outcropping stratigraphy, the Keuper basal unit, known as the Low

grey-green unit (Figure 1.4) is known in the Nogueres Zone as the Adons mudstone and carbonate formation, which crops out to the North East of CSPU and also in the localities around El Pont de Suert (Figure 1.3) (Salvany and Bastida, 2004). This formation is conformable above the Muschelkalk carbonates and is composed mainly of mudstones and interbedded dolostone beds of a few decimetres thick (Salvany and Bastida, 2004). The equivalent of this formation in Serres Marginals is the Canelles gypsum formation, named after the salt-cored anticline in the Noguera Ribagorçana river valley. The latter is mainly composed by gypsum with interbedded carbonate layers and minor presence of mudstones, interpreted to have originated in a wide evaporitic lagoon, likely extending to the south (Salvany and Bastida, 2004). The middle red unit, cropping out in the Nogueres Zone and also in Serres Marginals, is the Boix gypsum formation (Figure 1.4)(Salvany and Bastida, 2004), which consists of red and versicolor gypsum. In the Pyrenean domain tectonic subsidence was rapid at that time, and for this reason the middle red unit is thicker here than in other areas of Iberia (Ortí et al., 2017). The Senterada gypsum formation only crops out in the Pont de Suert and Senterada areas (Figure 1.3), where it reaches its maximum thickness of about 250m (Salvany and Bastida, 2004). This unit is composed of a very uniform succession of laminated gypsum beds with interbedded carbonate layers. The development of carbonate beds varies locally, and they are usually boudinaged or brecciated due to the intense deformation. In some localities there are anhydrite beds, which is not a very common feature among the Nogueres Zone Keuper (Salvany and Bastida, 2004). The upper green-grey unit (Figure 1.4), which crops out both in the Nogueres Zone and Serres Marginals is composed of the Avellanes mudstone and carbonate formation, named after the circular diapir of the Serres Marginals (Figure 1.3) (Salvany and Bastida, 2004). The lower part is predominantly mudstone but it becomes more carbonatic to the top, where it has been described as the base of the carbonate Isábena formation (Arnal et al., 2002; Salvany and Bastida, 2004). The final Keuper Evaporitic episode (Rhaetian to Hettangian), is represented in the Serres Marginals area by the sulfate lagoons of the Lécera formation, which is not present in the Nogueres Zone (Ortí et al., 2017).

Interbedded within the Keuper materials and remobilised by the diapiric movements there are dolerite bodies known in the Pyrenees as ophites, due to their microscopic

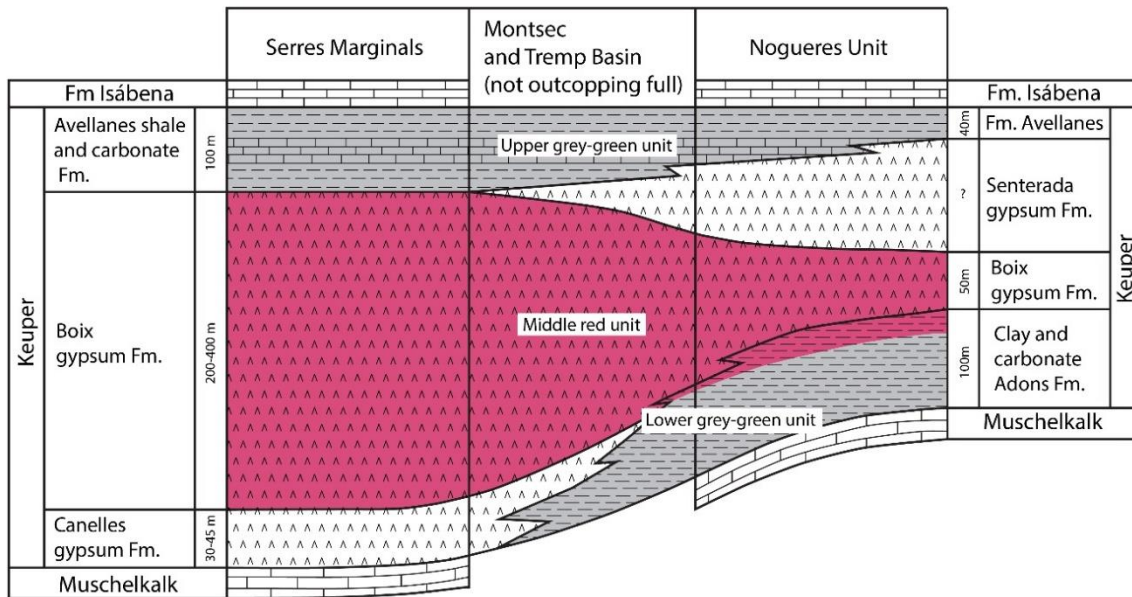


Figure 1.4. Correlation of the lithostratigraphic units of the Serres Marginals and Nogueres Keuper. *Salvany and Bastida, 2004.*

texture. The emplacement of the ophiolites within the hosting Keuper succession happened soon after its sedimentation, and before the sedimentation of the Rhaetian and Liassic carbonates (Azambre et al., 1987; Lago et al., 2000). The widespread presence of ophiolite interbeds all along the Pyrenean Keuper is very relevant to this work, since they produce the only preserved clasts that, in the Tertiary intramontane conglomerates, that can be unequivocally attributed to a broad Keuper source. In Chapter 3 of the thesis, ophiolite clasts are used as a marker to track diapir exposure during the orogeny.

Due to weathering, halite is not found in present-day outcrops. However, most wells that cut across the Keuper in the Southern Pyrenees, including Tamúrcia, Erinyà-1 and Isona-1 Bis in the study area (Figure 1.3), drilled through thick halite successions (Lanaja, 1987). Moreover, the salty water springs in localities as Gerri de la Sal, Peralta de la Sal and Vilanova de la Sal and many others, show that halite is an important component of the Keuper facies under the surface.

Seismic lines across the Pyrenees usually do not have good resolution at and below Keuper depths, and as a result, most cross-section interpretations tended to minimize the Triassic evaporite unit thickness below the Mesozoic sedimentary cover. This has led to the assumption of several stratigraphic repetitions of the Mesozoic-Cenozoic series

in the Serres Marginals area (Vergés and Muñoz, 1990; Teixell and Muñoz, 2000). Recent studies are challenging this procedure, presenting cross-sections with Keuper thicknesses between 1.5 to 3 km below the Serres Marginals and Montsec thrust sheets (Cámara and Flinch, 2017; Santolaria et al., 2017; Espurt et al., 2019a), emphasizing the role of salt structures during the Pyrenean orogeny and minimizing the amount of shortening.

As outlined above, present day volumes of the Triassic evaporites are not an ideal estimate for the original thickness, since there may have been large salt evacuation through the exposed diapirs and the frontal structures as well as deformation and dissolution. However, from the thickness of the remaining Keuper and the amplitude of the fold structures above we can tentatively estimate a minimum thickness of 2-3 km below the Serres Marginals. This is consistent with thicknesses reported in other areas of the Peri-Iberian Triassic rift system (Soto et al., 2017) and with what has been deduced in other deformed salt systems of the Pyrenees (references above).

1.2.2. The Central South-Pyrenean Unit

The Central South-Pyrenean Unit (CSPU) (Séguret, 1972), (Figure 1.3), comprises a system of cover thrust sheets of the Southern Pyrenees located between the basement units of the Noguera and Axial Zone antiformal stack to the north, and the Ebro Basin to the south. It is limited to the east and west by with oblique or lateral structures (Segre lateral ramp, Boltaña and Mediano anticlines, respectively) (Figure 1.3).

The CSPU has a prominent southward displacement with respect to adjacent units in the southern Pyrenean fold-and-thrust belt, attributed to the presence of an originally

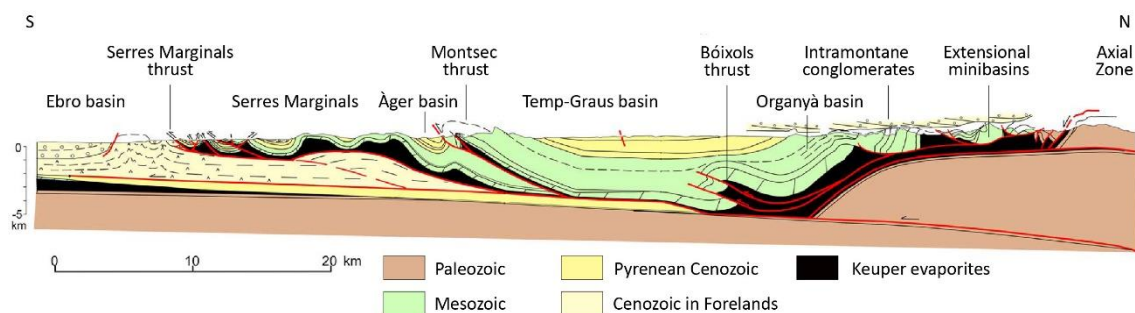
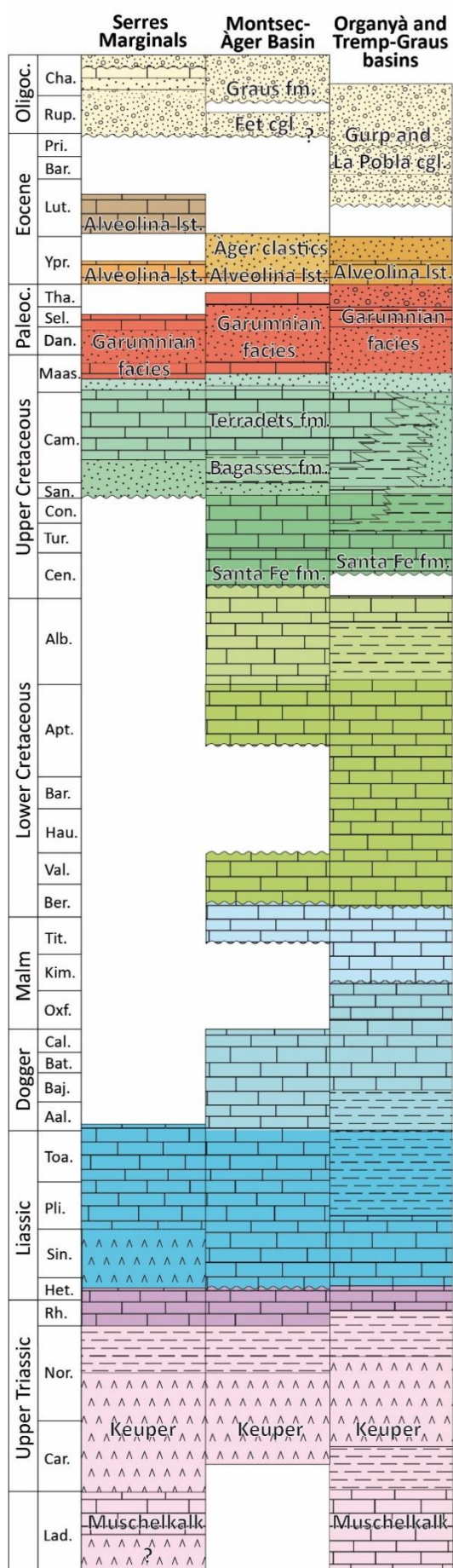


Figure 1.5. Cross section across the Central South-Pyrenean Unit along the Noguera Ribagorçana valley (Saura et al. 2016). The footwall structure of the Montsec thrust is reinterpreted in Chapter 2.

thicker Keuper series (Cámara and Klimowitz, 1985), an inherited Mesozoic basin geometry (Vergés, 1993), or to a mechanical contrast within the Keuper unit (Storti et al., 2007; Vidal-Royo et al., 2009; Muñoz et al., 2013). The CSPU developed progressively from the Late Cretaceous to the Oligocene, and was emplaced in an internal piggy-back thrust sequence (Vergés and Muñoz, 1990; Teixell and Muñoz, 2000), detached in the Triassic Keuper facies (Séguret, 1970; Cámara and Klimowitz, 1985)(Figure 1.5). It involves a Jurassic to Lower Cretaceous syn-rift carbonate succession, Cenomanian to early Santonian post-rift carbonates, and late Santonian to Oligocene mainly detrital and subordinately carbonate sediments, contemporaneous with the Pyrenean orogeny (Figure 1.6). The interaction of the developing fold-and-thrust belt with the sedimentation of synorogenic deposits has been a topic widely explored since the seventies (Séguret 1972; Garrido-Mejías 1973; Cámara & Klimowitz 1985; Barnolas *et al.* 1991; Vergés 1993; Meigs 1997; Teixell & Muñoz 2000, etc.).

The northernmost Bóixols thrust sheet (Figures 1.3 and 1.5) has the oldest age of emplacement in the CSPU, registering the onset of the Pyrenean compression starting in the late Santonian (Garrido-Mejías, 1973; Simó, 1986; Berástegui et al., 1990; Caus et al., 1990; García-Senz, 2002). The thrust sheet limits to the north with the wide Keuper outcrops of the Senterada-Gerri de la Sal area, which separate the CSPU Mesozoic cover from the thrust and overturned Paleozoic and Permo-Triassic units of the Nogueres Zone (Séguret, 1972) (Figures 1.3 and 1.5). In the Ribagorça area, complex salt-related Jurassic-Cretaceous minibasins have been reported (Sopeira and Faiada; Saura et al., 2016). In the east, the Cretaceous sedimentary succession of the structurally simpler Organyà synformal basin is over 5000m thick (Berástegui et al., 1990; García-Senz, 2002). The Cenomanian Santa Fe limestone formation (Mey et al., 1968) marks the post-rift angular unconformity (Figure 1.6). The Bóixols thrust, mostly blind or sealed under Maastrichtian calcarenites (Garrido-Mejías, 1973), formed from reactivated early Cretaceous extensional faults, producing fault-propagation anticlines with Keuper rocks at their cores (García-Senz, 2002).

To the south of Bóixols is the Montsec thrust sheet which has a Jurassic to Cretaceous succession that is about 3000m thick (Garrido-Mejías and Ríos, 1972; Vergés and Muñoz, 1990; Teixell and Muñoz, 2000)(Figure 1.6). The bulk of the thrust sheet succession has



a broad, flat-bottomed synformal shape (Figure 1.5) known as the Tremp basin, with Cretaceous and Tertiary sediments thinning towards the south. The emplacement of the Montsec thrust, detached in the Keuper, has been attributed to the Ypresian (Williams and Fischer, 1984; Rosell et al., 1985; Muñoz et al., 2018) regarding the progressive unconformity registered in the in the Montsec footwall (Àger syncline). In view of the structural and facies relationships, Teixell and Muñoz, 2000 extended the emplacement of the Montsec thrust sheet up to the late Eocene. The Montsec thrust is fossilized in the Noguera Ribagorçana river valley by the not precisely dated Fet conglomerates (Figure 1.6), derived from erosion of the ridge.

The structural geology of the Serres Marginals thrust sheet has been described in several works (Pocoví, 1978a; Martínez-Peña and Pocoví, 1988; Vergés and Muñoz, 1990; Muñoz, 1992; Vergés, 1993; Teixell and Muñoz, 2000). It presents a complex map configuration of several internal km-scale folds, imbricated synclines limited by Keuper-cored ridges and domes, and

Figure 1.6. Stratigraphy of the Serres Marginals, Àger basin-Montsec and Bóixols thrust sheets. The Àger clastics include the Baronia, Àger, Ametlla and Corçà fluviodeltaic formations. Stratigraphic units are from the ICGC 1:25000 maps and the Os de Balaguer sheet of the IGME 1:50000 geological map.

exposed diapirs (Figure 1.3). It has a much more reduced stratigraphic succession than the Montsec and Bóixols thrust sheets, where the Lower Cretaceous is completely missing (Figure 1.6).

The Early Oligocene thrusting of the Serres Marginals sheet above the Priabonian Barbastro gypsum formation and detrital equivalents of the Ebro Basin (Cámara and Klimowitz, 1985; García-Senz and Zamorano, 1992) transferred the deformation from the CSPU towards the Ebro foreland, where deformation occurred above an intra-basinal detachment level localized in upper Eocene evaporites.

1.3. Motivation and aims of this study

Since long ago, the knowledge on salt tectonics has evolved around the petroleum industry because many of the great productive provinces are salt basins (Gulf of Mexico, North Sea, West African margins, Red Sea, Precaspian basin, Brazilian offshore basins). More recently, salt tectonics have been pushed further by applying these concepts to understand the evolution of less productive areas, such as salt-detached fold-and-thrust belts. This has eventually led to the reassessment of the regional evolution of classic field areas like the Zagros mountains, the external parts of the Alps, the Tian Shan, the Atlas, the Andean Eastern Cordilleras and also the Pyrenees.

However, the study of salt tectonics in intensely shortened settings presents important challenges. One of them is the fact that the pre-existing diapiric structures and stratigraphic patterns inherited from the rifting stages are usually very deformed and sometimes obliterated. This is true as well for the halokinetic deformation happening contemporary to thrusting and buckle folding. It is frequent that the more evident imprint of thrusting is masking thickness differences in the syn-compressional strata, which are not solely related with folding. Moreover, the quick synorogenic rise of topography and associated fast erosion, usually erode the edges of the synclines and the anticlinal crests. This erases possible onlap geometries, thinning of the layers and unconformities, key elements to identify the imprint of halokinesis. It is the difficulty to find these elements that, in areas like Serres Marginals or the Montsec thrust has led to understand deformation as uniquely related to folding and thrusting, usually overlooking the role of vertical movements related to salt halokinesis.

This thesis wants to contribute to the discussion on the following fundamental salt tectonics questions:

- Which are the strata geometries characteristic of salt tectonics in the very early stages of compression?
- What factors determine the transition from load-induced subsidence to buckling and vice-versa?
- Are basal welding or shortening accumulation always the factors leading to thrusting?
- How does the thickness of the pre-shortening cover above the salt layer modify the impact of syn-tectonic sedimentation and erosion?

Regarding the Pyrenees, some of the fundamental questions that have inspired this thesis are:

- Is there a continuous salt tectonics activity from right after the Keuper evaporites sedimentation to the end of the orogeny?
- With the onset of buckle folding, did load-induced subsidence still play a significant role in the Pyrenean foreland?
- Why do the two provinces with important salt outcrops, Serres Marginals and the northern margin of the Organyà basin, present such different geometries?
- Can salt tectonics shed some light to the interpretation of not yet fully understood structures and geometrical relationships in the southern Pyrenees?

In this thesis I present a detailed tectono-stratigraphic study, integrating different disciplines to contribute to the knowledge on the salt tectonics evolution of the Central Southern Pyrenees. Rather than focusing on single diapiric structures, some of which have already been studied in detail, I have built a regional interpretation on the structural evolution of the two areas of the CSPU where salt tectonics had a major impact during the Pyrenean orogeny: The Montsec and Serres Marginals in the south, and the northern margin of the Organyà basin, limiting with the Noguères Zone (Figure 1.3) in the north. To do so, it has also been necessary to understand the role that salt tectonics played during the Jurassic-Cretaceous rifting stage in the Pyrenean basin. This

topic has been explored for the extensional basins of the northern CSPU, and in this work we contribute to the discussion. Although the study area is localized only in the Southern Pyrenees, field observations have been the starting point of a wider discussion, involving the fundamental processes and parameters conditioning compressional salt tectonics, as well as other field examples of fold-and-thrust belts and numerical and physical models.

The aims of this project are the following:

- To determine the diagnostic structural and sedimentary patterns of salt tectonics, in areas of the Southern Pyrenees strongly deformed by compression, where this type of tectonics is obliterated and often goes unnoticed.
- To discriminate patterns resulting from a) cases where there was a previous diapir structure formed in the rifting stages and b) cases where halokinesis started in the compressional stage.
- Understanding the influence of the geometry and orientation of the pre-compressive structures in the orogenic structural evolution.
- To determine the role of differential sedimentary accumulation loading (e.g. in synclinal zones) and erosion (e.g. in anticline crests and diapiric roofs) in salt migration/evacuation and in diapiric elevation and subsidence patterns.
- To study the influence of early compressive structures and associated salt tectonics on the source and sediment dispersion pattern of a foreland basin context.
- To integrate the salt tectonics evolution into the tectonostratigraphic framework of the Pyrenean Orogeny.

During the process, especially after starting a modelling approach, I have got into new topics such as the impact of cover thickness in allowing the development of early compressional structures, or the mechanisms of thrusting along diapiric cores, also discussed in the thesis.

1.4. Methods

Each of the chapters in this thesis follows a different methodological approach. For this reason, the specific methodology is detailed at the beginning of each one of the main chapters.

This PhD project has developed in three stages:

- The first stage involved identifying the fundamental questions on compressional salt tectonics that could be explored in a setting like the Pyrenees. In the initial fieldwork campaigns, in 2016, I revisited classic areas of Pyrenean geology not fully understood with thrust tectonics, as is the case of the Montsec footwall structure or the northward-tilted progressive unconformity of the La Pobla and Gulp conglomerates. I also did subsequent field campaigns in the Sierras Exteriores, the western equivalent to the Serres Marginalis, which finally have not been incorporated into the thesis. The campaigns involved field structural analysis, collection of extensive dip data, stratigraphic observations, and clast counts of conglomerates to investigate provenance.
- The second stage of the project involved putting together the field observations to build the first cross-sections and go back to the field to collect new structural and clast-composition data, while starting with the section restoration and the first regional interpretations. Specific structural analysis software (Midland Valley/*Petex Move*) was used for map handling of structural data and cross-section construction/restoration).
- In the third stage I started investigating the main questions raised from the field examples and comparing the Pyrenees case-study with other salt fold-and-thrust belts, and published numerical and physical experiments. From 2018 onwards, I undertook a modelling work in collaboration with the Applied Geodynamics Group of the Bureau of Economic Geology (University of Texas-Austin), to produce a series of 2D numerical simulations to address the fundamental parameters affecting the folding patterns of salt-detached foreland basins. During a four-month stay, we designed the main setup and went through a long

experimental phase to arrive at realistic deformation geometries. During 2019, back in Barcelona, I worked in the systematic studies on the effect of syn-compressional sedimentation in salt-related fold-thrust systems, and in the set-up of single diapir shortening numerical experiments. During the second visit to Austin, in February 2020, we implemented syn-compressional erosion, discussed the results reached so far, and outlined future experiments to be done. The details of the numerical code used are given in the corresponding chapter.

1.5. Thesis structure

This thesis is formally organized in a classic format. However, **Chapters 2 and 3** correspond to extracts of manuscripts already submitted for publication in scientific journals.

Chapter 1 is an introduction to the geological context and the aims and organisation of the thesis. The main chapters of the thesis are ordered with the field studies first (**Chapters 2 and 3**), and the numerical modelling studies later (**Chapter 4**), as the modelling approach was inspired by the field observations. Finally, Chapter 5 is a summary of the main conclusions reached in **Chapters 2, 3 and 4**. The complete list of references can be found at the end of the thesis.

Chapter 2 is under review in the Journal of the Geological Society as Burrell, L. and Teixell, A., *Compressional salt tectonics, foreland evolution and role of pre-existing diapiric structures in the southern Pyrenees (Montsec and Serres Marginals)*.

This manuscript has an extensive introduction to Pyrenean salt tectonics and to the structure of the Central South-Pyrenean unit. To avoid repetitions, the introductory part, which is relevant to the entire thesis, has been moved to Chapter 1. In consequence, Chapter 2 is a shorter version of the manuscript sent to the journal. The methodology, results, discussion and conclusions are the same as in the journal submitted version. The chapter presents a structural study of the Montsec and Serres Marginals area (Figures 1.3 and 1.7) based on field observations, published maps and newly acquired structural and stratigraphic data. We build new structural cross-sections reinterpreting the southern part of two classic transects of the Southern Pyrenees

(Noguera Ribagorçana and Noguera Pallaresa river transects, Figure 1.7). With the restoration of the sections, we focus on the role that pre-compressional salt structures had in determining the geometry of the Serres Marginals folds and the Montsec. We discuss the relative role between buckle folding and load-induced subsidence and the transition from folding to thrust sheet imbrication. Also, we compare the South Pyrenean case-study with other fold-and-thrust belts with similar characteristics.

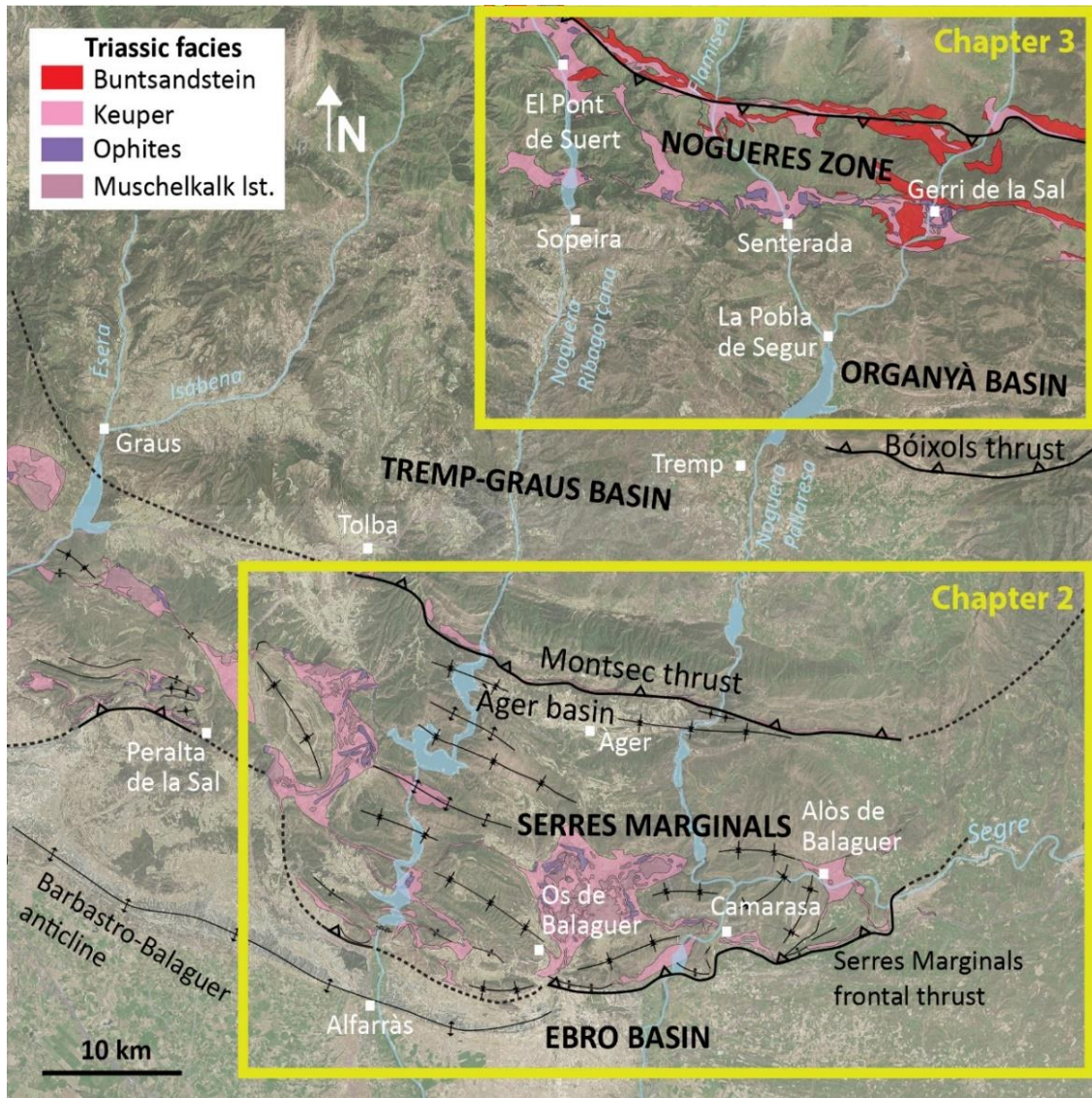


Figure 1.7. Aerial image of the study areas of the field work based thesis chapters. Wider location in Figure 1.3.

Chapter 3 is currently under review in the Bulletin de la Société Géologique de France as Burrel, L., Teixell, A., Gómez-Gras, D. and Coll, X., *Basement-involved thrusting, salt migration and intramontane conglomerates: a case from the Southern Pyrenees*.

Chapter 3 is presented in the same form as the manuscript submitted to the journal. The chapter focuses in the north of the Central South-Pyrenean Unit and Noguères Zone (Figures 1.3 and 1.7). The northern margin of the Organyà basin has a complex structure in which syn-rift Lower Cretaceous carbonates flank a wide Keuper evaporite province, featuring the leading edges of the basement-involved thrust sheets of the Pyrenean antiformal stack. In this study we use field observations and new and published structural data of the northern margin of the Organyà basin, combined with structural and clast provenance data from the Cenozoic alluvial conglomerates of Gorp and La Pobla, to understand the Lutetian to Oligocene evolution of the northern margin of the Central South-Pyrenean Unit. Previous studies have shown that the tectonostratigraphic evolution of this region was conditioned by the emplacement and exhumation of the Axial Zone antiformal stack. We present new paleogeographic maps and a cross-section illustrating how the movements over a mobile evaporite layer conditioned the geometry and catchment areas of the Cenozoic conglomeratic basins.

Chapter 4 corresponds to the 2D numerical modelling study of compressional salt tectonics. This chapter first presents an overview of the experimental process to get to a working setup. The following focus is on the systematic studies on shortening a salt-detached basin with syn-compressional sedimentation and erosion. They arrive to insights on how sedimentation rate and erosion intensity determine the transition between buckle folding and load-induced syncline subsidence. In the discussion of this chapter I compare the results obtained from numerical modelling with the field case studies, specially focusing on folding in Serres Marginals.

As mentioned before, **Chapter 5** summarizes the integrated conclusions of the previous three chapters.

Appendix I includes an A3 print of the restored structural cross-sections presented in Chapter 2, at a bigger scale for better visualization.

Appendix II includes the main figures of the numerical models in a bigger size.

Each of the three main chapters that contain the contributions of this thesis have reached specific conclusions and the thesis overall pursues a complete study. However, from the field and the numerical modelling studies new questions have arisen to

continue this line of research. The Pyrenees has proven once again to be a wonderful natural laboratory to gain understanding of many geological process, in this case for compressional salt tectonics.

Chapter 2

Compressional salt tectonics, foreland evolution and role of pre-existing diapiric structures in the southern Pyrenees (Montsec and Serres Marginals)

This chapter is under review in The Journal of the Geological Society as Burrell, L. and Teixell, A., *Compressional salt tectonics, foreland evolution and role of pre-existing diapiric structures in the southern Pyrenees (Montsec and Serres Marginals)*.

Abstract

Compressional salt tectonics, foreland evolution and role of pre-existing diapiric structures in the southern Pyrenees (Montsec and Serres Marginals)

Triassic evaporites have long been recognized as the main detachment level for thrusting in the Pyrenean fold-and-thrust belts. The deformed Late Cretaceous to Eocene foreland basins show evidence of diapirism often overlooked due to the more obvious imprint of shortening related structures. Based on field observations, published maps and newly acquired structural and stratigraphic data, we build new structural cross-sections reinterpreting two classic transects of the Southern Pyrenees (Noguera Ribagorçana and Noguera Pallaresa river transects). The sequential restoration of the structural sections explores the variations of the salt-tectonics structural style, addressing the role of halokinesis in the tectonic and sedimentary development of the basin. In the Serres Marginals area, we interpret that precursor salt pillows and diapirs started developing during the Mesozoic pre-orogenic extensional episode, evolving into a system of polygonal salt ridges and intervening synclines filled with early synorogenic sediments. During the Pyrenean compression, folding mechanisms transitioned from vertical halokinetic movements induced by sediment loading (bending) to buckle folding, and later to salt squeezing and thrust welding as salt ridges were unroofed. We examine the main field observations, that lead to this new interpretation and how it differs from the previous interpretations, currently under debate in light of recent compressional salt tectonics concepts.

To avoid repetitions, the sections of the paper on Pyrenean salt tectonics and the structure and stratigraphy of the Central South-Pyrenean Unit that are relevant for all the chapters of this thesis, have been moved to the introduction in Chapter 1. For this reason, Chapter 2 is a shortened version of the original submitted paper.

2.1. Introduction

In this paper we present a comprehensive reinterpretation of the tectonic evolution of the southern part of the central Pyrenees (Figure 2.1), based on field observations and cross-section construction and restoration. New observations allow to reassess the role of pre-and syn-compressional halokinetic movements in determining the structural style during the orogenic stage, incorporating concepts of contractional salt tectonics developed in recent years. Our interpretation has strong regional implications as it reduces the amount of shortening along the Montsec thrust and internal deformation within the Serres Marginals thrust sheet.

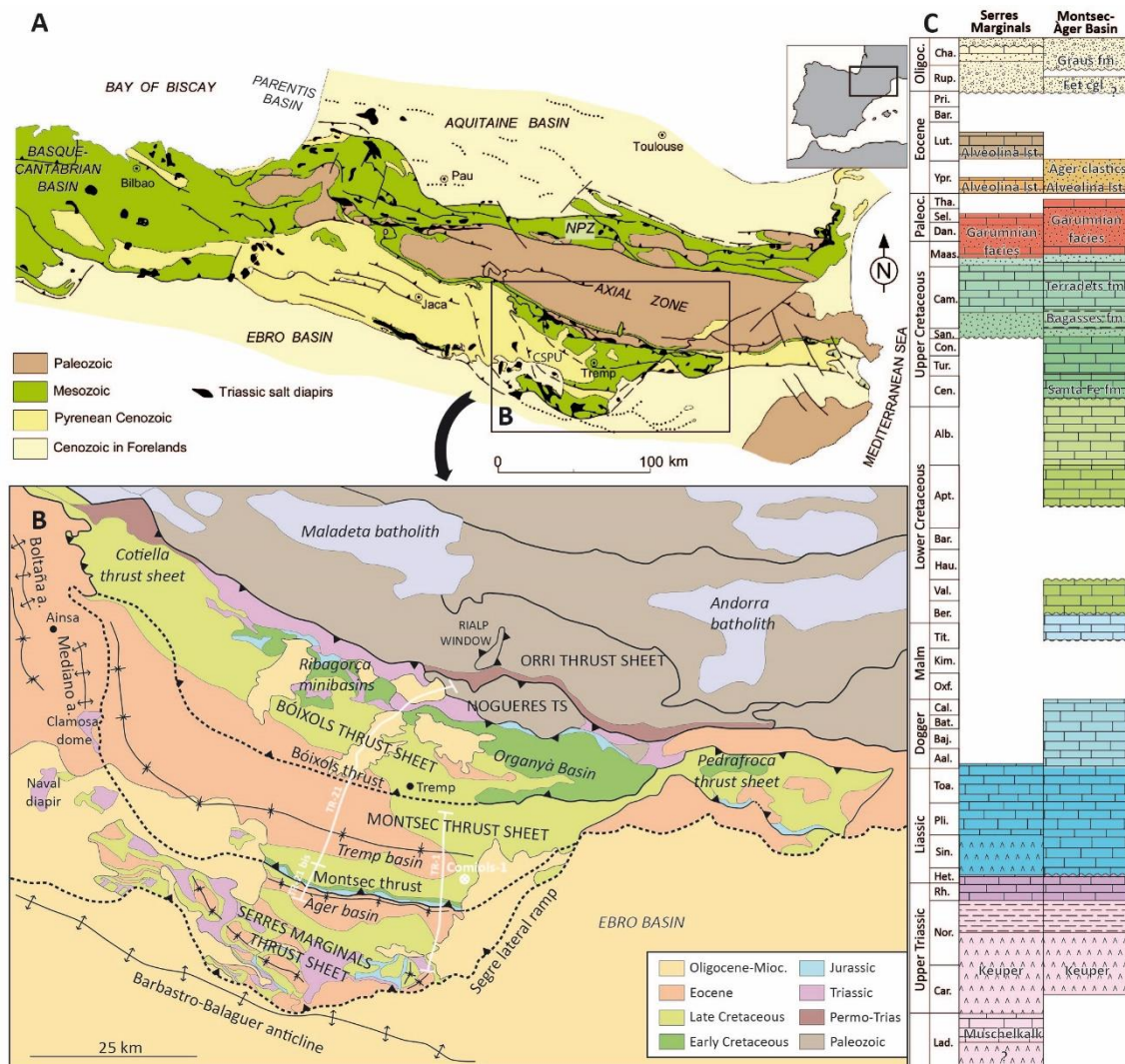


Figure 2.1 Error! Utilice la pestaña Inicio para aplicar O al texto que desea que aparezca aquí. -1. (a) Location map of the Pyrenean mountain belt, including the main Triassic salt structures (after Saura et al., 2016). NPZ: North Pyrenean Zone; CSPU: Central South-Pyrenean Unit. (b) Simplified geological map of the Central South Pyrenean unit, modified from the ICGC 1:250000 structural map. TS, Thrust sheet; a, anticline (c) Stratigraphy of the Serres Marginals and Àger basin-Montsec thrust sheets. The Àger clastics include the Baronia, Àger, Ametlla and Corça fluviodeltaic formations. Stratigraphic units are from the ICGC 1:25000 maps and the Os de Balaguer sheet of the IGME 1:50000 geological map.

2.2. Methods

We obtained the structural and stratigraphic data used in this study from field work and from bibliographic references. The 1:25.000 series of the geological map by the geological survey of Catalunya (Institut Cartogràfic i Geològic de Catalunya, ICGC) and the 1:50.000 series from the Spanish geological survey (Instituto Geológico y Minero de España, IGME), provide accurate cartographies of much of the area as well as stratigraphic logs and unit descriptions. Field campaigns were directed to collect new structural data in areas where they were insufficient or controversial, especially in the Montsec footwall.

We have considered the available 2D reflection seismic surveys from the 1960's to 1980's, which were acquired for hydrocarbon exploration in the Southern Pyrenees (Figure 2.1). The ECORS-PYRENEES deep seismic profile crosses the area near the Noguera Pallaresa River, and its interpretation has been widely discussed throughout the years (Roure et al., 1989; Muñoz, 1992; Vergés, 1993; Beaumont et al., 2000; Mouthereau et al., 2014; Teixell et al., 2018). The industrial TR-1 line crosses the area to the east of the Noguera Pallaresa valley (Figure 2.2), close to the Comiols-1 exploration well, and is interpreted in Muñoz et al., 2018. The TR-21 and 21bis lines (Figure 2.3) cross the area near the Noguera Ribagorçana River, and have been the base for the subsurface interpretation of the Montsec thrust geometry in that valley. While these seismic lines image well the hanging wall of the Montsec thrust, the footwall images are not clear (Figure 2.3), and their interpretation needs to rely largely on surface data. The Comiols-1 is the only exploration well in the area, which penetrates both the Montsec hanging wall and footwall, 15km to the east of the Noguera Pallaresa transect (Lanaja, 1987).

The integration of new structural data collected at the surface has been the basis for building the two structural cross-sections presented in this paper (Figure 2.4). These are 15 km apart, following the Noguera Ribagorçana and the Noguera Pallaresa river valleys (Referred as Ribagorçana and Pallaresa transects from now on, location in Figure 2.2), where fluvial incision provides the most complete exposures. The cross-sections have been built using the Move software and then restored step by step to several stages using the flexural slip unfolding algorithm built in the software.

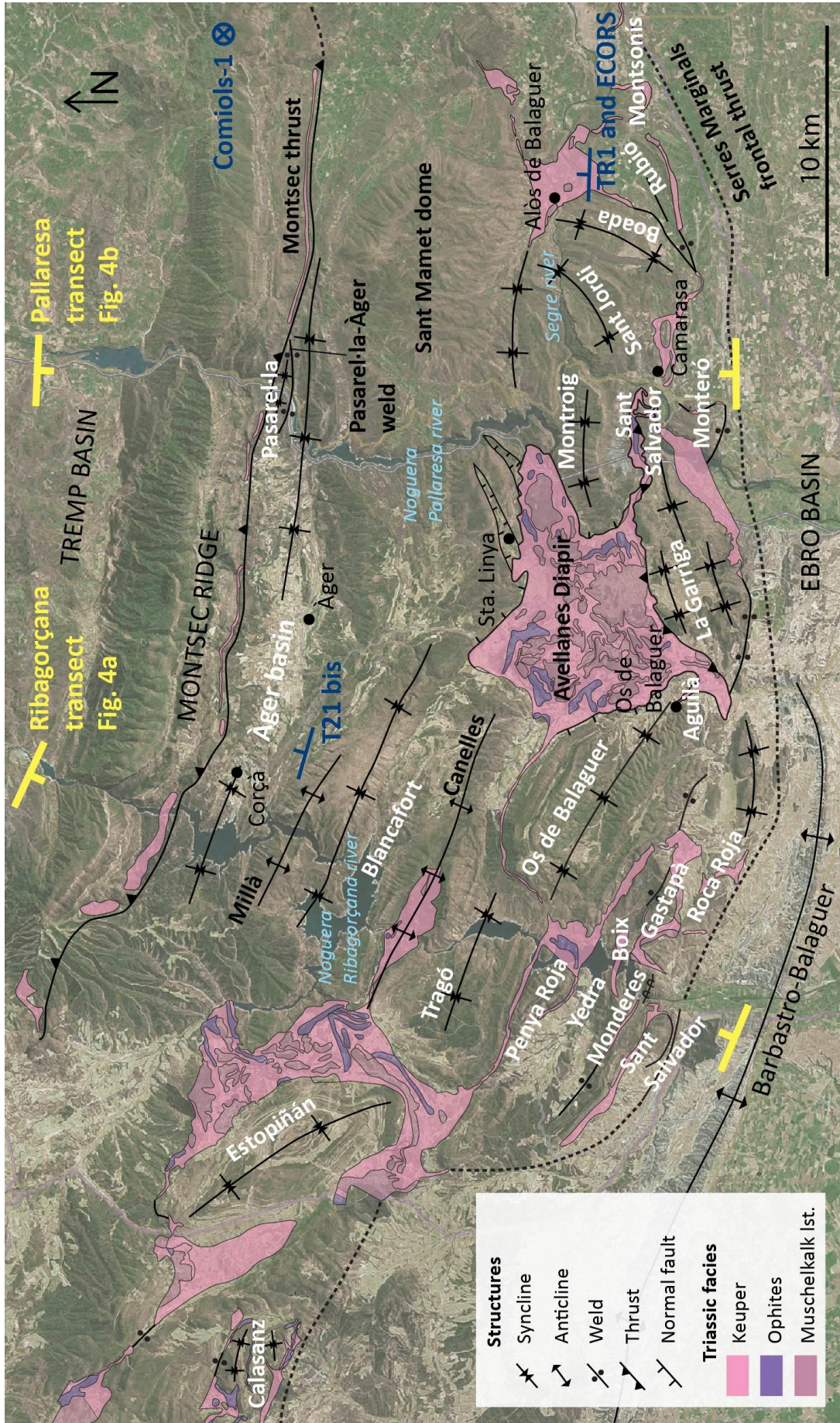


Figure 2.2. Detailed map of the Serres Marginals thrust sheet within the CSPU. Main structures (black) and synclines (white lettering) of the central Southern Pyrenees and location of the structural sections of Fig. 2.4 (yellow). Blue signs indicate seismic profiles analysed in this work.

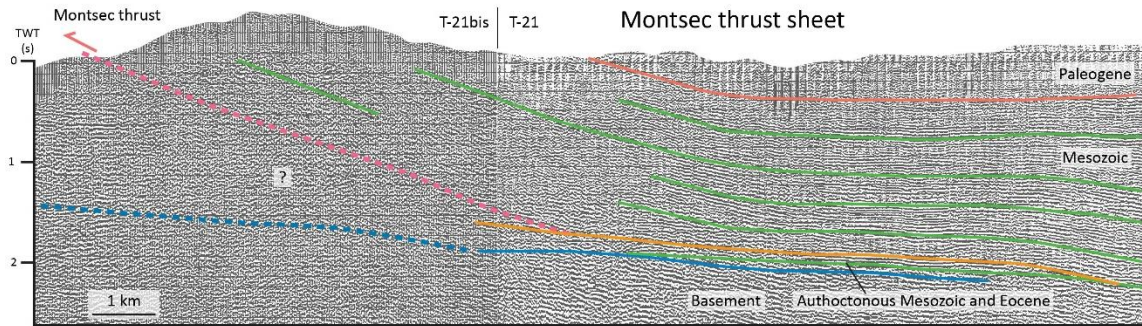


Figure 2.3. Sample seismic profiles across the study area: interpretation of seismic lines T-21 bis and T-21 (see location in figures. 2.1 and 2.2). The footwall is not interpreted due the poor seismic imaging and the discrepancies between the seismic horizons, likely artefacts, and the dips observed at the surface.

The unfolding algorithm does not work for layers with strong overturning or with remarkable thickness changes. In synclines with the latter characteristics, at the end of each stage it has been necessary to manually correct the restoration at the end of each stage, following the guidelines of area conservation except for the Keuper unit.

Since cross-sections in this work are based mostly on field data, it has been necessary to make some initial assumptions concerning the interpretation of bottom depth and thickness variations in synclines across the study area. Two subsurface end-members were considered when building the structural cross-sections:

- a) Where not constrained by surface data, the thickness of a layer is assumed the same at the core of the syncline as it is measured at the flanks
- b) In the case of existing lateral thickness variations and asymmetry in the syncline margins, we consider that it is likely that the same trend of thickening applies towards the centre of the syncline.

We have followed the second approach, where if complete thickness variation along one syncline or minibasin cannot be tracked, the observed variation between different synclines, and the observed pinchouts in the preorogenic succession indicate early folding and localized depocenters.

In the following sections we use salt tectonics terminology to describe the halokinetic features interpreted. Due to the relatively thin stratigraphic succession and the erosion that difficult the preservation of halokinetic sequences (Giles and Rowan, 2012), in most

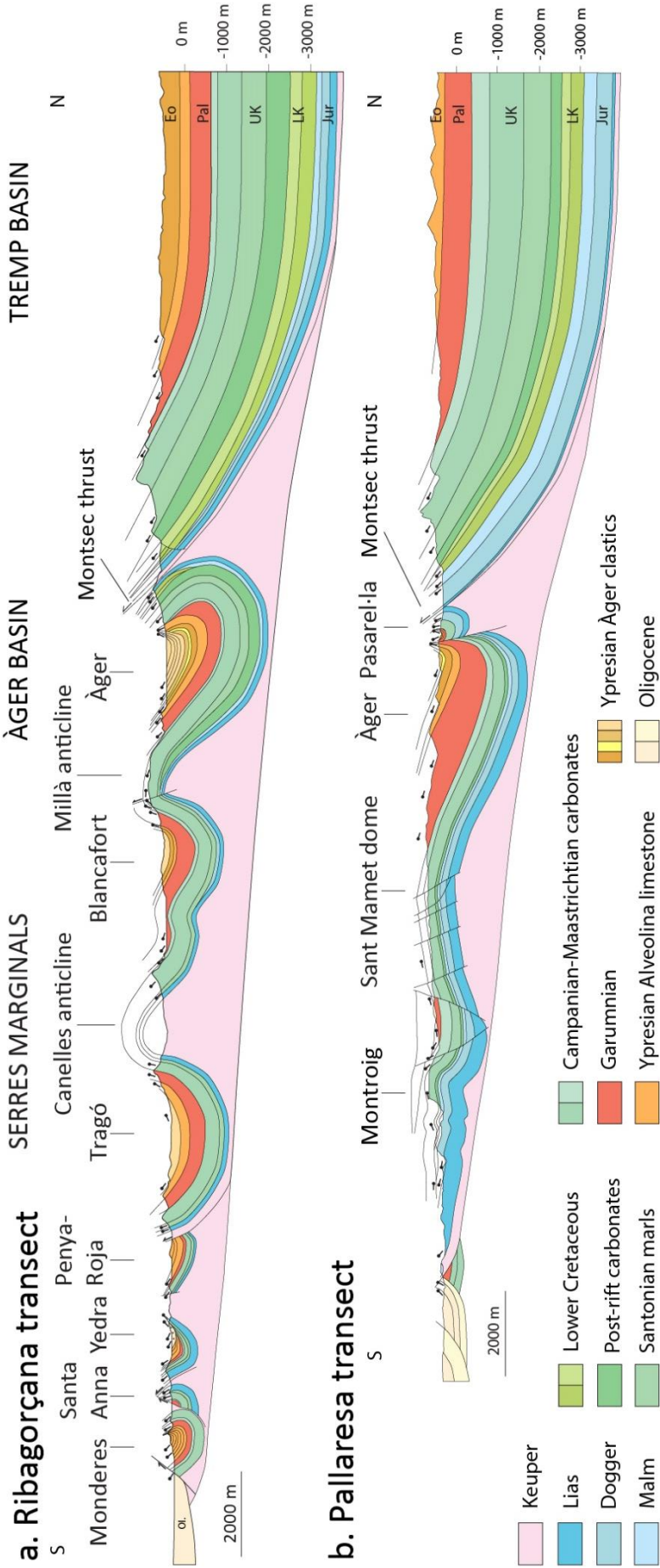


Figure 2.4. Present day cross-sections of the Ribagorçana and Pallaresa transects.

cases we will not use the term minibasins to define the Serres Marginals synclines, although they meet some of the requirements (e.g. completely surrounded by the evaporite unit; Rowan and Vendeville, 2006; Hudec et al., 2009). The term minibasin is only used to describe the Pasarel·la syncline which we interpret that grew on top of an exposed diapir.

2.3. Structure and stratigraphy of Montsec and Serres Marginals

To the south of Bóixols is the Montsec thrust sheet which has a Jurassic to Cretaceous succession that is about 3000m thick (Garrido-Mejías and Ríos, 1972; Vergés and Muñoz, 1990; Teixell and Muñoz, 2000). The bulk of the thrust sheet succession has a broad, flat-bottomed synformal shape (Figures 2.2 and 2.3) known as the Tremp basin, with Cretaceous and Tertiary sediments thinning towards the south. The emplacement of the Montsec thrust, detached in the Keuper, has been attributed to the Ypresian (Williams and Fischer, 1984; Rosell et al., 1985; Muñoz et al., 2018) regarding the progressive unconformity registered in the in the Montsec footwall (Àger syncline). In view of the structural and facies relationships, Teixell and Muñoz, 2000 extended the emplacement of the Montsec thrust sheet up to the late Eocene. The Montsec thrust is fossilized in the Ribagorçana river valley by the Fet conglomerates (Figure 2.1c), derived from erosion of the ridge.

The key elements for the lateral variation of the Montsec structure during the Pyrenean contraction are the pre-orogenic overburden thickness differences between the hanging wall and footwall succession and the availability of salt during the compression. As reflected in Table 2.1 in the supplementary material of this chapter, the thickness of the pre-orogenic (Jurassic to early Santonian) sedimentary succession preserved in the Montsec hanging wall is 1827m in the Comiols well (Lanaja, 1987), 1360m in the Pallaresa transect (1:25000 geological map, 290-1-2 sheet, ICGC, 2003) and 1037m in the Ribagorçana transect (1:25000 geological map, 289-2-2 sheet, ICGC, 2007). The thickest preorogenic sedimentary succession measured in the Serres Marginals thrust sheet is around 850m at Montroig (1:25000 geological map, 328-1-2 sheet, ICGC, 2014) but in all the other measured sections it is thinner than 400m (Table 2.1). Thus, it is safe

to infer a higher overburden vs evaporite thickness ratio in the present day Montsec hanging wall, than in the Àger basin and Serres Marginals.

A decreasing Triassic evaporite thickness towards the west of the Ribagorçana valley has been invoked as the reason for the differential thrust displacement and subsequent change in structural style from the South-Central Pyrenean Unit to the Ainsa oblique fold zone (Muñoz et al., 2013)(Figure 2.1). The origin of the Pedraforca and Segre ramps in the eastern CSPU (Figure 2.1b) has also been explained as a combination of the thinning of the Mesozoic sediments at the basin margin and the eastern pinch out of the Keuper (Vergés, 2003). Therefore, the original salt thickness decreased progressively from the central CSPU (Ribagorçana and Pallaresa transects) towards the margins of the CSPU (Comiols transect in the east). Due to the reduced Keuper thickness in the western part of the CSPU thrust unit, diapirism was not significant until the advanced stages of the compression in the mid Eocene (Teixell and Barnolas, 1995; Muñoz et al., 2013). These late diapiric movements were fed by salt being pumped towards the west, as sedimentary and thrust sheet load increased in the CSPU (Holl and Anastasio, 1993; Santolaria, 2015).

The structural geology of the Serres Marginals thrust sheet further south has been described in several works (Pocoví, 1978a; Martínez-Peña and Pocoví, 1988; Vergés and Muñoz, 1990; Muñoz, 1992; Vergés, 1993; Teixell and Muñoz, 2000). It presents a complex map configuration of several internal km-scale folds, imbricated synclines limited by Keuper-cored ridges and domes, and exposed diapirs (Figures 2.1 and 2.2). The Avellanes diapir, in a central position within the Serres Marginals, separates two different structural domains, hence the need to two regional cross-sections (Figure 2.4). The east domain, represented in the Pallaresa transect is characterized by gentle dipping domes and long-wavelength synclines with different axis orientations, whereas the west domain, represented in the Ribagorçana transect, contains tight anticlines and imbricated synclines with axis oblique to the Pyrenean shortening direction. For the synclines to the north of the Avellanes diapir are wide and have a complete stratigraphic succession, with the absence of the Lutetian *Alveolina* limestone. The synclines to the south of the diapir however, are much smaller and circular and have a very thinned stratigraphic succession, sometimes with the Lutetian *Alveolina* limestone on top of the

Rhaetian limestone. The previous works in Serres Marginals have not addressed the role of halokinesis in this variation of the structural style over such short distance.

Overall, the Serres Marginals show a much thinner and more irregular stratigraphic succession compared to the Bóixols and Montsec units to the north. The Jurassic is unevenly distributed, ranging from a thickness of up to 800m in the Montroig unit (Table 2.1; locations in Figure 2.2), to just a few tens of metres or absent in most other synclines. The Jurassic succession starts with Liassic white gypsum and anhydrite, the Rhaetian-Hettangian Lécera formation (Gómez and Goy, 1998), defined as the *Complexe evaporitique basal* of the Jurassic succession (Fauré, 1984), and represents the last widespread evaporitic episode of the Triassic-Jurassic in Iberia, defining a wide area of sulphate deposition known as the anhydrite zone (Ortí, 1982; Arnal et al., 2002). It reaches up to 400 m in the Montroig unit and only a few tens of metres the other southern synclines. The thick Liassic gypsum series is preserved on top of Rhaetian limestones, in the Montroig thrust, equivalent to the Imón formation in the Ebro basin and the Isábena formation in the Southern Pyrenees (Arnal et al., 2002; Salvany and Bastida, 2004; Ortí et al., 2017). The Jurassic units above are carbonates with a total thickness ranging from 150 to 570m (Table 2.1). The Lower Cretaceous is missing in the entire Serres Marginals except for the northern limb of the Àger syncline (Figures 2.1 and 2.4). The Serres Marginals synclinal cores are filled with synorogenic Palaeocene siliciclastic and lacustrine carbonate deposits (Garumnian facies), the Lower Ypresian Alveolina limestone, and the Upper Ypresian deltaic systems of the Baronia, Àger and Ametlla formations (Grouped in Figure 2.1 as Àger clastics), all of which often display growth strata fans (Garrido-Mejías and Ríos, 1972)(Figure 2.4). However, most synclines are eroded down to the Lower Ypresian Alveolina limestone, and only the Àger Basin and the Blancafort syncline have the complete series preserved (Figure 2.2). The Upper Ypresian fluvial channels of the Corçà formation (Part of Àger clastics in Figure 2.1) are the most recent preserved materials of the Àger basin infill. In the smaller synclines to the south of the Montroig thrust, a unit of Lutetian Alveolina limestone (Caus, 1973) is found unconformably above either the Upper Triassic, a thinned Upper Cretaceous series, or on the Ypresian limestone. The Lutetian Alveolina limestone does not exist to the north of the Avellanes Diapir and Montroig thrust (Teixell et al., 1996). Oligocene

outcrops in the Serres Marginals include locally-sourced conglomerates (Teixell et al., 1996) and interbeds of mudstones, sandstones and occasional gypsum deposits.

Oligocene conglomerates crop out throughout the Serres Marginals and fossilize the Ypresian progressive unconformities of the syncline limbs of e.g. Os de Balaguer, Tragó and Monderes. In the southern smaller synclines of Gastapà and Pere-Pau, the Oligocene sediments are cut by smaller scale thrusts and backthrusts. The bedding of these Oligocene conglomerates is tilted, indicating very localized deformation in the frontal part of the thrust sheet. Its composition is predominantly carbonate clasts of Ypresian Alveolina limestone and Upper Cretaceous and Palaeocene of very local provenance (Teixell et al., 1996). From the late Oligocene onwards, sedimentation moved to the Ebro Basin and the Serres Marginals thrust sheet was kept uplifted.

The thrusting of the Serres Marginals sheet above the Priabonian Barbastro gypsum formation and detrital equivalents of the Ebro Basin (Cámara and Klimowitz, 1985; García-Senz and Zamorano, 1992) transferred the deformation from the CSPU towards the Ebro foreland, where deformation occurred above an intra-basinal Upper Eocene detachment level.

2.4. Field observations in Montsec and Serres Marginals

In the following section we present key geometric and stratigraphic features in the Montsec thrust and the Serres Marginals which we interpret as salt-related and will be later referenced in the discussion on deformation timing.

The Montsec hanging wall

In map view (Figure 2.2), the hanging wall of the Montsec thrust has a very regular geometry from east to west. The stratigraphic record does not show significant lateral variations nor are there any major structures disrupting the north-dipping succession. Small-scale normal faults affect the pre-compressive succession and the Santonian Montsec sandstone alike. Formed during the post-rift stage, they do not propagate into the Upper Santonian Bagasses marls (Figure 2.1c) (1:25000 geological map, 289-2-2 sheet, ICGC, 2007). However, in the Ribagorçana and Pallaresa valleys, that provide good profiles of the Montsec hanging wall, angular unconformities can be observed between

the Jurassic and Lower Cretaceous carbonates and between the Lower Cretaceous and the Cenomanian Santa Fe limestone formation, highly erosive over the underlying units (Figure 2.5a), which suggests early halokinetic movements. As represented in the cross-sections of Figure 2.4, the pre-orogenic stratigraphy thins towards the frontal part of the Montsec hanging wall.

Montsec footwall, the Àger syncline and Pasarel·la minibasin

The Àger basin is an E-W elongated syncline situated at the Montsec thrust footwall (Figures 2.1 and 2.2). Its southern limb has a gentle northward dip and the northern limb of the syncline, on the other hand, is vertical to overturned and features important omissions in the series (Figures 2.4 and 2.5).

In the Ribagorçana transect, the Garumnian has been eroded out and the Campanian limestone is unconformably covered by the Ypresian Alveolina limestone, all overturned

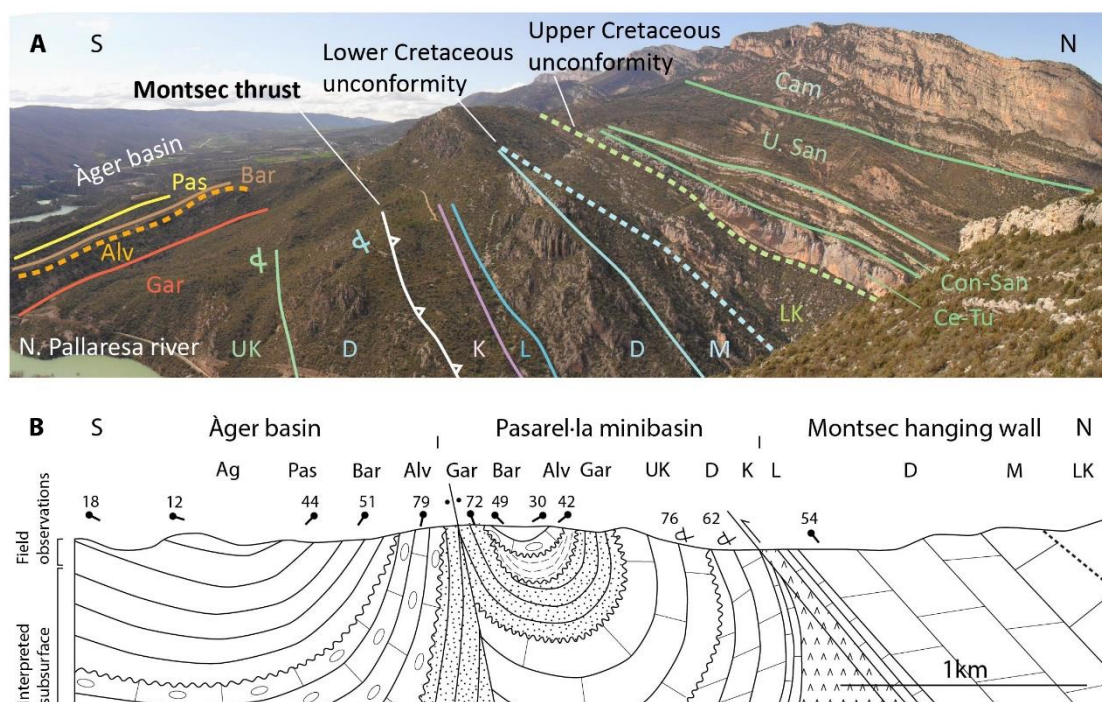


Figure 2.5. (a) View to the west of the Montsec hanging wall and the Pasarel·la minibasin in the Noguera Pallaresa valley. Note stacked unconformities in the Jurassic and Cretaceous of the Montsec thrust sheet (dashed) and the overturned but structurally continuous succession of the northern limb of the Pasarel·la synformal minibasin. K, Triassic Keuper; L, Lias, D, Dogger; LK, Lower Cretaceous; Ce-Te, Cenomanian-Turonian; Con-San, Coniacian-Santonian; U San, Upper Santonian; Cam, Campanian; UK, Undifferentiated Upper Cretaceous; Gar, Garumnian; Alv, Ypresian Alveolina limestone; Bar, Baronia sandstone fm., Pas, Pasarel·la marl fm., Ag, Àger sandstone fm. Image taken from coordinates 324773, 4653805, UTM 31. (b) Field sketch profile from the Montsec thrust to the Àger basin following the Noguera Pallaresa river. The boundary between the growth synformal structures of Pasarel·la and Àger basins is interpreted as a squeezed diapir, and so is the Montsec thrust, where welding has not been complete.

(Figure 2.6a). The Jurassic and pre-Santonian carbonates are overturned from 33 to 80 degrees. The uppermost Cretaceous is involved in a basin-wide progressive unconformity until the upper Ypresian (Figure 2.6).

In the Pallaresa transect, the northern limb of the Àger syncline is steep and presents a significant thinning of the Palaeocene-Ypresian stratigraphy, punctuated by an unconformity at the level of the Ypresian Alveolina limestone and Baronia deltaic formation (Figure 2.4b and 2.5). In sharp vertical contact, the small Pasarel·la syncline contains a very thin succession of Jurassic-Cretaceous, Garumnian and Ypresian (Alveolina limestone and Baronia formations). The pre-Campanian Cretaceous is missing and the Garumnian to Ypresian units define a fan of growth strata (Figure 2.5). The Jurassic and Upper Cretaceous strata show thicknesses comparable to those in the

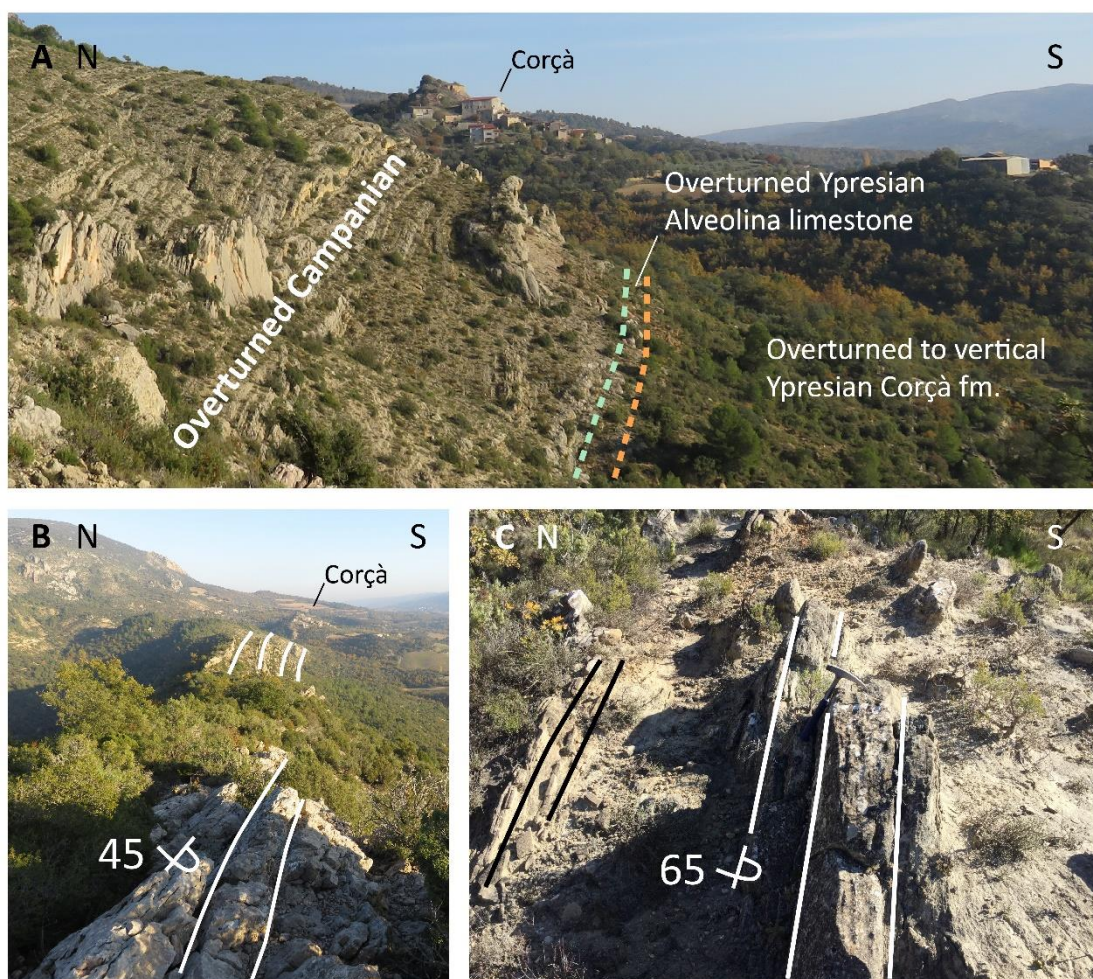


Figure 2.6. The overturned northern limb of the Àger basin in the Noguera Ribagorçana valley (a) General view looking east from UTM 31 307912 4655930 (b) Close-up of overturned Campanian limestone beds UTM 307149 4656367. (c) Close-up of overturned fluvial sandstone beds of the Ypresian Corça fm. at UTM 307884 4655841.

Ribagorçana transect. In the Pasarel·la syncline they are strongly overturned, and are cut by a fault-looking contact to the south. This structure was previously mapped as an imbricated thrust fan of overturned layers in the front of the Montsec thrust (ICGC 1:25000 map) but we reinterpret this contact as a weld.

The Sant Mamet dome

In the eastern Serres Marginals, the southern limb of the Àger basin syncline corresponds to the northern limb of the Sant Mamet dome (Figure 2.2), a gentle dipping arch with a four-way closure. The dome presents a dense network of fractures at its roof and flanks, with normal and strike-slip displacements that cut across the entire stratigraphic succession and are probably related to the halokinetic uplift of the dome. The Garumnian thickness decreases towards the crest of the dome, reflecting a Maastrichtian age of initial folding. In the northern limb of the dome, olistoliths of Alveolina limestone formation are interbedded within the Baronia deltaic sandstones (Gelabert, 1986). Sole marks indicate S-N paleocurrents, recording continued uplift during the Ypresian.

The oblique synclines of Sant Jordi, Boada, Rubió and Montsonís

The SE Serres Marginals is composed of four synclines with N-S and NE-SW axes, deviated from the E-W traces of most other folds to the west (Pocoví, 1978a) (Figure 2.2). In the easternmost Montsonís syncline, the stratigraphic succession starts with the Upper Cretaceous limestones directly on the Keuper, followed by a very thin unit of Garumnian red mudstone and the top Garumnian limestone. The core of the syncline contains the Alveolina limestone in angular unconformity. The eastern flank is overturned 60°, while the western shows a gentle progressive unconformity from 60 to 40 degrees. The Rubió syncline (Figure 2.2) has a stratigraphic succession similar in composition and thickness to the above described but the core of the syncline is filled by Oligocene evaporites and conglomerates in angular unconformity with the Cretaceous to Eocene succession (Soto et al., 2015). The southern flank is vertical overturned while the eastern flank is overridden by the Boada syncline. The Boada and Sant Jordi synclines (Figure 2.2), have a thick succession of Liassic carbonates and gypsum at the base, more similar to the succession in the Montroig area than to the two

eastern synclines, where Jurassic strata are missing. The flanks of the Boada and Sant Jordi synclines also show thickness variations and progressive unconformities, attributed to early folding during the Late Cretaceous to Ypresian (Soto et al., 2015). Vertical axis rotation as a mechanism to explain fold obliquity in these oblique synclines could not be unequivocally proven by palaeomagnetism (Dinarès-Turell, 1994).

Montroig unit and adjacent synclines of Monteró and Sant Salvador

Towards the west, the succession of the Serres Marginals becomes tabular in the Montroig area (Figure 2.2). The stratigraphic succession of the Montroig unit, similarly than that of the Sant Jordi syncline, contains the undeformed basal unit of Liassic gypsum, 290 m thick, on top of the Rhaetian limestones which overlie the Keuper which thins towards the west (Pocoví, 1978a; Salvany and Bastida, 2004).

To the south of the Montroig unit, the small Sant Salvador slices show vertical to overturned imbrications of a very thinned stratigraphic succession of Liassic and Upper Cretaceous limestones, Garumnian mudstones, and Ypresian and Lutetian Alveolina limestone surrounded by Keuper and Liassic gypsum outcrops (Figure 2.7a). Folds show strongly plunging axes and syncline limbs have internal deformation. The Monteró syncline to the south presents the same thin stratigraphy as the Sant Salvador slices, with thick Lutetian Alveolina limestone at the top. The syncline axis is N-S and the

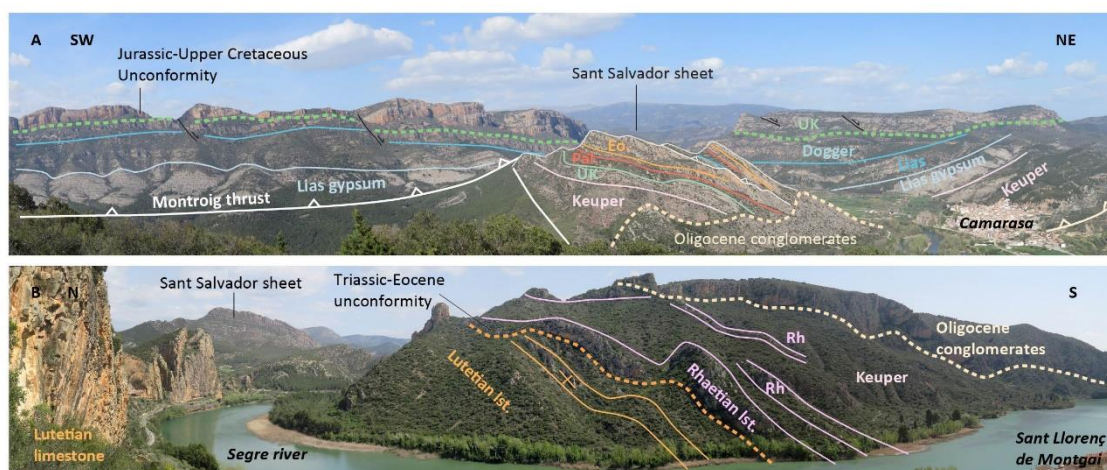


Figure 2.7. (a) View of the Montroig and Sant Salvador units of the Serres Marginals (see location of units in Fig. 2.2), photo looking NW from UTM coordinates 322460 4637940. Note the low-angle unconformity between the Jurassic and the Upper Cretaceous, and the strong unconformity of the Oligocene conglomerates on folded Mesozoic to Eocene beds. The conglomerates themselves are folded and cut by late thrusting. (b) View of the southeastern end of the La Garriga unit (Fig. 2.2) where the Lutetian Alveolina limestone (vertical to overturned) overlies the Rhaetian limestone and Keuper facies, looking west from UTM 320882, 4637403.

eastern limb is strongly overturned. Oligocene conglomerates tilted to the north truncate the western limb of the syncline.

The Avellanes diapir

The central part of the Serres Marginals thrust sheet contains the Avellanes diapir (Pocoví, 1978b) (Figure 2.2), a large equant planform outcrop of Keuper shales and evaporites that incorporates disrupted bodies of Muschelkalk carbonates and ophite. The E, W and S limits of the diapir appear as steep fault contacts where the Keuper abutts against the adjacent units, including the Oligocene sediments covering the Tragó and Os de Balaguer syncline limbs (Pocoví, 1978b; Teixell and Barnolas, 1996). The southern limb of the diapir thrusts over Early Oligocene conglomerates of the La Garriga Unit (Figure 2.2), which we describe below, progressively closing to the west and joining the Montroig thrust to the east. The Avellanes diapir is also in thrust contact with the Os de Balaguer syncline to the west. Only the NW limit of the diapir, is a concordant contact with the Jurassic and Cretaceous succession, while in the rest of the northern boundary the Keuper is in high-angle fault contact with the Upper Cretaceous. Rocks to the north (Àger basin) and east (Montroig unit) of the diapir are internally deformed by sets of normal faults affecting from the Upper Cretaceous to the Oligocene, similar to those described bounding the Clamosa diapir in the western CSPU (Teixell and Barnolas, 1995).

In the southern part of the Avellanes diapir, on top of the Keuper there is the small Aguilà syncline (Figure 2.2), with a N-S oriented axis. It has as a very thin stratigraphic succession, consisting only of Liassic and Upper Cretaceous limestones and no Garumnian nor Eocene. The north-eastern flank of the Aguilà syncline is almost vertical and has a progressive unconformity affecting the Upper Cretaceous carbonates. The reduced sedimentary succession in the Aguilà syncline also supports the idea that the Avellanes diapir was an inflated area since the Maastrichtian.

The Garriga unit

South of the Avellanes diapir, the NE-SW oriented La Garriga thrust system (Figure 2.2) comprises a fan of imbricated slices. The stratigraphic succession is similar to the adjacent Monteró and Sant Salvador synclines (Figure 2.7a), showing a thinned Upper

Cretaceous and Ypresian succession but with a thick unit of Lutetian Alveolina limestone on top. In the southern slices the Lutetian limestone is directly on top of Keuper and Rhaetian carbonates by a low-angle unconformity (Figure 2.7b). Mildly deformed Oligocene conglomerates partially cover the unit, fossilizing the imbricate thrusts. It is worth noting that locally the Oligocene conglomerates lie directly on top of the Keuper, a common observation in the southern synclines.

The Os de Balaguer and Tragó synclines

To the west of the Avellanes diapir, the Os de Balaguer and Tragó synclines (Figure 2.2) are large E-W oriented folds, with a relatively thick succession of Jurassic and Upper Cretaceous carbonates, Garumnian carbonates and clastics and Ypresian Alveolina limestone. The Os de Balaguer northern limb unfolds from 49 degrees of overturning in the Lower Jurassic limestones at the base, adjacent to the Avellanes diapir, to very gently dipping Ypresian Alveolina limestones at the core of the syncline (Figure 2.8a). In the southern limb the stratigraphic succession is thicker and does not show a fan of growth strata. The core of the Tragó syncline is filled by Ypresian fluvial beds in angular unconformity over the underlying Alveolina limestone. Upper Oligocene fine-grained sandstones, mudstones and evaporites outcrop in the southern limb of the syncline and are overthrust by the Os de Balaguer syncline.

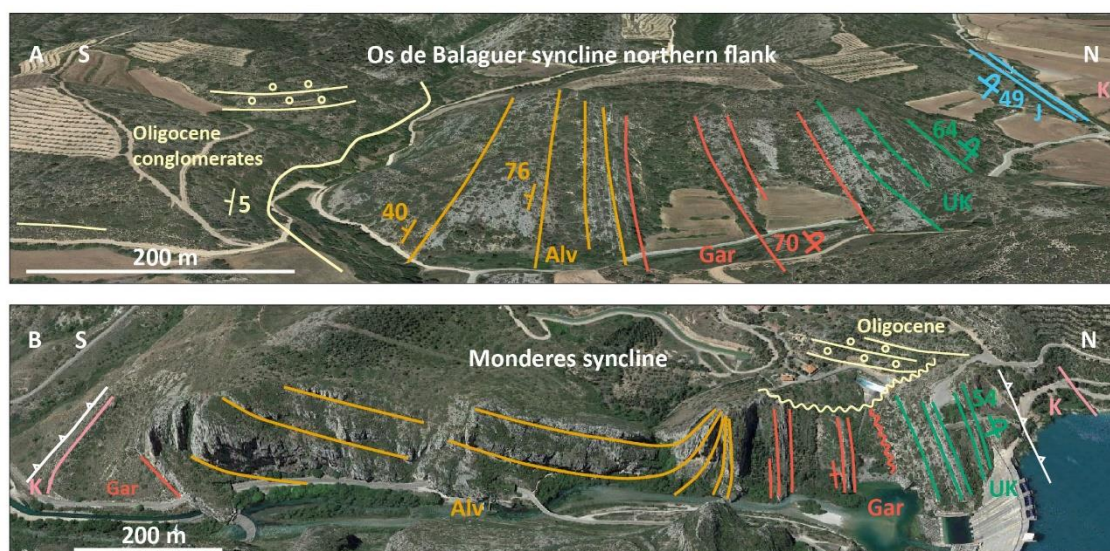


Figure 2.8. Examples of fans of growth strata at the flanks of the Serres Marginals synclines. (a) Northern flank of the Os de Balaguer syncline, photo coordinates UTM 310363 4640384. (b) Northern limb of the Monderes syncline (see location in Fig 2), UTM 299128 4639091. Both images are taken from Google Earth. K, Keuper; J, Jurassic; UK, Upper Cretaceous; Gar, Garumnian; Alv, Ypresian Alveolina limestone.

The salt-cored anticlines and imbricated synclines of the Ribagorçana valley

From north to south, the structure of the western Serres Marginals in the Ribagorçana valley comprises the salt-cored km-scale anticlines of Millà and Canelles, linked by the Bancafort and Tragó synclines (Figures 2.2 and 2.4a), and then a system of smaller-scale imbricates. The latter often show a synformal internal structure, displaying growth strata fans from the Upper Cretaceous limestones onwards. The most evident of these is in the northern flank of the Monderes syncline (Meigs, 1997), involving the Upper Cretaceous to Eocene succession, from a 60 degrees overturn in the Campanian limestones, to 40 degrees of normal polarity in the Ypresian *Alveolina* limestone (Figure 2.8b). These long-lived unconformities are present in other synclines with strong overturning such as Os de Balaguer, but also occur in the less steep flanks of Os de Balaguer, Bancafort, Monteró or Boada synclines.

The salt-cored anticlines of the north show an E-W-oriented axis and relatively high cylindricity, contrasting with the circular structures of the Sant Mamet dome and Avellanes diapir, and the adjacent oblique synclines described above. The northern folds are not affected by thrusting (Figure 2.4a), whereas to the south, where the stratigraphic succession is thinner, the Keuper rocks between the synclines served as preferential site for late thrusting, as thrusts frequently cut Oligocene conglomerates, unconformable over folded Cretaceous-Eocene beds (Figure 2.8a). This is the case of the Yedra and Boix units in the southern part of the Ribagorçana transect. In places where two oblique

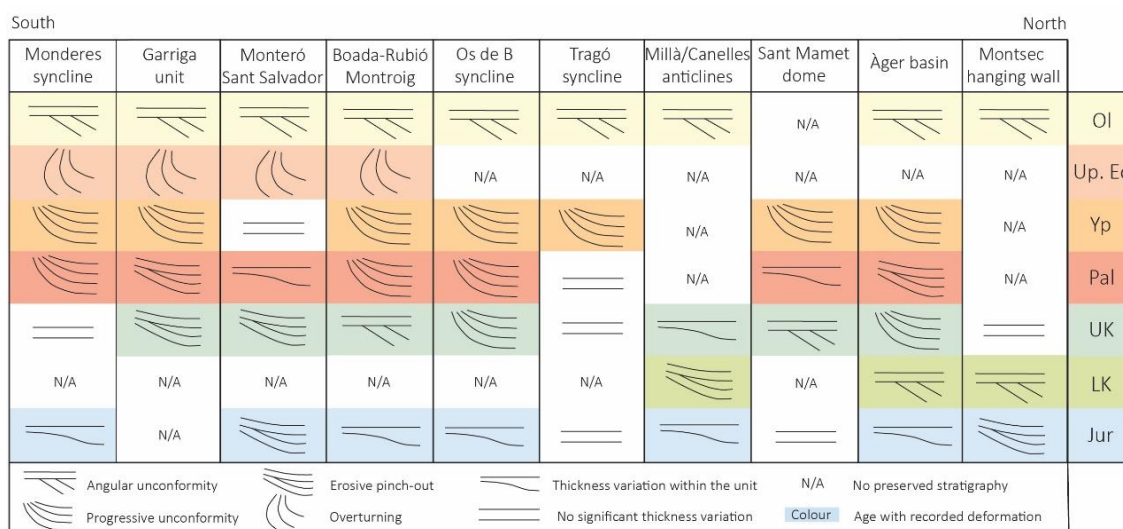


Figure 2.9. Summary of field observations on tectono-sedimentary relationships in the Serres Marginals and Montsec main structures.

Keuper ridges intersect, as it happens east of the *Penya Roja* syncline and to the north of *Boada* syncline, there are small-scale diapiric extrusions with deformed *Muschelkalk* bodies within (Figure 2.2).

The field observations reported above have been summarized in figure 2.9, where structures and stratigraphic discontinuities in each of the studied anticlines/faulted ridges and intervening synclines from north to south have been classified by time of occurrence.

2.5. Salt Tectonics interpretation

Acknowledging thickness variations among the Jurassic in *Serres Marginals* synclines leads to an interpretation of an early evolution of the fold structures in the absence of compressional stress, just by load-induced salt withdrawal and diapirism (e.g. Hudec et al., 2009; Peel, 2014). In experimental fold-and-thrust belts detached above a viscous décollement, deformation quickly propagates and reaches the frontal pinch-out of the salt, although initial shortening accommodates in the thrust sheets at the back (Costa and Vendeville, 2002; Li and Mitra, 2017). Hence, if the Central South Pyrenean fold and thrust belt is understood as detached above a continuous viscous décollement (Soto et al., 2002; Storti et al., 2007; Santolaria et al., 2017), it is likely that compressional stresses reached the *Montsec* and *Serres Marginals* a short time after the onset of the Pyrenean compression in the Late Santonian.

From the previous observations we identify a pre-orogenic and a synorogenic phase of halokinesis in the *Montsec* and *Serres marginals* domain. During Late Jurassic and Early Cretaceous rifting stage, sedimentation rate was very reduced in *Serres Marginals*, where evidence of diachronous subsidence can be found in the thickness differences of the Jurassic succession. Evidence for significant extensional faulting is lacking, so it is unlikely that regional extension propagated so far to the south. However, it is possible that salt migration was enhanced by regional rifting from the Late Jurassic onwards in the *Tremp* and *Àger* basins, contributing to the development of the a salt pillow in the *Montsec* area, from now on referred to as *Montsec pillow*. In the *Tremp* basin, the more uniform and thicker carbonate sedimentation was not accompanied by the development of early salt structures in the area (Figure 2.3). We interpret that during

the rifting stage the Montsec structure developed as a salt pillow that separated an area of high subsidence, the Tremp basin, from an area that remained relatively uplifted, the Àger basin. The Cretaceous unconformities in the Montsec hanging wall and footwall reflect stratigraphic thinning towards the salt pillow.

Sedimentology and clastic provenance data show that the Montsec was a growing structure during the Garumnian sedimentation in the late Maastrichtian and Palaeocene (Cuevas et al., 1989; Deramond et al., 1993; Gómez-Gras et al., 2016).

We interpret that in the Ribagorçana transect, the Montsec grew as a salt-cored anticline as a combination of compressional buckling and halokinetic growth, fed by the salt evacuated by sedimentary loading from the Tremp and Àger basins. The progressive deepening of the Àger syncline is registered in the long-lived unconformity of its northern limb. With the progressive uplifting the Montsec pillow evolved into a salt anticline that unroofed progressively, which favoured the partial welding and thrusting in the later stages of the orogeny.

In the Pallaresa transect, the intervening Pasarel·la syncline, with its condensed succession, is here interpreted as a minibasin on top of the exposed Montsec salt pillow, unroofed from earlier on and later welded to the Montsec thrust and Àger syncline. An alternative interpretation is to consider the Pasarel·la syncline a deformed piece of the Montsec anticline crest. However, due to the fairly continuous stratigraphic record in the syncline, the small wavelength of the fold and the absence of faulting we favour the first interpretation.

Previous to the arrival of the Pyrenean deformation front to Serres Marginals, unconformities within the synclines were diachronous through the different synclines (Figure 2.9). The onset of the Pyrenean deformation at the Palaeocene is evidenced by the widespread growth strata and thickness changes of the Garumnian facies observed contemporary in most synclines (Figure 2.9). We interpret that structures as the Millà and Canelles salt-cored anticlines in the Ribagorçana transect grew during the Pyrenean orogeny as a combination of compressional buckling and halokinesis. The Garumnian and Ypresian clastic loading in the northern area of the Serres Marginals -Àger basin, Blancafort and Tragó synclines- enhanced salt migration towards the anticline cores. The

Sant Mamet dome and the Avellanes diapir also grew fed by the downbuilding of the Àger basin and adjacent synclines but maintained their equant planform. The unroofing of the Avellanes diapir during the late stages of the compression caused the subsidence of the cover units around to accommodate diapir rising. The lack of clastic sedimentation in the southern area of Serres Marginals during the Ypresian kept the area relatively uplifted and the synclines deformed mostly by compressional buckling.

2.6. Discussion

Regarding the previous observations and integrating them with compressional salt tectonics concepts from other natural examples and physical and numerical models, we propose a new interpretation for the structural evolution of the Montsec ridge, Àger Basin and Serres Marginals area, illustrated in figures 2.10 and 2.11. This has strong regional implications, but also raises general questions on foreland basin evolution above thick evaporite detachments that we will address in this discussion.

2.6.1. Reinterpretation of the Montsec footwall structure

Classically, the Àger basin has been described as comprising the sedimentary rocks from the Garumnian facies upwards, which fill the syncline at the Montsec thrust footwall. The angular and progressive unconformities affecting the Ypresian deposits of the Àger basin (Garrido-Mejías, 1973; Martínez-Peña and Pocoví, 1988; Zamorano, 1993) were explained as a result of the growth of footwall syncline during the main Montsec thrust displacement (Vergés and Muñoz, 1990; Muñoz, 1992; Vergés, 1993). The overturned succession of Jurassic to Upper Cretaceous strata in the northern limb of the syncline was interpreted as part of the Montsec hanging wall anticline (Vergés and Muñoz, 1990; García-Senz and Zamorano, 1992; Teixell and Muñoz, 2000). In the Ribagorçana transect the thrust plane has been placed across the contact between the overturned Upper Cretaceous and the Eocene clastics near the Corçà locality (Teixell and Muñoz, 2000). Our observations lead us to challenge these interpretations, with a new framework for the understanding of the significance of the Àger basin unconformities and structural evolution.

We propose that in the Ribagorçana transect (Figure 2.4a), the fan of growth strata of the northern limb of the Àger syncline comprises the sediments from the Jurassic to the Ypresian, punctuated by unconformities. We reinterpret the steep to overturned stratigraphic succession of the Montsec-Ager basin as unfaulted from the Mesozoic to the Eocene. The succession is continuous in upright position except for gaps of the Garumnian and the Lower Ypresian deltaic sediments that crop out in the southern limb of the syncline but are lost by erosion in the exposed northern limb (Figure 2.4a). The dips of the growth strata range from 38 to 70 degrees overturned measured in the Lower Cretaceous, to the 60 to 10 degrees right way-up dips measured in the Ypresian Corçà fluvial beds in the core of the syncline (Figure 2.6). Regarding the continuous nature of this growth strata fan, our new field observations of the profile provided by the Ribagorçana river incision indicate that if a thrust were to be placed between the Upper Cretaceous and the Ypresian *Alveolina* limestone, it would be parallel to the steep overturned stratigraphy, which is a very unlikely geometry. Instead, we now propose an interpretation where the main Montsec thrust is localized further north in the Keuper core of the Montsec anticline, where previous works represented only a minor axial-plane thrust.

While the hanging wall flat structure is very regular along the 35 km-long in the Montsec ridge, there are differences in the thrust footwall. The surface geology at the Pallaresa transect (Figure 2.4b) differs from the Ribagorçana structure described above. Between the main Àger syncline and the Montsec there is the minor, fault bounded synformal unit that we refer to as the Pasarel·la syncline. Similarly to the Ribagorçana transect, the overturned Upper Cretaceous and Jurassic strata of northern limb of the Pasarel·la syncline have been interpreted as part of the hanging wall anticline of the Montsec thrust sheet (Berástegui et al., 1993; Zamorano, 1993). Again, this solution implies a thrust fault parallel to overturned stratigraphy, with no alteration of the stratigraphic order (1:25000 geological map, 290-2-2 sheet, ICGC, 2003), or a blind thrust under the Ypresian sediments of the Àger basin (Zamorano, 1993). Although the latter interpretation cannot be discarded, we advocate for a stratigraphic continuity of the Jurassic to Ypresian succession of the Pasarel·la syncline and interpret that the main Montsec thrust is between this succession and the right-way-up succession of the

Montsec ridge, which shows a distinct and much thicker stratigraphy (Figures 2.4b and 2.5).

Our interpretation has strong regional implications, as it decreases the amount of shortening in the Montsec thrust, which originates from the closure of the diapir and the minor displacement across the thrust weld. The two combined produce a total shortening in the order of 6 to 8 km. Although the presence of a blind shortcut thrust below the Ypresian sediments of the Àger basin cannot be discarded, our interpretation implies substantially less shortening than the 11 km estimated for the Ribagorçana transect by Teixell and Muñoz (2000), which interpreted a continuous footwall ramp under the Montsec hanging wall. Acknowledging pre-compressional salt tectonics role in the evolution of the Serres Marginals synclines also reduces the amount of internal shortening within the thrust sheet, as the early stage of folding is not produced by buckling but by differential loading in the Jurassic-Upper Cretaceous stage.

2.6.2. Rationale and uncertainties in cross-section construction

The limited quality of the available seismic images and the large distance to the nearest wells challenge the understanding of the subsurface geometry, especially in an area where surface geology varies over a short distance. We do not disregard the seismic interpretation of the deep structure of the Montsec hanging wall and Tremp basin (Teixell and Muñoz, 2000; Muñoz et al., 2018), since reflectors are continuous and unambiguous in the hanging wall (Figure 2.3). The footwall imaging, however, is poor and stratal geometries cannot be identified with confidence, as apparent reflectors contradict surface observations (Figure 2.3). The nearest well penetrating the Montsec footwall is Comiols-1, located 15 km to the east of the Pallaresa transect, and 31 km from the Ribagorçana (Figure 2.2).

The Comiols-1 well drilled a right way-up footwall succession 1200m thick, including 600m of Upper Cretaceous. The structure that can thus be deduced for the well area differs significantly from that inferred for the Pallaresa and Ribagorçana transects in this work where the entire footwall succession, starting from the Jurassic, is thinned and upturned in the northern limb of the Àger syncline. At the surface, near the well longitude, the Àger basin shows no longer a synformal structure, and the immediate

footwall of the Montsec thrust is constituted by Eocene strata gently dipping to the north between 10 and 30 degrees (ICGC, 2007b).

The progradation of the Garumnian and Eocene clastic systems of the Àger basin and Serres Marginals towards the west and the subsequent salt withdrawal, progressively depleted the salt layer in the eastern Serres Marginals. This favoured the development of a hanging wall flat and footwall ramp in the Comiols transect, as opposed to the transects to the west, where the availability of salt in the source layer fed the growth of the Montsec as a salt structure until the advanced stages of the compression. The contrasting structural style here described were already reported as end-member solutions for the Montsec deep thrust structure by Garrido-Megías and Ríos (1972); we propose that both are valid, but for different areas.

2.6.3. Salt tectonics and evolution of the central southern Pyrenees from extension to contraction

The good record of the pre- and synorogenic stratigraphy in the Montsec and Serres Marginals thrust sheets enables the restoration of the cross-sections from the present day to the Jurassic. The aim of restorations in figures 2.10 and 2.11 is to provide elements for discussion on the evolution of this thrust belt and proximal foreland basin with a proposed strong influence of halokinesis. The stages restored depend on the constraints provided by stratigraphic formation tops preserved for specific intervals. For this reason, the Ribagorçana and Pallaresa restored stages do not always represent the same time interval. Lower Cretaceous rocks are missing in the Serres Marginals, so this epoch will not be shown in restoration.

The basement structures that conditioned the Keuper deposition and its original sedimentary thickness distribution during the Triassic rifting are no longer in place since the CSPU thrust sheets have been transported to the south. Following the idea discussed in Espurt et al. (2019b) for the Provence fold-and-thrust belt in France, Triassic rifting could have generated a network of small-scale basement horsts and grabens that conditioned evaporite deposition in the Triassic, resulting in initial salt thickness variations within the Serres Marginals domain. The basement below present day Tremp basin, if it was rheologically stronger, was not affected by this close faulting and thus

Ribagorçana transect

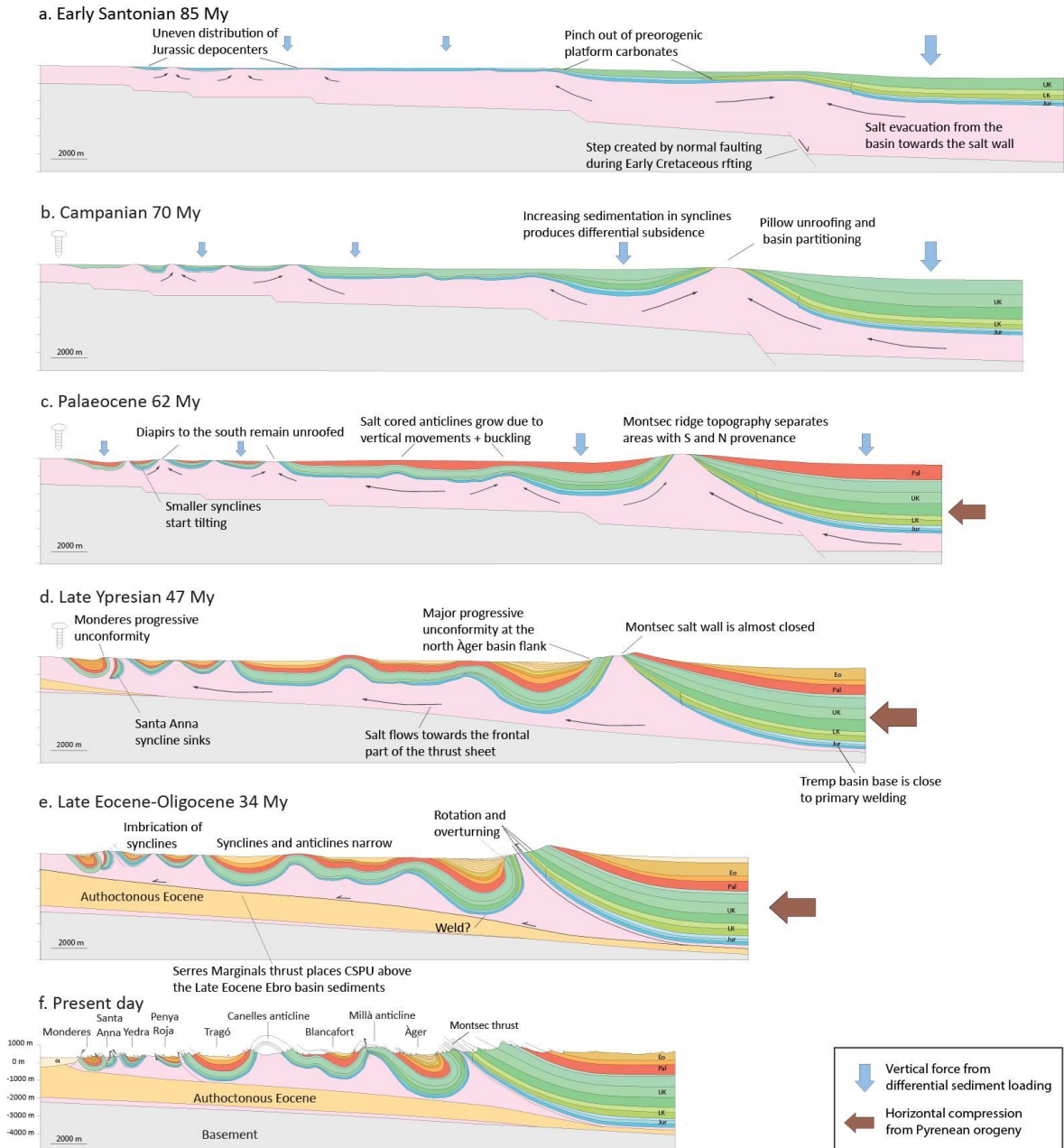


Figure 2.10. Structural evolution of the Ribagorçana transect. A3 applied version in the appendix of the thesis.

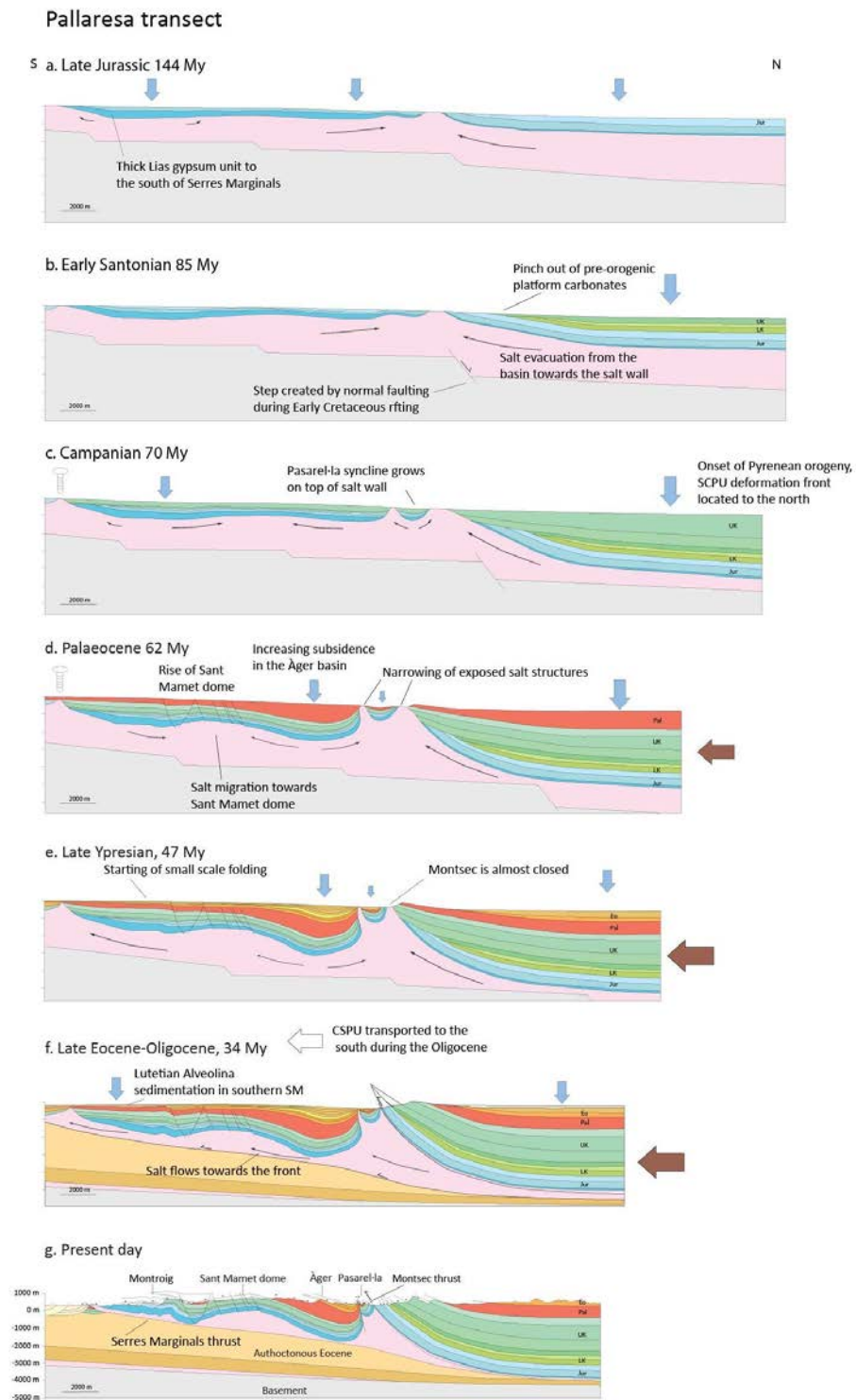


Figure 2.11. Structural evolution of the Pallaresa transect. A3 applied version in the appendix of the thesis.

maintained a uniform thickness salt layer throughout. Another option is to understand the differences between Montsec hanging wall and Serres Marginals entirely as a consequence of the differences in the salt to overburden ratio during the Jurassic and Lower Cretaceous.

Jurassic

In the Serres Marginals the thick lower Liassic gypsum succession to the south of the Montroig thrust is irregularly distributed and thicker in the Pallaresa (Figure 2.11a) than in the Ribagorçana transect (Figure 2.10a). The Upper Liassic and Dogger limestones and dolomites also show important thickness variations between the different synclines, indicating the existence of differentiated depocentres and structural highs from early on, particularly in the Ribagorçana transect.

Cretaceous rifting and Late Cretaceous post-rift

From the Late Jurassic to the early Santonian, the Serres Marginals and Àger basin were located in the southern shoulder of the Pyrenean rift, at the uplifted footwall of the ancient basement Rialp normal fault (Teixell et al., 2018). Thus, the sedimentary overburden in the Serres Marginals and Àger Basin was shallow and thin compared to the thicker syn and post-rift sedimentary accumulations to the north in the CSPU, closer to the main rift axis in the northern Pyrenees. Before the Santonian time, the southern extent of the carbonate platform sedimentation in the south Pyrenean realm was located to the south of the present day Montsec thrust (Simó, 1993).

Since there is no preserved record of Lower Cretaceous or pre-compressive Upper Cretaceous in most of the Serres Marginals area, we have used the top Jurassic to restore the pre-compressional stage in this area. The restoration of this stage in the Montsec hanging wall also includes the Cenomanian-Turonian platform carbonates of the Santa Fe formation and the Coniacian to Santonian calcarenites (Figure 2.1c).

During the post-rift stage, subsidence related to salt evacuation was slow in the Tremp basin and shallow carbonate deposits accumulated. Loading in the Tremp basin pushed the evaporites towards the south, where the Serres Marginals area had a thinner stratigraphic succession and maintained its buoyancy. The lack of sedimentation in the

Serres Marginals domain kept a lower overburden vs evaporite thickness ratio throughout the pre-contractonal stage.

In the pre-compressive stages of evolution there is already important differences between the two transects: while in the Ribagorçana transect the Montsec initially grew as a salt pillow with Jurassic and Lower Cretaceous roof (Figure 2.10a), the Pallaresa transect pillow was partially unroofed earlier during the rifting stage, and the thin Jurassic roof was incorporated into what later became the Pasarel·la minibasin (Figure 2.10b).

Late Santonian to mid Maastrichtian

During the early Pyrenean convergence stages, the deformation front of the sedimentary cover in the Southern Pyrenees was located in the Organyà Basin (Figure 2.1), reactivating Early Cretaceous normal faults such as the Bóixols thrust (Berástegui et al., 1990). In the Ribagorçana transect of the Serres Marginals, the Montsec salt pillow continued growing, fed by the salt evacuated below the Tremp and Àger basins under the weight of the post-rift platform carbonates. The uplifting progressively unroofed the thinner top of the pillow and the southern part of the carbonate platforms was incorporated into the northern limb of the active Àger syncline (Figure 2.10b). In the Pallaresa transect the carbonate sedimentation on top of the unroofed pillow started the subsidence in the Pallaresa minibasin and evacuated salt towards the Montsec diapir to the north and the Pasarel·la-Àger diapir to the south (Figure 2.11c).

Throughout the Serres Marginals, the sedimentation of the Upper Santonian clastics and the Campanian-Maastrichtian carbonates kept the differential subsidence in synclinal depocentres. Associated salt withdrawal initiated the growth of the Canelles and Millà anticlines in the Ribagorçana transect (Figure 2.10b), the Avellanes and the Sant Mamet domes in the Pallaresa transect (Figure 2.11c).

Early Palaeocene

During the Palaeocene, the deformation front reached the Montsec and Serres Marginals area. The Garumnian clastic systems present different provenance signals at each side of the Montsec salt ridge: the Àger basin systems came from the Ebro massif to the south, while the Tremp basin systems were fed by the material eroded from the

uplifted Bóixols high (Gómez-Gras et al., 2016). This suggests that the Montsec was a continuous salt structure with positive topographic relief that separated two depocentres with differential subsidence (Figs. 2.10c and 2.11d).

As Pyrenean contraction intensified, evaporites evacuated from the subsiding Tremp basin and Àger syncline were likely displaced to the frontal part of the foreland or extruding through the Montsec and Pasarel·la-Àger diapirs. The Pasarel·la minibasin started to tilt to the south.

In the Pallaresa transect, the thickening of the Garumnian towards the south suggests that the Sant Mamet dome was growing fast at that time, fed by the salt evacuated from the Àger basin depocentre, which was located further to the south of the present day axis of the Àger syncline (Figure 2.11d). In the Ribagorçana transect, the sum of vertical load by Garumnian sediments together with the compressional buckling resulted in the progressive rotation and steepening of the northern flank of the Àger syncline (Figure 2.10c).

The Garumnian succession forms a progressive unconformity together with the underlying Upper Cretaceous in most of the Serres Marginals synclines (Figure 2.9). The widespread occurrence of the unconformities indicate that the synclines kept filling and slowly subsiding into the evaporites at the same time that they started to close due to the horizontal compressional stress.

Ypresian

During the Early Eocene, the loading of the basement thrust stack of the Axial Zone hinterland increased flexural subsidence in the South Pyrenean basin. The Early Ypresian Alveolina carbonate platform shows a progradation geometry towards the east in the northern limb of the Àger syncline (Figure 2.5a). However, during the Late Ypresian the denudation of the growing orogen shifted sedimentation in the Serres Marginals area from shallow carbonate platforms to deltaic systems and increased sedimentation rates in the E-W prograding deltaic to fluvial systems of the Àger basin.

The Montsec salt wall was progressively narrowing due to compression, most of the Keuper evaporites at its core were progressively evacuated. In the Pallaresa transect (Figure 2.11e) part of the contraction at that time was buffered by the folding of the

Pasarel·la minibasin and salt evacuation through the Pasarel·la-Àger diapir, which prevented the overturning of the northern limb of the Àger basin (Figure 2.11e). The Pasarel·la minibasin presents a much thinner Ypresian series than the Àger basin, as it was kept uplifted between the Montsec and Pasarel·la-Àger welds, something common observed in numerical modelling (Fernandez et al., 2020). However, it retained enough mobility to keep tilting to the south the erosive unconformity of the Ypresian Alveolina limestone above the upper part of the Garumnian. The sedimentary cover in the southern part of the Pallaresa transect was quite continuous; the Sant Mamet dome was not unroofed, and this favoured transmission of stress and folding into the Montroig, and Sant Jordi and Boada synclines.

In the western part of Serres Marginals, the synclines and anticlines continued tightening and the Alveolina limestones and deltaic sandstones of the Baronia, Àger, and Ametlla systems record angular and progressive unconformities in the Blancafort, Tragó and Os de Balaguer synclines. The contraction also caused the tilting of the smaller synclines in the southern part of the Ribagorçana transect. During the Eocene, the Santa Anna syncline was tilted 90 degrees to the south and sank into the Keuper. Only the overturned northern limb is outcropping at present day, fossilized by gently dipping Oligocene conglomerates (Figure 2.10d).

Middle Eocene to Oligocene

The only preserved record of the Mid to Late Eocene in the area is a sequence of Lutetian Alveolina Limestone deposited in the smaller synclines in the leading edge of the Serres Marginals thrust sheet, to the south of the Avellanes diapir. The Lutetian limestone lies directly above the Rhaetian carbonates or above a much thinner succession of Upper Cretaceous limestone. This indicates that the southern domain of the Serres Marginals was an uplifted area for a long history with limited sedimentation and/or erosion. The opposite is the case in the bigger synclines to the north, such as Os de Balaguer and Tragó, which have preserved a large thickness of Palaeocene and Ypresian succession but no Lutetian Alveolina limestone. With the available data we cannot tell whether the Lutetian limestone existed in the northern Serres Marginals and has been eroded, or whether it was restricted to the south due to localized accommodation in the area related with salt withdrawal.

The Fet conglomerates, not conclusively dated yet but, by analogy with the Serres Marginals, of possible Oligocene age, fossilize the Montsec thrust in the Noguera Ribagorçana valley, lying horizontally in angular unconformity above Ypresian Àger basin clastics or directly on top of the Keuper and Mesozoic succession of the unroofed Montsec ridge (Figure 2.10e). The post-Ypresian history of the Montsec ridge is not recorded by syntectonic sediments, but is likely that the main emergence of the thrust (locally thrust weld) occurred during mid to late Eocene times, as the Ypresian formations do not record the existence of significant mountain relief north of the Àger basin.

During the Oligocene, the squeezing of the Serres Marginals salt anticlines transitioned to thrusting, partly as the entire Serres Marginals thrust sheet overrode the autochthonous Ebro basin (Figure 2.10e and 2.11f). Continued horizontal compression caused secondary welding accompanied by syncline imbrication.

2.6.4. Role of key parameters in structural evolution

The Serres Marginals province is a good example of how basins with isolated pre-compressive diapirs and elongated structures in different orientations influence shortening distribution and result in compressional structures with complex geometries and high spatial variability. In synclines with such a thin pre-compressive succession, synorogenic sedimentation and erosion will also play a primary role in the evolution of salt structures. In the following sections we discuss how these parameters condition the evolution of the Montsec and Serres Marginals in framework of a developing orogen (Figure 2.12) and compare it with other case studies of salt detached fold-and-thrust belts and analogue physical models.

Pre-compressional salt structures

Complex structures with polygonal synclines and intervening salt walls and diapirs indicate the existence of pre-compressive salt structures conditioning shortening localisation (Rowan and Vendeville, 2006). In the Serres Marginals and the Montsec, sedimentation played a key role in shaping the pre-compressional basin configuration since the Jurassic. Serres Marginals synclines have a thin succession of preorogenic sediments, but carbonates and gypsum are denser than salt, so density-driven

subsidence is a valid initiation mechanism in absence of tectonic stresses or significant basement slope (Hudec et al., 2009; Warsitzka et al., 2013). Low levels of carbonate sediment supply during the Jurassic allowed salt ridges to rise without being buried, isolating adjacent polygonal depocentres with important thickness differences from early on. Sedimentation at low rates induced by salt withdrawal was also invoked as the main mechanism controlling the polygonal syncline configuration of the Karayün fluvial formation of the Sivas basin (Ribes et al., 2017). Pre-existing structures in the subsalt basement are thought to have an important role in determining the initial location of these early depocentres in Sivas (Callot et al., 2012). In the Fars region in the south-east Zagros fold-and-thrust belt pre-compressive diapirism has also been identified soon after the evaporite sedimentation, determining local patterns of subsidence and subsequent differential thickness in the synclines from early on (Jahani et al., 2009). This early phase of diapirism has also been identified the Kuqa foldbelt in the Tian Shan (Shiqin Li et al., 2012). In these field examples, as in the Serres Marginals, the structural configuration after compression still reflects the early depocentres controlled by salt withdrawal.

Contrasting with the polygonal pattern of Serres Marginals, the Montsec salt-cored anticline has an elongated structure. Elongated salt-cored folds without much lateral variability, usually imbricated, are typical of fold-and-thrust belts developed above a thick viscous detachment level without significant pre-compressive salt structures (Costa and Vendeville, 2002; Duffy et al., 2018) such as the central Zagros (Sherkati et al., 2006) and the Salt Range and Potwar Basin (Grelaud et al., 2002). In contrast, elongated diapirs in the Prebetics ranges developed during the rifting stage and during the subsequent compression were first transported passively and later squeezed in thrust-welds (Roca et al., 2006; Escosa et al., 2018).

The case of the Montsec, is between these two end-members. The angular unconformities in the hanging wall and the long-lived progressive unconformities and lateral variation in the footwall indicate a salt pillow growth during the rifting stage. With the onset of shortening, the salt structure continued growing as a salt-cored anticline in the western area and as an exhumed diapir in the central area. We favour the idea that the main trigger of the Montsec pillow growth was an E-W oriented basement fault

formed during the rifting stage, and hence its elongated shape. Subsequent differential load due to the thicker sedimentation in the downthrown domain -the Tremp basin- kept mobilising salt towards the pillow during the rift and post-rift stage. This has been proven a useful mechanism to produce elongated salt pillows in analogue models (Warsitzka et al., 2015).

Shortening distribution

The complex pre-compressive configuration of the Serres Marginals conditioned the preferential accumulation of shortening during the orogeny. First, the Avellanes diapir and the Sant Mamet Dome, are circular salt structures isolated from each other that did not close with shortening. It is an interesting case as it is known from analogue models and field examples that usually diapirs are the first structures to shorten under compression due to the weaker mechanics of salt compared to surrounding rock (Decarlis et al., 2014; Duffy et al., 2018). A possible explanation for that is that the Sant Mamet roof was thick enough to retain strength and prevent the closure. In the case of the Avellanes diapir, where we do not have any evidence of roof thickness and timing of unroofing, additional factors need to be considered.

A similar case to the Serres Marginals is found in the diapirs of the Fars region in the south-eastern Zagros, which instead of closing, increased their size during compression. This is attributed to the shift of carbonate sedimentation to clastic sediment supply and the increment of sedimentation rates, which accelerated the upwards movement of the salt, preventing the burial of the diapirs (Trocmé et al., 2011). As in the Serres Marginals case, by the start of increased sedimentation rates, the Fars diapirs were already close to the surface, and this had an important role in keeping the diapir active. Additionally, the equant planform of the Avellanes diapir and the Sant Mamet dome made it harder to accumulate strain, which accumulated in salt structures preferentially orientated perpendicular to stress direction. Also, the presence of numerous slabs of Muschelkalk carbonates interbedded within the evaporites in the diapirs could have contributed to disrupt and slow down the evaporite flow, an effect that has been pointed out by numerical models (Shiyuan Li et al., 2012), and could have decreased the evacuation rate through the exposed salt structures.

Instead of closing the big diapirs, shortening gradually tightened the salt-cored anticlines which were not unroofed during the early stages of compression and closed the diapirs between the smaller synclines in the southern area. With the progressive closure of the small breached salt anticlines and diapirs, the Serres Marginals synclines came closer together and the intervening salt structures arranged perpendicular to shortening direction. The rearrangement of synclines and salt structures network related to shortening direction is also observed in the Gulf of Mexico, the Flinders Range and the Sivas basin (Rowan and Vendeville, 2006; Kergaravat et al., 2017). As it is the case for the Sivas basin, the composition of the source salt layer in the Serres Marginals outcrops is mostly gypsum, anhydrite and mudstone. Although original halite proportion is thought to be much higher, the presence of gypsum and anhydrite, with higher viscosity values, likely contributed to slow down the closing of structures.

Another important point of discussion is what parameters promote the transition from folding to thrusting. The depletion of salt from the base layer, but also the secondary welding between synclines, increases the overall rigidity of the sedimentary cover and enhances coupling with the remaining salt, promoting thrusting and minibasin imbrication in the advanced stages of shortening. This effect has been observed in minibasins with high initial mobility such as in the Precaspian basin (Duffy et al., 2017; Fernandez et al., 2017) and the Sivas basin (Kergaravat et al., 2017; Legeay et al., 2019). In the Serres Marginals case study, due to the translation of the thrust sheet towards the south and lack of seismic profiling we do not have evidence of primary welding having produced or its timing. Secondary welding happened in the structures that were unroofed by the later stages of compression and were orientated perpendicular to the main stress direction. This is the case of the Montsec thrust-weld and the thrusts between the imbricated synclines in the central and southern part of Serres Marginals. Syncline imbrication started soon after the southwards translation of the Serres Marginals thrust sheet above the Ebro basin in the Serres Marginals thrust, as evidenced by tectonostratigraphic relationships of the thrusts with the Oligocene conglomerates. It is possible that thrust sheet translation contributed to mobilise the remaining salt towards the frontal part of the thrust sheet, which increased friction in the base of the synclines and thrusting promotion.

Role of syncompressional sedimentation and erosion

In absence of syntectonic sedimentation, shortening quickly closes the diapirs oriented perpendicular to stress direction (Rowan and Vendeville, 2006; Duffy et al., 2018). However, analogue models reveal that differential sedimentation in a salt-detached foreland basin is key to initiate fold tightening, preventing the rapid translation of deformation towards the frontal ramp (Darnault et al., 2016). At the onset of Pyrenean compression, the Serres Marginals frontal part was already a relatively raised area (there is a very thin pre-Lutetian sedimentary succession south of the Montroig thrust). For this reason, the early syn-compressional sedimentary systems, i.e. the E-W directed fluvial channels of the Garumnian concentrated in the Àger basin and the northern synclines of the Serres Marginals. With the advance of compression, sedimentation progressively displaced to the frontal part of the basin, with the sedimentation of the Lutetian Alveolina limestone. The southern Serres Marginals was no longer an uplifted area, which is something counterintuitive, as salt expulsion towards the frontal pinchout usually promotes bulging of the frontal areas of the foreland with the advance of compression.

It has been reported how the tectonically induced foreland subsidence and associated increase of sedimentation rates promotes lateral continuity of the sedimentary systems, sometimes burying the preexisting diapiric structures and overtaking the salt induced accommodation patterns (Ribes et al., 2017). In the Serres Marginals, the shift from halokinetic-induced accommodation patterns to shortening, local accommodation and differential loading happened during the Garumnian (Figure 2.12). The clastic systems that entered Serres Marginals area and followed E-W routing systems, perpendicular to shortening direction and parallel to the growing salt anticlines, which did not become completely buried. Garumnian strata but also the Eocene deltaic and fluvial systems thin towards the growing structures (Canelles and Millà anticlines, Sant Mamet dome, Montsec footwall) and record progressive unconformities because the structures uplifted faster than the rate of sedimentation. During the Campanian, Maastrichtian, Palaeocene and early Eocene accommodation was created as a combination of increasing regional subsidence and local salt induced downbuilding (Figure 2.12). The combination of both allows the creation of local accommodation above diapiric

structures (Ribes et al., 2017, figure 15), resulting in small secondary minibasins such as the Pasarel·la minibasin.

Progressive erosional unroofing of the Montsec diapir/salt-cored anticline, which happened earlier than in Serres Marginals, had an important role in the fast subsidence of the Àger syncline from the Garumnian onwards which became the preferential route for the sedimentary systems. The sedimentary loading promoted salt migration towards the frontal part of the basin. To the south of the Àger basin, the Canelles and Millà anticlines were unroofed in the later stages of the orogeny or not unroofed at all, which likely contributed to the flanking synclines being shallower.

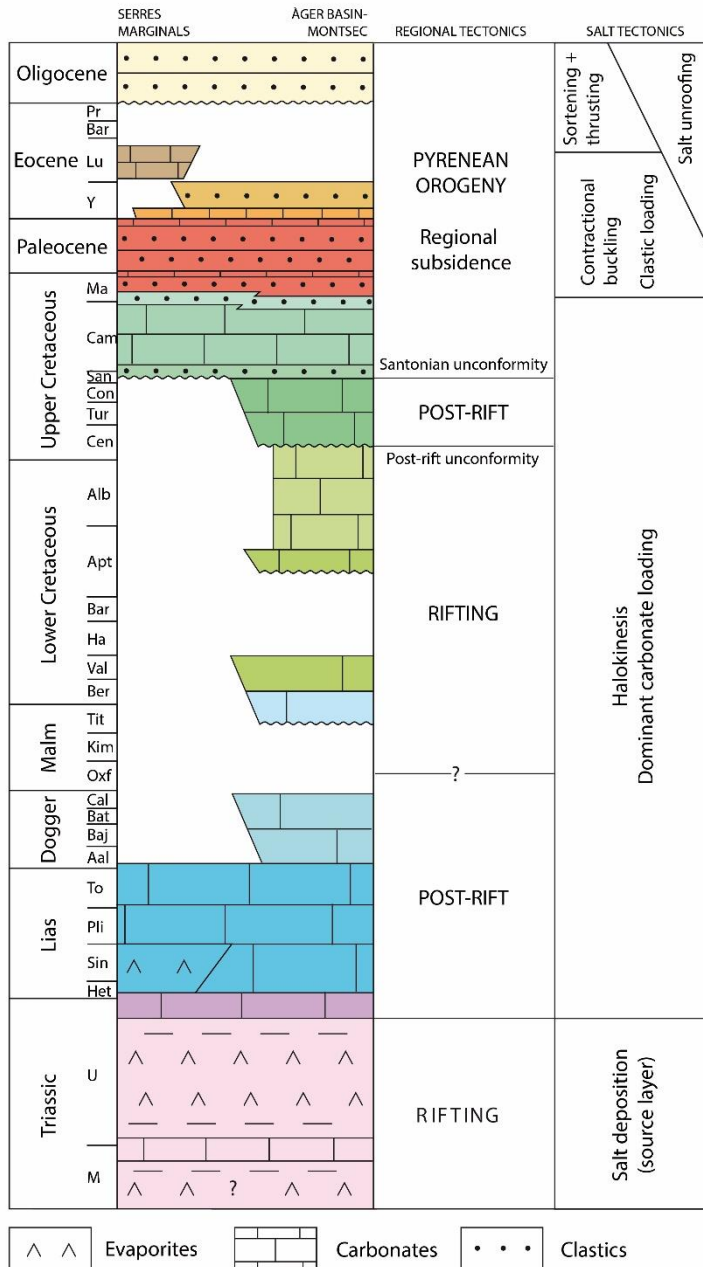


Figure 2.12. Stratigraphic succession of the Serres Marginals and Montsec areas juxtaposed to the regional tectonic events and salt-tectonics related events interpreted in this study.

2.7. Conclusions

In this study we present a reinterpretation of the Montsec and Serres Marginals foreland thrust-fold structures of the southern Pyrenees based on new field observations and incorporating salt tectonics concepts. The result has been two new regional cross-sections across the Montsec ridge and the Serres Marginals thrust sheet. With a sequential restoration up to the Jurassic time, we substantially modify the interpretation on the mechanisms that controlled the structural evolution of the southern Pyrenees and reduce the amount of estimated shortening along the Montsec thrust-weld.

Halokinetic features can be identified in the long-lived unconformities and thickness differences at the syncline flanks in the Serres Marginals and Montsec-Àger basin. The variability in size, geometry and preserved stratigraphic record indicate an independent subsidence rate for each structure, with separate depocentres locally operating since the Jurassic. This conditioned a pattern of polygonal synclines and intervening salt structures in the Serres Marginals before the arrival of the Pyrenean deformation front.

We reinterpret the origin of the Montsec as an elongated salt pillow, its rising likely triggered by basement normal faulting during the Early Cretaceous rifting stage. The significant throw of the fault enabled greater subsidence in the sedimentary cover of the Tremp basin while the Àger basin and Serres Marginals were relatively uplifted. Salt withdrawal from the Tremp basin to the south maintained a slow but steady subsidence with no drowning of the carbonate platform.

With the onset of compression in the Late Santonian the driving mechanisms for deformation in the Àger basin and the Serres Marginals progressively shifted from predominantly vertical movements (bending) due to differential loading of synclines to structure narrowing by predominant compressional buckling from the Paleocene onwards. Increasing sedimentation rates during the orogeny kept the synclines subsiding into the salt, but salt structures were close enough to the surface to keep growing and not be buried. It is likely that the Oligocene imbrication of the synclines in the Ribagorçana transect responds to primary welding of the basal evaporite layer in the deeper synclines (Àger basin, Os de Balaguer and Tragó).

The structural variability across the Montsec footwall and Serres Marginals is a direct consequence of the high evaporite vs sedimentary cover thickness ratio, the presence of pre-compressive diapiric structures and the constant sediment supply during the contraction, as part of a broken foreland basin system.

This case study provides an example of the evolution of the frontal part of a fold-and-thrust belt evolving above a thick basal evaporite layer with pre-compressional structures under continuous synorogenic sedimentation. The discussion of fundamental parameters in its compressional evolution, introduced in other salt fold-and-thrust belts, as well as in analogue and numerical models, is enriched by the addition of the South Pyrenean case study.

SUPPLEMENTARY MATERIAL

	<i>Mo</i>	<i>Mr</i>	<i>ODB and Tg</i>	<i>Mill ant</i>	<i>St M dome</i>	<i>Ag Rib</i>	<i>Ag Pall</i>	<i>Mts Rib</i>	<i>Mts Pall</i>
<i>Oligocene</i>	855	200	350	90	0	0	0	0	0
<i>Lutetian</i>	220	0	0	0	0	0	0	0	0
<i>Ypresian</i>	40	180	350	655	580	480	1210	0	0
<i>Garumnian</i>	30	245	310	665	740	300	35	55	0
<i>Maastrichtian-Campanian</i>	20	325	350	450	450	0	50	1270	1105
<i>Upper Santonian</i>	0	80	30	75	75	95	0	370	440
<i>Coniacian-Lower Santonian</i>	0	0	0	0	0	20	0	200	60
<i>Cenomanian-Turonian</i>	0	0	0	0	0	100	0	80	70
<i>Lower Cretaceous.</i>	0	0	0	0	105	130	0	470	480
<i>Malm</i>	0	70	0	0	0	0	0	0	200
<i>Dogger</i>	0	200	0	75	150	100	0	80	250
<i>Lias</i>	20	300	155	150	0	80	0	197	280
<i>Lias gypsum</i>	0	290	30	0	0	0	0	0	0
<i>Rhaetian limestone</i>	40	0	50	0	0	0	0	10	20
<i>Keuper</i>	120	120	50	50	0	0	0	40	115

Table A.1. Thickness of the stratigraphic succession in representative sections of the study area (in metres). Data from stratigraphic logs in the ICGC 1:25.000 maps. *Mo*, Monteró; *Mr*, Montroig; *ODB and Tg*, Os de Balaguer and Tragó; *Mill ant*, Millà anticline; *St M dome*, Sant Mamet dome; *Ag Rib*, Àger basin Ribagorçana transect; *Ag Pall*, Àger basin Pallaresa transect; *Mts Rib*, Montsec hanging wall Ribagorçana transect; *Mts Pall*, Montsec hanging wall Pallaresa Transect.

Chapter 3

Basement-involved thrusting, salt migration and intramontane conglomerates: a case from the Southern Pyrenees

This chapter is under review in le Bulletin de la Société Géologique de France as Burrel, L., Teixell, A., Gómez-Gras, D. and Coll, X., Basement-involved thrusting, salt migration and intramontane conglomerates: a case from the Southern Pyrenees

Abstract

Basement-involved thrusting, salt migration and intramontane conglomerates: a case from the Southern Pyrenees

The northern margin of the Organyà basin (Southern Pyrenees) has a complex structure in which syn-rift Lower Cretaceous carbonates flank a wide Keuper evaporite province, featuring the leading edges of the basement-involved thrust sheets of the Pyrenean antiformal stack. Recent observations show that Keuper diapirs and salt walls grew during the Cretaceous extensional episode, conditioning the development of differentiated depocenters and minibasins. The role of salt tectonics during the Pyrenean orogeny has not been addressed in previous structural studies, but present-day cross-sections indicate a Keuper evaporite-bearing vertical thickness of up to 3000 m in the Senterada-Gerri de la Sal area. We infer that salt migration was a determinant mechanism in triggering a gentle northward tilting of the Organyà basin during the Eocene-Oligocene, recorded in the La Pobla de Segur and Gulp syn-tectonic conglomerates in a basin-wide progressive unconformity and a large north-directed onlap, opposite to the main sedimentary influx direction. Contemporaneously, salt migration, promoted by conglomerate differential loading, enabled the sinking and rotation of the unrooted Noguères thrust units (*têtes plongeantes*). We use new and published structural data for the Lower Cretaceous margin of the Organyà basin, combined with structural and clast provenance data from the Cenozoic alluvial fan conglomerates of La Pobla and Gulp, to understand the Lutetian to late Oligocene evolution of the northern margin of the Central South-Pyrenean Unit. The tectono-sedimentary evolution of this area and the salt evacuation patterns are closely related to the exhumation history of the stacked Paleozoic thrust sheets of the Pyrenean hinterland to the north. In this study we correlate the movements over a mobile substratum and the paleogeographic changes of conglomeratic basins at the toe of an exhuming orogenic interior.

Résumé

Chevauchements de socle, migration du sel et conglomérats intramontagneux: un cas des Pyrénées méridionales

La marge nord du bassin d'Organyà (Pyrénées méridionales) présente une structure complexe dans laquelle les carbonates du Crétacé inférieur, syn-rift, flanquent un vaste domaine d'évaporites du Keuper, en interaction avec la partie frontale des nappes chevauchantes de l'empilement axial pyrénéen (têtes plongeantes des Nogueres). Des observations récentes montrent que des diapirs de Keuper se sont développés pendant l'épisode d'extension créacée, conditionnant le développement de dépocentres et de minibassins différenciés. Le rôle de la tectonique salifère pendant l'orogénèse pyrénéenne n'a pas été abordé dans ce secteur dans les études structurales précédentes, mais les coupes transversales actuelles indiquent une épaisseur verticale de Keuper à évaporites allant jusqu'à 3000 m dans la région de Senterada-Gerri de la Sal. Nous en déduisons que la migration du sel a été un mécanisme déterminant dans le déclenchement d'un léger basculement vers le nord du bassin d'Organyà pendant l'Éocène-Oligocène, enregistré dans les conglomérats syn-tectoniques de La Pobla de Segur et de Gulp par une discordance progressive à l'échelle du bassin et un onlap régional dirigé vers le nord, à l'opposé de la direction principale du flux sédimentaire. Simultanément, la migration du sel, favorisée par la charge différentielle des conglomérats, a permis l'enfoncement et la rotation des têtes plongeantes des Nogueres, séparées de leur racine par l'érosion. Nous utilisons des données structurales nouvelles et publiées sur la marge du Crétacé inférieur du bassin d'Organyà, combinées aux données structurales et de provenance des clastes des conglomérats alluviaux du Cénozoïque de La Pobla et de Gulp, pour comprendre l'évolution du Lutétien à l'Oligocène tardif de la marge nord de l'Unité Sud-Pyrénéenne Centrale. L'évolution tectono-sédimentaire de cette zone et les modèles d'évacuation du sel sont liés à l'histoire de l'exhumation des nappes chevauchantes de matériel paléozoïque empilées au nord dans la Zone Axiale pyrénéenne. Dans cette étude, nous corrélons les mouvements sur un substrat mobile avec les changements paléogéographiques des bassins conglomératiques au pied d'un intérieur orogénique en exhumation.

3.1. Introduction

In basins that evolve on top of thick evaporite detachment levels, differential loading of prograding sedimentary systems triggers salt mobilization towards areas with a smaller overburden load and associated depocentre migration (Ge et al., 1997). In salt-bearing foreland basins, load-induced halokinetic movements in addition to the compressional forces from the orogeny can play an important role in shaping the architecture of alluvial fans. Nevertheless, due to the evident imprint of compressional structures such as thrusts and fault-related folds, the contribution of halokinesis in syn-orogenic sediments of fold-and-thrust belts has been often disregarded.

The intramontane alluvial fans of the Central South-Pyrenean Unit (CSPU) are late Lutetian to late Oligocene in age and crop out in three main areas known from East to West as the La Pobla de Segur, Gulp, and Sis conglomeratic basins (Rosell and Riba, 1966; Mellere, 1993; Vincent, 2001)(Figure 3.1). Additionally, to the north of the La Pobla and Gulp basins, the Senterada conglomeratic basin is an E-W through that comprises three smaller isolated outcrop areas, on top of the Paleozoic and Triassic of the Nogueres thrust sheet. From south to north, the alluvial fans progressively retrograde, displacing the apical areas to the north, shifting sedimentation from the Organyà basin northern margin towards the unrooted leading edge of the Axial Zone antiformal stack (the Nogueres têtes plongéantes; Séguret, 1972) and a Keuper evaporite province in between, which we call the Senterada salt province (Figure 3.2). The evolution of the catchment areas and geometry of these alluvial systems (Figures 3.2 and 3.3) has been strongly influenced by the joint effects of the Axial Zone uplift, horizontal shortening and salt evacuation. With the intervention of such diverse factors, the geological history registered within the Middle Eocene to Oligocene intramontane conglomerates in the South-Pyrenean thrust belt puts forward an interesting case study.

The starting point of this study involved revisiting the work by Rosell and Riba (1966), who noted a unusual dip and apparent downlap to the north in the lower alluvial systems of the La Pobla basin (Figure 3.4a). This observation contrasted with the major northward provenance of the fans, so they attributed the downlap to the synsedimentary tilting of the conglomeratic basin towards de north, progressively

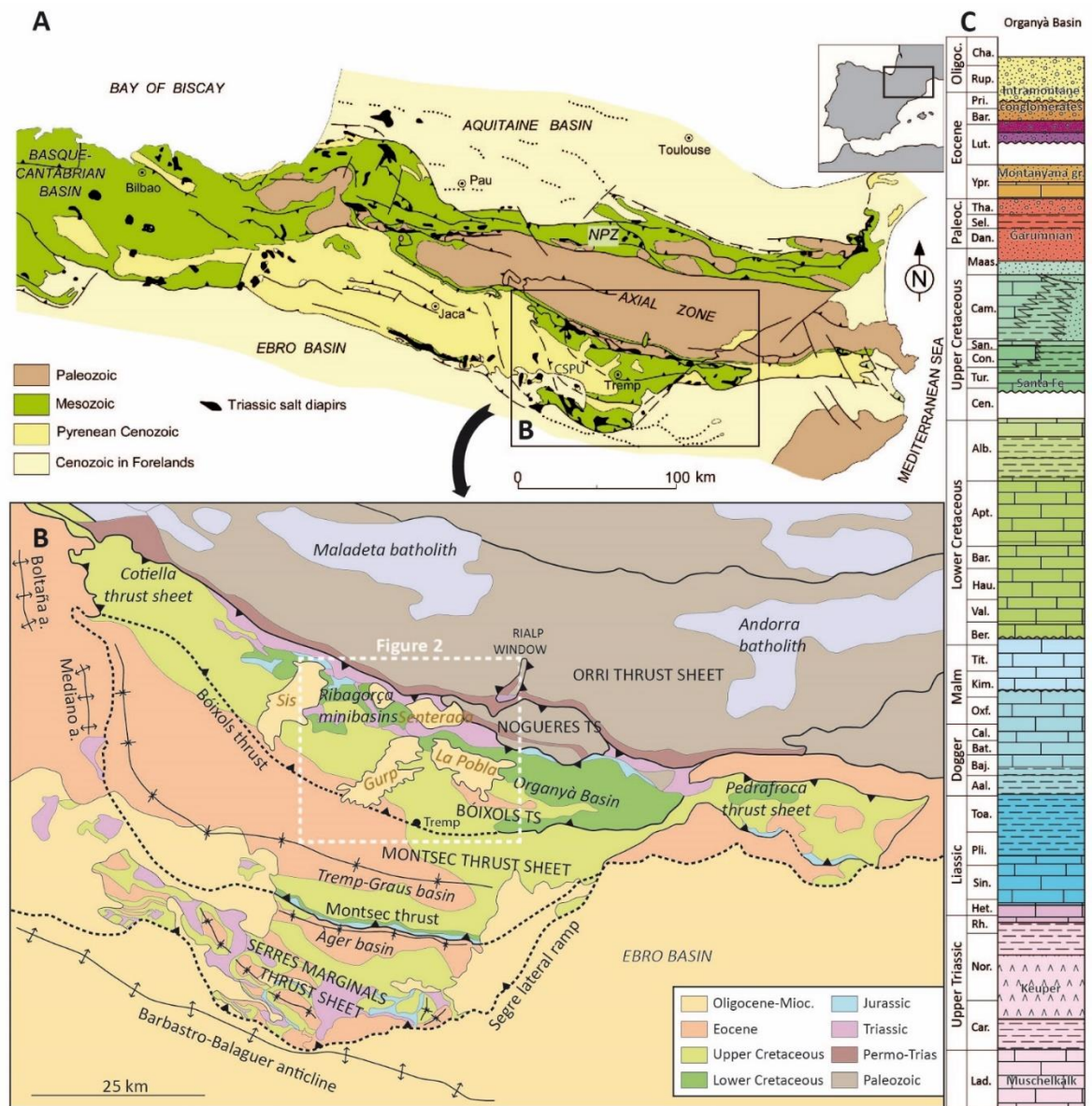


Figure 3.1. (a) Geologic sketch map of the Pyrenean orogen. (b) Geological map of the South-Central Pyrenean unit indicating the location of the study area (Fig. 2). (c) Stratigraphic column of the Organyà and Tremp-Graus basins.

shifting the basin depocentre in that direction. In this study we return to this idea in the light of the more recently developed salt tectonics concepts, invoking load-induced salt migration as the main factor inducing the north-directed tilting and associated depocentre migration.

Salt tectonics may quickly modify the connection between catchment areas, routing systems and depocentres. In the framework of a growing orogen, sudden local changes in provenance often indicate smaller-scale tectonic activity related to salt expulsion, but can often be overprinted by basement thrusting and related growth structures. Originally interbedded with Triassic Keuper evaporites, the uninterrupted presence of

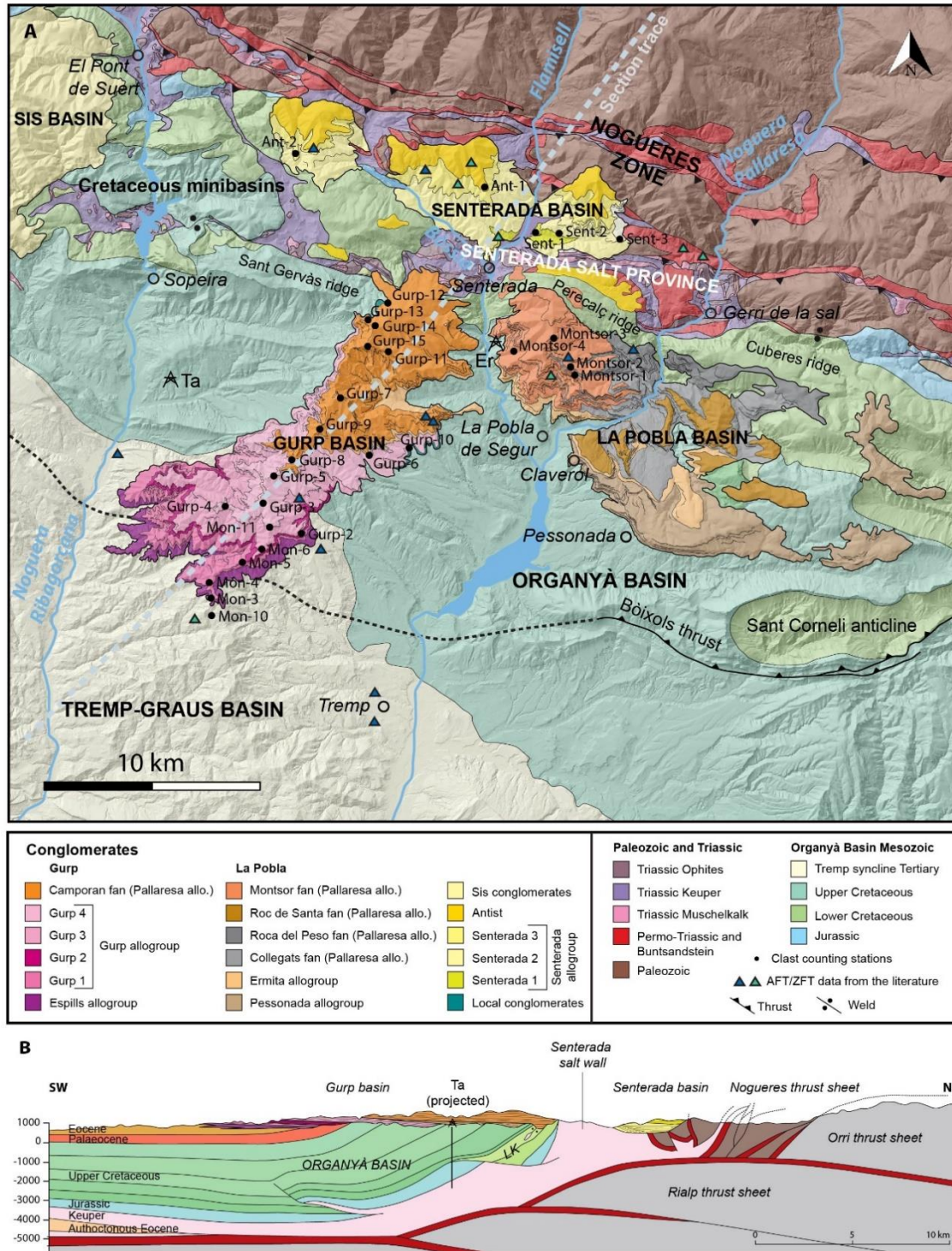


Figure 3.2. (a) Detailed geological map of the study area showing the location of the clast counting stations. Ta, Tamúrcia well, Er, Erinyà well. The limits of the conglomerate fans are modified from the ICGC 1:25000 maps of Tremp and Espills for the Gulp basin, and from Saura (2004) and Barsó (2007) for the La Pobla and Senterada Basins. The Organyà Basin and the Nogueres Zone have been drawn from the ICGC 1:50000 map of the Pallars Jussà. The AFT/ZFT sample locations refer to the papers by Beamud et al., 2011, Whitchurch et al., 2011, Fillon et al., 2013, and Michael (2013). **(b)** Schematic cross-section along the Gulp basin transect. LK, lower Cretaceous. The Organyà basin structure is modified from the sections in Mencos et al. (2015) and Muñoz et al. (2018), the Nogueres shallow structure is from Saura and Teixell (2006), and the deep structure of the antiformal stack is modified from Muñoz et al. (2018).

ophite clasts within the intramontane conglomerate of the Southern Pyrenees indicates the continuous erosion of Keuper exposures of the Senterada salt province. This provides an excellent marker to track salt-related movements from the late Lutetian to the Oligocene, where exposed diapirs and salt walls were part of the source area. Focusing on the geometry and provenance indicators of the Gurp, La Pobla and Senterada basins, we present new palaeogeographic maps and cross-sections, illustrating the evolution of the conglomeratic basins in relation to the uplifting antiformal stack and the halokinesis of the Keuper evaporites.

3.2. Geological setting and previous studies

The antiformal stack structure of the Axial Zone of the Pyrenees has been extensively studied since the 1970s (Séguret, 1972; Williams and Fischer, 1984; Vergés and Martínez, 1988; Roure et al., 1989; Muñoz, 1992; Beaumont et al., 2000; Mouthereau et al., 2014; Muñoz et al., 2018; Teixell et al., 2018), defined as a duplex structure of Paleozoic basement-involved, south-directed thrust sheets. The frontal part of the antiformal stack, detached by erosion from its root to the north, consists of foreland-dipping thrusts and related downward-facing folds referred to as the Noguères *têtes plongeantes* (Séguret, 1972). Recent numerical modelling studies have explored the role of the Keuper evaporites in crustal-scale orogenic inversion, which are key in enabling gliding, stacking and rotation of the duplex thrusts (Grool et al., 2019; Jourdon et al., 2020). In the South-Central Pyrenees, the Noguères thrust sheet consists internally of a set of minor imbricates of Silurian and Devonian metasedimentary rocks with Permo-Triassic deposits unconformably on top (Muñoz, 1992; Saura and Teixell, 2006). These subunits are interleaved with Triassic shales and evaporites of the Keuper facies (Figure 3.2a). The Variscan structure of the Noguères units, preceding the Pyrenean Orogeny, and the Permo-Triassic basin configuration has been documented in several works (Mey, 1968; Zwart, 1979; Muñoz, 1992; Saura, 2004; Saura and Teixell, 2006; Lloret et al., 2018). Under the Noguères thrust sheet, the Orri thrust sheet, bearing the igneous and metamorphic complexes of the Axial Zone (Muñoz, 1992), crops out to the north of the Noguères thrust sheet (Figure 3.1).

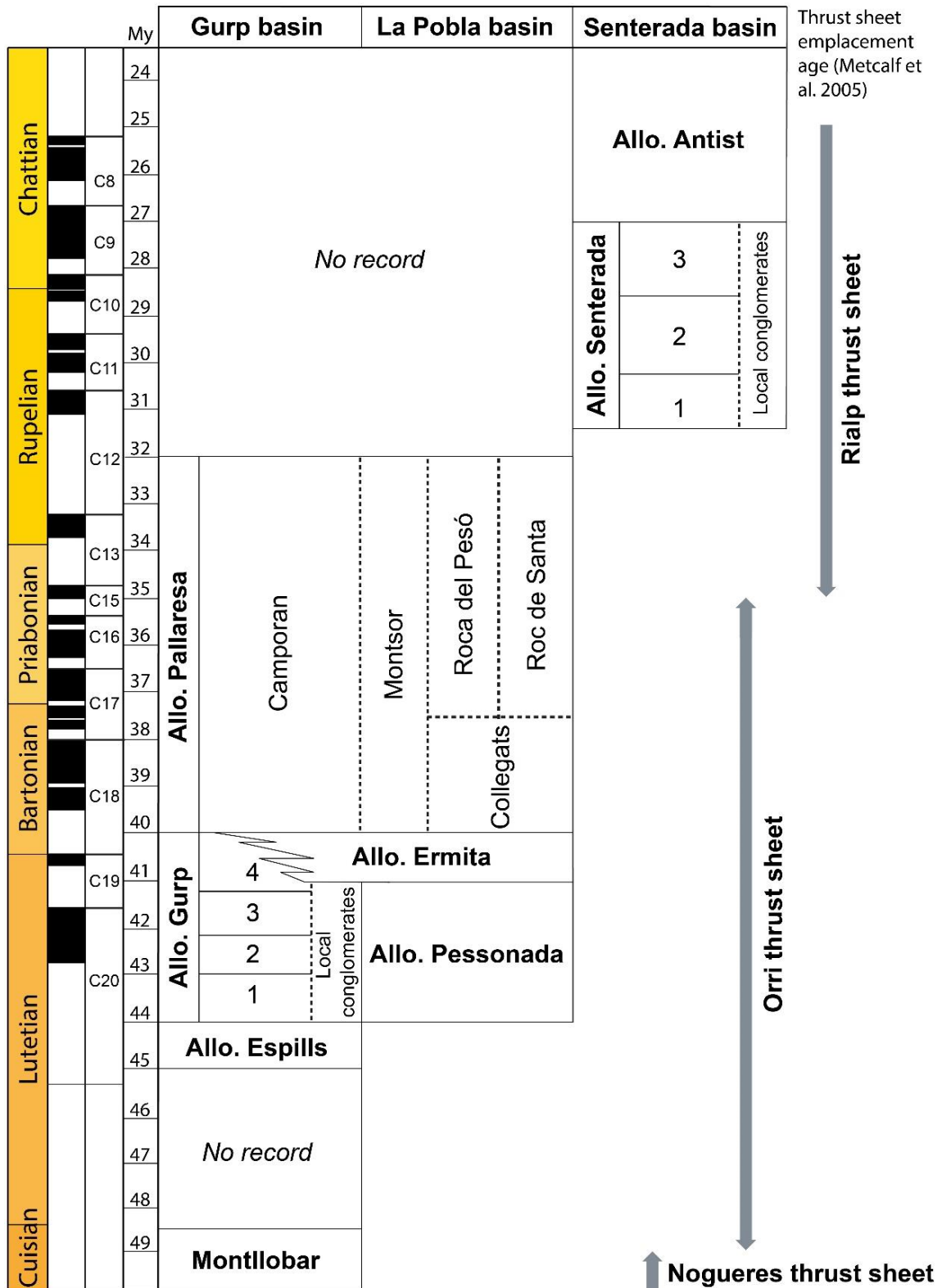


Figure 3.3. Tectonostratigraphic framework for the syn-orogenic conglomerate units used in this study. Modifications from previous works are explained in the text.

According to thermochronological data (apatite and zircon fission tracks: AFT, ZFT) by Fitzgerald et al. (1999) and Metcalf et al. (2009), a first stage of heating around 70-50 My in the Orri thrust sheet can be attributed to burial by the upper thrust sheets as the Nogueres (Figure 3.3). Oldest cooling ages of the Lacourt massif of the North Pyrenean zone (the root zone to the Nogueres zone according to Teixell et al., 2018) at 70 (ZFT) and 55 My (AFT) (Yelland, 1991; Fitzgerald et al., 1999) could be consistent with this. From 50 to 30 My, the uplift of the Orri thrust sheet accelerates the amplitude growth of the Axial Zone antiformal stack, rapidly lifting and cooling the granite massifs contained in the sheet (Ribérot, Maladeta, Marimanya, etc.). Rapid cooling continued in the massifs of the North Pyrenean Zone (Vacherat et al., 2016). Finally, the emplacement of the lowermost Rialp thrust sheet, at around 30 My, starts a stage of slower cooling up to the present day (Metcalf et al., 2009; Whitchurch et al., 2011).

The Axial Zone antiformal stack is flanked to the south by the thin-skinned South-Pyrenean fold-and-thrust belt, constituted by Mesozoic and Paleogene rocks detached from the basement units by the Triassic Keuper, which is also the source layer for diapirism. The eastern part of the thrust belt in the central Pyrenees was referred to as the Central South-Pyrenean Unit (CSPU; Séguret, 1972) (Figure 3.1), a name we retain for convenience in the description. The Keuper outcrops extensively between the Nogueres thrust slices and the CSPU, forming what we call the Senterada salt province. Over the mid-Triassic Muschelkalk carbonates, the Keuper facies of the Senterada salt province is composed of four different formations (Salvany and Bastida, 2004): a) the Adons mudstones and carbonates; b) the Boix gypsum formation, consisting of red and versicolor gypsum; c) the Senterada gypsum formation, cropping out in the Pont de Suert and Senterada areas; and finally d) the Avellanes mudstones and carbonates formation. Due to the weathering conditions, halite is not found in the outcrops. However, most wells that cut across the Keuper in the SCPU, including Erinyà and Tamúrcia wells in the study area (Figure 3.2), indicate thick halite successions (Lanaja, 1987). Moreover, the salty water springs in Gerri de la Sal show that halite is an important component of the Keuper facies under the surface.

The evaporite depositional thickness within the Keuper facies in the Senterada province is hard to estimate, due to compression leading to intense deformation and repetitions

within the succession. The Erinyà and Tamúrcia wells (Figure 3.2) stopped drilling after 130m into the Keuper halite and mudstone, so the basal depth of the evaporite unit is unknown. The presence of abundant Muschelkalk carbonate lenses within the deformed Keuper facies suggests that Middle Muschelkalk evaporites, not clearly identified at the surface but reported in wells in the Iberian and Ebro basins (Bartrina and Hernández, 1990; Jurado, 1990; Ortí et al., 2017), could have acted as the basal level of the source layer for fault detachment and diapirism.

Halokinetic deformation has been reported along the northern margin of the CSPU in the Cotiella thrust sheet (McClay et al., 2004; Lopez-Mir et al., 2014) and the Ribagorça basin (Saura et al., 2016) (Figure 3.1) during the Pyrenean Mesozoic rifting stage. To the southeast of these halokinetic depocenters, the lower Cretaceous Organyà basin was a synformal basin filled with a thick carbonate succession (Berástegui et al., 1990; Caus et al., 1990; García-Senz, 2002). The Jurassic and lower Cretaceous succession of northern limb of the Organyà syncline is shown as isopach, terminating sharply against the Morreres backthrust, which is understood as an Eocene structure that uplifts the basin above the Senterada Keuper province (Berástegui et al., 1990; Muñoz, 1992; García-Senz, 2002). In this study we revise this concept, reinterpreting the Morreres backthrust as a diapiric contact at the edge of the Organyà basin.

The Organyà basin is limited to the south by the Bóixols thrust, the oldest of the South-Pyrenean piggy-back succession, emplaced during the late Santonian as a reactivation of an extensional fault system (Berástegui et al., 1990; Vergés and Muñoz, 1990). Berástegui et al. (1990) and García-Senz (2002) report a progressive onlap of the Lower Cretaceous carbonates against the Jurassic pre-rift strata in the Bóixols hanging-wall and interpret it as a roll-over anticline against a listric fault, inspired by the geometries observed in physical models by Ellis and McClay (1988). To the south of the Bóixols thrust, the central part of the CSPU is the broad, flat-bottomed syncline known as the Tremp-Graus basin, filled by the synorogenic sediments from the upper Santonian to the Eocene, and limited to the south by the Montsec thrust (Figure 3.1).

Mid to Late Eocene and Oligocene alluvial conglomerate inliers of the South-Pyrenean thrust belt were sedimented unconformably above deformed Mesozoic and Tertiary rocks of the SCPU (Figure 1)(Rosell and Riba, 1966). The major basal unconformity at the

base of these intramontane conglomerates, and an apparent downlap to the north of the conglomerate beds against it (Figure 3.4a), has been studied since the 19th century. During the first half of the 20th century, the fossil-bearing levels of Sossís in the lower part of the succession were dated as Bartonian (Misch, 1934; Bataller, 1943; Crusafont et al., 1956). Rosell and Riba (1966) published the first complete stratigraphic description, and mapped the La Pobla basin. The study also included clast compositional identification, differentiating alluvial fan units with predominant Paleozoic or Mesozoic

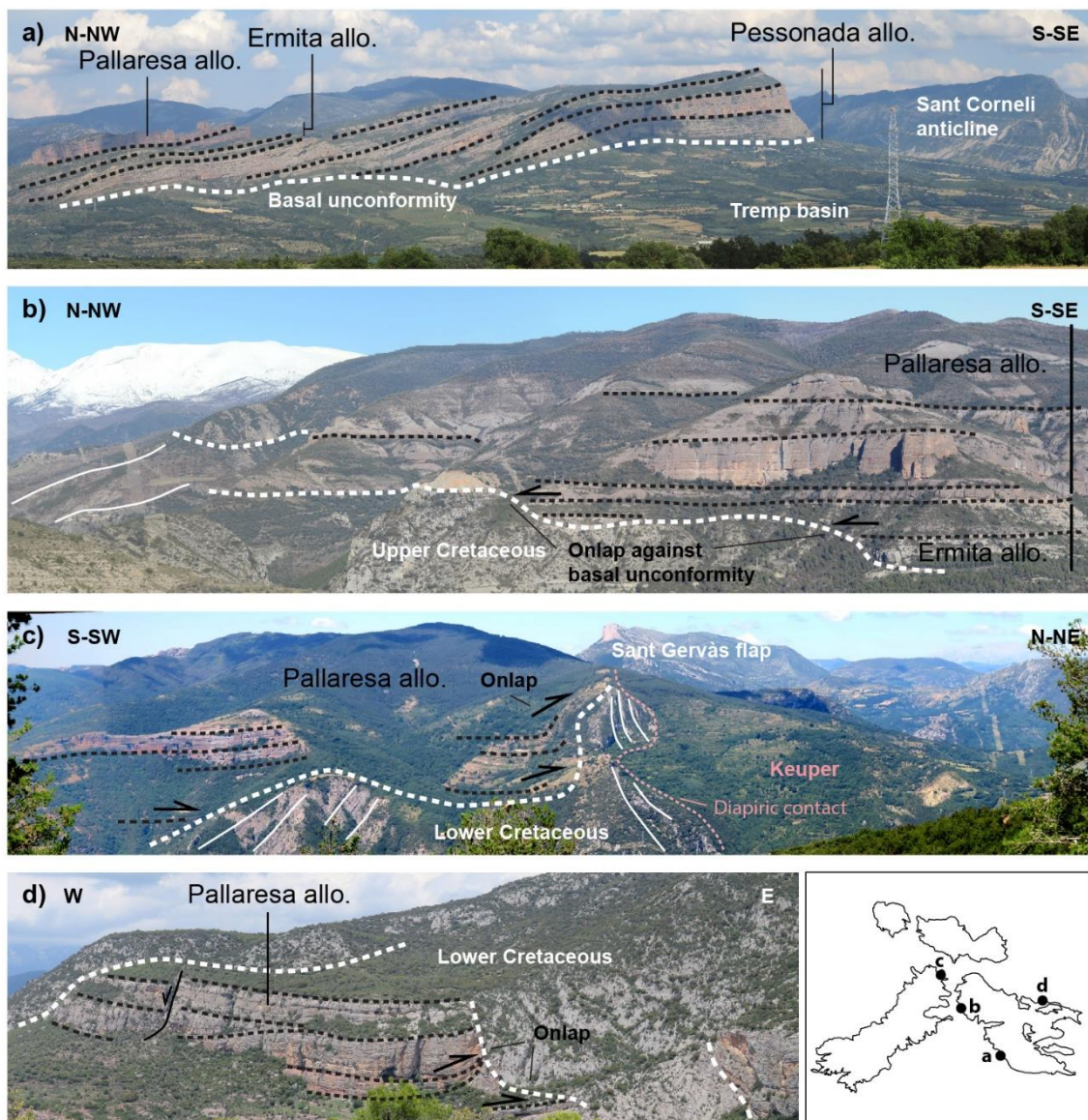


Figure 3.4. (a) Flat basal unconformity and north-directed downlap of the conglomerates in the Serra de Pessonada. Field of view is 5km. (b) Ermita and Pallaresa allogroups onlapping against the irregular basal unconformity in the Flamisell valley (Serra de Montsor). The horizontal dip of the beds is apparent due to the orientation of the photo. Tilting of the beds ranges from 20°N at the bottom of the Pallaresa allogroup to nearly horizontal at the top. Field of view is 6km (c). Onlap of the Pallaresa allogroup conglomerates (Camporan system) against the Lower Cretaceous ridge in the northern Gulp basin. Field of view is 4km. (d) Pallaresa allogroup conglomerates (Roca del Pesó system) infilling Lower Cretaceous palaeoreliefs in the NE margin of the Organyà basin. Field of view is 2km.

provenance and interpret the downlap against the basal unconformity as produced by the tilting of the basin, pointing towards a progressive development of the basal unconformity, rather than a post-depositional tilting. Robles and Ardévol (1984) studied the relationships between the alluvial fans and the Sossís and Claverol lacustrine deposits, differentiating climatic cycles within the stratigraphic succession that were correlated with the progradation and retrogradation of the Ermita fan, and produced a series of palaeogeographic maps. The carbonate and marly members of the lacustrine units, often interbedded with coal beds, are very rich in vertebrate and invertebrate fossil content (i.e. compilation of palaeontological data in López-Martínez et al., 1998).

Studies by Mellere and Marzo (1992) and Mellere (1993) proposed a new stratigraphic framework for the La Pobla de Segur conglomerates, which was based on mappable unconformity surfaces and clast compositional changes. Five allogroups were defined: Pessonada, Ermita, Pallaresa, Senterada, and Antist. The apparent downlap of the conglomerate beds against the basal unconformity was attributed to the reactivation of the Bóixols thrust or deeper structures. Magnetostratigraphic dating of the La Pobla conglomerates (Beamud et al., 2003, 2011) was anchored in the lacustrine fossil localities, and covered an age span of around 18 My. These data, combined with AFT data in granitic clasts (Beamud et al., 2011), in detrital samples of the CSPU (Whitchurch et al., 2011; Fillon et al., 2013) and thermal modelling (Beamud et al., 2011; Whitchurch et al., 2011) led to a refined chronostratigraphic framework for the La Pobla and Sis conglomerates, which range from the late Lutetian to the late Oligocene. Provenance studies in the La Pobla conglomerates by Barsó (2007), focused on clast counting and heavy minerals identification. The observed provenance changes were correlated with exhumation data in the Axial Zone antiformal stack (Beamud et al., 2011). These studies explain the Oligocene disconnection of the La Pobla and Senterada basins as a result of the Morreres backthrust emergence.

Contrary to what happens in the La Pobla basin, there are no extensive stratigraphic studies nor a solid chronostratigraphic framework for the Gulp conglomerates. The southern part of the Serra de Gulp is mapped in the ICGC 1:25000 maps of Tremp and Espills (ICGC, 2009, 2010), outlining the sedimentological and compositional characteristics of the main conglomerate units. The Gulp basin succession starts with

the Espills allogroup, which is followed by the Gulp allogroup and the Ermita and Pallaresa allogroups, the latter two equivalents to the La Pobla basin. Michael (2013) correlated the Gulp conglomerates with the Escanilla fluvial system of the Ainsa basin based on clast counting, and also provided sparse detrital AFT data. In this study, we will use the unit divisions proposed by Mellere and Marzo (1992) for the La Pobla and Senterada basins and the ICGC maps for the Gulp basin.

3.3. Methods

Field campaigns were carried out to obtain additional structural data of the northern Organyà Basin flanking with the Senterada salt province. Structural data have also been gathered within the conglomeratic basins to constrain their geometry, with special focus in the less studied Gulp basin. The deep structure of the Organyà basin adopted in this work is modified from the sections in Mencos et al. (2015) and Muñoz et al. (2018), the Nogueres Zone shallow structure is from Saura and Teixell (2006) and the deep structure of the antiformal stack is modified from Muñoz et al. (2018).

Quantification of the main clast lithologies in the conglomerate units was performed in the outcrop locations indicated in Figure 3.2. We have analyzed a total of 18 clast-counting stations, 11 of which are located in the Gulp basin, 4 in the La Pobla basin, and 3 in the Senterada basin. In the La Pobla and Senterada basins fewer stations were required given that clast counting had been previously performed by Barsó (2007). The method used was that by Howard (1993), which consists in counting subsets of 100 clasts each to obtain lithology percentages. The repetition of four clast-countings, which are closely spaced in each station, was not possible in some localities due to the limited outcrop space and conditions. In cases where in-situ identification of clasts was difficult, their lithology was determined by thin-section observations under microscope.

To simplify the clast counting results, we have grouped the 42 identified lithologies (Table in the supplementary data of this chapter) into 8 provenance groups:

- a. Tertiary limestones and sandstones: Alveolina limestones, and deltaic and fluvial Eocene sandstones from the Tremp basin.

- b. Mesozoic carbonates: Dogger black dolomites and breccias, orbitolina-bearing limestones, rudist bearing limestones, sparitic limestones, black shales, and bioclastic limestones from the Cretaceous of the CSPU.
- c. Micritic limestone: Grey coloured limestone clasts with no visible fossil content. Likely to belong to the Triassic Muschelkalk, the Jurassic, or the lower Cretaceous.
- d. Triassic dolerites (ophites), originally interbedded with the Keuper evaporites and mudstones.
- e. Permo-Triassic clasts: Permian red sandstones and breccias, Buntsandstein quartz conglomerates and quartz pebbles, Buntsandstein white sandstones, caliche nodules, and pumite fragments. They were likely sourced from the Nogueres area (the thrust sheet and its autochthon).
- f. Carboniferous: Microconglomerate and sandstone typical of the Culm facies, sourced from the Nogueres thrust sheet.
- g. Silurian and Devonian: Silurian black slates, ochre Devonian limestones and calcareous slates, and crinoid or goniatites bearing Devonian limestones (Griotte facies), sourced from the upper subunits of the Nogueres thrust sheet.
- h. Paleozoic granites.
- i. Paleozoic metasediments: marbles (occasionally with pyrite and andalusite crystals), slates, gneiss, deformed quartz and quartzites.

3.4. Tectonostratigraphy of the La Pobla, Gulp and Senterada conglomeratic basins

The substratum of the northern margin of the Organyà basin

This study addresses the role that salt tectonics played in the Eocene and Oligocene evolution of the northern half of the Organyà basin. However, to understand the role of pre-compressional diapirism, it has been necessary to conduct new field investigations of the Mesozoic syn-rift strata. The Aptian and Albian carbonate and marl strata in the Flamisell river valley (Figure 3.2) describe a progressive unconformity from dips of 60-80 degrees overturned adjacent to the Senterada Keuper province to right way-up dips

of 40-50 degrees further south (Figure 3.4c), suggesting diapiric rise. In the Noguera Pallaresa river valley, the Perecalç overturned syncline (Figure 3.2) has a complex faulted structure (García-Senz, 2002), which has challenged the identification of growth patterns in this area.

The Albian Lluçà marls (Figure 3.1c) appear locally sheared, and in the Flamisell valley contain interbedded lenses of Keuper evaporites (Figure 3.2b). Regarding their position within the succession and the proximity with the Senterada salt province we interpret that these lenses can be the remnants of a salt sheet extruded from the Senterada diapir during the rifting stage.

In the light of observations suggesting syn-rift diapir rise in the northern margin of the Organyà basin, we reinterpret the contact between the Lower Cretaceous carbonates at the basin edge and the Keuper province primarily as a diapiric contact (Figure 3.2b), and not as a thrust as it was previously understood (e.g. Morreres backthrust, Muñoz, 1992, Mellere, 1993), although some fault reactivation may not be discarded. The unconformities within the Pessonada conglomerates (Figure 3.4a), previously attributed to the displacement of the Morreres backthrust (e.g. Beamud et al., 2011), can be reinterpreted as halokinetic unconformities caused by Paleogene diapir reactivation.

Towards the east, in the Cuberes ridge (Figure 3.2a) the diapiric contact between the Keuper province and the Mesozoic overburden cuts across older carbonates of the Upper Jurassic, Neocomian and Barremian (García-Senz, 2002). Dips change from 65 degrees overturned in the Noguera Pallaresa valley to around 50 to 30 in the eastern part of the study area where Keuper evaporites have been completely squeezed out and the Jurassic strata are directly in contact with the Paleozoic of the Nogueres thrust sheet (Figure 3.2a).

In section 3.7, we use these observations to put forward a case for salt tectonic activity during the Cretaceous rifting and the Cenozoic orogeny. In the following sections, we focus on observations for the syn-orogenic evolution of the intramontane conglomeratic basins. In view of the variability of the alluvial systems through space and time, we describe them unit by unit using the allogroup classification by Mellere and Marzo

(1992) for the La Pobla basin, but incorporating some modifications in the stratigraphy (Figure 3.3).

The Espills allogroup (Middle Lutetian)

The Espills allogroup (ICGC, 2009) is the first unit above the basal unconformity in the Gulp basin. In the southern area, the Espills conglomerates are deposited in a low angle unconformity with the Cuisian Montanyana group of the Tremp-Graus basin (Figure 3.1c). The Espills strata dip about 10 degrees N and the underlying Cuisian layers are close to horizontal.

The maximum vertical thickness of the allogroup is 110m (ICGC, 2010). To the north, the Espills conglomerates onlap and pinch out against the Alveolina limestone ridge of the Tremp-Graus basin (Figure 3.2a). Paleocurrent directions in the Espills allogroup are SSW directed and the clast composition is mainly Paleozoic, with a significant number of metamorphic clasts and granites (Figure 3.5b), indicating a northern provenance. Within the Espills allogroup there are also clasts with provenance from the Mesozoic and Tertiary cover, as well as Triassic dolerites (ophites). Although no studies have conclusively dated the Espills allogroup yet, based on the correlation with the units above, this allogroup has been assigned to the Middle Lutetian (Beamud et al., 2003; ICGC, 2010), older than the Pessonada Allogroup.

The Gulp allogroup (Upper Lutetian)

The Gulp allogroup (ICGC, 2010) was deposited unconformably above the Espills allogroup. ICGC cartography divided this allogroup in four units: Gulp 1, 2, 3 and 4, based on mappable photohorizons, with a total thickness of about 500m.

The Gulp conglomerates also register the tilting to the north, with dips of 10 to 20 degrees towards the N and NE. The northern extent of the allogroup is limited by the Upper Cretaceous limestone and sandstone ridges of the Tremp-Graus basin, where the Gulp allogroup units onlap and pinch out. The paleocurrents in the Gulp units are SSW directed (ICGC, 2010), recording a northern provenance mainly constituted by Devonian limestones and calcareous slate clasts (calcshists), metamorphic rocks and scarce granites. There is also an important fraction of Triassic ophitic dolerites and Lower and Upper Cretaceous clasts (Figure 3.5c and d).



Figure 3.5. Images of clast-counting stations, illustrating different clast lithologies (locations in Fig.2a). (a) Mon-10, Montillobar conglomerates. (b) Mon-3, Espills allogroup. (c) Mon-5. Gurp allogroup, unit 1. (d) Gurp-5. Gurp allogroup, unit 4. (e) Montsor-1, Pallaresa allogroup, Montsor fan. (f) Montsor-3, Pallaresa allogroup, Montsor fan. (g) Sent-1, Senterada allogroup, unit 1. (h) Ant-2, Antist allogroup. Dev Ist: Devonian limestone; Mz Ist: Mesozoic limestone, Gr: Granite; P-T sst: Permo-Triassic sandstone; Bunts: Buntsandstein conglomerate; Culm: Culm conglomerate and sandstone; Of: Ophiolite; Sil met: Silurian metamorphic schist; Dev sch: Devonian schist; UK Ist: Upper cretaceous limestone; LK Ist: Lower cretaceous limestone; Met: Metamorphic rock fragment; Ter sst: Tertiary sandstone.

The Pessonada allogroup (Late Lutetian)

The Pessonada allogroup (Robles and Ardévol, 1984; Mellere and Marzo, 1992), named after the conglomerate ridge east of La Pobla de Segur, is the first and southernmost in the La Pobla basin. It has a thickness of about 1000m (Mellere, 1993) and lays directly on the basal unconformity, flat or tilted to the north in this part of the La Pobla basin (Figure 3.3a). There are smaller-scale angular intraformational unconformities related to minor thrusts (Mellere and Marzo, 1992). The Pessonada conglomerates dip 30 to 40 degrees N, in the apparent downlap against the basal unconformity. The unconformities within the Pessonada conglomerates have been attributed to the displacement of the Morreres backtrust (Beamud et al., 2011), but we reinterpret them as halokinetic unconformities caused by the tilting of the basin edge.

The Pessonada allogrup is the proximal and middle part of a locally sourced alluvial fan. Paleocurrent directions are mostly SSW orientated (Mellere, 1993). However, cobble imbrications suggest that additional smaller fans were sourced from the E and S. The conglomerates are clast-supported and their composition is almost exclusively Mesozoic micritic grey limestones, probably Cretaceous in age, as well as minor Upper Cretaceous sandstone (Mellere, 1993; Rosell et al., 1994). Magnetostratigraphic data places the base of the Pessonada allogroup in the upper Lutetian at 44My (Beamud et al., 2003, 2011)(Figure 3.3).

The Ermita allogroup (Uppermost Lutetian to Bartonian)

The Ermita allogroup (Robles and Ardévol, 1984; Mellere and Marzo, 1992) is a fan-delta system which progrades into lacustrine environments to the south, and reaches a total thickness of 200-250m (Mellere, 1993). The Ermita conglomerates overlie the Pesonada allogrup in the south of the La Pobla basin, while to the north they sit on top of the flat basal unconformity (Figure 3.4a).

As is the case in the Pessonada allogroup, the clast composition of the Ermita conglomerates is local Mesozoic limestone and paleocurrents are also SSW directed. The Ermita allogroup also crops out in the eastern sector of the Gulp basin, overlying the Gulp allogroup, with a vertical thickness no greater than 100m.

Based on mammal fossil chronostratigraphy and magnetostratigraphy, the Ermita allogroup sedimentation happened near the Lutetian-Bartonian boundary, at ~41-40My (Beamud et al., 2011)(Figure 3.3).

The Pallaresa allogroup (Bartonian to Rupelian)

The Pallaresa allogroup (Mellere and Marzo, 1992) comprises five interfingering alluvial fan systems, with different composition and provenance: Collegats, Roc de Santa, Roca del Pesó and Montsor in the La Pobla Basin, and Camporan fan in the Gurp basin.

The lower ones lie unconformably over the Gurp and Ermita allogroups (Figure 3.4a and b). Towards the north of the Gurp and La Pobla basins, the Pallaresa allogroup conglomerates lie directly above the basal unconformity over the Mesozoic. In this area, the basal unconformity transitions from being flat-lying in its lowest point in the Noguera Pallaresa valley, to become irregular and climbing up the uplifted carbonate ridges of the northern margin of the Organyà basin (Figure 3.4b and c). The conglomerates of the La Pobla basin cut across the ridges of Perecalç and Cuberes ridge, the most likely entering points of the alluvial systems into the basin. Dips in the La Pobla basin for the Pallaresa allogroup are around 10 to 30 degrees towards the north and NW. In contrast, the conglomerate beds of the allogroup in the Gurp basin are tilted to the east (dips of 15 to 25 degrees NE). This eastward component is likely depositional, since the conglomerates truncate the Sant Gervàs cretaceous ridge and progressively onlap to the north (Figures 3.2 and 3.4c). The erosive incision indicates a possible entry point of the conglomerate sediments into the basin.

The Pallaresa allogroup in the La Pobla basin transitions gradually from the Ermita allogroup. The Collegats system maintains a very local source area and small size (2km² extension and 200m thick). Between the Noguera Pallaresa and Flamisell valleys, the Collegats system interfingers with the Montsor fan system (Rosell and Riba, 1966; Robles and Ardévol, 1984), around 800m thick (Beamud et al., 2003) and active during the entire sedimentation of the Pallaresa allogroup. Montsor fans covered larger areas (more than 50km²) (Mellere, 1993). In the south, the Montsor layers sit on top of the basal Collegats system, dipping between 8 and 27 degrees to the N. In the Flamisell river valley, the Montsor conglomerates directly onlap the basal unconformity over the Lower

Cretaceous palaeoreliefs (Figure 3.4b). On top of the Collegats system in the SE of the La Pobla Basin, the Roc de Santa system dips around 20 degrees to the NE and show W-directed palaeocurrents. The Roca del Pesó system infill the Lower Cretaceous palaeoreliefs in the northern La Pobla Basin (Figure 3.4d). The irregularities in the basal unconformity cause a variety of dips, but the regional dip to the north is still predominant.

Barsó (2007), loosely assigned the Pallaresa allogroup of the Gulp basin to the Montsor alluvial fan system. However, our new clast counting results (Figure 3.6) show very different clast composition between the stations in the Montsor fan in the La Pobla basin, and the fan in the Gulp basin. The most remarkable difference is the presence of Carboniferous Culm clasts in Montsor fan (Fig 3.5d and 3.6) and their total absence in the Gulp basin (Camporan area), which indicate two time-equivalent fans but with different catchment areas. Hence the Gulp and La Pobla upper Pallaresa allogroup conglomerates belong to different fans, even if time-equivalent. We have named the newly identified fan at Gulp the Camporan fan, after the name of the highest peak in the Serra de Gulp (Figs. 3.2 and 3.3).

The Pallaresa allogroup fans were active from the Lutetian-Bartonian boundary to the late Priabonian, about 34 My ago (Beamud et al., 2011). Previous studies (Mellere and Marzo, 1992; Mellere, 1993; Beamud et al., 2003; Barsó, 2007) considered the upper part of the Serra de Montsor succession as belonging to the Oligocene Senterada and Antist allogroups (Figure 3.3). In the following sections, we discuss the reasons to keep the conglomerates of the upper part of the Serra de Montsor within the Pallaresa allogroup.

The Senterada allogroup (Rupelian to Chattian)

The Senterada allogroup (Mellere and Marzo, 1992) has been reported as cropping out in the upper part of the Serra de Montsor in the La Pobla basin, as well as in the Senterada basin to the north, which is a narrow E-W trough disconnected from the Pobla basin to the south (Figure 3.2a). The Senterada basin section is around 400m thick (Beamud et al., 2011), and in the present day it is considerably lower in the topography. Progressive unconformities within the Senterada allogroup (Saura, 2004) open to the

north and onlap against the margin of the Faiada Lower Cretaceous minibasin (Saura et al., 2016). The lower units have very irregular dip directions as the beds are infilling an irregular topography, usually sitting directly above the Keuper evaporites and ophites (Figure 3.2). The clasts in this basal unit are heterometric and angular, indicating limited transport, and Permo-Triassic and Devonian lithologies reflect the composition of the nearby Nogueres sheet. Saura (2004), named these deposits Sarroca group, after the locality to the NW of Senterada.

The Senterada allogroup conglomerates are here divided into three different units. The lower one is characterized by dominant Permo-Triassic clasts (Figure 3.5g), the second is predominantly made up of Devonian and Carboniferous clasts, and the third without a clear lithologic predominance. The third unit of Senterada is usually matrix-supported and heavily weathered, so the poor outcrop conditions challenge a systematic clast composition analysis. The matrix in the Senterada conglomerates is composed of fine-grained material with reddish coloration, characteristic of the Buntsandstein sandstone and lutites. It is worth noting that, within the Senterada basin conglomerates, the Mesozoic carbonate clasts are almost non-existent.

The age of the Senterada allogroup, determined by palaeomagnetism in the Senterada basin profile, has been determined as Rupelian to early Chattian, 33 to 27My (Beamud et al., 2011). The magnetostratigraphic profiles by Beamud et al. (2011) in the Pallaresa allogroup were sampled across a continuous section from the base of the allogroup to halfway up the Montsor mountain. The sampling was resumed at the base of the Senterada basin in the Flamisell valley, assumed to be time-equivalent to the upper part of Serra de Montsor, attributed to Senterada and Antist allogroups. As a consequence of the sampling interruption, the data show a hiatus of around 3My (34-31My) between the last sample in the Montsor mountain and the first sample in the Senterada basin. However, the stratigraphic succession at Serra de Montsor ridge appears fairly continuous, with no major unconformities or identifiable paraconformities. We have not observed any significant change in the clast composition between the lower Montsor fan and the conglomerates in the upper part of the ridge. For this reason, we assign the upper part of the Montsor mountain to the Pallaresa allogroup (Figure 3.2 and 3.3), and not to the Senterada and Antist allogroups as defined in the separate Senterada basin

which, in contrast, do present a significantly different composition from the Montsor fan (Figure 3.6).

Another important reason to consider the upper part of the Serra de Montsor ridge as not equivalent to the Senterada basin conglomerates is the present-day difference in topographic elevation between the two. While the base of the unsampled upper section of the Montsor mountain is around 1330m high, the base of the conglomerates in the Senterada basin succession is around 800m high in the Flamisell and Bòssia river valleys (Figure 3.2). To sediment on top of the Montsor ridge, the north-derived Senterada alluvial systems would have had to climb up a topographic difference of more than 500m. This appears to be an unlikely scenario, taking into account the height of the Lower Cretaceous ridges. We consider that a potential sinking of the Senterada basin, or an uplift of La Pobla basin due to a late-Oligocene to Miocene backthrust after the deposition of the Senterada and Antist conglomerates would not account for the compositional differences between the upper Montsor ridge and the Senterada basin.

Instead, we interpret that the small scale of the alluvial fans (with very local provenance and matrix support) and the significant height of the Lower Cretaceous ridges prevented the Senterada conglomerates to overspill into the upper parts of the La Pobla basin. We favour the idea that Senterada conglomerates had a very local catchment area within the nearby Nogueres thrust sheet (hence the mainly Permo-Triassic and Devonian composition, Figures 3.5g and 3.6).

The Antist allogroup (Chattian)

The Antist allogroup, 300m thick (Mellere and Marzo, 1992), has been reported to crop out in the Senterada basin and in the upper part of the Serra de Montsor in the La Pobla basin. As the upper Senterada unit, the Antist conglomerates are very coarse and matrix-supported, so the outcrop conditions are an impediment to a systematic composition analysis. The Antist alluvial fan is very proximal and contains a clast composition characteristic of the Nogueres thrust sheet, predominantly Devonian limestones and Permo-Triassic red clasts. Triassic ophites, green quartzites, and marbles are common clasts as well. To the west there are local areas with abundant granite clasts (Figure 3.5h). The presence of Carboniferous Culm sandstones has also been reported for the

eastern area. The Antist allogroup is not deformed or tilted, so it has been stated that the Antist conglomerates register the end of the Pyrenean deformation in this area (Mellere and Marzo, 1992; Beamud et al., 2003).

The age of the Antist system has been determined as Chattian, 27-24My (Figure 3.3), and it is time-equivalent to the Sis Collegats alluvial system in the Sis valley (not to be mistaken with the Pallaresa allogroup Collegats system) and the Graus fluvial sediments of the Tremp-Graus basin (Beamud et al., 2011).

3.5. Clast-counting lithology results

A profile through the Gulp basin records significant changes in provenance from base to top. The Montllobar conglomerates (Figure 3.5a), from the underlying Montanyana group, the upper part of the filling of the Tremp-Graus syncline, are mostly sourced from Mesozoic and Tertiary carbonates from the surrounding palaeoreliefs (69%). However, the proportion of Paleozoic clasts is around 31%, indicating a clear northern provenance already in the late Ypresian (Figure 3.6, complete results can be found in table in the supplementary material in this chapter).

In the Lutetian Espills unit (Mon-3 station) (Figure 3.5b) over 50% of the clasts derive from Paleozoic rocks: Silurian black slates (10,9%) and Devonian brown limestones (14,6%) and calcareous slates (29,3%) with occasional granite (1,2%) and gneiss (1,2%) pebbles. Post-Paleozoic lithologies are in a lesser proportion: Tertiary calcarenites (12,2%), Alveolina limestone (4,9%), Micritic grey limestone (19,5%), Orbitolina limestone (5,3%) and rudist limestone (1,2%). It is also worth noting that 4,9% of the clasts are Triassic ophites, despite this being a weak lithology that quickly weathers during transport. This proportion is similar to that of the lower sections of the overlying Gulp allogroup (Figure 3.5c).

Several counting stations were analysed in the Gulp allogroup (Figures 3.2, 3.5c, 3.5d and 3.6): the allogroup is mainly constituted by clasts of grey micritic limestones (42,7% Gulp 1; 21,4% Gulp 2; 30,3% and 27,2% Gulp 3; and 15,3% and 28,9% Gulp 4), Devonian limestones (18,6% Gulp 1; 8,3% Gulp 2, 11,2% and 18,5% Gulp 3; 24,7% and 11,1% Gulp 4) and Devonian calcareous slates (13,3% Gulp 1, 36,9% Gulp 2, 29,2% and 19,8% Gulp

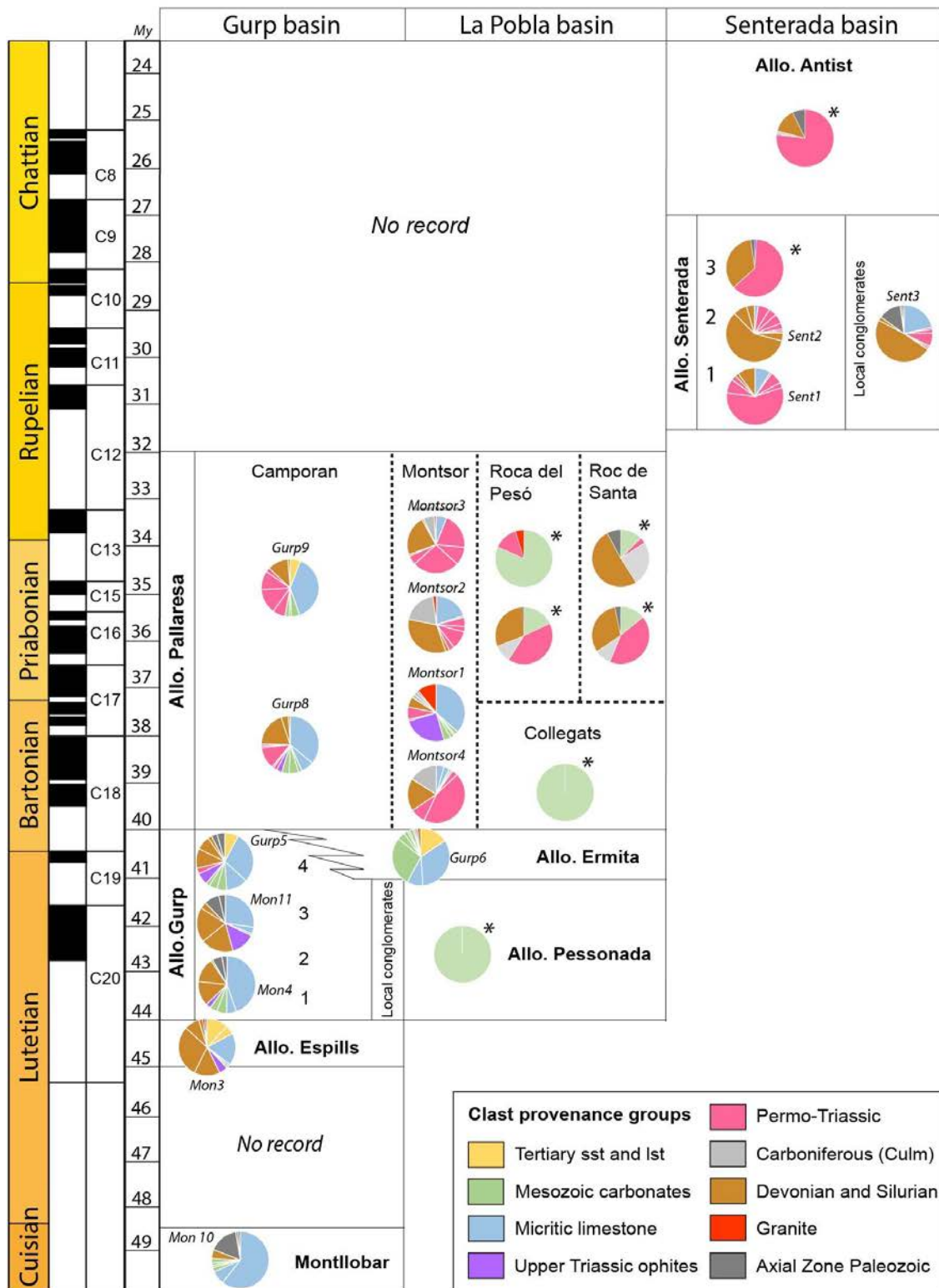


Figure 3.6. Pie charts documenting the clast lithology percentages in the counting stations. Location of samples in figure 2. The charts marked with * are from Barsó (2007).

3, 12,9% and 7,8% Gurp 4) . Triassic ophites (2,7% Gurp 1; 9,5% Gurp 2, 9% and 13,6% Gurp 3; 14,1% and 6,7% Gurp 4) are also well represented. Minor proportions of Axial Zone metamorphic pebbles (8% Gurp 1, 1,2% Gurp 2, 1,1% and 12,3% Gurp 3, 5,9% and 7,7% Gurp 4) and granites (around 1% in Gurp 2, Gurp 3 and Gurp 4) have also been found. It should be noted that the Permo-Triassic clasts are absent in the Espills, Gurp 1, Gurp 2, Gurp 3 units and in the lower and middle part Gurp 4 unit (Figure 3.5d). These begin to appear at the top of Gurp 4 unit (3,3%) and are common throughout the Camporan unit (Pallaresa allogroup) at the top of the Gurp basin (17,5 to 34,2%). These Permo-Triassic clasts mainly derive of detrital red beds. White to green colored ignimbrite clasts are also occasionally found.

The Ermita allogroup in the Serra de Gurp section (Gurp-6 station) is predominantly composed of 82,1% Mesozoic cover (42,4% grey micritic limestones, 38,8% Mesozoic carbonates, and 1,1% ophites). Tertiary sandstone and limestone clasts (15,6%) are also present. Additionally, there is an occasional appearance of Devonian limestones (2,2%)(Figure 3.6), very similar to the proportions reported by Mellere and Marzo, (1992) and Barsó (2007) for the La Pobla basin. However, the finding of epidote detrital grains in the Ermita allogrup of the La Pobla basin may indicate that the catchment area went through of Triassic ophites.

The transit from the Gurp to the Pallaresa allogroup, where the Ermita group is absent (Gurp-8 station), is marked by an increasing proportion of Permo-Triassic clasts (17,5%). Silurian black slates (1%), Devonian calcareous slates (4,1%) and Devonian ochre limestones (19,6%) clasts are still present in a significant proportion (24,6%). The Mesozoic lithologies (grey micritic limestones 43,3%, Orbitolina bearing limestones (5,2%), undifferentiated Mesozoic carbonates (6.3%), ophites (3,1%) represent more than half of the clasts throughout the Pallaresa allogroup in the Gurp basin. To the top of the Pallaresa Allogrup (Gurp-9 station) in the Gurp basin (Camporan fan), the presence of Mesozoic lithologies decreases (47.1%) and Permo-Triassic (34,2%) clasts increase with a minor contribution of Devonian limestone (11,8%) and Axial Zone clasts (1,2%).

Clast-counting data in the Montsor system of the Pallaresa allogroup of the La Pobla basin (Figures 3.2, 3.5e, 3.5f and 3.6), in contrast, provides significantly different results.

The Mesozoic clasts content is much lower than in the Gulp basin, ranging from 20% to just 6% in the upper part. The proportion between Permo-Triassic clasts on the one hand, and Silurian and Devonian on the other, varies throughout the unit. At the base (Montsor-4 station), the proportion of Permo-Triassic pebbles is 55,9% while for Silurian and Devonian clasts it is 18,3% and for grey Mesozoic limestones it is 7,5%. An important observation is the presence of Carboniferous Culm sandstones and microconglomerates (Figure 3.5f) in a proportion of 16,1%, even though this lithology is completely absent in the Gulp basin succession. The Montsor-1 clast-counting station (Figure 3.5e) is located in a bed with unique clast proportions, to such an extent that the layer has a distinct colour in the outcrop and it can be distinguished in aerial images, so much that the bed was specifically mapped in the 1:50000 geological map Tresp chart (Rosell et al., 1994). This is due to a comparatively high proportion of Mesozoic carbonates (45%), some of them light-coloured, and green ophites (25%) together with a significant presence of granites and leucogranites (10,9%). This is the highest proportion of ophites reported in the entire conglomerate succession. Permo-Triassic (7,9%), Devonian limestones (5,9%) and Culm clasts (2%) are also represented.

In the following stations in Serra de Montsor succession (Montsor-2 and Montsor-3 stations) (Figure 3.5f) the Permo-Triassic clasts increase significantly towards the top (21,8% Montsor-2; 55,9% Montsor-3) together with Silurian and Devonian clasts (35,4% Montsor-2; 24,4% Montsor-3). The proportion of Culm clasts increases and then decreases to the top (19,8% Montsor-2; 6,1% Montsor-3). Mesozoic carbonates (19,8% Montsor-2; 6,1% Montsor-3) decrease from base to top. There are no clasts of green ophites and the weathered granites, frequent in the white layer appear in very minor proportions in the upper part of the succession (2,1% Montsor-2, 1% Montsor-3).

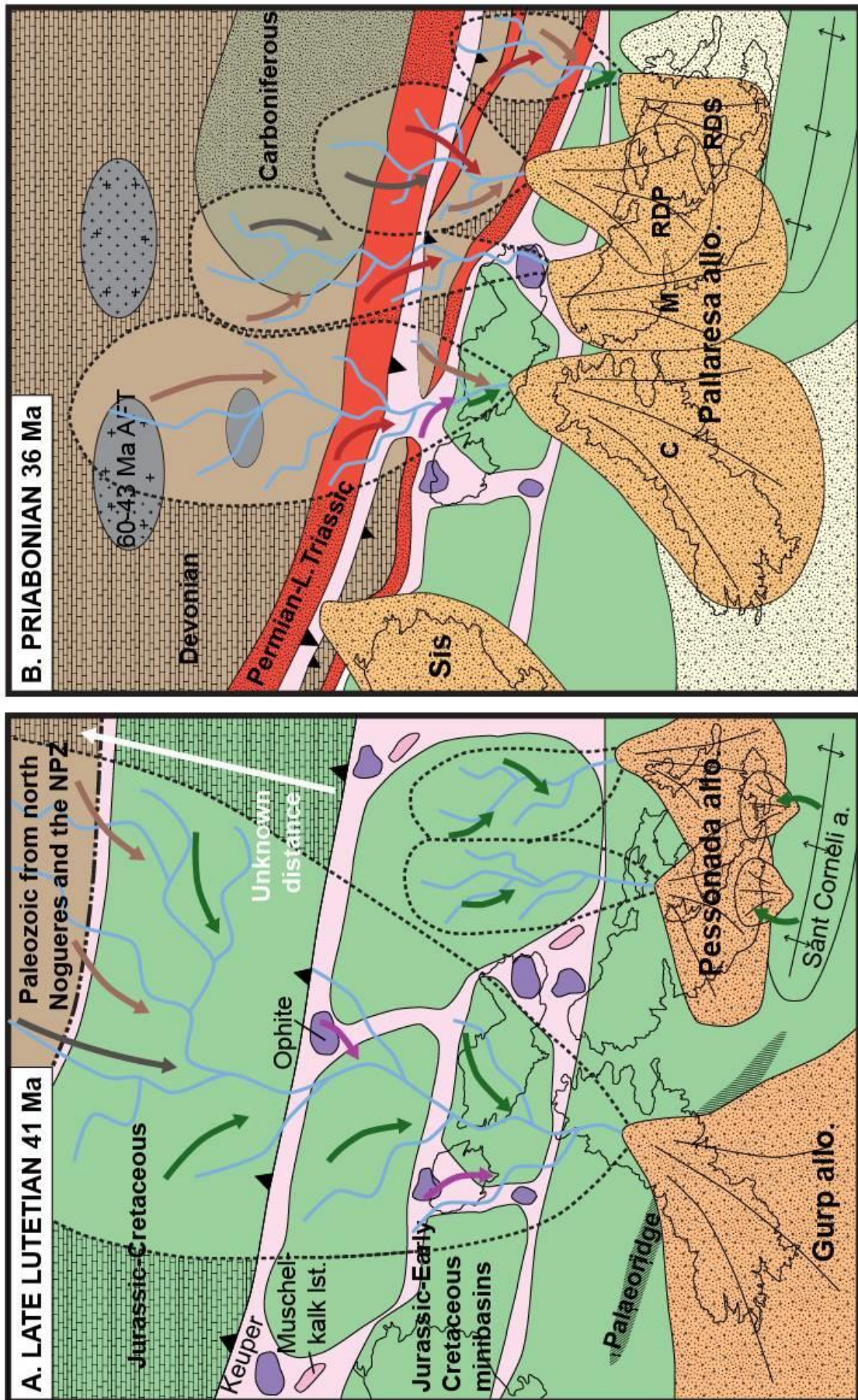
The results of the Senterada basin reveal a very different clast composition between the Senterada 1 unit (Sent-1 station; figures 3.5g and 3.6), with predominantly cobbles of Permo-Triassic lithologies (78%) in a fine-grained matrix of red sand, and the Senterada 2 unit (Sent-2 station; Figure 6), mostly composed of Devonian clasts (76,4%, with brown crinoidal limestone and pink *Goniatites*-bearing limestone of Griotte facies). In this latter unit, the Permo-Triassic conglomerates and sandstones are in 21,3%, whereas Mesozoic limestones are represented in a very minor proportion (2,2%). The upper Senterada 3

unit has very poor outcrop conditions, due to the high proportion of matrix content, so we were unable to set a clast counting station in any of the areas surveyed. It has been reported as having a clast proportion of approximately half Devonian limestones and half Permo-Triassic clasts (Barsó, 2007). The poor outcrop conditions have also prevented systematic clast-counting in the Antist allogroup. Field observations have shown that clast composition within the Antist allogroup varies in different outcrops. In certain there is a predominance of granite clasts (Figure 3.5h), while in other areas the predominance is pebbles of Buntsandstein conglomerates and sandstones and Devonian limestone clasts (Barsó, 2007). Axial Zone well-rounded metamorphic clasts as green quartzites with folded quartz veins, marbles, dark-metasandstones, slates and quartz pebbles are lithologies widely represented.

3.6. Evolution of alluvial fan catchment areas

The middle Lutetian Espills allogroup at the base of the Serra de Gulp succession has no time-equivalent in the La Pobla basin. It is composed of 50% of Paleozoic clasts, mostly originated in Devonian and Silurian lithologies of the Nogueres thrust sheet but with the occasional appearance of granite and gneiss pebbles. The upper Lutetian Pessonada allogroup fans in the La Pobla basin are entirely composed of Cretaceous carbonate clasts, while the equivalent Gulp allogroup fans in the Gulp basin have around 40-60% of clast composition from the Nogueres Devonian and Silurian, metamorphic clasts and Triassic ophites (Figure 3.6).

Based on the counting results and the geometrical observations in section 3.4, we interpret the Pessonada allogroup as a small system of local alluvial fans sourced from Cretaceous carbonate minibasins that probably existed to the north over the Senterada salt province (now eroded), equivalent to the Ribagorça diapir and minibasin province (i.e. Saura et al., 2016), and from the northern margin of the Organyà basin (Figure 3.7a). To the southern part of the basin, the Pessonada alluvial fans likely overlapped the relief of the Sant Corneli anticline, which could have also provided carbonate clasts in smaller-scale flows. In contrast, the catchments of the Gulp fans (Espills and Gulp allogroups) were much larger, extending throughout a larger area in the hinterland (Figure 3.7a). Although an important contribution was from the Cretaceous reliefs immediately to the



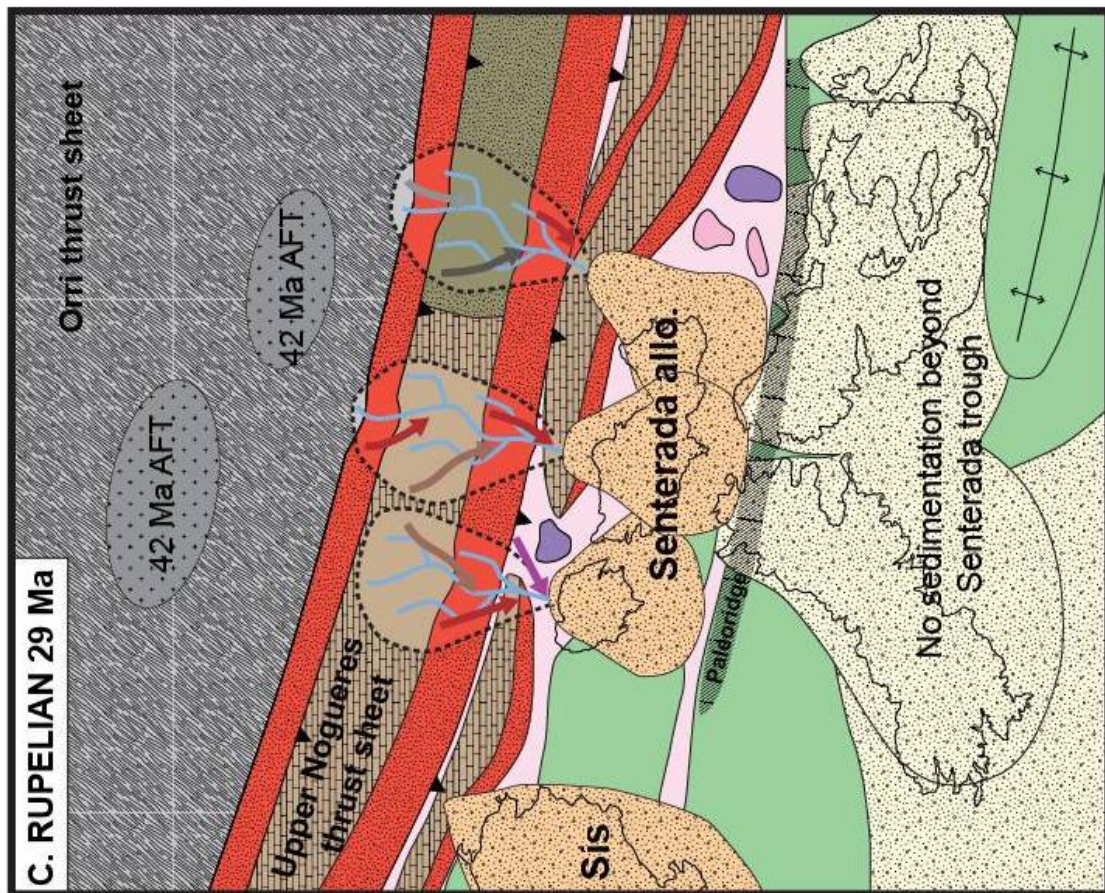
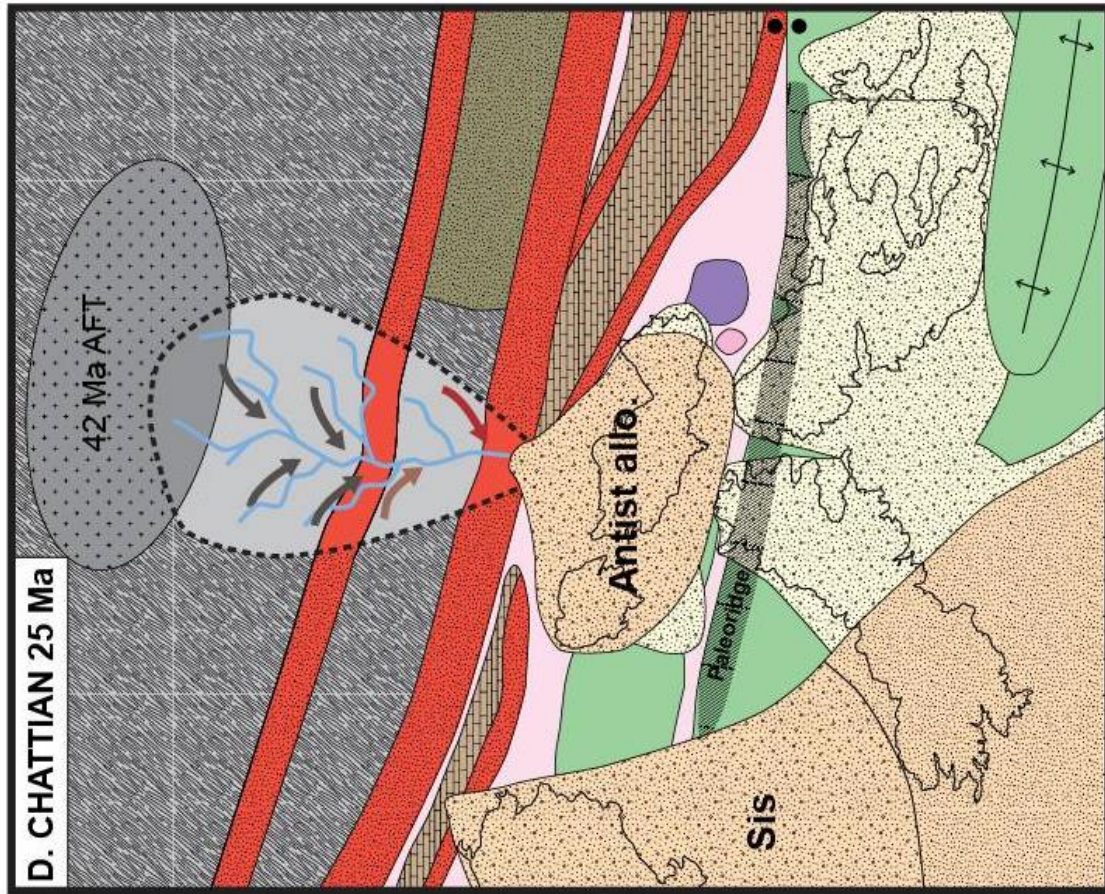


Figure 3.7. Palaeogeographical reconstruction showing the evolution of the intramontane alluvial fans and their catchment areas from Late Lutetian to Late Oligocene. AFT data from Beamud et al., 2011. C, Camporan fan; M, Montsor fan; RDS, Roc de Santa fan; RDP, Roca del Pesó fan.

north, the catchment area extended up to the exposed salt province, supplying the Triassic ophitic dolerites, as well as further north into the Nogueres thrust sheets supplying Devonian and Silurian clasts. The absence of Permo-Triassic clasts in the Espills and lower Gulp allogroups, suggests that the Paleozoic clasts were sourced from an area where Cretaceous carbonates were directly overlying the Silurian and Devonian (Figure 3.7a). The omission of the Permo-Triassic succession is most probably caused by a northern termination of the Permo-Triassic basins in the Nogueres thrust sheet (as inferred in the Nogueres reconstruction by Teixell et al., 2018, and similarly to what happens in parts of Axial Zone today). The precise position of the northern limit of the Permo-Triassic basins and the extent of the Mesozoic cover during the Late Lutetian are unknown.

The granite and gneiss pebbles however, were sourced by more distant areas. The most likely source are the Lower Paleozoic gneiss massifs and Hercynian plutons like those of Castillon, Trois Seigneurs and Lacourt, located at the root of the Nogueres thrust sheet in the North Pyrenean zone (following the tectonic reconstruction by Teixell et al., 2018). These massifs have AFT and ZFT cooling ages from the Late Cretaceous to the early Oligocene (Sinclair et al., 2005; Whitchurch et al., 2011), therefore it is possible that they were exposed at the surface by the late Lutetian, the age of sedimentation of the first alluvial fan of the Gulp basin. This is further supported by fission-track cooling ages of 75-55Ma in clasts of the upper Gulp and Pallaresa allogroups in the Gulp basin (Michael, 2013) and geomorphological criteria that place the middle Eocene watershed past the North-Pyrenean zone (Ortuño and Viaplana-Muzas, 2018). It is worth noting that the crystalline massifs of the present-day Axial Zone yielded younger fission-track cooling ages (centered on 45-30My), with which they are unlikely sources for the Lutetian conglomerates.

Regarding clast composition, the Bartonian-Priabonian Pallaresa allogroup systems can be separated into two groups: on one hand local fans (Collegats system) predominantly sourced from adjacent reliefs formed by Mesozoic carbonates, and on the other, more extensive fans with larger catchment areas predominantly sourced from the Nogueres

thrust sheet Siluro-Devonian, Carboniferous and Permo-Triassic rocks (Camporan, Montsor, Roca del Pesó and Roc de Santa systems)(Figure 3.6 and 3.7b). The abundance of Buntsandstein and Permian clasts in all the Nogueres-sourced fans indicates that the leading edge of the thrust sheet, containing the Permo-Triassic lithologies, was cropping out during the Bartonian.

The almost total absence of gneiss and other Lower Paleozoic lithologies within the Pallaresa allogroup fans we interpret it reflects the progressive southward displacement of the Pyrenean water divide: during the Lutetian the North-Pyrenean massifs were part of the drainage area (Roigé et al., 2017; Ortuño and Viaplana-Muzas, 2018), while in the Bartonian and Priabonian a local southward migration of the divide localized the drainage area in the southern Nogueres thrust sheet domain (Figure 3.7a and b). The few granite pebbles found within the Pallaresa allogroup could have been sourced from minor intrusions within the Nogueres thrust sheet, now eroded (Beamud et al., 2011).

The southern extent of the eastern fans in the La Pobla basin was probably still limited by the Sant Corneli anticline, while the Camporan and Montsor fans infilled the Lower Cretaceous reliefs to the north and then expanded freely to the south, stacking flat above the Pessonada, Ermita, and Gulp allogroups (Figure 3.4a and 3.4b, Figure 3.7b). The proximity between the present-day outcrops of the Camporan and Montsor systems, together with the reported dip measurements, suggests that the two could have interfingered in the area of the present-day Flamisell river valley (Figure 3.2a).

As explained in section 3.4, we consider the Oligocene conglomerates of the Senterada and Antist groups as restricted to the Senterada basin. These conglomerate systems were trapped and confined in an E-W oriented synformal trough, sitting directly above the Keuper, and finally overlapping onto the Paleozoic to the north and the Sant Gervàs and Perecalç ridges to the south (Figure 3.7c). The clast composition within the Senterada units, with predominant Buntsandstein and Siluro-Devonian limestones and slates (Figure 3.6) reflects the composition of the nearby Nogueres thrust subunits. There is very little contribution of granites or high-grade metamorphics from areas further north, indicating that the fans had small catchment areas (Figure 3.7c). In the Antist allogroup, however, the presence of Lower Paleozoic metamorphics and granite pebbles indicates that the late Oligocene the catchment areas expanded, draining also

from the plutons of the Orri thrust sheet at the core of the antiformal stack (Figure 3.7d) that was progressively unroofed during the late Eocene and Oligocene, as indicated by thermochronology (Metcalf et al., 2009).

3.7. Role of salt tectonics and basement thrusting in the evolution of the synorogenic conglomeratic basins

The conglomeratic basin evolution during mid Eocene to late Oligocene times appears very influenced by the structures inherited from the rift and post-rift stages in the Southern Pyrenees. These structures limited the extent of the synorogenic basins and acted as topographic barriers that diverted the alluvial routing systems (Figure 3.7).

From the observations of growth strata and Keuper sheets, we interpreted that for most of the Early Cretaceous rifting stage the Senterada province was already a complex salt wall system, probably exposed in the surface. The differential load of syn-rift sediments in the Organyà basin likely mobilized salt withdrawal from under the basin towards the salt walls, contributing to the rising and tilting of the northern basin margin and forming the basin-wide progressive unconformity. The northern boundary of the Organyà basin observed today is primarily the diapiric contact with the Senterada salt province (previously interpreted as the Morreres backthrust to account for Jurassic and Cretaceous layer truncations over the Keuper).

Salt wall rise was reactivated by the early Pyrenean shortening, by squeezing between the Organyà basin and the Nogueres thrust sheet emplaced onto the Keuper. The uninterrupted contribution of Triassic ophite clasts in the Gurb and La Pobla conglomerates (Figure 3.6) indicates that diapirs of the Senterada salt province were exposed at the surface throughout the entire evolution of the conglomeratic basins, between the Lutetian to the late Rupelian-Chattian (and possibly since the Early Eocene as witnessed by the Triassic clasts in the upper Montanyana group Montllobar conglomerates, Figure 3.6). This had a major effect in enabling uninterrupted load-induced salt withdrawal and associated basin tilting, that would not have happened if the salt province was covered and salt had nowhere to extrude.

On the basis of the structural and provenance data presented above, we propose new palaeogeographic and cross-section reconstructions (Figures 3.7 and 3.8) of four stages in the evolution of the intramontane conglomeratic basins of Gulp, La Pobla, and Senterada between the mid Eocene to the Oligocene.

As explained in the previous section, the Gulp and La Pobla basins were separate depocentres in the interior of a low-relief, South-Pyrenean thrust belt during the mid and late Lutetian (Figure 3.7a). Differential loading caused by the conglomerate weight triggered low-amplitude salt evacuation of the evaporites under the Organyà basin towards the Senterada salt walls (Figure 3.8a). However, the Mesozoic carbonate succession of the Organyà basin edge is much thicker compared to the synorogenic conglomerates (Figure 3.2b). For this reason, load-induced movements produce only a moderate tilting of the basin margin, reflected in the apparent north-directed downlap of the La Pobla and Gulp conglomerates against the basal unconformity and the long-lived progressive unconformity within the conglomerate beds (Figure 3.4a).

In the latest Lutetian, stacking under the Nogueres thrust sheet begun: the Orri thrust sheet was in the early stages of emplacement (Muñoz, 1992; Sinclair et al., 2005; Metcalf et al., 2009). The Nogueres thrust sheet was under further exhumation but not yet eroded enough to disconnect the downward facing leading edge from the root zone to the north. The Orri thrust sheet granites (e.g. Maladeta, figure 3.2a) have late Lutetian and younger AFT cooling ages, indicating that they were still covered by an important thickness of rock (Figure 3.8a).

From the Bartonian onwards, the Orri thrust sheet uplift completely eroded the Nogueres thrust sheet Mesozoic cover and the Cretaceous minibasins to the east of the Flamisell river (Figure 3.8b). This exposed the Permo-Triassic rocks of the Nogueres leading edge, which became the main source area for the Pallaresa allogroup fans in the Gulp and La Pobla basins (Figure 3.7b). The fact that the La Pobla fans are enriched in Carboniferous clasts, while this lithology is absent in the Gulp basin, suggests that the Gulp and La Pobla systems were different fans with distinct catchment areas, but likely interfingered in a shared alluvial plain (Figure 3.7b). The differential loading of the conglomerates and the retrogradation of the systems kept pumping salt towards the

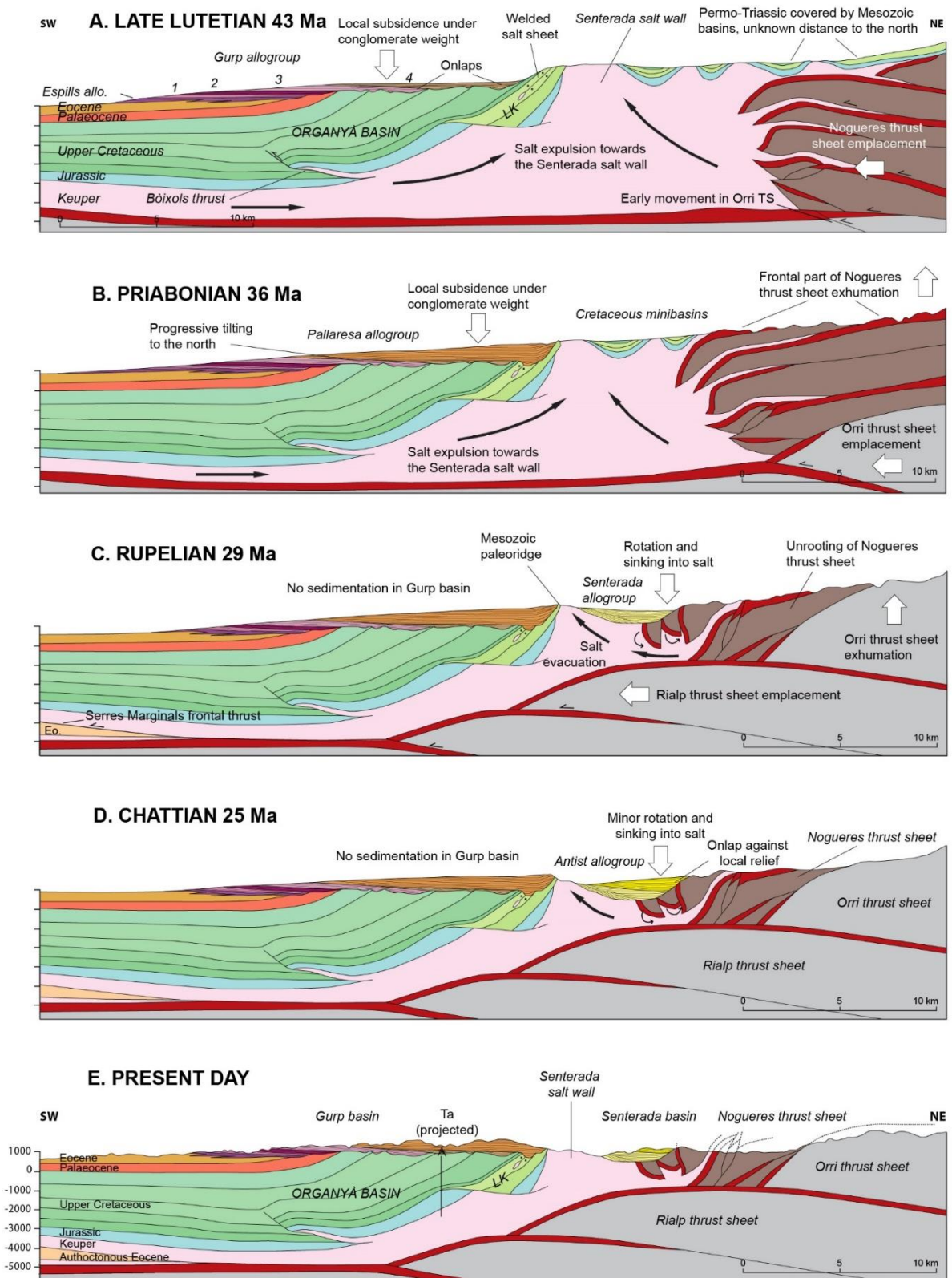


Figure 3.8. Restored cross-sections of the sequential evolution (Late Lutetian to present day) of the northern margin of the Organyà basin and the adjacent salt province as a response of the growth of the Axial Zone antiformal stack and the differential loading by synorogenic alluvial sediments. Ta, Tamúrcia well

Senterada salt province, continuing the northward tilting of the conglomeratic basins (Figure 3.8b).

Detrital AFT data from the upper Gurb and Pallaresa allogroups of the Gurb basin yield cooling ages between 75 and 55My (Michael, 2013), reflecting the ages of the Nogueres sheet emplacement. The absence of younger detrital AFT ages from the Orri sheet is consistent with the evidence gathered from clast composition, indicating that the Nogueres thrust sheet was the main contributor to the upper fans in the Gurb basin (Beamud et al., 2011).

By the start of the Oligocene, with the emplacement of the lower basement thrust sheets (Rialp and others, Muñoz et al., 2018), the leading edge of the Nogueres thrust sheet was detached from its root, and gravitationally sank into the Keuper salt (Figure 8c). Sinking into the Keuper may partly account for the strong rotation and complete overturning of the Triassic layers of the Nogueres “têtes plongées”. The immersion of the overturned thrust leading edge into the Senterada salt province, together with regional shortening, further mobilized of the underlying Keuper evaporites towards the salt diapirs. In a positive feedback loop, the loading of the conglomerates on top of the Triassic and the detached Paleozoic sheets accelerated their gravitational sinking in the salt (Figure 3.8c). This caused the development of an E-W orientated sedimentary trough along the Senterada evaporite province (a “minibasin”). The locally sourced conglomerates were confined to this depression (Senterada basin), too low to be able to climb up the Cretaceous ridges to the south and overspill onto the La Pobla basin (Figure 3.7c). Due to salt evacuation to the south, the Senterada basin depocentre progressively displaced to the north, and sediments overlapped the Paleozoic and Triassic outcrops (Figure 3.8c).

The flat-lying, late Oligocene Antist allogroup had a wider catchment area, including Axial Zone granites and metamorphic clasts from the then exhumed Orri thrust sheet, but sedimentation was still confined to the Senterada trough (Figure 3.7d). The sedimentation of the Antist conglomerates during the Chattian is contemporary to the Rialp thrust sheet emplacement. As interpreted by Teixell and Muñoz (2000) and Muñoz et al. (2018), the leading edge of the Rialp thrust sheet has significant displacement below the Senterada basin and even the northern edge of the Organyà basin (Figure

3.8d). However, the basement thrusting did not translate in deformation of the Mesozoic cover or the Eocene-Oligocene conglomerates, which crop out flat and undeformed. A possible explanation for this is that the thick Keuper accumulations within the Senterada salt province promoted the complete decoupling between the basement and the cover above. In this case, shortening was accommodated by the expulsion of great volumes of salt through the exposed Senterada salt walls and the pumping of salt towards the foreland. A second interpretation is that the conglomerates and the Mesozoic cover do not register deformation during the Rupelian because the Rialp thrust sheet did not reach that far south as interpreted. With this solution, the thick volumes of Keuper would not have extruded, and present day Senterada salt province would still have preserved several kms of vertical evaporite thickness underneath. In the restorations in figure 3.8 we have followed the first approach, relying on the displacement attributed to Rialp thrust sheet by the authors cited above. We would like to emphasize again the large initial volumes of Keuper involved in either of the two interpretations.

3.8. Conclusions

In this study we present a reinterpretation of the evolution of the intramontane conglomeratic basins in the northern part of the Southern Pyrenees based on new field observations, clast counting and revisiting previous structural interpretations taking into account the recent advances in salt tectonics. The results are illustrated in new palaeogeographic maps and a representative cross-section sequentially restored at four stages from the late Lutetian to the late Oligocene of the La Pobla, Gulp and Senterada conglomeratic basins and their drainage areas. The maps and the restored cross-section highlight the role of the interplay between hinterland basement thrusting and Keuper salt migration in conditioning the dimensions and shape of the intramontane alluvial fan systems.

Halokinesis is identified in the northern margin of the Organyà Mesozoic basin since the Early Cretaceous rifting times: thinning stratigraphy towards the Senterada salt province, progressive unconformities and interbedded Keuper lenses within the Lower Cretaceous carbonates and shales are strong evidence for salt diapirism in this epoch,

as has been recently documented in other areas of the Southern Pyrenees. Consequently, we reinterpret the Morreres backthrust structure as a diapiric contact between the northern margin of the Organyà basin and the Senterada salt wall province. The salt walls were exposed at the surface at least during the rifting stage first, and then at least from the upper Ypresian to the Oligocene, as evidenced by the widespread presence of Triassic ophite clasts in all the conglomerate units.

Alluvial fans sourced in the reliefs of the growing antiformal stack of the Axial Zone rapidly deposited the gravel load over a mobile salt-bearing substratum at its toe. From Lutetian times onwards, the differential load of the alluvial systems of the La Pobla and Gulp basins contributed to generate accommodation space and caused a moderate and progressive northward tilting of the northern Organyà basin margin, enabled by the expulsion of salt through the exposed Senterada salt province. This is reflected in the north-directed onlap of the Pessonada and Gulp conglomerates against the basal unconformity, opposite to the main sediment influx direction, and a long-lived progressive unconformity within the conglomerate succession.

During the late Lutetian, the La Pobla basin was receiving only local sediments from the Mesozoic carbonates of the extensional minibasins and northern Organyà basin margin. At the same time, the alluvial fans of Espills and Gulp allogroups drained from a much more extensive area; the North Pyrenean zone metamorphic and granite massifs likely sourced the gneiss, marble and granite pebbles, while the Siluro-Devonian limestones and slates were supplied by the Nogueres thrust sheet, not yet unrooted by erosion. By the Priabonian, the emplacement of the Orri thrust sheet uplifted the Nogueres thrust sheet and the topographic uplift of the antiformal stack initiated the migration of the watershed divide to the south. This is reflected in the increasing proportion of proximal lithologies derived from the Nogueres Zone in the Pallaresa allogroup fans, such as Permo-Triassic lithologies of the frontal part of the Nogueres sheet and Carboniferous Culm sandstone pebbles. The alluvial fans progressively retrograded to the north, infilling the palaeoreliefs of the northern Organyà basin. In any case, the total subsidence and Eocene-Oligocene strata rotation was moderate due to the thick Mesozoic succession existing between the fan conglomerates and the Keuper salt. The erosional unrooting of the Nogueres thrust sheet during the Oligocene enabled the

sinking and rotation of the detached leading edge into the evaporites of the Senterada salt province, explaining partly their strong overturning. Subsidence was enhanced by the sedimentation of the Senterada and Antist conglomerates on top, which due to load-induced salt withdrawal kept trapped into the Senterada trough, defined by the width of the salt province.

The study of the northern margin of the South-Pyrenean Central Unit revisits important observations regarding intramontane conglomerate geometries. With the addition of new structural and compositional data, and making use of salt tectonics concepts developed in the last decades we propose a new interpretation of the structural evolution of this complex area of the Southern Pyrenees. This study presents a good example of how halokinesis, induced by differential sedimentary loading, can interact with compressional structures and their unroofing, having a strong effect in basin geometry and shaping of alluvial routing systems.

SUPPLEMENTARY MATERIAL

Sample Unit	Mon10 Monlobar	Mon3 Espills	Mon4 Gurp1	Mon6 Base Gurp3	Mon11 Top Gurp3	Gurp2 Gurp2	Gurp3 Gurp4	Gurp5 Top Gurp4	Gurp6 Ermita	Gurp8 Camporan1	Gurp9 Camporan 1	Sent1 Senterada1	Sent2 Senterada2	Sent3 Senterada loc	Montsor1 Mont ophite	Montsor2 Montsor midc	Montsor3 Montsor top	Montsor4 Montsor base
Ochre sandstone	0	0	0	0	0	0	0	7,8	15,6	0	5,9	0	0	0	0	0	0	0
Ochre calcarenite	0	12,2	0	0	0	0	0	0	0	0	0	0	0	0	0	0	0	0
Alveoline limestone	0	4,9	0	0	0	0	0	0	0	0	0	0	0	0	0	0	0	0
Micritic limestone	57,1	18,3	42,7	30,3	27,2	21,4	15,3	28,9	33,3	36,1	38,8	9	2,2	21,5	36,6	19,8	6,1	4,3
Grey limestone with white veins	7,1	1,2	5,3	1,1	3,7	0	0	12,2	8,9	7,2	4,7	0	0	0	0	0	0	3,2
Ochre bioclastic limestone	0	0	0	0	0	0	0	0	0	0	1,2	0	0	0	0	0	0	0
Bioclastic limestone	2,4	0	4	0	1,2	2,4	3,5	0	27,8	2,1	0	0	0	0	2	0	0	1,1
Orbitolina limestone	0	0	5,3	1,1	0	2,4	1,2	5,6	0	5,2	2,4	0	0	0	1	1	0	0
White limestone	0	0	0	0	0	0	0	0	4,4	0	0	0	0	0	0	0	0	0
Sparitic white limestone	0	0	0	0	0	0	0	0	2,2	0	0	0	0	0	0	0	0	0
Rudist limestone	1,2	1,2	4	0	0	6	1,2	4,4	1,1	4,1	0	0	0	0	0	0	0	0
Jurassic Breccia	0	0	0	0	0	0	0	2,2	0	0	0	0	0	0	2	0	0	1,1
Marl	1,2	0	0	0	0	0	0	0	2,2	0	0	0	0	0	0	0	0	0
Intraformational mudstone	0	0	0	0	0	0	0	0	1,1	0	0	0	0	0	0	0	0	0
Black dolomite	0	0	0	0	0	0	0	0	0	0	0	0	0	0	4	0	0	0
Ophite	0	4,9	2,7	9	13,6	9,5	14,1	6,7	1,1	3,1	0	1	0	0	24,8	0	0	0
Buntsandstein conglomerate	0	0	0	0	0	0	0	0	0	2,1	7,1	7	6,7	1,1	1	5,2	20,4	3,2
Quartz	0	0	0	0	0	0	0	0	0	1	0	3	4,5	2,2	0	3,1	10,2	0
Permo-Triassic red sandstone	0	0	0	0	0	0	0	3,3	0	12,4	14,1	57	5,6	7,5	6,9	10,4	26,5	44,1
Buntsandstein white sandstone	0	0	0	0	0	0	0	0	0	1	10,6	8	3,4	1,1	0	3,1	5,1	8,6
Pumite	0	0	0	0	0	0	0	0	0	0	0	0	1,1	0	0	0	0	0
Permo-Triassic breccia	0	0	0	0	0	0	0	0	0	1	2,4	0	0	0	0	0	0	0
Permo-Triassic Caliche	0	0	0	0	0	0	0	0	0	0	0	3	0	0	0	0	0	0
Griotte limestone	0	0	0	0	0	0	0	0	0	0	0	0	1,1	1,1	0	2,1	1	0
Red limestone	0	0	0	0	0	0	0	0	2,2	0	0	0	0	0	0	0	0	0
Oxidized devonian limestone	0	0	0	0	0	0	0	0	0	0	0	2	4,5	0	0	0	0	0
Devonian limestone	6	14,6	13,3	11,2	18,5	8,3	24,7	11,1	0	19,6	11,8	10	58,4	48,4	5,9	33,3	22,4	18,3
Ochre limestone	2,4	0	0	0	0	0	0	0	0	0	0	0	0	0	0	0	0	0
Devonian limestone with chrinoids	0	0	0	0	0	0	0	0	0	0	0	0	7,9	2,2	0	0	0	0
Calcarous slate (calcschist)	4,8	29,3	13,3	29,2	19,8	36,9	12,9	7,8	0	4,1	0	0	4,5	12,9	0	0	1	0
Culm sandstone	0	0	0	0	0	0	0	0	0	0	0	0	0	0	2	19,8	6,1	16,1
Carboniferous slate	0	0	0	0	0	0	0	0	0	0	0	0	0	0	2	0	0	0
Black lutititic shale	0	8,5	1	10,1	3,7	8,3	20	2,2	0	1	0	0	0	0	0	0	0	0
Black shale with andalusite	0	2,4	0	5,6	0	2,4	0	0	0	0	0	0	0	0	0	0	0	0
Limestone with andalusite	0	0	5,3	0	8,6	0	2,4	3,3	0	0	1,2	0	0	0	0	0	0	0
Marble	0	0	0	1,1	0	0	0	0	0	0	0	0	0	0	1	0	0	0
Marble limestone	15,5	0	2,7	0	3,7	1,2	3,5	4,4	0	0	0	0	0	0	0	0	0	0
Black limestone with pyrite	1,2	0	0	0	0	0	0	0	0	0	0	0	0	0	0	0	0	0
Foliated quartz	1,2	0	0	0	0	0	0	0	0	0	0	0	0	0	0	0	0	0
Gneiss	0	1,2	0	0	0	0	0	0	0	0	0	0	0	0	0	0	0	0
Cambro-ordovician Schist	0	0	0	0	0	0	0	0	0	0	0	0	0	1,1	0	0	0	0
Quarsita	0	0	0	0	0	0	0	0	0	0	0	0	0	1,1	0	0	0	0
Granite	0	1,2	0	1,1	0	1,2	1,2	0	0	0	0	0	0	0	10,9	2,1	1	0
Total	100	100	100	100	100	100	100	100	100	100	100	100	100	100	100	100	100	100

Table 3.1. Results of the clast counting stations. Locations of the stations are in figure 3.2. The color legend is in the following page.

Categories			
a. Tertiary limestones and sandstones			
b. Mesozoic carbonates			
c. Micritic limestone			
d. Triassic dolerites			
e. Permo-triassic clasts			
f. Carboniferous			
g. Silurian and Devonian			
h. Paleozoic granites			
i. Paleozoic metasediments			

Chapter 4

*2D numerical study on folding in a
salt-detached basin*

4.1. Introduction

Thin skinned fold-and-thrust belts are the result of compression of a sedimentary cover over a weaker detachment level. The presence of salt as a detachment level results in wide fold-and thrust belts with low taper angles (Davis and Engelder, 1985). A basal detachment of salt can also accelerate the propagation of the deformation front and determine the fold geometry, given its low viscosity and that the coupling with the underlying rock units is reduced (Davis and Engelder, 1985; Costa and Vendeville, 2002). This usually leads to a pattern of regularly spaced anticlines and synclines, with dimensions and spacing (predominant wavelength, (λ_{dom})) that are dependent on the sedimentary cover and detachment level viscosity (η), thickness (h), and power law exponent (n) (Schmalholz et al., 2002):

$$\lambda_{dom} = 1,2\pi \left(\frac{\eta_{sed}}{3n\eta_{salt}} \right)^{\frac{1}{6}} \sqrt{\frac{h_{salt}}{h_{sed}}} h_{sed} \quad [1]$$

Following this equation, the thicker the pre-shortening sedimentary cover, the higher the dominant wavelength of folds will result.

The growth rate of the folding instability (q_{dom}) over the background strain-rate ($\dot{\epsilon}$) (Schmalholz et al., 2002) can be described as:

$$\frac{q_{dom}}{\dot{\epsilon}} = 2.5n \left(\frac{\eta_{sed}}{n\eta_{salt}} \right)^{\frac{1}{3}} \frac{h_{salt}}{h_{sed}} \quad [2]$$

These equations provide an accurate approximation in fold-and-thrust belts where folding dominates over thrusting. Recent numerical modelling studies incorporate additional geological parameters or variations related to salt tectonics that, as seen in natural field examples, also play an important role in the geometry and spacing of detachment folds. These include the cohesion of the sedimentary cover (Meng and Hodgetts, 2019a), syntectonic sedimentation and erosion (Heydarzadeh et al., 2020), or the presence of intermediate detachment levels within the sedimentary succession (Yamato et al., 2011; Ruh et al., 2012; Fernandez and Kaus, 2014; Meng and Hodgetts, 2019b).

In Chapter 2 of this thesis we interpreted the Serres Marginals as a salt province developed from the interaction of compressional buckling and load-induced subsidence of a sedimentary cover with pre-existing diapiric structures. The discussion in Chapter 2 presented some questions that we thought important to address through modelling. Due to the very thin pre-shortening sedimentary cover in Serres Marginals, the sedimentary load in the synclines during the compression had a major effect in influencing folding patterns. Also, from the restoration of structural cross-sections, we concluded that the erosion rate of the salt-cored anticline crests and diapiric roofs likely played an important role in determining whether these structures evolved into thrust welds or remained open. The big effect that erosion plays in influencing folding is very unique of subaerial fold-and-thrust belts (Simpson, 2006; Cruz et al., 2011; Darnault et al., 2016), and can explain some of the major differences in folding and thrusting geometries between these and submarine compressional systems involving gravity-induced salt-detachment folds (Simpson, 2006). However, due to the many factors intervening in fold-and-thrust belts affected by salt tectonics, syntectonic erosion has rarely been implemented in analogue or numerical models of fold-and-thrust belts so far.

The initial aims of this study were to provide via numerical modelling some insight on the following questions:

- 1) Under which circumstances a salt province with synclines and intervening salt anticlines and diapirs is formed during shortening without pre-existing diapiric structures?
- 2) Is the ratio of salt vs pre-shortening cover thickness a predominant factor in determining the fold spacing and geometry? How does sedimentation rate affect?
- 3) How does syntectonic erosion affect syncline subsidence? Does faster erosion accelerate depletion of the salt layer?
- 4) How does syntectonic erosion affect the transition from buckling-dominated folding to load-induced subsidence?

These questions are addressed through a modelling setup inspired in the tapered system of the Southern Pyrenees with two pre-shortening diapirs and a frontal salt pinch-out. In light of the reconnaissance of thrust-faulted or welded salt anticlines and diapirs in the Pyrenean natural examples, we also considered necessary to address specifically the products of shortening of pre-existing diapirs, testing the effect of varying initial diapir shape and other parameters as salt/overburden thickness, or syntectonic erosion and sedimentation.

In this thesis chapter I present first an overview of the experimental process leading to build a 2D setup and the lessons learned from it. Second, I focus on the systematic 2D numerical studies on folding and downbuilding with syntectonic sedimentation and erosion and the systematic study on thrusting across a single diapir.

4.2. Method

4.2.1. *Governing equations and numerical method*

For this study I worked in collaboration with Dr. Naiara Fernández from the Applied Geosciences Laboratory in the Bureau of Economic Geology to adapt the code to the setup geometry and implement syntectonic sedimentation and erosion. We use the 2D finite element code MVEP2 (Kaus, 2010; Ruh et al., 2012). MVEP2 is used to solve the equations below for incompressible rocks with visco-elasto-plastic rheology, using MILAMIN (Dabrowski et al., 2008), a MATLAB solver that allows to perform computations more efficiently. MVEP-2 code follows a Lagrangian approach, where the material properties are tracked by markers distributed randomly across the model grid. The markers get their rheological properties from the different phases defined in the setup. The location of the markers is recorded at the end of each timestep by a deformable numerical grid. As our simulations involve continuous compression, the grid will shorten and reduce its spacing for each timestep.

The numerical method uses a continuum mechanics approximation, where the governing equations are the conservation of mass and the momentum for incompressible materials with visco-elasto-plastic rheology:

$$\frac{\delta v_i}{\delta x_i} = 0 \quad [3]$$

$$-\frac{\partial P}{\partial x_i} + \frac{\partial \tau_{ij}}{\partial x_j} = \rho g_i \quad [4]$$

Where v is the velocity of the particles, x is the position, ij are the spatial coordinates, τ is the deviatoric stress tensor $\tau = \sigma_{ij} + P$, σ is stress, P is pressure, $P = \sigma_{ij}/3$, ρ is density and g is the gravitational constant.

The rheology of the sedimentary cover phase has been approached as a visco-elasto-plastic material, which follows the Maxwell visco-elasto-plastic equations where the deviatoric strain rate tensor is the sum of the three terms:

$$\dot{\epsilon}_{ij} = \dot{\epsilon}_{ij}^{viscous} + \dot{\epsilon}_{ij}^{elastic} + \dot{\epsilon}_{ij}^{plastic} \quad [5]$$

The viscous term of the equation is:

$$\dot{\epsilon}_{ij} = \frac{1}{2\eta} \tau_{ij} \quad [6]$$

The elastic term is:

$$\dot{\epsilon}_{ij} = \frac{1}{2G} \frac{D\tau_{ij}}{Dt} \quad [7]$$

Where G is the elastic shear modulus.

The plastic term is:

$$\dot{\epsilon}_{ij} = \dot{\lambda} \frac{\partial Q}{\partial \sigma_{ij}} \quad [8]$$

Where $\dot{\lambda}$ is the plastic multiplier, σ_{ij} is the total stress tensor and Q is the plastic flow potential.

The resolution of the equations and the numerical implementation in the code can be found in the articles referenced above. A comparison of MILAMIN_VEP with other codes used for modelling brittle thrust wedges and fold systems can be found in Buitter *et al.* (2016).

4.2.2. Numerical setup and boundary conditions

In the first simulations without sedimentation and in the simulations with only sedimentation (no erosion), the number of markers was 1000 in the X direction. To implement erosion, the number of markers is reduced to 300, to optimize computation time. This has no major impact in the resolution of the simulations. In the shorter single-diapir setup the number of markers in the models is 500.

The boundary conditions in setup are different for each boundary of the modelling box (Figure 4.1). For the bottom boundary there is no slip, as the basement does not deform. The right boundary of the model has free-slip condition, meaning that materials can only move parallel to the boundary, as it acts as the equivalent of an end wall in sandbox modelling. The left boundary, which acts as the moving wall, has a constant strain rate of 1^{-15} in all the simulations, a value usually used in studies on folding of visco-elasto-plastic materials (Kaus, 2010; Jourdon et al., 2020).

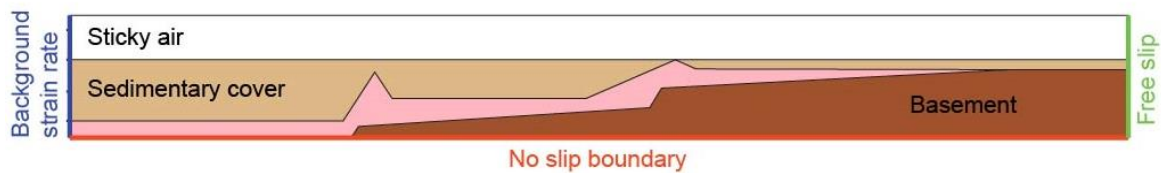


Figure 4.1. Boundary conditions and phases of the regional setup simulations

In the first simulations the upper boundary of the simulation box is the top of the rock phases and has an upper boundary condition of no stress, where the markers are free to move in any direction. This allows to create topography as the deformation progressed by deforming the top of the grid. However, the model box has to recalculate the geometry at each timestep and it becomes a slow process.

After realizing that a no-stress upper boundary was not very efficient, we tried using an internal free-stress boundary, which uses the “sticky” air approach (Crameri et al., 2012). This way, a layer of zero density and very low viscosity (1^{16} Pa/s) is added in the area between the rocks and the top boundary, simulating air. This low viscosity layer works effectively as a no-stress boundary, allowing to create topography, and to implement sedimentation and erosion. Topography is recorded by particle displacement, not requiring the constant redimensioning of the modelling box, and therefore it is a quicker

process. We did model runs of the same simulation using the two methods, and the final result did not differ significantly. For this reason, all the models from the simulation 5.0 onwards use the sticky air method.

4.2.3. Material properties

Apart from air, three rock phases are used in the modelling (Figure 4.1): a rock salt phase, a sedimentary cover phase and basement phase. The sediments in simulations with syntectonic sedimentation have the same rheological properties as the pre-shortening sedimentary cover (Table 4.1). Salt is modelled as a viscous fluid, with halite properties, with a density of 2200 kg/m³ and a viscosity of 1e-18 Pa/s (Ings and Beaumont, 2010; Mouthereau et al., 2012; Goteti et al., 2013; Fernandez et al., 2020). The sedimentary cover is modelled as a visco-plastic material with brittle behavior, with a cohesion of 20 e⁶ Pa (Yamato et al., 2011; Goteti et al., 2013) and a friction angle of 30° (Shiyuan Li et al., 2012; Goteti et al., 2013; Heydarzadeh et al., 2020). The rheological properties used for each phase are summarized in the following table:

<i>Phase</i>	Density ρ (kg/m³)	Viscosity μ (Pa/s)	Friction angle φ (°)	Cohesion C (Pa)	Elastic shear modulus
<i>Salt</i>	2200	1e 18	N/A	N/A	N/A
<i>Sedimentary cover</i>	2650	1 e25	30	20 e6	2 e9
<i>Basement</i>	2650	1 e25	30	40 e6	N/A
<i>Air</i>	0	1 e16	N/A	N/A	N/A

Table 4.1. Material properties of the modelled phases

4.2.4. Erosion and sedimentation

4.2.4.1. Aggrading reference level

Syntectonic sedimentation is implemented by vertically displacing an horizontal reference level by aggrading material at rates of 0.01, 0.015 or 0.020 cm/yr. At each time step, the newly aggraded sediments fill the empty space, for example the core of a syncline fold, up to a reference level imposed. The combination of subsidence of the

synclines and the sedimentation rate will control how much sediment is added to the system each time step. In simulations without erosion there is no mass redistribution, just an addition of sediments, which is implemented by converting from 'air phase' to 'sediment phase' all the particles below the horizontal reference level at each time step (See figure 3 in Fernandez *et al.* 2020). Each 500.000 years the layers of new sediment aggraded alternate the colours to better display the geometry and potential discontinuities (unconformities) within the syncline infills.

4.2.4.2. Hillslope diffusion

In simulations that incorporate syntectonic erosion, surface processes simulating syntectonic sedimentation and erosion are implemented using the hillslope diffusion equation:

$$\frac{\partial h_s}{\partial t} = \kappa \cdot \frac{\partial^2 h_s}{\partial x^2} \quad [9]$$

Where κ is the diffusion constant, h_s is the surface topography and x the spatial coordinate.

This equation has long been used to model geomorphological processes (e.g. Fernandes & Dietrich 1997), and more recently in numerical studies on folding with erosion (Simpson, 2006; Heydarzadeh et al., 2020). In our simulations, this equation was implemented by turning into sediment all particles of sedimentary cover phase that were above a given horizontal level. The rate at which this occurs is determined by the diffusion constant κ , which we changed in the successive model runs. The higher the κ value, the more intense the erosion is.

The difference between simulations with just sedimentation and the models with erosion and redistributed sedimentation is that instead of sediment just appearing filling the empty space below a certain horizontal level, the amount of sediment generated is proportional to the amount of sedimentary cover destroyed by erosion. An important limitation, however, is that the particles of 'phase salt' that are destroyed are also turned into sediment instead of disappearing, as it would happen by dissolution at the surface.

4.2.5. Model setup geometries

4.2.5.1. Target and model setup

The dimensions and initial geometry of the models is inspired in a simplification of the south Pyrenean fold-and-thrust belt structure (Figure 4.2). The three domains with different pre-shortening cover thickness, are roughly equivalent to: Domain A, the Serres Marginals thrust sheet, Domain B, the Montsec thrust Sheet and Domain C, the Bóixols thrust sheet. The modelling box used is 70 km long and 8 km high, where the top 3 km are 'air phase' to allow topography to develop.

The initial thickness of these domains is the same in all the model runs for domains B and C, which is 2,5 and 4 km respectively and a thickness that varies between 0,5 and 1 km for domain A. In some model runs of the experimental phase the Domain A is tapered, thinning towards the foreland.

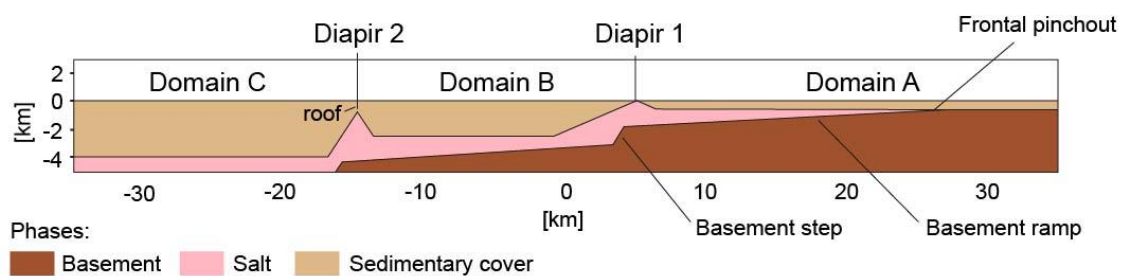


Figure 4.2. Phase distribution and geometry of the long setup

The dimensions of the model are designed to have a frontal area with a thin pre-shortening sedimentary cover that easily nucleates small wavelength folds, the Domain A, whereas the thicker domains B and C, will have tendency to tilt or fold in a much bigger wavelengths. The moving wall, adjacent to Domain C is considered the hinterland side of the model, while the opposite boundary with the salt pinch-out will be referred to as the foreland side.

Between the pre-compressional domains are the diapirs (Figure 4.2) inspired in the early diapiric structures of Bóixols and the Montsec, possibly growing since the Jurassic or Early Cretaceous, as it has been discussed in the previous sections of the thesis. From present-day geometry it is hard to estimate the original geometry of these structures at the onset of compression. However, the goal of these simulations was not just

reproducing the specific case of the Pyrenees, but more importantly, testing the influence of geometrical and physical parameters intervening in the shortening of diapir-bearing tapered basins (i.e. analogous to foreland basins or external thrust belts), so the shape of the diapirs was modified through the different simulations. This also varied the initial area of salt across the simulations.

The basement height was also changed through the successive model runs to accommodate salt thickness variations. However, in all the simulations the basement lowers towards the hinterland simulating pre-existing normal faults formed during the previous rifting stage of the natural target. The last experimental setup configurations and all the systematic series have a basement configuration as the one represented in figures 4.1 and 4.2.

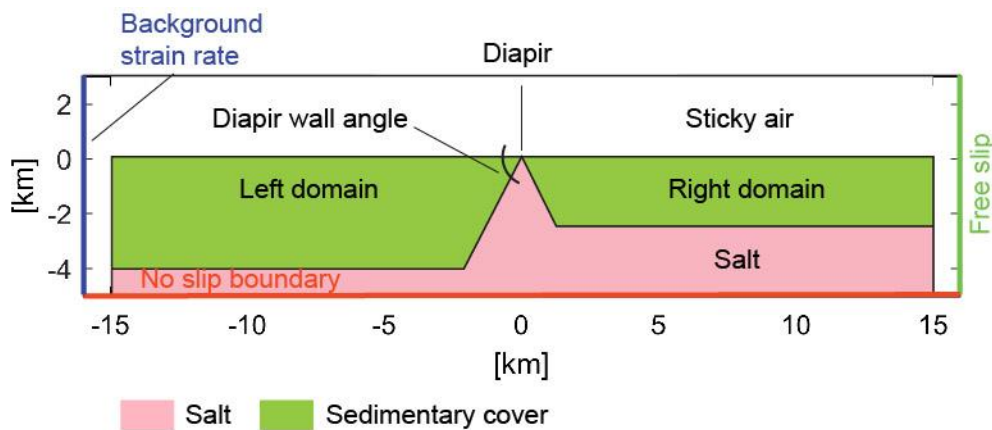


Figure 4.3. Boundary conditions, geometry and phases of the single diapir setup

4.2.5.2. Single diapir setup

The modelling box of the systematic series with the single diapir setup is 30 km long and 8 km high, and is a simplification B and C domains in the multiple-diapir setup (Figure 4.3). Boundary conditions are the same as in the previous setup and so are the rheological parameters used for the three phases (Table 4.1). There is no basement topography and the bottom boundary is no-slip.

To explore the effect of the diapir overture in combination with the relative flank thickness we have produced a series of simulations testing different angles of the diapir

margins and different levels of asymmetry in the overburden thickness at both sides of the diapir.

4.2.6. *Model runs*

We have run a total of 125 simulations, distributed in the following categories:

- 65 simulations of the multiple-diapir setup, varying geometrical and rheological parameters and implementing syntectonic sedimentation.
- 3 simulations testing the effect of increased background strain rate in the multiple-diapir setup. Such a setup resulted in unrealistic geometries.
- 14 simulations for a systematic study including syntectonic erosion and sedimentation and
- 43 simulations of the single diapir setup

All the simulation runs and the variables used are detailed in the tables at the appendix of this chapter, but to be concise I only discuss and include figures of the most representative simulations within each category. To present the results, section 4.3 gives a quick overview of the experimental process leading to a functional setup for the folding studies. Section 4.4 focuses on the three systematic studies, the first two on the effect of erosion and sedimentation on fold development, and the third one on shortening at the core of a single diapir.

4.3. Preliminary experiments to develop a functional setup

4.3.1. *Diapirs with roof: the effect of diapir width*

4.3.1.1. *Deformation of narrow diapirs (2km)*

In the first simulations diapirs were 2km wide and had a roof thickness of 0.5 km or 1 km. The basement topography had two steps and ramp which localized the salt pinch-out. The parameters that varied in this set of simulations are the thickness of the roof of both diapirs and the boundary conditions (free air instead of a no stress-boundary).

In the simulations with narrow diapirs and a basement configuration of two steps and a frontal ramp, there are two general observations (Figure 4.4):

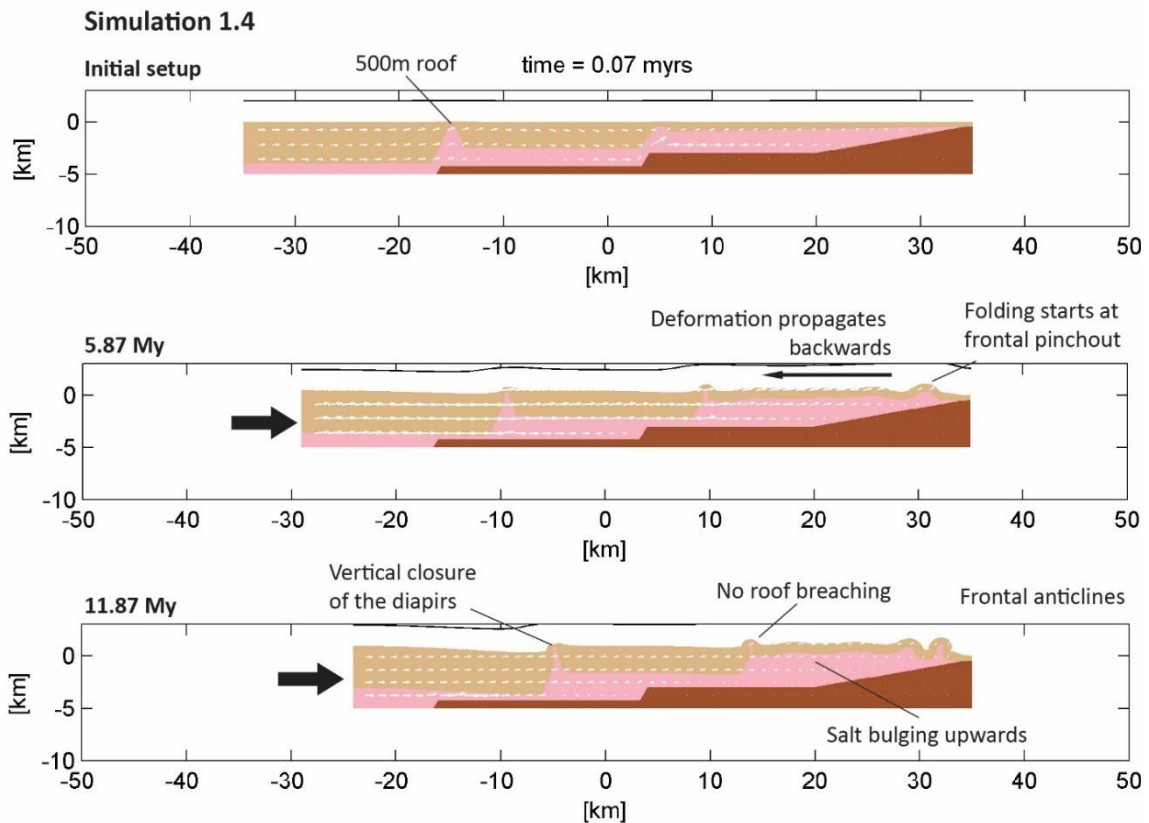


Figure 4.4. Simulation 1.4 with narrow diapirs.

A) Deformation propagates fast to the frontal part of Domain A, creating a frontal anticline, and then backwards forming new folds behind the frontal anticline but with lower topography. Salt under Domain A remains inflated.

B) The two pre-existing diapirs narrow vertically and are transported passively above the salt. No tilting or thrusting develops. Modifying roof thickness has no major effect on how deformation propagates towards the frontal part of Domain A. In none of the simulations the diapir roof has been breached.

4.3.1.2. Setups with wide diapirs

Models with narrow diapirs do not show thrusting along the cores of the pre-existing diapirs, which start to close vertically. This contrasts with the Pyrenees natural example, where Bóixols diapir (equivalent to Diapir 2 in the models), starts thrusting soon after the onset of compression. Simulations with wider diapirs (Figure 4.5) tested if extra salt and lower angle of the diapir margins would promote the closure of the diapirs and

thrusting along the core. This variable will be explored further in the systematic simulations of the single-diapir setup.

The increase in the total amount of salt in the wider diapirs translates in less folding in Domain A, as salt from the diapir cores moves towards the foreland promotes the bulging of Domain A (fig. 4.5). Only a single frontal anticline forms, verging towards the model end.

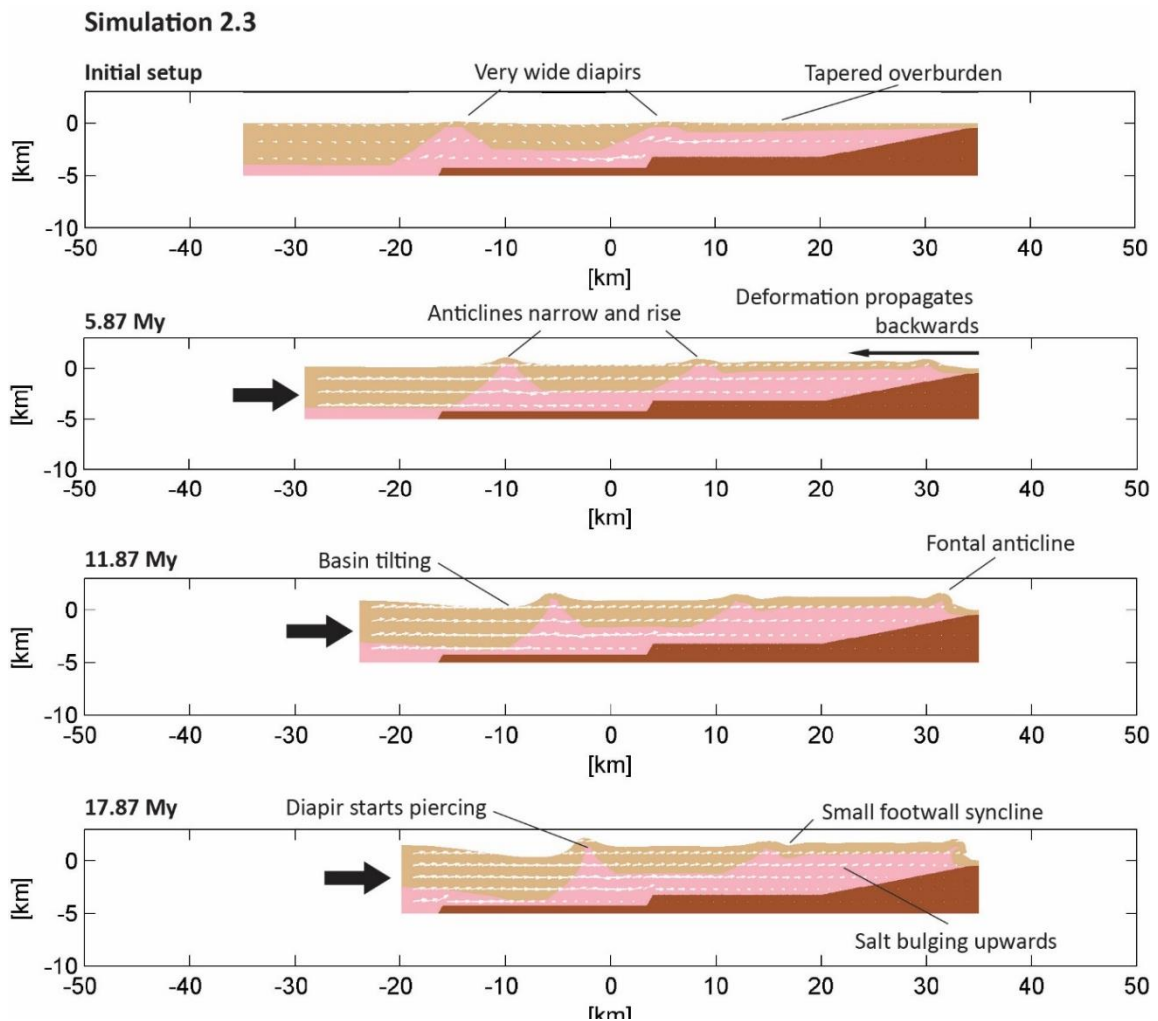


Figure 4.5. Simulation 2.3 with wide diapirs.

4.3.1.3. Diapirs without roof

Diapirs 1 and 2 still did not develop any significant thrusting across the diapir core in any of the previous model runs. Observing that in the previous model runs roof thickness had no major effect on how folding evolved in Domain A, we ran simulations with unroofed diapirs. The simulations of diapirs without roof (Figure 4.6), show incipient thrusting and suggests that the absence of roof favours forethrusting towards the

foreland. With no roof, diapirs accommodate more shortening. Part of the salt in the diapirs extrudes to the surface, but mostly salt is remobilized towards the foreland and contributes to the inflation of Domain A. The inflation of Domain A due to the excess of salt is clearly preventing the formation of additional folds.

So far, the models that accommodate more shortening in Diapirs 1 and 2 develop less folds in Domain 1 because the deformation front takes longer to reach the foreland end of the model. Additionally, the absence of diapir roof disrupts the continuity of the pre-shortening cover, difficulting the transmission the advance of the deformation front through the cover. Deformation then is localized in the salt, which mobilizes towards the foreland, contributing to the bulging of Domain 1.

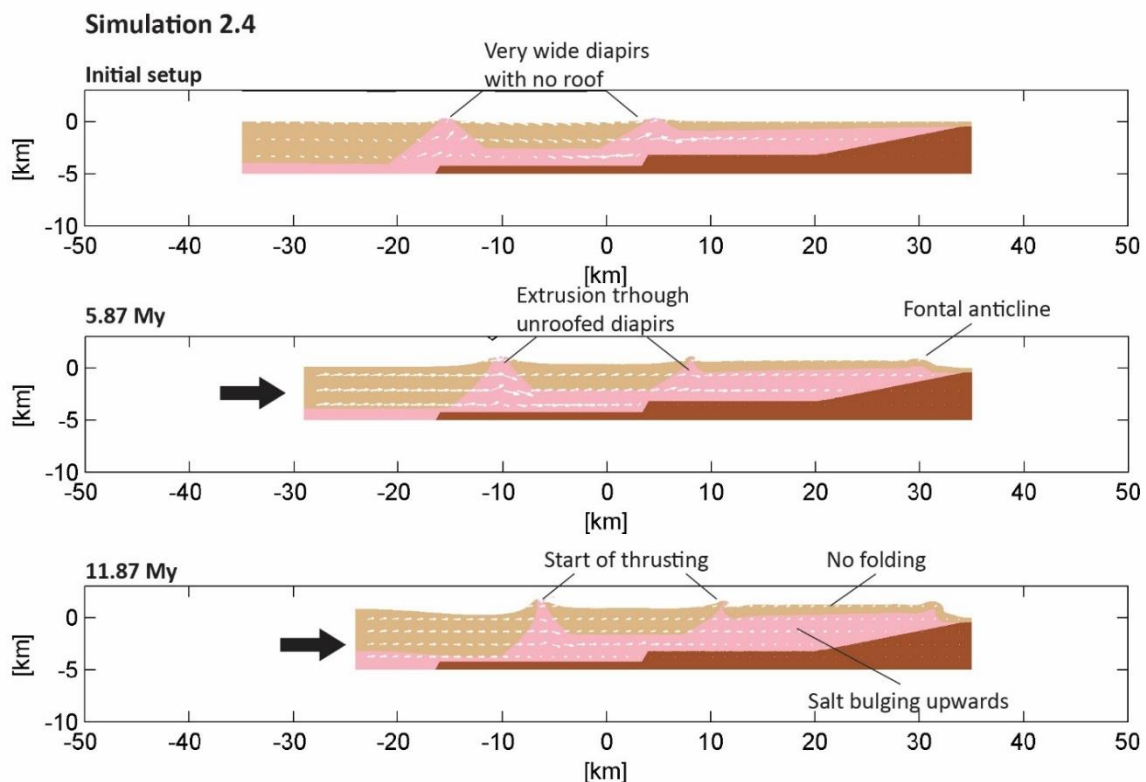


Figure 4.6. Simulation 2.4 with wide diapirs with no roof

4.3.2. Adding syntectonic sedimentation

The next step was to add sedimentation in the multiple-diapir modelling to test the working hypothesis that sedimentation would limit the bulging of the salt in Domain A, enabling folding as observed in the natural case of the Serres Marginals. Also, it was expected that it could promote withdrawal and subsidence of Domains B and C. We ran

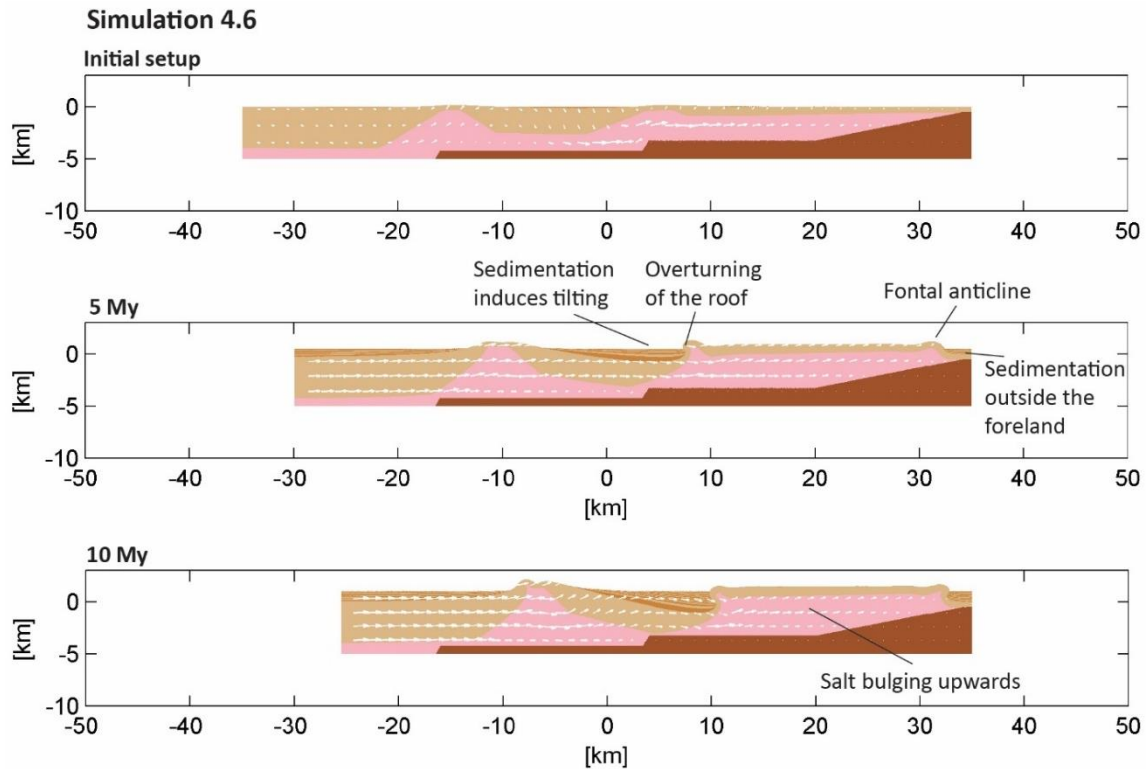


Figure 4.7. Simulation 4.6 with wide diapirs and implementing syntectonic sedimentation. Syntectonic sediments are shown as layers of alternating brown and beige colours.

simulations with sedimentation in the narrow-diapir setup, but for the sake of better comparison, we will focus on the description of the effects of sedimentation in the wide-diapir models (with diapirs of varying width).

At this point, we had tried with different diapir width combination, to test if diapir width had any influence in how fast the deformation front propagates to the frontal end, and if certain diapiric geometries would enhance thrusting. With syntectonic sedimentation, the wider the diapirs, the more Domain B tilts under the sediment weight of the sediments. The domain tilts to the south, and for larger diapirs (6km wide, Figure 4.7) Domain B tends to underthrust Domain A, producing a backthrust. No thrust or footwall syncline develops to the right (foreland side) of Diapir 1. Domain C, with less salt beneath, does not tilt and just accumulates sedimentation evenly.

A very significant effect of syntectonic sedimentation is that it quickly fills the frontal end of the foreland, locking the frontal anticline and enhancing a sort of backstop.

In the first simulations with syntectonic sedimentation the folds still do not appear in Domain A, because the whole area is bulging upwards (Figure 4.7). Just the frontal

anticline develops. At this point we concluded that the excess of salt in the frontal part of the model is preventing further fold nucleation and this effect cannot be counteracted just by adding sedimentation.

Since one of the goals of the study is to test the parameters affecting folding in Domain A, equivalent to the folded area of Serres Marginals, the next step was to run the models with a basement configuration that reduced the amount of salt below Domain A but still keeping a taper angle, and test if this reduced the salt bulging upwards. Even in the absence of sedimentation, with the new basement configuration the situation changed very much in domains A and B (Figure 4.8).

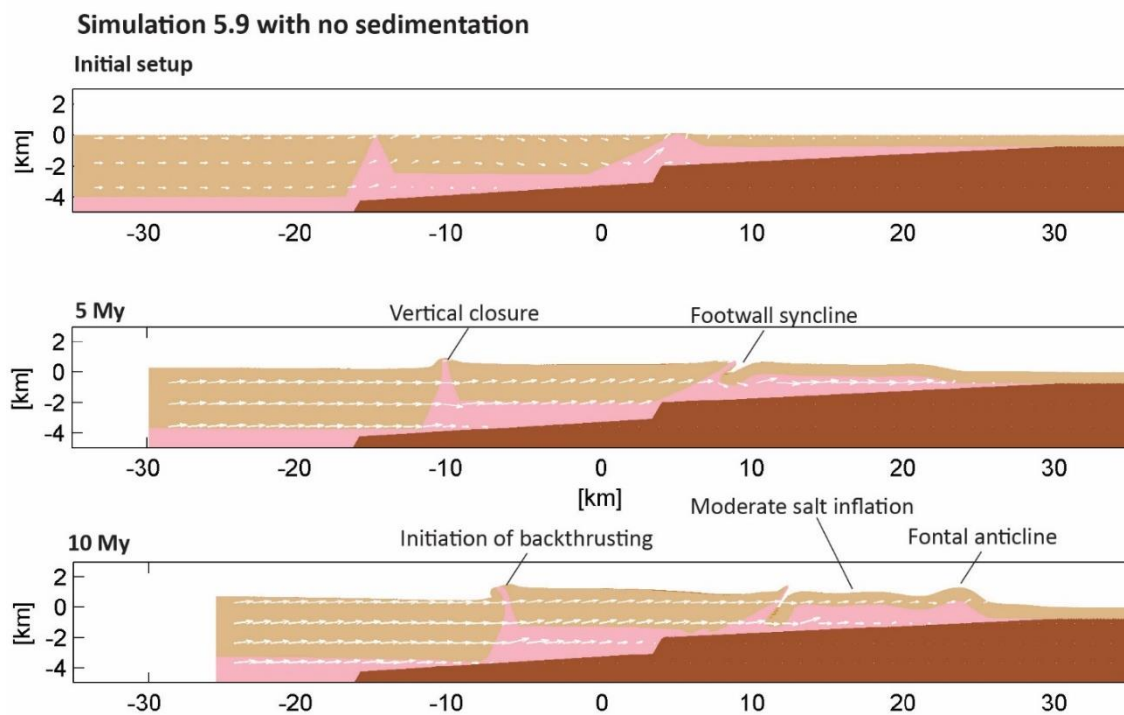


Figure 4.8. Simulation 5.9 with reduced initial salt thickness and no sedimentation

Reduced salt below Domain A favours the nucleation of more folds besides the frontal anticline. However, the area still lifts much due to the ascending salt. Diapir 1 leans towards the south in initiating a forethrust with a footwall syncline, and Diapir 2 just squeezes vertically with the upper part forming a backthrust as happened with the previous basement configuration. Adding sedimentation to one of the setups with the higher basement configuration changed the resulting fold geometry in Domain A (Figure 4.9). There is not so much bulging upwards of the salt, and the folds that developed had

a wider wavelength than in the previous simulations. As it happened with the previous basement configuration, the sedimentation in the foreland end pins the frontal anticline, creating a primary weld and preventing the displacement of salt towards the foreland. The syncline at the footwall of the inclined Diapir 1 accumulates thick sediment, whereas syncline in Domain A does not, because the area remains too inflated to accumulate sediments. Domain B tilts slightly to the south, accumulating sediments in the syncline closest to Diapir 1, but does not subside as much as in the previous simulations because there is less salt to withdraw from below. When changing thickness of Domain A to a constant layer of 0.75km, instead of a thinning wedge from 0.5 to 1km, the number of folds developed is the same, but they are closer together and grow higher vertically. This may be due to the thicker cover at the frontal end, that pinches the salt out and causes the frontal anticline to develop more to the north, narrowing the space available for the development of the other folds.

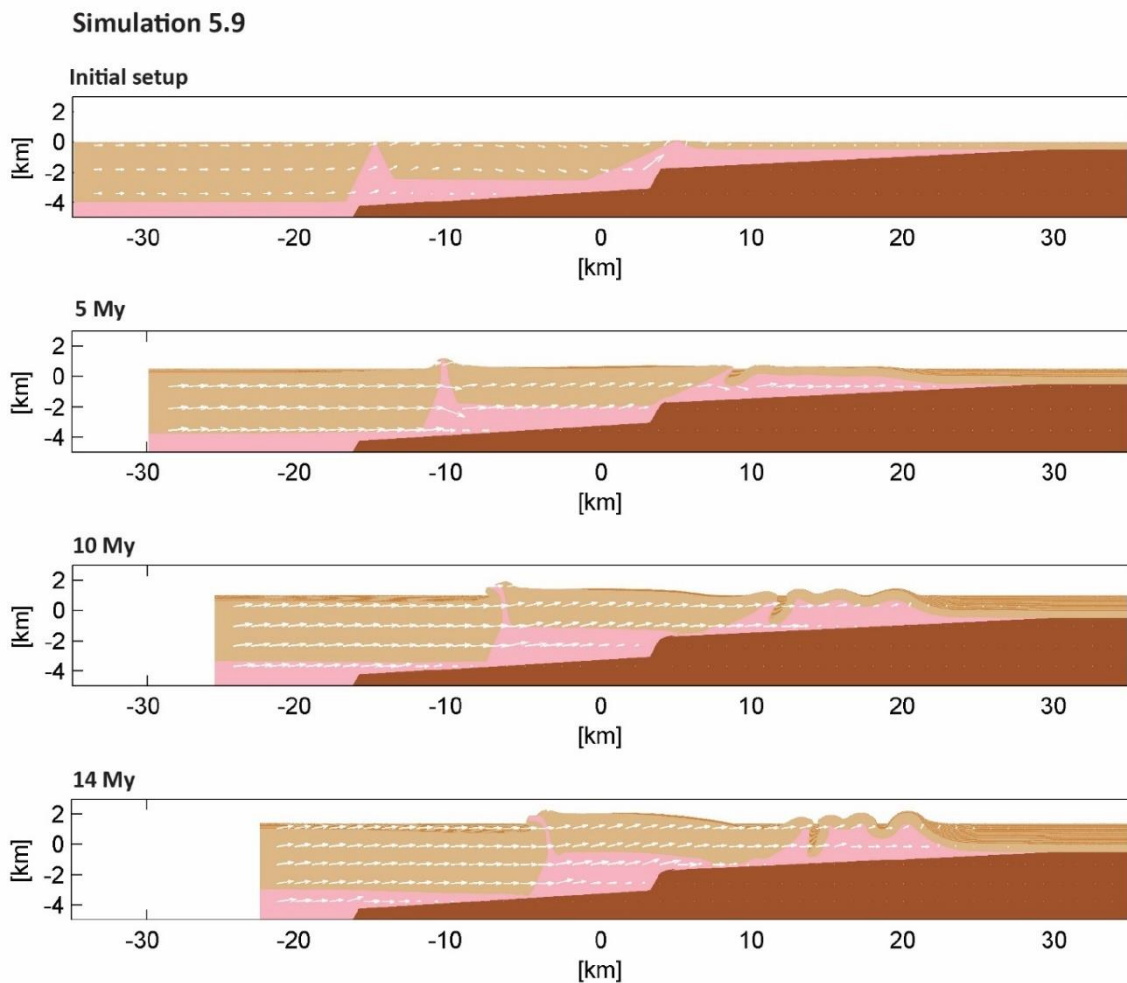


Figure 4.9. Simulation 5.9, the initial geometry that is the base for the following systematic experiments in the next section of the chapter.

In simulations from 5.9 onwards, a smaller thickness of salt reduced the bulging of the Domain A, developing a greater number of folds. The southernmost syncline starts to accumulate sediments and the footwall syncline of inclined Diapir 1 (which we view as analogue to the Àger basin in the Pyrenees natural case) evolves to a deep pouch or drop shape. As the frontal anticline is the first that forms in the sequence, the oldest sediments deposited remain on its crest because there is no erosion. Decreasing the amount of salt below the Domain A is a key factor to produce folding, so this was the basement configuration used in subsequent simulations.

4.3.3. Lessons learned from the preliminary experimental attempts

From the process of building an initial setup that showed realistic geometries that could offer analogies to the natural cases and processes we wanted to understand, we have come to the following conclusions:

- It is possible to form folds with syntectonic sedimentation in the absence of pre-existing diapiric structures in Domain A. However, this requires a very specific salt vs overburden thickness ratio. For this reason we conclude that pre-compressional structures are very determinant in facilitating fold development.
- A high evaporite vs sedimentary cover thickness ratio promotes salt bulging upwards and prevents the formation of folds.
- With the geometrical and rheological parameters used, pre-existing diapirs have a tendency to close vertically and to develop very limited to no thrusting across the cores.
- Syntectonic sedimentation can enhance folding, basin tilting and the displacement of the frontal backstop towards the moving wall, thus reducing the extension of the frontal domain.

To progress into the systematic studies on folding with syntectonic sedimentation, and with syntectonic sedimentation and erosion, we always use variations of setup 5.9, as the evaporite vs sedimentary cover thickness ratio was favourable for producing folding. In the systematic runs, rheological parameters are the same as in the experimental runs

(Table 4.1) and all the changes to the geometry of simulation 5.9 are explained within the text.

4.4. Systematic studies

4.4.1. *Effects of syntectonic sedimentation vs pre-shortening cover thickness*

Once we set a valid model configuration to produce folds in Domain A, we observed that the wavelength and number of folds were mostly dependant on the syntectonic sedimentation rate and the salt-cover thickness ratio. We designed a set of model runs with the basic geometry of model 5.9 (Figure 4.8) and varying the pre-shortening cover thickness and the sedimentation rate. The values of sedimentation rate and cover thickness are as reflected in Table 4.2 below. Domains 2 and 3 and diapir geometry have remained unchanged throughout all the model runs.

Cover thickness/ sed. rate	0,01 cm/yr	0,015 cm/yr	0,02 cm yr
0,5 km	Simulation 5.9	Simulation 5.17	n/a
0,75 km	Simulation 5.10	Simulation 5.12	Simulation 5.11
1 km	Simulation 5.18	Simulation 5.19	Simulation 5.13

Table 4.2. Variation of parameters in the systematic study on syntectonic sedimentation

In this section we will focus on folding development in Domain 1; for this reason the figures show the models cut at 0 km for better visualisation. Also, the figures from now on are reversed to match the orientation of the geological cross-sections of the Montsec and Serres Marginals of the Southern Pyrenees presented in the previous chapters. All the models in this series have been run to 1200 timesteps, here equivalent to 12 My.

4.4.1.1. The effect of sedimentation rate

Increasing the sedimentation rate from 0.01 cm/yr to 0.015 cm/yr to 0.02 cm/yr affects substantially the fold development of Domain A and its final structure (Figure 4.10). The faster accumulation of sediments accelerates the development of internal structures in the domain and acts as a backstop for the salt migration, preventing salt from flowing towards the foreland. After 12 My, the simulations with 0,01 cm/yr show thick sedimentation outside Domain A from the horizontal coordinates -35 to -22 km (Simulations 5.9, 5.10, 5.19, figure 4.10), while in the models with sedimentation rates

of 0,02 cm/yr the thicker sedimentation in the outer domain extends from -35 up to -15 km (Simulations 5.11, 5.13, figure 4.10). This makes Domain A around 7 km shorter due to increasing sedimentation rates. As salt cannot be distributed along all the domain, it gets trapped between the sediment accumulations at both sides of the domain, and an anticline starts to form in the central part of the Domain A. As the higher sediment accumulation is in the outer domain, the big anticline leans towards the hinterland, with early sediments in the foreland flank progressively verticalising. With a faster sedimentation rate, the footwall syncline of Diapir 1 becomes a depocenter sooner. For Domain B, faster sedimentation rates cause the basin to tilt deeper towards the foreland under the sediment load. As compression progresses, the advance of Domain B squeezes shut Diapir 1. There is little to no thrusting along the diapir core, since the sedimentation rate is so high that keeps Domain B sinking and it cannot uplift.

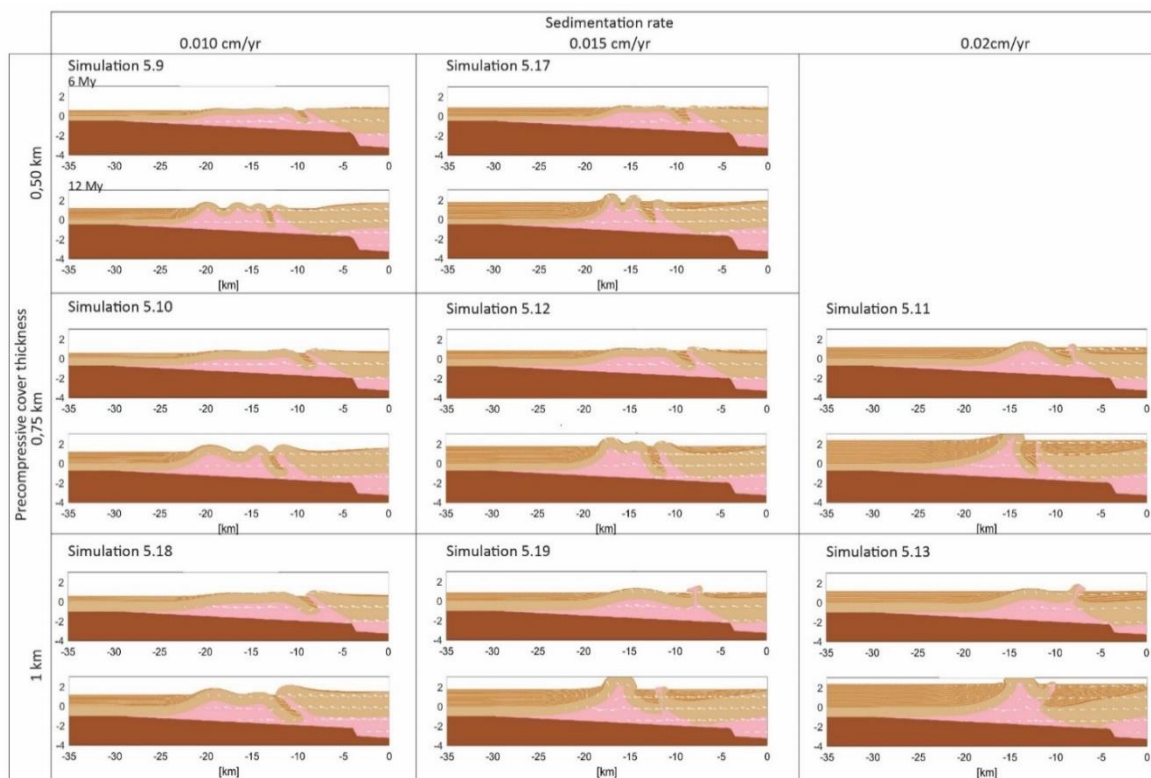


Figure 4.10. Results of the systematic study on syntectonic sedimentation, geometries after 6 and 12 My

4.4.1.2. The effect of the overburden to salt ratio

In the simulations with a lower sedimentation rate (Simulations 5.9, 5.10 and 5.18 in figure 4.10), increasing the overburden thickness promotes the rigid behaviour of the

overburden decreasing the number of anticlines formed by buckling from three (Simulation 5.9) to just two, which are shallower and show a larger wavelength (Simulations 5.10 and 5.18). In the simulations with 0.015cm/yr sedimentation rate, the rigidity promotes the shift from two anticlines (Simulations 5.17 and 5.12) to just a single anticline that is unrealistically tall (Simulation 5.20).

To understand the influence of cover thickness in counteracting the effect of higher sedimentation rates, we ran the simulations with thicker overburden of 1 km constant across Domain A. In simulation 5.13, the thick overburden and the higher sedimentation rate has an effect on the final shape of the footwall syncline in Diapir 1. This time it does not form a drop shaped basin, because the overburden is too thick to be able to fold in the first stages of shortening, so just forms a shallow syncline accumulating a small amount of sediment. In simulations 5.19 and 5.13 the anticline in Domain A is too rigid to lean towards the hinterland as it does in simulation 5.11, and the shape tends more towards a box fold geometry.

4.4.1.3. Lessons learned from the study on syntectonic sedimentation

To sum up, the main observations in the systematic study with syntectonic sedimentation are:

- Higher sedimentation rates decrease the extension of Domain A, as sedimentation in the outer domain of the foreland propagates the pinch-out towards the hinterland by a migrating primary weld.
- Higher sedimentation rates promote upright structures, specially the footwall syncline in Diapir 1, and anomalously tall anticlines in Domain A.
- Higher sedimentation rates promote an early tilting of Domain B towards the foreland, which may even underthrust below Domain A.
- A lower evaporite to cover thickness ratio increases the overall rigidity of the domain, reducing the number of folds and their amplitude (i.e. the depth of the synclines).
- The joint effect of a high sedimentation rate and a thicker cover tends to produce a lower number of folds, which grow slower.

4.4.2. Study with syntectonic erosion

The next step into the systematic study on folding was to add erosion in order to introduce anticline unroofing and salt extrusion. Syntectonic erosion counteracts the bulging of the salt by unroofing the anticlines and promoting syncline subsidence as a combination of loading and compression. On top of varying the erosion intensity, in these simulations we have continued testing the influence of evaporite vs overburden thickness ratio, as we did with the simulations with only sedimentation. All the simulations in this series have run for 2000 timesteps, equivalent to 20 My.

Simulations have been arranged in the following matrix in order to test the influence of erosion and sedimentation rate and cover thickness:

Cover thickness/ κ	$1 e^{-9}$	$1 e^{-8}$	$5 e^{-8}$	$1 e^{-7}$
0,5 km	Simulation M1	Simulation M2	Simulation M3	Simulation M4
0,75 km	Simulation M5	Simulation M6	Simulation M7	Simulation M8
1 km	Simulation M9	Simulation M10	Simulation M11	Simulation M12

Table 4.3. Variation of parameters in the systematic study with syntectonic sedimentation and erosion.

As introduced in the methods section, κ is the diffusion constant. It is expressed as a power of 10. The value $1 e^{-9}$ corresponds to 1×10^{-9} . The higher the κ , the more intense will be the effect of erosion.

The results are displayed in figures 4.10, 4.11, 4.12 and 4.13 in the following pages. A larger version of the figures can be found at the appendix of the thesis. Timing of anticline unroofing is a very important factor determining the final fold geometry, so three moments in the evolution of each simulation are shown in figures 4.10, 4.11 and 4.12: After 6My, 12 My and 18 My. Figure 4.13 reflects the final geometry of the twelve simulations.

In the following section we outline the main results regarding the variation of erosion and cover thickness and also will discuss the plots reflecting the progressive loss of salt in the folded domain.

4.4.2.1. Number and geometry of folds

The main effect of erosion in the models is that, if it is intense enough, it will eventually unroof the crests of the anticlines, thus promoting the subsidence of the synclines under the sedimentary load and decreasing the quantity of salt available. The rate of erosion in these models represented by the parameter kappa (κ), and will determine how fast unroofing occurs. A fold dominant wavelength based on diapir spacing divided by number of folds (Equation 1, page 107) is difficult to measure in our simulations due to the limited amount of folds. The values reflecting the final number of folds and their geometry have been measured just for the synclines and not averaged, since the final number of folds is too low for the average to be informative.

In the model runs with the thinnest pre-shortening cover, **0,5 km**:

Simulation	κ	Number of synclines	Wavelength	Amplitude	Anticline topography/ unroofing
M1	1e-9	4	2,5- 3 km	1-1,5 km	No unroofing/ high topography
M2	1e-8	3	2-3,75 km	1-1,3 km	Partial unroofing/ high topography
M3	5e-8	3	2,5- 3 km	1-1,3 km	Total unroofing/ low topography
M4	1e-7	2	3,5- 4 km	1,5-1,7 km	Total unroofing flat topography

Table 4.4. Model runs for a 0,5 km pre-shortening cover with an increasing erosion rate. κ 1e-9 is the lowest erosion rate and 1e-7 is the highest.

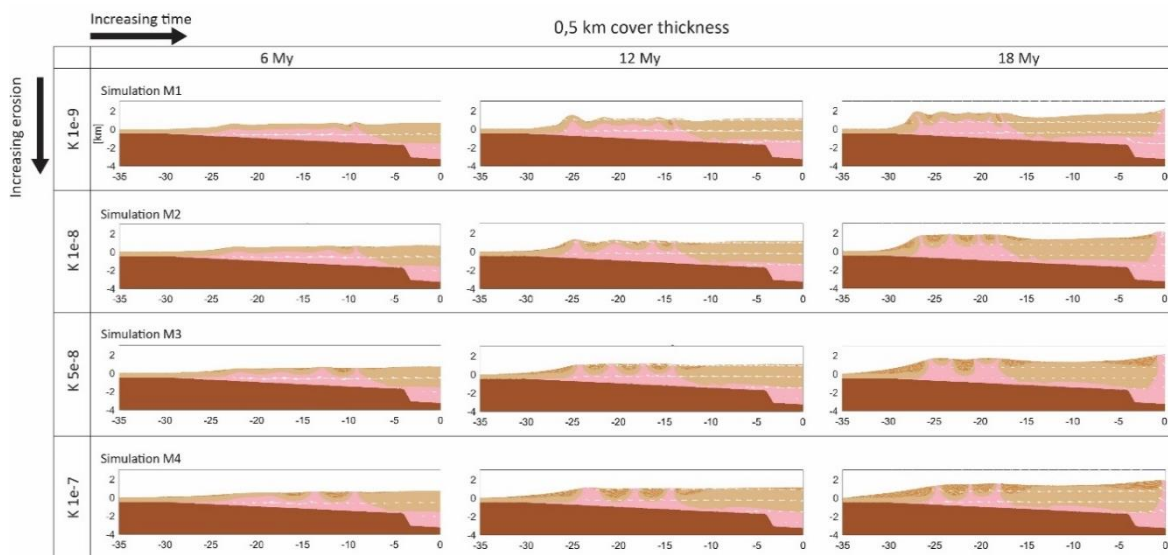


Figure 4.11. Results of the simulations with 0,5 km cover thickness of the systematic study on syntectonic sedimentation and erosion. Geometries after 6, 12 and 18 My.

Pre-shortening cover, **0,75 km**:

Simulation	κ	Number of Synclines	Wavelength	Amplitude	Anticline topography/ unroofing
M5	1e-9	3	1,5 km- 4 km	1-2,5 km	No unroofing/high topography
M6	1e-8	3	3 km- 4 km	1-2 km	No unroofing/ low topography
M7	5e-8	2	4 km- 5 km	1,5- 2 km	Total unroofing/ no topography
M8	1e-7	2	4,5 km- 5 km	1,5- 2 km	Total unroofing/ no topography

Table 4.5. Model runs for a 0,75 km pre-shortening cover with an increasing erosion rate. κ 1e-9 is the lowest erosion rate and 1e-7 is the highest.

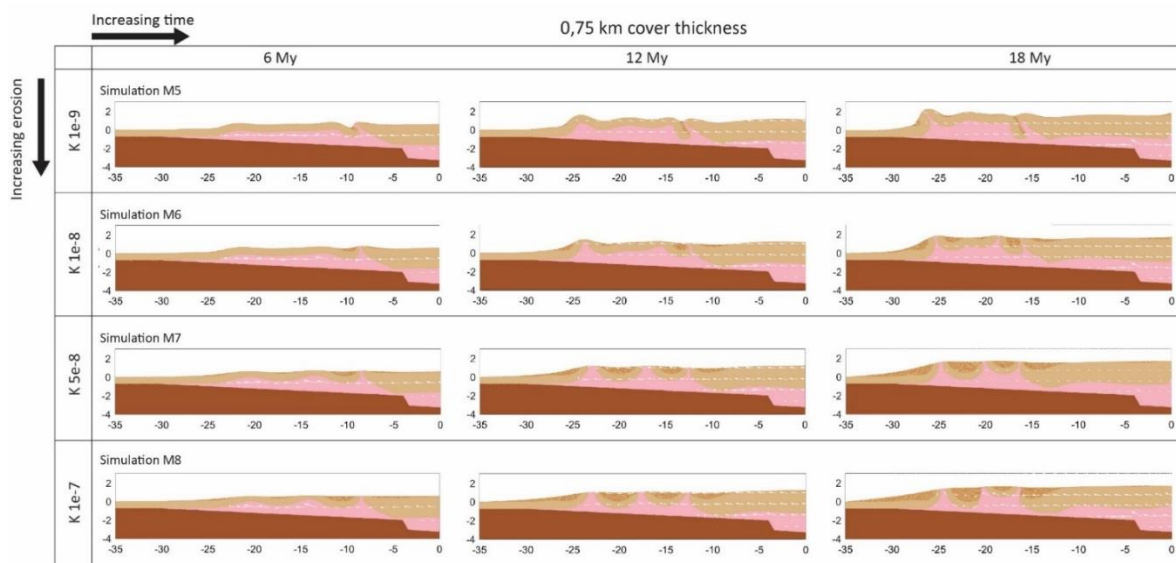


Figure 4.12. Results of the simulations with 0,75 km cover thickness of the systematic study on syntectonic sedimentation and erosion. Geometries after 6, 12 and 18 My

Pre-shortening cover **1 km**:

Simulation	κ	Number of synclines	Wavelength	Amplitude	Anticline topography/ unroofing
M9	1e-9	2	4- 7,5 km	2-3 km	No unroofing/high topography
M10	1e-8	2	4,3- 6,8 km	2-2,5 km	No unroofing/high topography
M11	5e-8	2	5- 5,6 km	2 km	Partial unroofing/ flat topography
M12	1e-7	1	8 km	2,2 km	Total unroofing/flat topography

Table 4.6. Model runs for a 1 km pre-shortening cover with an increasing erosion rate. κ 1e-9 is the lower erosion rate and 1e-7 is the higher.

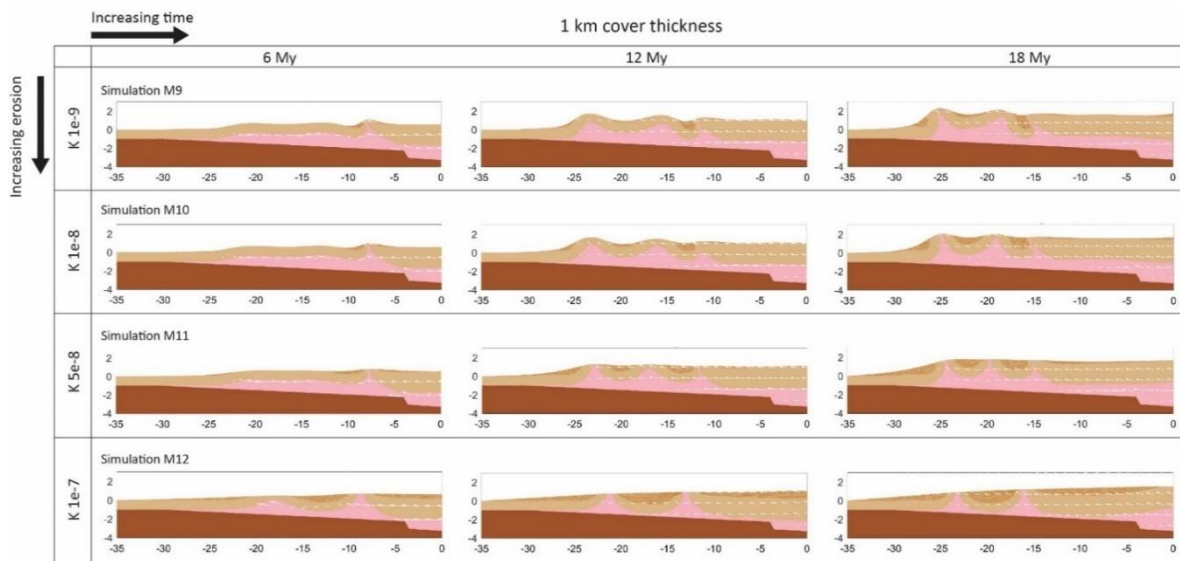


Figure 4.13. Results of the simulations with 1 km cover thickness of the systematic study on syntectonic sedimentation and erosion. Geometries after 6, 12 and 18 My

Final stage of the twelve simulations with syntectonic sedimentation and erosion after 18 My:

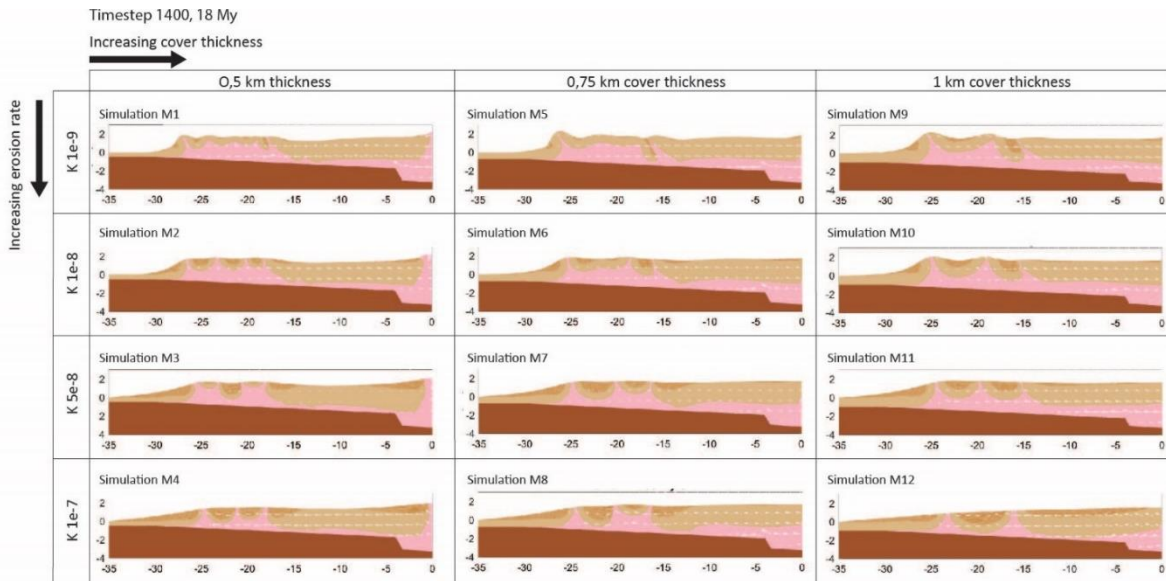


Figure 4.14. Geometries after 18 My of all the simulations of the study on syntectonic sedimentation and erosion.

As reflected in tables 4.4, 4.5 and 4.6, in each of the three cover thickness groups the increasing of erosion rate results in a higher fold wavelength, and folds develop earlier in time. This is clear in the simulations with thinner cover (Figures 4.11, 4.12 and 4.13). This is because with low erosion rates (M1 and M2, Figure 4.11) folds are able to nucleate and grow by buckling before their crest is eroded. (Stage 6 My). When erosion unroofs the anticlines, they begin to close and synclines increase their subsidence (Stage 12 and 18 My, Figure 4.11). In contrast, in the models with higher erosion intensity (M3 and M4), the cover is disconnected earlier by eroding the higher areas when the train of folds is not yet fully developed. Buckling and load-induced subsidence coexist since early on and the latter one is predominant. Losing the rigid roof on top of the anticlines at the early stages also means that the diapirs will be easier to squeeze and close, and the space previously occupied by the anticlines is used by synclines growing by sedimentary loading. In simulations with high κ and cover thickness of 0,5 or 0,75 km, it can be seen how the pre-compressional cover sinks quickly and the syncline flanks are buried under the syntectonic sediments (M7 and M8, Figure 4.12).

As predicted by buckling theory, in setups with a thicker pre-compressional sedimentary cover, the early development of folds by buckling is delayed due to the rigidity of the

cover, an effect also seen in the models with no erosion. The result is a lower number of folds with bigger wavelength and amplitude (Table 4.6). The most clear example on this is simulation M12, where a wide syncline is formed occupying all the domain (Figure 4.13). The syncline is formed mostly by load-induced subsidence instead of buckle folding because the pre-compressional cover is no longer connected to be able to transmit the stress from the hinterland towards the foreland. Shortening is accommodated by the expulsion of salt and the closure of anticlines.

4.4.2.2. Effect of salt evacuation rate

A useful way to analyse the effect of anticline unroofing in salt loss is to plot the sectional surface of model salt at each timestep. As mentioned before, the effect of faster erosion

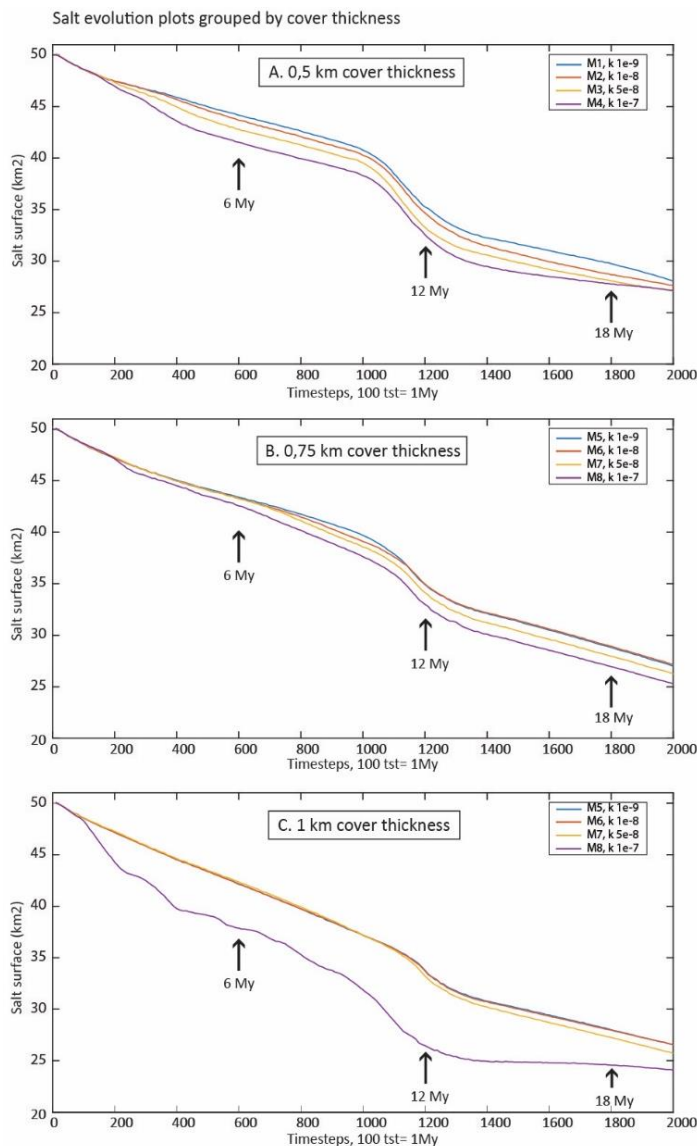


Figure 4.15. Salt loss plots grouping simulations with the same cover thickness.

can be counteracted by thicker overburdens, for this reason salt loss plots in figure 4.15 group the simulations with the same cover thickness and plots in figure 4.16 group simulations with the same erosion intensity.

The plots comparing salt loss in simulations with the same overburden thickness varying erosion rate (Figure 4.15) show the expected direct relationship between more intense erosion and a faster loss of salt. The final amount of salt available after 2000 timesteps (20My) is lower in all the simulations with a more intense erosion rate. During the first two million

years, all the simulations with 0,5 and 0,75 km cover thickness loose salt at the same rate, regardless of the erosion intensity. In the case of simulations with 1km cover thickness, this just happens during the first My (Figure 4.15). After 6My, there is already differential unroofing of the anticlines, which are unroofed in the simulations with faster erosion but are not in the ones with lower values of kappa (Figures 4.11, 4.12 and 4.13). In the salt loss plots, this translates into a wider separation between the curves. In the plot of 1km, salt loss curves of M9, M10 and M11 simulations, with the lower erosion rates, are very similar while the curve of $k 1e-7$ loses more salt and much faster (Figure 4.15). This is due to the growth and sinking of the wide syncline, that quickly mobilises the salt below towards the diapir and the unroofed anticlines, and also to the more intense erosion widening the overture of Diapir 1. In the three plots, from timestep 1000 to 1400 (10 to 14 My) there is an increase on salt loss, which reflects the unroofing of the anticlines. From timesteps 1400 to 2000, the loss of salt is steady in all the simulations, as all the anticlines have been unroofed (except in simulation M1 and M5, where erosion rate was too low, Figures 4.11 and 4.12) and they are nearly closed due to shortening. The final amount of salt remaining in the model is always lower for higher erosion rates.

Comparing the salt-loss curves grouping the plots of the same erosion rate (Figure 4.16), shows that for all erosion rates, the simulations with the thicker pre-compressional cover (1km) are the ones to experience a faster loss. This may seem counterintuitive, as a thicker cover is harder to erode, but the simulations with a thicker cover develop a lower number of folds, with larger synclines that to sink deeper, displacing a greater amount of salt. Once the first structure is unroofed, sinking happens much faster when the cover is thicker. Comparing between the simulations with cover thicknesses of 0,5 and 0,75 km, salt loss occurs at a very similar pace for all the values of κ , and both curves often overlap. After 20 My the simulation with a thinner cover always finishes with slightly more salt left but the final amount does not differ significantly, except for the case with the higher erosion rate (Figure 4.16, D).

It is interesting to note that the salt-loss plots of all the simulations end up with a similar amount of salt, between 24 and 28 km². However, fold geometries differ between all the models, mostly due to the timing of the transition from buckling to load-induced syncline subsidence, determined by the timing of anticline unroofing.

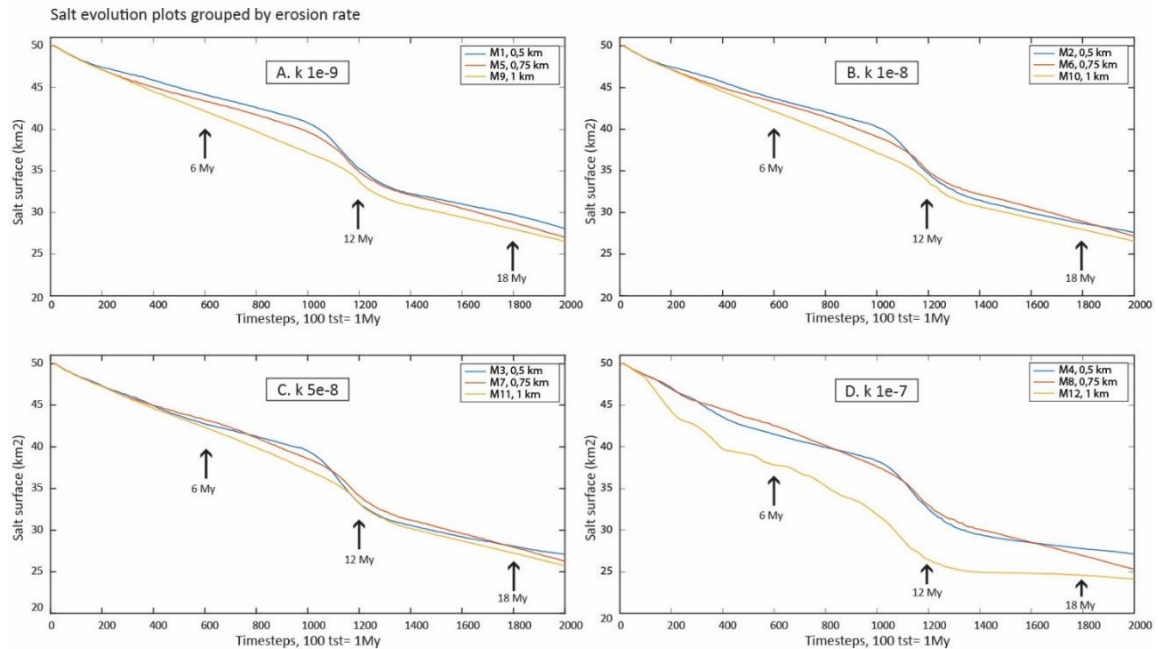


Figure 4.16. Salt loss plots grouping simulations with the same erosion rate.

4.4.2.3. Lessons learned from the systematic study with syntectonic erosion

The main lessons obtained in the systematic study on folding with syntectonic erosion and sedimentation are:

- Syntectonic erosion has an impact in fold wavelength and amplitude. In models with slower erosion, the initial buckle folding phase before fold crest erode determines the final fold geometry. Slower erosion results in a higher number of folds with smaller wavelength and amplitude. Fast erosion and unroofing promotes a quick transition from buckle folding to load-induced subsidence in synclines (minibasins).
- When the anticline unroofing disconnects the pre-tectonic layer, deformation is no longer ruled by buckling. Instead, shortening is accommodated through salt expulsion and associated anticline closure.
- A thicker pre-compressional cover increases the resistance to buckling, so the initial buckle folding phase is not as quick. Folding mostly occurs by load-induced subsidence

once the anticlines have been unroofed. This promotes faster salt expulsion because synclines tend to sink deeper.

- Load-induced subsidence creates synclines with higher symmetry than these created by buckle folding, where structures develop a definite vergence as a consequence of the frontal salt pinch-out of the model setup.

- Timing of unroofing impacts the final fold geometry but not so much the amount of salt lost.

4.4.3. Study of thrusting through a single diapir

As seen in the experimental phase of the studies with a longer setup, diapirs 1 and 2 close shut vertically in most simulations and do not show thrusting along the core of the diapir. Vertical welding without thrusting is very frequent in physical models also, even in the cases where the diapir walls are not vertical (Callot et al., 2012; Duffy et al., 2018; Roma et al., 2018). In these cases once the diapir is fully closed, the deformation is usually accommodated by a shortcut thrust in front of the diapir. Although we observe vertical welding in our numerical simulations, shortcuts do not happen.

The fact that numerical simulations and physical models rarely predict thrusting along the core of preexisting diapirs presents a paradox when compared with cross sections from field examples of fold-and-thrust belts with pre-compressional diapirs, where thrusting along welds is frequent (Graham et al., 2012; Kergaravat et al., 2016; López-Mir et al., 2016; Saura et al., 2016; Labaume and Teixell, 2020). However, there are also field examples where vertical welding does not have any associated thrusting (Rowan and Vendeville, 2006; Jahani et al., 2017).

The goal of this study with a shorter setup is to test under which conditions thrusts are produced or inhibited during the shortening of a diapir. In particular, we investigate by means of numerical modelling whether the asymmetry of overburden thickness in each flank of a diapir and the dip angle of the diapir margins have an effect on the occurrence of thrusting at diapir cores. To test this we have run 12 simulations varying the cover thickness of the flank to the right of the diapir (4 km, 3 km and 2.5 km) and varying the angle of the diapir margins (vertical, 63°, 45°, 34°) (Table 4.7). To simplify the number of variables involved in the study, both diapir margins have the same dip, diapir roof is 0,5 km thick in the diapirs with vertical margins and sedimentation rate is constant and the same in all the simulations (0,01 cm/yr).

Diapir margin dip	Right flank thickness 4 km	3 km	2.5 km
Vertical	Simulation 11.4	Simulation 10.4	Simulation 12.4
63°	Simulation 11.1	Simulation 10.1	Simulation 12.1
45°	Simulation 11.2	Simulation 10.2	Simulation 12.2
34°	Simulation 11.3	Simulation 10.3	Simulation 12.3

Table 4.7. Parameters varied in the systematic study on thrusting through a diapir core

The initial and final geometries after 12 My of shortening are summarized in figure 4.17.

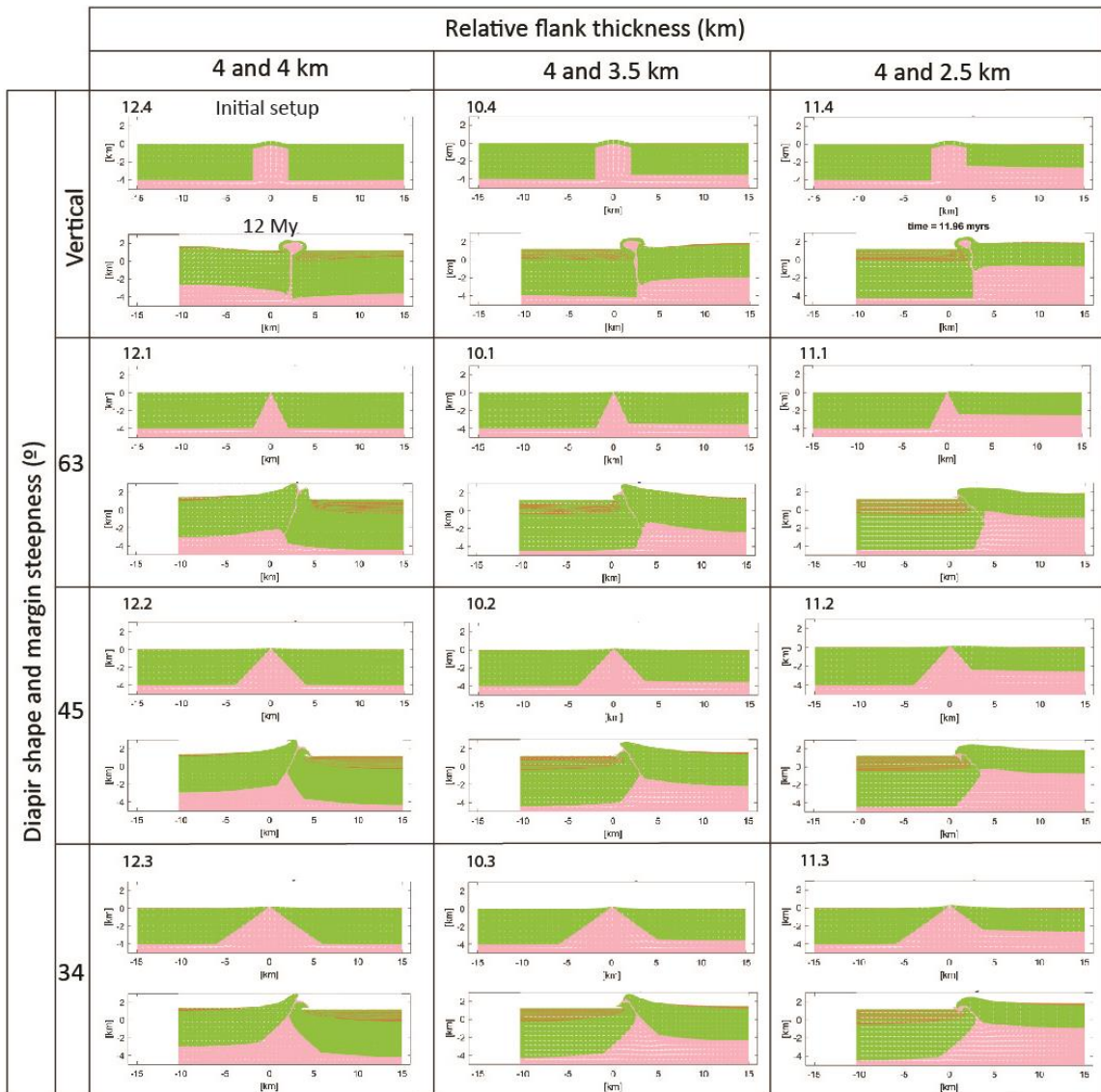


Figure 4.17. Initial setup and final geometries of the single diapir simulations

Simulations with diapirs with less steep margins have wider diapirs at the base, and this has a major impact during shortening because the wider pedestals never get to fully close. After welding or partially welding the upper part of the diapir, thrusting happens in all the simulations except these with vertical diapir walls, where the diapir just closes vertically to form a secondary weld (Figure 4.17). In the simulations with vertical walls, the diapir is unable to breach the roof and extrude salt. The unbreached roof folds into an anticline with both limbs overturned at the base (Figure 4.17), which is not a realistic geometry.

Relative flank thickness is the most important factor in determining the vergence of diapir thrusting. In our numerical simulations, the thinner flank always overrides the thicker one, and the larger initial asymmetry between the flanks, the more the thin one is uplifted. This can be a priori expected, but it contrasts with the observations of many natural examples, as the Southern Pyrenees, where thicker basins like the Montsec or Montroig hanging walls, among others, overthrusts the thinner units to the south. It is possible that, contrary to what happens in the models, in natural examples the direction of the compression has a bigger effect than the differences of thickness at both sides of the diapir and this favours forethrusts even in the cases with high asymmetry. Syntectonic erosion, basement configuration and the tapering of the salt layer are not tested in the models with a single diapir setup, but are parameters likely to affect whether the thicker unit can thrust above the thinner one or not.

In the simulations with the same overburden thickness in both flanks, vergence of the thrust is always towards the right, influenced by the fact that the moving wall is at the right boundary, so the right side is the one that overthrusts preferentially. However, in the simulations with asymmetric flank thickness it is always the thin flank that overrides the thick one, in this setup producing backthrusts.

Syntectonic sediments quickly accumulate in the footwall domain, contributing to sink it faster. Salt mobilised from under the footwall domain moves towards the hanging wall, where overburden is lighter and salt is less pressurised, thus contributing to its buoyancy and its lifting above the original regional. Syntectonic sedimentation also enables the folding and rotation of the pre-compressional cover in the footwall, which creates an overturned flank for the footwall syncline (a compressional flap).

4.4. Discussion of modelling results

The simulations presented provide interesting results to discuss the questions raised at the start of the modelling process, and provide also some insight on the evolution of the Montsec-Serres Marginals province of salt ridges and synclines.

As interpreted from field evidence in chapter 2 of this thesis, halokinetic structures in the Serres Marginals salt province had started when differentiated depocentres formed during the Jurassic. This conditioned the later compressional evolution of salt ridges and

synclines once the deformation front had clearly reached the area during the time of the Garumnian sedimentation (late Cretaceous to Paleocene) (Figure 2.9 in chapter 2). However, previous studies in Serres Marginals (Pocoví, 1978b; Teixell and Muñoz, 2000) interpreted that structures in the area initiated by buckling and thrusting during the compressional stage. In our 2D simulations we aimed to test if geometries like the Montsec footwall and Serres Marginals could be achieved by buckling alone, in the absence of pre-existing salt structures. It was evident that placing pre-compressional salt structures across the Serres Marginals analogue domain would condition folding, as pre-existing diapirs tend to localize deformation since the start of the model runs and determine where the subsequent folds would form (Callot et al., 2012; Fernandez, 2014; Dooley and Hudec, 2020). The generation of folds of comparable wavelength to those in Serres Marginals without pre-existing diapirs has been achieved after several experimental runs varying the salt vs cover thickness ratio and the sedimentation rate. The final wavelength of folds can be substantially modified by introducing erosion. However, in the different model runs we have observed that, as the initial setups had no salt exposed in the surface in the Serres Marginals analog domain, the tendency of the salt of broadly bulging upward counteracted deformation by buckling and inhibited the nucleation of folds.

Recent structural studies include cross-sections with present-day Keuper thickness between 1.5 to 3 km below the Serres Marginals and Montsec thrust sheets (Cámara and Flinch, 2017; Santolaria et al., 2017; Espurt et al., 2019a). Our models have a pre-compressional salt thickness between 1 and 2 km, tapering towards the frontal pinch-out. Despite our moderate salt thickness, salt bulging has been an issue in most simulations, except in those with very intense erosion rates, which led to a few, wide synclines. In the western Serres Marginals there is a high number of synclines of small wavelength that evolved above a thick layer of salt. In eastern Serres Marginals, however, the wide wavelength of the Sant Mamet dome and the Avellanes diapir is more similar to the simulations with initial bulging. For this reason we propose that there were initial thickness differences within the thrust sheet pre-shortening cover which triggered load-induced subsidence, seeding folding from early on. Also, unroofed diapiric structures such as the Montsec and Avellanes diapirs evacuated salt during the buckling

phase and this prevented the salt bulging upwards during the more advanced stages of the compression. This is not the case of the Sant Mamet dome to the east, which still preserves most of its roof. Most salt-cored of the smaller wavelength anticlines were unroofed at the later stages of the orogeny, or were not unroofed at all. Most of the sedimentary cover stayed connected and for this reason the buckling stage lasted until the end of the orogeny, similar to what is observed in simulations with lower erosion rates.

The only pre-compressional salt structures in our models have been the two wide diapirs separating the three domains with different cover thickness, representing the diapiric structures of Bóixols and Montsec, formed during the Pyrenean rifting stage (Chapter 2). Although the vertical welding of the diapirs and the lack of thrusting across the diapir cores has been an unexpected observation, the pre-existing diapir in the Montsec analogue has still conditioned the evolution of the deformation in the different domains. When the deformation front reaches Domain A, equivalent to Serres Marginals, the first fold to evolve in the simulations with syntectonic erosion is the southern syncline at the toe of the equivalent to the Montsec diapir. In simulations with lower erosion rates, the phase dominated by buckle folding lasts longer and the footwall syncline develops a drop or pouch shape. On the other hand, in simulations with more intense erosion rate, where connection of the sedimentary cover is soon broken, the syncline evolves predominantly by load-induced subsidence. This tends to develop syncline limbs with similar dips and more symmetrical overall.

The Àger basin, in the footwall of the Montsec thrust, has the thicker Paleogene sedimentary succession of the Serres Marginals thrust sheet (Figure 2.3, chapter 2), likely indicating a faster subsidence compared to the other synclines. Subsidence was continuous, as evidenced by the complete stratigraphic record and the long-lived unconformity at its northern limb. With respect to the geometries of diapir-flanking synclines obtained in the models, the Àger syncline is more similar to the drop shapes that evolve in simulations with less intense erosion where folding is predominantly developed by buckling (see also Brun & Fort, 2004), rather than the semi-circular synclines, characteristic of intense erosion and predominant load-induced subsidence. This supports our interpretation based on field observations, where buckling had the

predominant role in deformation at the Serres Marginals from the Garumnian stage onwards.

Syntectonic erosion is a very important parameter in the evolution of deformed foreland basins with salt, as its intensity will determine the unroofing of salt-cored anticlines, accelerating salt expulsion and promoting anticline closure. This does not happen in underwater settings such as gravity-driven fold-and thrust-belts at the toe of passive margin slopes (e.g. Brun & Fort 2004). Running a systematic series of simulations first with syntectonic sedimentation alone and then with syntectonic sedimentation and erosion has allowed us to address the importance of the erosion rate in determining fold geometries. In the simulations with no erosion, high sedimentation rates result in unrealistic geometries, promoting verticality of the anticlines, very fast subsidence in the synclines, and an overall decrease in the number of folds, inhibited by the thick pile of sediments on top of the pre-compressional layer. Even with moderate sedimentation rates, the absence of erosion meant that the vertical growth of the structures was not counteracted and this led to the bulging of the salt upwards, pinned by sedimentation concentrated in the outer foreland domain and in the diapir-flanking syncline. Any realistic effect that the variation of pre-compressional cover thickness could have had in the final geometry of the folds was shadowed by the disproportion in the development of the topography.

After incorporating erosion to the simulations, the key factors to determine fold geometry are the timing of anticline unroofing, and how many anticlines get unroofed. We have learned that the thickness of the pre-compressional cover does not affect much its erodibility. The main role of the cover thickness is in regulating the rigidity and susceptibility to fold during the buckling stage. As expected, a thin cover will develop a higher number of folds with smaller wavelength during the folding phase, while a thicker, more rigid cover will result in fewer and wider folds. The effect of erosion intensity and sediment supply will become more important if anticlines become unroofed, as they both will determine how fast and deep the synclines will subside.

None of the simulations ended with syncline imbrication, in spite of anticline unroofing. When simulations were left to run for longer time, synclines were uplifted and eroded rather than overthrusting each other. This is similar to the issue of the absence of

thrusting at diapir cores. Through the simulations with a single diapir setup we have learned that thrusting across the diapir core is possible if the diapir margins have a favourable dip angle, and that the thinner flank will always override the thicker one, effect that is enhanced by syntectonic sedimentation. However, we are still left to understand the fact that in the field there are examples of the thicker basin overriding the thinner one as in the case of the Montsec and Serres Marginals. A possibility is that thrusting across the Montsec diapir has as little displacement as the one achieved in our simulations, but it is more likely that in the natural example there are other factors that we have not been able to reproduce in our simulations.

This modelling project is still work in progress; the following steps involve testing the same setup with material properties that give a more rigid behaviour to the sedimentary cover and including a final stage of shortening without sedimentation or erosion.

In summary, erosion intensity will determine the timing of salt anticline unroofing and cover thickness will determine the geometry of the folds at that stage. But a thicker cover will not necessarily delay significantly the moment of unroofing.

4.5. Conclusions

This 2D numerical study has been useful to answer, at least partially, the questions raised the beginning of this chapter and has also brought up new points for discussion.

In 2D, it is possible to produce a fold system with salt anticlines and intervening synclines without pre-compressional salt structures. However, if the salt layer is too thick, the tendency is to broadly inflate the domain, preventing the nucleation of folds. If pre-compressional sedimentary cover is too thick, it will behave rigidly, also inhibiting buckle folding.

The implementation of syntectonic sedimentation enhances the formation of folds, and quickly localizes the deformation. It also promotes verticality in the structures. If sedimentation rate is too high, however, it masks the effect of cover thickness variations and can result in unrealistic geometries. For this reason in this kind of setting is necessary to implement erosion to achieve realistic results.

The intensity of erosion determines the timing of unroofing of salt anticlines, and therefore the transition from buckle folding, when the sedimentary cover is connected, to sedimentary load-induced subsidence, when synclines are individualised and anticlines are being closed. The effect of a thicker cover, will condition the geometry of the folds formed during the buckling phase, but will not have much influence in the timing of unroofing.

As for fold geometry, when erosion is less intense and the buckling phase lasts longer, there is a higher number of folds with smaller wavelength, and more asymmetric. It is in these cases where synclines flanking pre-existing diapirs form preferentially. The drop shape of the Åger basin is very similar to the synclines at the diapir flank in simulations with low erosion and a long buckling phase. This is also coincident with the field observations in chapter 2 that demonstrate that buckling was the predominant mechanism of folding in Serres Marginals for much of the Pyrenean orogeny. The fact that only some of the salt structures in Serres Marginals were unroofed by the end of the orogeny also supports this hypothesis.

In the simulations with the single diapir setup, welding and subsequent thrusting occurs in all the simulations except the ones where the diapir has vertical walls. The vergence of the thrust is determined by the thickness of the pre-shortening cover at both sides of the diapir, as it is always the thinner flank which overrides the thicker one. Sedimentation enhances this effect by accumulating faster in the thicker domain and salt gets displaced towards the opposite side, increasing its buoyancy. In the cases where the pre-shortening cover thickness is the same at both sides of the diapir, thrusting always occurs towards the opposite direction from the moving wall.

Trying to gain some insight in the mechanisms of thrusting across the diapir cores and the factors leading to syncline imbrication are two lines to continue investigating with this kind of simulations.

SUPPLEMENTARY MATERIAL

Table A.1. Setups with narrow diapirs

	Boundary Condition	Basement geometry	Width Diapirs	Roof	Domain A	Time Steps	Time End	Sedimentation
	Sticky Air/ No Stress		Km		Taper/Constant Thickness?			NO/YES (cm/yr)
1.1	No stress	Two taller steps, ramp	2	0.5	1 a 0.5	600	11.87	No
1.2	No stress	Two taller steps, ramp	2	1	1 a 0.5	600	11.87	No
1.3	No stress	Two steps, ramp	2	0.5	1 a 0.5	600	11.87	No
1.4	Free air	Two steps, ramp	2	0.5	1 a 0.5	600	11.87	No
1.5	No stress	Two steps, ramp	2	0.5	1 a 0.5	600	11.87	No

Table A.2. Setups with wide diapirs

	Boundary condition	Basement geometry	Width diapirs	Roof	Domain 1	Time steps	Time End	Sedimentation
	StickyAir/No stress		Km	Km	Taper/ Constant Thickness			
2.1a	No stress	Two steps, ramp	4	0.5	1 a 0.5	600	11.87	No
2.2	No stress	Two steps, ramp	6	0.5	1 a 0.5	600	11.87	No
2.3	Free air	Two steps, ramp	6	0.5	1 a 0.5	1000	19.87	No
2.4a	Free air	Two steps, ramp	6	No roof	1 a 0.5	1000	19.87	No
2.4b	Free air	Two steps, ramp			2 a 0.5	1000	19.87	No
2.5	Free air	Two steps, offsetted, ramp	6	0.5	1 a 0.5	1000	19.87	No
2.6	Free air	Two steps, ramp	6	0.25	1 a 0.5	1000	19.87	No
2.7	No stress	Two steps, ramp	6	0.5	1 a 0.5	600	11.87	No

2.8	No stress	Two steps, ramp	6	0.5	1 constant	600	11.87	No
2.9	No stress	Two steps, ramp	6	0.5	0.75 constant	600	11.87	No

Tables A.3. Adding syntectonic sedimentation

	Boundary conditions	Basement geometry	Diapir width	Diapir roof	Domain A thickness	Time Steps	Time End (My)	Sedimentation
4.1	No stress	Two steps, ramp	2	0.5	0.5 to 1	1000	9.96	0.01
4.2	No stress	Two steps, ramp	4	0.5	0.5 to 1	1000	9.96	0.01
4.3	No stress	Two steps, ramp	6	0.5	0.5 to 1	1200	11.96	0.01
4.4	No stress	Two steps, ramp	6	0.5	0.5 to 1	1000	9.96	No
4.5	No stress	Two steps, ramp	6	0.25	0.5 to 1	1000	9.96	0.01
4.6	No stress	Two steps, ramp	7	0.5	0.5 to 1	1160	11.56	0.01

	Boundary conditions	Basement geometry	Diapir width	Diapir roof	Domain A thickness	Time steps	Final End (My)	Sedimentation (cm/yr)
5.0	Sticky air	Twosteps, ramp	2 and 6	0	0.5 to 1	900	17,87	No
5.1	Sticky air	step-ramp-step-ramp	2 and 6	0	0.5 to 1	1000	19,87	No
5.2	Sticky air	continuous ramp	2 and 6	0	0.5 to 1	1000	19,87	No
	Sticky air	Two steps, ramp	4	0,5	0.5 to 1	1000	19,87	No
5.3	Sticky air	continuous ramp	2 and 6	0	0.5 to 1	1000	19,87	No
5.,4	Sticky air	step-ramp-step-ramp	2 and 6	0	0.5 to 1	1200	11,96	0,01
5.5	Sticky air	continuous ramp	2 and 6	0	0.5 to 1	1200	11,96	0,01
5.6	Sticky air	Two steps, ramp	2 and 6	0	0.5 to 1	730	7,26	0,01

5.7	Sticky air	step-ramp- step-ramp	2 and 6	0	0.75 constant	1200	11,96	0,01
5.8	Sticky air	step-ramp- step-ramp	2 and 6	0	0.5 constant	1200	11,96	0,01
5.9	Sticky air	step-ramp- step-ramp	2 and 6	0	0.75 constant	1200	11,96	0,01
5.10	Sticky air	step-ramp- step-ramp	2 and 6	0	0.5 constant	1200	11,96	0,01
5.11	Sticky air	step-ramp- step-ramp	2 and 6	0	0.75 constant	1200	11,96	0,02
5.12	Sticky air	step-ramp- step-ramp	2 and 6	0	0,75 constant	1200	11,96	0,015
5.13	Sticky air	step-ramp- step-ramp	2 and 6	0	1 constant	1200	11,96	0,02
5.14	Sticky air	step-ramp- step-ramp	2 and 6	0	0,5 constant	1200	11,96	0,015
5.15	Sticky air	step-ramp- step-ramp	2 and 6	0	0,75 to 1	1200	11,96	0,015
5.16	Sticky air	step-ramp- step-ramp	2 and 6	0	0,5 to 1	1200	11,96	0,015
5.17	Sticky air	step-ramp- step-ramp	2 and 6	0	0,5 constant	1200	11,96	0,015
5.18	Sticky air	step-ramp- step-ramp	2 and 6	0	1 constant	1200	11,96	0,01
5.19	Sticky air	step-ramp- step-ramp	2 and 6	0	1 constant	1200	11,96	0,015
5.20	Sticky air	step-ramp- step-ramp	2 and 6	0	0,5 to 1	1200	11,96	0,01

Table A.4. Simulations with the short diapir setup

Name	Boundary conditions	Diapir angle	Diapir roof	Thickness left domain	Thickness right domain	Time steps	Final time	Sediment. (cm/yr)
10.1	Sticky air	63	0	4 km	3,5 km	1200	12 My	0,01
10.2	Sticky air	45	0	4 km	3,5 km	1200	12 My	0,01
10.3	Sticky air	34	0	4 km	3,5 km	1200	12 My	0,01
10.4	Sticky air	Vertical	0,5	4 km	3,5 km	1200	12 My	0,01
11.1	Sticky air	63	0	4 km	2,5 km	1200	12 My	0,01
11.2	Sticky air	45	0	4 km	2,5 km	1200	12 My	0,01
11.3	Sticky air	34	0	4 km	2,5 km	1200	12 My	0,01
11.4	Sticky air	Vertical	0,5	4 km	2,5 km	1200	12 My	0,01
12.1	Sticky air	63	0	4 km	4 km	1200	12 My	0,01
12.2	Sticky air	45	0	4 km	4 km	1200	12 My	0,01
12.3	Sticky air	34	0	4 km	4 km	1200	12 My	0,01
12.4	Sticky air	Vertical	0,5	4 km	4 km	1200	12 My	0,01

Table A.5. Simulations with syntectonic erosion

Name	Boundary conditions	Diapir roof	Thickness Domain A	Erosion intensity (k)	Time steps	Final time
M1	Sticky air	0	0,5 km	1e-9	2000	20 My
M2	Sticky air	0	0,5 km	1e-8	2000	20 My
M3	Sticky air	0	0,5 km	5e-8	2000	20 My
M4	Sticky air	0	0,5 km	1e-7	2000	20 My
M5	Sticky air	0	0,75 km	1e-9	2000	20 My
M6	Sticky air	0	0,75 km	1e-8	2000	20 My
M7	Sticky air	0	0,75 km	5e-8	2000	20 My
M8	Sticky air	0	0,75 km	1e-7	2000	20 My
M9	Sticky air	0	1 km	1e-9	2000	20 My
M10	Sticky air	0	1 km	1e-8	2000	20 My
M11	Sticky air	0	1 km	5e-8	2000	20 My
M12	Sticky air	0	1 km	1e-7	2000	20 My

Chapter 5

Conclusions

In a multidisciplinary study integrating structural and stratigraphic data and numerical modelling, this thesis presents new results on the orogenic evolution of the Central Southern Pyrenees and the role of salt tectonics. The conclusions reached from the Pyrenean case study can also be integrated into the wider discussion on the fundamental parameters driving salt-related tectonic deformation. Here is a summary of the main conclusions reached by this study:

5.1. Structural reinterpretation

- The field study of the progressive unconformity the Àger basin (Chapter 2) has led to the reinterpretation of the Montsec footwall structure. The continuity of the stratigraphic succession and the dips of the growth strata have led to reinterpret the Àger basin northern limb as an unfaulted succession from the Mesozoic to the Ypresian and thus, localize the main thrust plane along the axial surface of the Montsec anticline. This interpretation implies substantially less shortening than the 11 km estimated previously for the Montsec thrust in the Ribagorçana transect, in interpretations that showed a continuous footwall ramp under the Montsec hanging wall anticline.
- The identification of the progressive unconformity described in the Aptian and Albian carbonates adjacent to the Senterada Keuper province, to the north of the Organyà basin, and the Keuper lenses interbedded within the Albian marls, has led to the reinterpretation of the contact between the two (Chapter 3). The contact between the Lower Cretaceous carbonates of the basin edge and the Keuper province, previously understood as the Morreres backthrust is here reinterpreted as primarily a diapiric contact, although some fault reactivation during the Pyrenean orogeny may not be discarded.

5.2. Tectonostratigraphy and alluvial systems provenance

- Identifying an absence of Permo-Triassic clasts in the late Lutetian Espills and lower Gulp allogroups of the Gulp basin intramontane conglomerates suggests that the Paleozoic clasts were sourced from an area where the Cretaceous

carbonates were directly overlying the Silurian and Devonian from the Nogueres thrust sheet. The omission of the Permo-Triassic succession is most probably caused by a northern termination of the Permo-Triassic basins in the Nogueres thrust sheet, while the granite and gneiss pebbles were likely sourced by more distant areas like the Lower Paleozoic gneiss massifs and Hercynian plutons (e.g. Castillon, Trois Seigneurs and Lacourt), located at a root of the Nogueres thrust sheet in the North Pyrenean zone. The water divide during mid Eocene times was located more to the north than it is today.

- Compositional differences between the clasts of the upper fans of the Pallaresa allogroup in the La Pobla de Segur basin and the Gulp basin have led to the differentiation of a new alluvial fan in the Gulp basin, here named the Camporan fan. This fan is characterised by a predominance of Permo-Triassic and Devonian limestone pebbles, and a lack of Carboniferous pebbles, as opposed to the time-equivalent fans of the La Pobla basin, where Culm facies pebbles are abundant.
- Based on a local source dominated clast composition and the stratigraphic relationships with the substratum, the Senterada allogroup is reinterpreted as a very local system, restricted to the Senterada basin only. These conglomerate fans were trapped and confined in an E-W oriented synformal trough (a minibasin), sitting directly above the Keuper, and finally overlapping onto the Paleozoic to the north and the Sant Gervàs and Peralç ridges to the south.

5.3. Salt tectonics evolution in the Southern Pyrenees

5.3.1. *Pre-compressional stage*

- Halokinetic features are identified in the long-lived unconformities and thickness differences at the syncline flanks in the Serres Marginals and Àger basin. The variability in size, geometry and preserved stratigraphic record indicate an independent subsidence rate for each structure, with separate depocentres locally operating since the Jurassic. This conditioned a pattern of polygonal synclines and intervening salt structures in the Serres Marginals before the arrival of the Pyrenean deformation front.

- In this context, the precursor of the Montsec ridge is interpreted as an elongated salt wall, its initiation likely triggered by basement normal faulting during the Early Cretaceous rifting stage. The significant throw of the basement fault enabled greater subsidence in the sedimentary cover of the Tremp basin, while the Àger basin and Serres Marginals remained relatively uplifted. Hence the Lower Cretaceous succession is almost non-existent in these domains.
- Halokinetic features are also identified during the Early Cretaceous rifting stage in the northern margin of the Organyà basin, indicated by the thinning stratigraphy towards the Senterada salt province, progressive unconformities, and interbedded Keuper lenses within the Lower Cretaceous carbonates and shales, likely remnant of a partially-welded salt sheet.

5.3.2. *Pyrenean orogeny*

- With the onset of Pyrenean compression, in the late Santonian, the driving mechanisms for deformation in the Àger basin and the Serres Marginals progressively shifted from predominantly vertical movements due to differential loading (bending), to structure narrowing by predominant compressional buckling from the latest Cretaceous-Palaeocene onwards. Increasing sedimentation rates during the orogeny kept the synclines subsiding into the salt, but the continuity of the pre-shortening cover, due to lack of anticline unroofing, meant that buckling could remain as the predominant folding mechanism. It is likely that the Oligocene imbrication of the synclines in the Ribagorçana transect responds to primary welding of the basal evaporite layer in the deeper synclines, in parallel to the unroofing of some of the diapirs and anticline crests.
- The overturned panel of the Àger basin footwall syncline in the Noguera Ribagorçana transect is interpreted as a flap that was further verticalized and rotated during the orogeny. The overturned strata of the Pasarel·la syncline are interpreted as the northern margin of a minibasin that grew at the top of the Montsec salt pillow. During the compression, the smaller diapir flanking the Pasarel·la minibasin to the south was closed into the Pasarel·la weld.

- In the Organyà basin, the salt walls from the Senterada salt province were exposed at the surface at least during the rifting stage first, and then from the upper Ypresian to the Oligocene, as evidenced by the widespread presence of Triassic ophite clasts in all the intramontane conglomerate units. From Lutetian times onwards, the differential load of the alluvial systems of the La Pobla and Gulp basins generated accommodation space and caused a moderate and progressive northward tilting of the northern Organyà basin margin, enabled by the expulsion of salt through the exposed Senterada salt province. The alluvial fans progressively retrograded to the north, infilling the palaeoreliefs of the northern Organyà basin and displacing the load towards the Senterada salt province.
- The erosional unrooting of the Nogueres thrust sheet during the Oligocene enabled the sinking and rotation of the detached leading edge (the Nogueres têtes plongeantes) into the evaporites of the Senterada salt province, explaining partly their strong overturning. Subsidence was enhanced by the sedimentation of the Senterada and Antist conglomerates on top, which due to load-induced salt withdrawal kept trapped into the Senterada trough, defined by the width of the salt province.

5.4. Folding mechanisms in a salt-detached foreland basin

- During the pre-compressional stage, load-induced subsidence was predominant in the Serres Marginals synclines, as indicated by diachronous thickness variations and unconformities, indicating independent subsidence rates between the synclines. The onset of compressional buckling is marked by the contemporary occurrence of the growth strata and stratigraphic discontinuities in all the synclines.
- In the 2D numerical models of compressional salt tectonics, it is possible to form a domain with salt anticlines and intervening synclines and without pre-shortening salt diapirs, which could be taken as analogues to parts of the Serres Marginals. In models reproducing the configuration of the south-central Pyrenees (Organyà, Tremp and Serres Marginals units), the deformation front

quickly reaches the frontal domain without deforming significantly the thicker basins in the rear or closing the large pre-existing diapirs. However, thick salt layers favour the inflation of the external domain, preventing the formation of smaller-wavelength folds. Thick pre-shortening overburdens behave rigidly, also inhibiting buckle fold nucleation. This favours the hypothesis of Mesozoic thickness differences caused by halokinesis in much of the Serres Marginals domain (occurring since the Jurassic), helping to nucleate early compressional folding.

- The intensity of erosion determines the timing of unroofing of the anticlines, and therefore the transition from buckle folding, when the sedimentary cover is connected, to load-induced subsidence, when synclines are individualised and anticlines are being closed. This supports idea that the sedimentary cover in Serres Marginals was fairly continuous (anticlines and diapirs not fully unroofed) up to the last orogenic stages, thus enabling folding by buckling as has been deduced by field evidence. However, the early unroofing of structures as the Avellanes diapir or the Montsec, and associated salt extrusion likely prevented widespread inflation, which would have inhibited buckle folding.
- When erosion is less intense and the buckling phase lasts longer there is a higher number of folds, with higher asymmetry. It is in these cases where flanking synclines tend to form at the foreland side of the main diapirs. The drop shape of the Àger basin is very similar to the synclines at the diapir flanks in simulations with low erosion and a long buckling phase.
- Thrusting across the diapir cores after welding nor syncline imbrication has happened in the regional setup of the numerical simulations. In the short setup thrusting always occurred with the thinner unit overriding the thicker one, as opposed to what happens in the Montsec thrust-weld. From field observations it looks like primary welding could have had an important effect in the unroofing of the structures and subsequent secondary welding and syncline imbrication. Since the synclines in the regional setup models never got to weld at the base, this hypothesis needs to be tested in further simulations.

References

References

- Almela, A., Rios, J.M., 1943. Contribución al conocimiento de la zona surpirenaica catalana. *Boletín Igme* 18, 41–65.
- Alves, T.M., Manuppella, G., Gawthorpe, R.L., Hunt, D.W., 2003. The depositional evolution of diapir- and fault-bounded rift basins : examples from the Lusitanian Basin of West Iberia. *Sedimentary Geology* 162, 273–303. [https://doi.org/10.1016/S0037-0738\(03\)00155-6](https://doi.org/10.1016/S0037-0738(03)00155-6)
- Arche, A., López-Gómez, J., 1996. Origin of the Permian-Triassic Iberian Basin , central-eastern Spain. *Tectonophysics* 266, 443–464.
- Arnal, I., Calvet, F., Márquez, L., Márquez-Aliaga, A., Solé de Porta, N., 2002. La plataforma carbonatada epeírica (Formaciones Imón e Isábena) del Triásico superior del Noreste de la Península Ibérica. *Acta Geologia Hispanica* 37, 4, 299–328.
- Azambre, B., Rossy, M., Lago, M., 1987. Caractéristiques pétrologiques des dolérites tholéitiques d' âge triasique (ophites) du domaine pyrénéen. *Bulletin de la société française de Minéralogie et de Cristallographie* 110, 379–396.
- Barnolas, A., Samsó, J.M., Teixell, A., Tosquella, J., Zamorano, M., 1991. Evolucion sedimentaria entre la cuenca de Graus-Tremp y la cuenca de Jaca-Pamplona, in: I Congreso Del Grupo Español Del Terciario, Libro-Guía.
- Barsó, D., 2007. Análisis de la procedencia de los conglomerados sinorogénicos de La Pobla de Segur (Lérida) y su relación con la evolución tectónica de los Pirineos centro-meridionales durante el Eoceno medio-Oligoceno. Tesis de la Universitat de Barcelona.
- Bartrina, T., Hernández, E., 1990. Las unidades evaporíticas del Triásico del subsuelo del Maestrazgo, in: Formaciones Evaporíticas de La Cuenca Del Ebro y Cadenas Periféricas y de La Zona de Levante. Nuevas Aportaciones y Guía de Superficie. Universitat de Barcelona, pp. 34–38.
- Bataller, J.R., 1943. El Anoplotherium commune CUV. del Eocénico de Sossís. *Las Ciencias* 8.
- Beamud, E., Garcés, M., Cabrera, L., Muñoz, J.A., Almar, Y., 2003. A new middle to late Eocene continental chronostratigraphy from NE Spain. *Earth and Planetary Science Letters* 216, 501–514. [https://doi.org/10.1016/S0012-821X\(03\)00539-9](https://doi.org/10.1016/S0012-821X(03)00539-9)
- Beamud, E., Muñoz, J.A., Fitzgerald, P.G., Baldwin, S.L., Garcés, M., Cabrera, L., Metcalf, J.R., 2011. Magnetostratigraphy and detrital apatite fission track thermochronology in syntectonic conglomerates: Constraints on the exhumation of the South-Central Pyrenees. *Basin Research* 23, 3, 309–331. <https://doi.org/10.1111/j.1365-2117.2010.00492.x>
- Beaumont, C., Muñoz, J.A., Hamilton, J., Fullsack, P., 2000. Factors controlling the Alpine evolution of the central Pyrenees inferred from a comparison of observations and

- geodynamical models. *Journal of Geophysical Research* 105, B4, 8121–8145. <https://doi.org/10.1029/1999JB900390>
- Berástegui, X., García-Senz, J., Losantos, M., 1990. Tecto-sedimentary evolution of the Organyà extensional basin (central south Pyrenean unit, Spain) during the Lower Cretaceous. *Bulletin de la Societé Géologique de la France* 8, VI, 251–64.
- Berástegui, X., Losantos, M., Munoz, J.A., Puigdefabregas, C., 1993. Tall geológic del Pirineu central 1:200000, Institut Cartogràfic de Catalunya.
- Bodego, A., Iriarte, E., López-Horgue, M.A., Álvarez, I., 2018. Rift-margin extensional forced folds and salt tectonics in the eastern Basque-Cantabrian rift basin (western Pyrenees). *Marine and Petroleum Geology* 91, November 2017, 667–682. <https://doi.org/10.1016/j.marpetgeo.2018.02.007>
- Brun, J.P., Fort, X., 2004. Compressional salt tectonics (Angolan margin). *Tectonophysics* 382, 3–4, 129–150. <https://doi.org/10.1016/j.tecto.2003.11.014>
- Buiter, S.J.H., Schreurs, G., Albertz, M., Gerya, T. V., Kaus, B., Landry, W., le Pourhiet, L., Mishin, Y., Egholm, D.L., Cooke, M., Maillot, B., Thieulot, C., Crook, T., May, D., Souloumiac, P., Beaumont, C., 2016. Benchmarking numerical models of brittle thrust wedges. *Journal of Structural Geology* 92, 140–177. <https://doi.org/10.1016/j.jsg.2016.03.003>
- Callot, J.-P., Trocme, V., Letouzey, J., Albouy, E., Jahani, S., Sherkati, S., 2012. Pre-existing salt structures and the folding of the Zagros Mountains. *Geological Society of London Special Publication* 363, 1, 545–561. <https://doi.org/10.1144/SP363.27>
- Cámara, P., Flinch, J.F., 2017. The Southern Pyrenees: A Salt-Based Fold-and-Thrust Belt. *Permo-Triassic Salt Provinces of Europe, North Africa and the Atlantic Margins* 395–415. <https://doi.org/10.1016/B978-0-12-809417-4.00019-7>
- Cámara, P., Klimowitz, J., 1985. Interpretación geodinámica de la vertiente centro-occidental surpirenaica (Cuencas de Jaca-Tremp). *Estudios geológicos* 41, 391–404.
- Canérot, J., 1988. Manifestations de l’halocinèse dans les Chaînons Béarnais (Zone Nord Pyrénéenne) au Crétace inférieur. *Comptes Rendus Académie des Sciences de Paris* 306, 1099–1102.
- Canérot, J., Hudec, M.R., Rockenbauch, K., 2005. Mesozoic diapirism in the Pyrenean orogen: Salt tectonics on a transform plate boundary. *AAPG Bulletin* 89, 2, 211–229. <https://doi.org/10.1306/09170404007>
- Caus, E., 1973. Aportaciones al conocimiento del Eoceno del anticlinal de Oliana (prov. Lérida). *Acta Geológica Hispánica* 8, 1, 7–10.
- Caus, E., Rod, D., Sire, A., 1990. Stratigraphy of the Lower Cretaceous (Berriasian-Barremian) sediments in the Organyà Basin, Pyrenees, Spain. *Cretaceous Research* 11, 313–320.
- Costa, E., Vendeville, B.C., 2002. Experimental insights on the geometry and kinematics of fold-and-thrust belts above weak, viscous evaporitic décollement. *Journal of Structural Geology* 24, 1729–1739. <https://doi.org/10.1016/j.jsg.2004.04.001>

- Cramer, F., Schmeling, H., Golabek, G.J., Duretz, T., Orendt, R., Buitert, S.J.H., May, D.A., Kaus, B.J.P., Gerya, T. V., Tackley, P.J., 2012. A comparison of numerical surface topography calculations in geodynamic modelling: An evaluation of the “sticky air” method. *Geophysical Journal International* 189, 1, 38–54. <https://doi.org/10.1111/j.1365-246X.2012.05388.x>
- Crusafont, M., Vilalta, J., Truyols, J., 1956. Caracterización del Eoceno continental en la cuenca de Tremp y edad de la orogénesis pirenaica. *Ile Congr. Int. Etud. Pyr. Toulouse* 2, 1, 29–53.
- Cruz, L., Malinski, J., Hernandez, M., Take, A., Hilley, G., 2011. Erosional control of the kinematics of the Aconcagua fold-and-thrust belt from numerical simulations and physical experiments. *Geological Society of America Bulletin* 39, 5, 439–442. <https://doi.org/10.1130/G31675.1>
- Cuevas, J.L., Mercadé, L., Puigdefábregas, C., Nijman, W., Muñoz, J.A., 1989. The first stage of the foreland basin: the Tremp Group, in: *In Guidebook 4th International Conference on Fluvial Sedimentology. Servei Geològic de Catalunya*, pp. 23–29.
- Dabrowski, M., Krotkiewski, M., Schmid, D.W., 2008. MILAMIN: MATLAB-based finite element method solver for large problems. *Geochemistry, Geophysics, Geosystems* 9, 4, 1–24. <https://doi.org/10.1029/2007GC001719>
- Dalloni, M., 1930. Étude géologique des Pyrénées catalanes. *Annales de la Faculté des sciences de Marseille* 26, 3, 373.
- Darnault, R., Callot, J.-P., Ballard, J.-F., Fraise, G., Mengus, J.-M., Ringenbach, J.C., 2016. Control of syntectonic erosion and sedimentation on kinematic evolution of a multidecollement fold and thrust zone: Analogue modeling of folding in the southern subandean of Bolivia. *Journal of Structural Geology* 89, 30–43. <https://doi.org/10.1016/j.jsg.2016.05.009>
- Davis, D.M., Engelder, T., 1985. The role of salt in fold-and-thrust belts. *Tectonophysics* 119, 67–88.
- Decarlis, A., Maino, M., Dallagiovanna, G., Lualdi, A., Masini, E., Seno, S., Toscani, G., 2014. Salt tectonics in the SW Alps (Italy-France): From rifting to the inversion of the European continental margin in a context of oblique convergence. *Tectonophysics* 636, 293–314. <https://doi.org/10.1016/j.tecto.2014.09.003>
- Deramond, J., Souquet, P., Fondécave-Wallez, M.J., Specht, M., 1993. Relationships between thrust tectonics and sequence stratigraphy surfaces in foredeeps: Model and examples from the Pyrenees (Cretaceous-Eocene, France, Spain). *Geological Society Special Publication* 71, 71, 193–219. <https://doi.org/10.1144/GSL.SP.1993.071.01.09>
- Dinarès-Turell, J., 1994. Remagnetizaciones asociadas a diagenesis y su relación con el emplazamiento de láminas cabalgantes en el Pirineo meridional. *Geogaceta* 15, 105–108.
- Dooley, T.P., Hudec, M.R., 2020. Extension and inversion of salt-bearing rift systems. *Solid Earth Discussions* In review. <https://doi.org/https://doi.org/10.5194/se->

2020-3

- Duffy, O.B., Dooley, T.P., Hudec, M.R., Jackson, M.P.A., Fernandez, N., Jackson, C.A.L., Soto, J.I., 2018. Structural evolution of salt-influenced fold-and-thrust belts: A synthesis and new insights from basins containing isolated salt diapirs. *Journal of Structural Geology* 114, April, 206–221. <https://doi.org/10.1016/j.jsg.2018.06.024>
- Duffy, O.B., Fernandez, N., Hudec, M.R., Jackson, M.P.A., Burg, G., Dooley, T.P., Jackson, C.A.L., 2017. Lateral mobility of minibasins during shortening: Insights from the SE Precaspian Basin, Kazakhstan. *Journal of Structural Geology* 97, 257–276. <https://doi.org/10.1016/j.jsg.2017.02.002>
- Dupuoy-Camet, J., 1953. Triassic diapiric salt structures, south-western Aquitaine basin, France. *AAPG Bulletin* 37, 10, 2348–2388.
- Ellis, P.G., McClay, K.R., 1988. Listric extensional fault systems - results of analogue model experiments. *Basin Research* 1, 1, 55–70. <https://doi.org/10.1111/j.1365-2117.1988.tb00005.x>
- Escosa, F.O., Roca, E., Ferrer, O., 2018. Testing thin-skinned inversion of a prerift salt-bearing passive margin (Eastern Prebetic Zone, SE Iberia). *Journal of Structural Geology* 109, February, 55–73. <https://doi.org/10.1016/j.jsg.2018.01.004>
- Espurt, N., Angrand, P., Teixell, A., Labaume, P., Ford, M., de Saint Blanquat, M., Chevrot, S., 2019a. Crustal-scale balanced cross-section and restorations of the Central Pyrenean belt (Nestes-Cinca transect): Highlighting the structural control of Variscan belt and Permian-Mesozoic rift systems on mountain building. *Tectonophysics* 764, December 2018, 25–45. <https://doi.org/10.1016/j.tecto.2019.04.026>
- Espurt, N., Wattellier, F., Philip, J., Hippolyte, J.C., Bellier, O., Bestani, L., 2019b. Mesozoic halokinesis and basement inheritance in the eastern Provence fold-thrust belt, SE France. *Tectonophysics* 766, December 2018, 60–80. <https://doi.org/10.1016/j.tecto.2019.04.027>
- Fauré, P., 1984. Le Lias de la partie centro-orientale des Pyrénées espagnoles (Provinces de Huesca, Lerida et Barcelona). *Bulletin de la Société d'histoire naturelle de Toulouse* 121, 23–27.
- Fernandes, N.F., Dietrich, W.E., 1997. Hillslope evolution by diffusive processes: The timescale for equilibrium adjustments. *Water Resources Research* 33, 6, 1307–1318. <https://doi.org/10.1029/97WR00534>
- Fernandez, N., 2014. 2D and 3D numerical modelling of multilayer detachment folding and salt tectonics. Phd Thesis, Johannes Gutenberg-Universität Mainz.
- Fernandez, N., Duffy, O.B., Hudec, M.R., Jackson, M.P.A., Burg, G., Jackson, C.A.L., Dooley, T.P., 2017. The origin of salt-encased sediment packages: Observations from the SE Precaspian Basin (Kazakhstan). *Journal of Structural Geology* 97, 237–256. <https://doi.org/10.1016/j.jsg.2017.01.008>
- Fernandez, N., Hudec, M.R., Jackson, C.A.-L., Dooley, T.P., Duffy, O.B., 2020. The competition for salt and kinematic interactions between minibasins during density-

- driven subsidence: observations from numerical models. *Petroleum Geoscience* 26, 1, 3–15. <https://doi.org/10.1144/petgeo2019-051>
- Fernandez, N., Kaus, B.J.P., 2014. Fold interaction and wavelength selection in 3D models of multilayer detachment folding. *Tectonophysics* 632, C, 199–217. <https://doi.org/10.1016/j.tecto.2014.06.013>
- Ferrer, O., Jackson, M.P.A., Roca, E., Rubinat, M., 2012. Evolution of salt structures during extension and inversion of the Offshore Parentis Basin (Eastern Bay of Biscay). *Geological Society Special Publication* 363, 1, 361–380. <https://doi.org/10.1144/SP363.16>
- Fillon, C., Gautheron, C., van der Beek, P., 2013. Oligocene–Miocene burial and exhumation of the Southern Pyrenean foreland quantified by low-temperature thermochronology. *Journal of the Geological Society* 170, 1, 67–77. <https://doi.org/10.1144/jgs2012-051>
- Fitzgerald, P.G., Muñoz, J.A., Coney, P.J., Baldwin, S.L., 1999. Asymmetric exhumation across the Pyrenean orogen: Implications for the tectonic evolution of a collisional orogen. *Earth and Planetary Science Letters* 173, 3, 157–170. [https://doi.org/10.1016/S0012-821X\(99\)00225-3](https://doi.org/10.1016/S0012-821X(99)00225-3)
- Flinch, J.F., Casas, J.M., 1996. Inversion of a transfer system into lateral ramps: An example from the South-Central Pyrenees (Spain). *International Journal of Earth Sciences* 85, 2, 372–379. <https://doi.org/10.1007/s005310050082>
- García-Senz, J., 2002. Cuencas extensivas del Cretácico Inferior en los Pirineos centrales, formación y subsecuente inversión. Phd thesis, Universitat de Barcelona.
- García-Senz, J., Zamorano, M., 1992. Evolución tectónica y sedimentaria durante el Priaboniense superior-Mioceno inferior, en el frente de cabalgamiento de las Sierras Marginales occidentales. *Acta Geológica Hispánica* 27, 1–2, 195–209.
- Garrido-Mejías, A., 1973. Estudio geológico y relación entre tectónica y sedimentación del Secundario y Terciario de la vertiente meridional pirenaica en la zona central. Phd thesis, Universidad de Granada.
- Garrido-Mejías, A., Ríos, L.M., 1972. Síntesis geológica del Secundario y Terciario entre los ríos Cinca y Segre (Pirineo Central de la vertiente sur pirenaica, provincias de Huesca y Lérida). *Boletín Geológico y Minero* 83, 1, 1–47.
- Ge, H., Jackson, M.P.A., Vendeville, B.C., 1997. Kinematics and Dynamics of Salt Tectonics Driven by Progradation. *AAPG Bulletin* 81, 3, 398–423. <https://doi.org/10.1306/522B4361-1727-11D7-8645000102C1865D>
- Gelabert, B., 1986. Estratigrafía física y análisis de facies de la fm. Baronia entre Perauba y Coll d’Orenga. Undergraduate thesis, Universitat Autònoma de Barcelona.
- Giles, K.A., Rowan, M.G., 2012. Concepts in halokinetic-sequence deformation and stratigraphy. *Geological Society of London Special Publication* 363, 1, 7–31. <https://doi.org/10.1144/SP363.2>
- Gómez-Gras, D., Roigé, M., Fondevilla, V., Oms, O., Boya, S., Remacha, E., 2016.

- Provenance constraints on the Tremp Formation paleogeography (southern Pyrenees): Ebro Massif vs Pyrenees sources. *Cretaceous Research* 57, 414–427. <https://doi.org/10.1016/j.cretres.2015.09.010>
- Gómez, J., Goy, A., 1998. Las unidades litoestratigráficas del tránsito Triásico-Jurásico en la región de Lécera (Zaragoza). *Geogaceta* 23, 63–66.
- Goteti, R., Beaumont, C., Ings, S.J., 2013. Factors controlling early stage salt tectonics at rifted continental margins and their thermal consequences 118, April, 3190–3220. <https://doi.org/10.1002/jgrb.50201>
- Graham, R., Jackson, M., Pilcher, R., Kilsdonk, B., 2012. Allochthonous salt in the sub-Alpine fold-thrust belt of Haute Provence, France. *Geological Society of London Special Publications* 363, 1, 595–615. <https://doi.org/10.1144/SP363.30>
- Grelaud, S., Sassi, W., Frizon de Lamotte, D., Jaswal, T., Roure, F., 2002. Kinematics of eastern Salt Range and South Potwar Basin (Pakistan): a new scenario. *Marine and Petroleum Geology* 19, 1127–1139.
- Grool, A.R., Huismans, R.S., Ford, M., 2019. Salt décollement and rift inheritance controls on crustal deformation in orogens. *Terra Nova* 31, 6, 562–568. <https://doi.org/10.1111/ter.12428>
- Heydarzadeh, K., Ruh, J.B., Vergés, J., Hajjalibeigi, H., Gharabeigli, G., 2020. Evolution of a structural basin: Numerical modelling applied to the Dehdasht Basin, Central Zagros, Iran. *Journal of Asian Earth Sciences* 187, July 2019, 104088. <https://doi.org/10.1016/j.jseaes.2019.104088>
- Holl, J.E., Anastasio, D.J., 1993. Paleomagnetically derived folding rates, southern Pyrenees, Spain. *Geology* 21, 3, 271–274.
- Howard, L., 1993. The statistics of counting clasts in rudites: a review, with examples from the upper Palaeogene of southern California, USA. *Sedimentology* 40, 2, 157–174. <https://doi.org/10.1111/j.1365-3091.1993.tb01759.x>
- Hudec, M.R., Jackson, M.P.A., 2007. Terra infirma: Understanding salt tectonics. *Earth-Science Reviews* 82, 1–2, 1–28. <https://doi.org/10.1016/j.earscirev.2007.01.001>
- Hudec, M.R., Jackson, M.P.A., 2006. Advance of allochthonous salt sheets in passive margins and orogens. *AAPG Bulletin* 90, 10, 1535–1564. <https://doi.org/10.1306/05080605143>
- Hudec, M.R., Jackson, M.P.A., Schultz-Ela, D.D., 2009. The paradox of minibasin subsidence into salt: Clues to the evolution of crustal basins. *Geological Society of America Bulletin* 121, 1/2, 201–221. <https://doi.org/10.1130/B26275.1>
- ICGC, 2014. 328-1-2 sheet, Camarasa, 1:25000 geological map.
- ICGC, 2010. 251-2-2 sheet, Espills, 1:25000 geological map.
- ICGC, 2009. 252-1-1 sheet, Tremp, 1:25000 geological map.
- ICGC, 2007a. 289-2-2 sheet, Sant Esteve de la Sarga, 1:25000 geological map.
- ICGC, 2007b. 328-2-1 sheet, Vilanova de Meià, 1:25000 geological map.

- ICGC, 2003. 290-1-2 sheet, Llimiana, 1:25000 geological map.
- Ings, S.J., Beaumont, C., 2010. Shortening viscous pressure ridges, a solution to the enigma of initiating salt “withdrawal” minibasins. *Geology* 38, 4, 339–342. <https://doi.org/10.1130/G30520.1>
- Jackson, M.P.A., Hudec, M.R., 2017. *Salt tectonics: Principles and practice*. Cambridge University Press.
- Jackson, M.P.A., Vendeville, B.C., Schultz-Ela, D.D., 1994. Structural Dynamics of Salt Systems. *Annual Review of Earth and Planetary Sciences* 22, 93–117. <https://doi.org/10.1146/annurev.earth.22.1.93>
- Jahani, S., Callot, J.P., Letouzey, J., Frizon de Lamotte, D., 2009. The eastern termination of the Zagros Fold-and-Thrust Belt, Iran: Structures, evolution, and relationships between salt plugs, folding, and faulting. *Tectonics* 28, 1–22. <https://doi.org/10.1029/2008TC002418>
- Jahani, S., Hassanpour, J., Mohammadi-Firouz, S., Letouzey, J., Frizon de Lamotte, D., Alavi, S.A., Soleimany, B., 2017. Salt tectonics and tear faulting in the central part of the Zagros Fold-Thrust Belt, Iran. *Marine and Petroleum Geology* 86, 426–446. <https://doi.org/10.1016/j.marpetgeo.2017.06.003>
- James, V., Canérot, J., 1999. Diapirisme et structuration post-triasique des Pyrénées occidentales et de l’Aquitaine méridionale (France). *Eclogae Geologicae Helveticae*.
- Jourdon, A., Mouthereau, F., Le Pourhiet, L., Callot, J., 2020. Topographic and Tectonic Evolution of Mountain Belts Controlled by Salt Thickness and Rift Architecture. *Tectonics* 39, 1. <https://doi.org/10.1029/2019TC005903>
- Jurado, M., 1990. El Triásico y el Liásico basal evaporíticos del subsuelo de la cuenca del Ebro, in: *Formaciones Evaporíticas de La Cuenca Del Ebro y Cadenas Periféricas, y de La Zona de Levante*. ENRESA-GPPG, Universidad de Barcelona, pp. 21–28.
- Kaus, B.J.P., 2010. Factors that control the angle of shear bands in geodynamic numerical models of brittle deformation. *Tectonophysics* 484, 1–4, 36–47. <https://doi.org/10.1016/j.tecto.2009.08.042>
- Kergaravat, C., Ribes, C., Callot, J.P., Ringenbach, J.C., 2017. Tectono-stratigraphic evolution of salt-controlled minibasins in a fold and thrust belt, the Oligo-Miocene central Sivas Basin. *Journal of Structural Geology* 102, 75–97. <https://doi.org/10.1016/j.jsg.2017.07.007>
- Kergaravat, C., Ribes, C., Legeay, E., Callot, J.P., Kavak, K.S., Ringenbach, J.-C., 2016. Minibasins and salt canopy in foreland fold-and-thrust belts: The central Sivas Basin, Turkey. *Tectonics* 35, 6, 1342–1366. <https://doi.org/10.1002/2016TC004186>
- Koyi, H., 1998. The shaping of salt diapirs. *Journal of Structural Geology* 20, 4, 321–338. [https://doi.org/10.1016/S0191-8141\(97\)00092-8](https://doi.org/10.1016/S0191-8141(97)00092-8)
- Labaupe, P., Teixell, A., 2020. Evolution of salt structures of the Pyrenean rift (Chaînons Béarnais, France): From hyper-extension to tectonic inversion. *Tectonophysics* 92, 63–72, 228451. <https://doi.org/10.1016/j.tecto.2020.228451>

- Lago, M., Galé, C., Arranz, E., Vaquer, R., Gil, A., Pocovi, J., 2000. Triassic tholeiitic dolerites («ophites») of the el grado diapir (Pyrenees, Huesca, Spain): Emplacement and composition. *Estudios Geológicos* 56, 1–2, 3–18. <https://doi.org/10.3989/egeol.00561-2152>
- Lanaja, J., 1987. Contribución de la exploración petrolífera al conocimiento de la geología de España.
- Legeay, E., Ringenbach, J.C., Kergaravat, C., Pichat, A., Mohn, G., Vergés, J., Kavak, K.S., Callot, J.P., 2019. Structure and kinematics of the Central Sivas Basin (Turkey): salt deposition and tectonics in an evolving fold-and-thrust belt, in: *Fold and Thrust Belts: Structural Style, Evolution and Exploration*. Geological Society of London, Special Publications, 490.
- Letouzey, J., Colletta, B., Vially, R., Chermette, J., 1995. Evolution of salt-related structures in compressional settings, in: Jackson, M., Roberts, D.G., Snelson, S. (Eds.), *Salt Tectonics, Sediments and Prospectivity*. pp. 41–60.
- Li, J., Mitra, S., 2017. Geometry and evolution of fold-thrust structures at the boundaries between frictional and ductile detachments. *Marine and Petroleum Geology* 85, 16–34. <https://doi.org/10.1016/j.marpetgeo.2017.04.011>
- Li, Shiyuan, Abe, S., Reuning, L., Becker, S., Urai, J.L., Kukla, P.A., 2012. Numerical modelling of the displacement and deformation of embedded rock bodies during salt tectonics: A case study from the South Oman Salt Basin. *Geological Society, London, Special Publications* 363, 1, 503–520. <https://doi.org/10.1144/sp363.24>
- Li, Shiqin, Wang, X., Suppe, J., 2012. Compressional salt tectonics and synkinematic strata of the western Kuqa foreland basin, southern Tian Shan, China. *Basin Research* 24, 4, 475–497. <https://doi.org/10.1111/j.1365-2117.2011.00531.x>
- Lloret, J., Ronchi, A., López-Gómez, J., Gretter, N., De la Horra, R., Barrenechea, J.F., Arche, A., 2018. Syn-tectonic sedimentary evolution of the continental late Paleozoic-early Mesozoic Erill Castell-Estac Basin and its significance in the development of the central Pyrenees Basin. *Sedimentary Geology* 374, 134–157. <https://doi.org/10.1016/j.sedgeo.2018.07.014>
- López-Martínez, N., Civis, J., Casanovas, M.L., Daams, R., 1998. *Geología y Paleontología del Eoceno de la Pobla de Segur (Lleida)*. Edicions i Publicacions de la Universitat de Lleida.
- López-Mir, B., Muñoz, J.A., García-Senz, J., 2016. 3D geometric reconstruction of Upper Cretaceous passive diapirs and salt withdrawal basins in the Cotiella Basin (southern Pyrenees). <https://doi.org/10.1144/jgs2016-002>
- López-Mir, B., Muñoz, J.A., García-Senz, J., 2015. Extensional salt tectonics in the partially inverted Cotiella post - rift basin (south - central Pyrenees): structure and evolution 419–434. <https://doi.org/10.1007/s00531-014-1091-9>
- Lopez-Mir, B., Muñoz, J.A., García Senz, J., 2014. Restoration of basins driven by extension and salt tectonics: Example from the Cotiella Basin in the central Pyrenees. *Journal of Structural Geology* 69, PA, 147–162.

- <https://doi.org/10.1016/j.jsg.2014.09.022>
- Martínez-Peña, M.B., Pocoví, A., 1988. El amortiguamiento frontal de la estructura de la cobertera surpirenaica y su relacion con el anticlinal de Barbastro-Balaguer. *Acta Geológica Hispánica* 23, 2, 81–94.
- Masclé, A., Puigdefábregas, C., 1998. Tectonics and sedimentation in foreland basins: results from the Integrated Basin Studies project. Geological Society of London Special Publication 134, 1–28. <https://doi.org/10.1144/GSL.SP.1998.134.01.02>
- McClay, K., Muñoz, J.A., García-Senz, J., 2004. Extensional salt tectonics in a contractional orogen: A newly identified tectonic event in the Spanish Pyrenees. *Geology* 32, 9, 737–740. <https://doi.org/10.1130/G20565.1>
- Meigs, A.J., 1997. Sequential development of selected Pyrenean thrust faults. *Journal of Structural Geology* 19, 96, 3–4. [https://doi.org/10.1016/S0191-8141\(96\)00096-X](https://doi.org/10.1016/S0191-8141(96)00096-X)
- Mellere, D., 1993. Thrust-Generated, Back-Fill Stacking of Alluvial Fan Sequences, South-Central Pyrenees, Spain (La Pobla De Segur Conglomerates). *Special publications International Association of Sedimentology* 20, February, 259–276. <https://doi.org/10.1002/9781444304053.ch14>
- Mellere, D., Marzo, M., 1992. Los depósitos aluviales sintectónicos de la Pobla de Segur: alogrupos y su significado tectonoestratigráfico. *Acta Geol. Hispánica, Volum homenatge a Oriol Riba*. 27, 1–2200009, jv, 145–159.
- Mencos, J., Carrera, N., Muñoz, J.A., 2015. Influence of rift basin geometry on the subsequent postrift sedimentation and basin inversion: The Organyà Basin and the Bóixols thrust sheet (south central Pyrenees) 1452–1474. <https://doi.org/10.1002/2014TC003692>.Received
- Meng, Q., Hodgetts, D., 2019a. Combined control of décollement layer thickness and cover rock cohesion on structural styles and evolution of fold belts : A discrete element modelling study. *Tectonophysics* 757, 58–67. <https://doi.org/10.1016/j.tecto.2019.03.004>
- Meng, Q., Hodgetts, D., 2019b. Structural styles and decoupling in stratigraphic sequences with double décollements during thin-skinned contractional tectonics : Insights from numerical modelling. *Journal of Structural Geology* 127, May, 103862. <https://doi.org/10.1016/j.jsg.2019.103862>
- Metcalf, J.R., Fitzgerald, P.G., Baldwin, S.L., Muñoz, J.A., 2009. Thermochronology of a convergent orogen: Constraints on the timing of thrust faulting and subsequent exhumation of the Maladeta Pluton in the Central Pyrenean Axial Zone. *Earth and Planetary Science Letters* 287, 3–4, 488–503. <https://doi.org/10.1016/j.epsl.2009.08.036>
- Mey, P.H.W., 1968. Geology of the Upper Ribagorzana valleys, Central Pyrenees, Spain. *Leidse Geol. Mededelingen* 41, 229–292.
- Mey, P.H.W., Nagtegaal, P.J.C., Roberti, K.J., Hartevelt, J.J.A., 1968. Lithostratigraphic subdivision of post-Hercynian deposits in the south-central Pyrenees, Spain. *Leidse Geologische Mededelingen* 41, 221–228.

- Michael, N.A., 2013. Functioning of an ancient routing system, the Escanilla Formation, South Central Pyrenees Nikolaos. PhD thesis, Imperial College of London.
- Misch, P., 1934. Der Bau der mittleren Südpirenen. *Abhandlungen der Königlichen Gesellschaft der Wissenschaften in Göttingen* III, 12, 1–168.
- Moragas, M., Vergés, J., Saura, E., Martín-Martín, Messenger, G., Merino-Tome, O., Suarez-Ruiz, I., Razin, P., Grelaud, C., Malaval, M., Jousiaume, R., Hunt, D.W., 2016. Jurassic rifting to post-rift subsidence analysis in the Central High Atlas and its relation to salt diapirism. *Basin Research* 1–27. <https://doi.org/10.1111/bre.12223>
- Mouthereau, F., Filleaudeau, P.Y., Vacherat, A., Pik, R., Lacombe, O., Fellin, M.G., Castellort, S., Christophoul, F., Masini, E., 2014. Placing limits to shortening evolution in the Pyrenees: Role of margin architecture and implications for the Iberia/Europe convergence. *Tectonics* 33, 12, 2283–2314. <https://doi.org/10.1002/2014TC003663>
- Mouthereau, F., Lacombe, O., Vergés, J., 2012. Building the Zagros collisional orogen: Timing, strain distribution and the dynamics of Arabia/Eurasia plate convergence. *Tectonophysics* 532–535, 27–60. <https://doi.org/10.1016/j.tecto.2012.01.022>
- Muñoz, J.A., 1992. Evolution of a continental collision belt: ECORS-Pyrenees crustal balanced cross-section, in: *Thrust Tectonics*. Springer, Dordrecht, pp. 235–246. https://doi.org/10.1007/978-94-011-3066-0_21
- Muñoz, J.A., Beamud, E., Fernández, O., Arbués, P., Dinarès-Turell, J., Poblet, J., 2013. The Ainsa Fold and thrust oblique zone of the central Pyrenees: Kinematics of a curved contractional system from paleomagnetic and structural data. *Tectonics* 32, 5, 1142–1175. <https://doi.org/10.1002/tect.20070>
- Muñoz, J.A., Mencos, J., Roca, E., Carrera, N., Gratacós, O., Ferrer, O., Fernández, O., 2018. The structure of the South-Central-Pyrenean fold and thrust belt as constrained by subsurface data. *Geologica Acta* 16, 4, 439–460. <https://doi.org/10.1344/GeologicaActa2018.16.4.7>
- Ortí, F., 1982. Sur les conditions de dépôt, la diagenese et la structure des évaporites triasiques dans l'est de l'Espagne. *Sciences de la Terre* 25, 179–199.
- Ortí, F., Pérez-López, A., Salvany, J.M., 2017. Triassic evaporites of Iberia: Sedimentological and palaeogeographical implications for the western Neotethys evolution during the Middle Triassic – Earliest Jurassic. *Palaeogeography, Palaeoclimatology, Palaeoecology* 471, 157–180. <https://doi.org/10.1016/j.palaeo.2017.01.025>
- Ortuño, M., Viaplana-Muzas, M., 2018. Active fault control in the distribution of elevated low relief topography in the Central-Western Pyrenees. *Geologica Acta* 16, 4, 499–518. <https://doi.org/10.1344/GeologicaActa2018.16.4.10>
- Pedrera, A., Ruiz-Constán, A., García-Senz, J., Azor, A., Marín-Lechado, C., Ayala, C., Díaz de Neira, J.A., Rodríguez-Fernández, L.R., 2020. Evolution of the South-Iberian paleomargin: from hyperextension to continental subduction. *Journal of Structural Geology* in press, June.

- Peel, F.J., 2014. How do salt withdrawal minibasins form? Insights from forward modelling, and implications for hydrocarbon migration. *Tectonophysics* 630, C, 222–235. <https://doi.org/10.1016/j.tecto.2014.05.027>
- Pocoví, A., 1978a. Estudio geológico de las Sierras Marginales Catalanas (Prepirineo de Lérida)*. *Acta Geológica Hispánica* 13, 3, 73–79.
- Pocoví, A., 1978b. Estudio geológico de las Sierras Marginales Catalanas (Prepirineo de Lerida). PhD thesis, Universitat de Barcelona.
- Ribes, C., Kergaravat, C., Crumeyrolle, P., Lopez, M., Bonnel, C., Poisson, A., Kaan, K.S., Callot, J.P., Ringenbach, J.C., 2017. Factors controlling stratal pattern and facies distribution of fluvio-lacustrine sedimentation in the Sivas mini-basins, Oligocene (Turkey). *Basin Research* 29, 596–621. <https://doi.org/10.1111/bre.12171>
- Robles, S., Ardévol, L., 1984. Evolución paleogeográfica y sedimentológica de la cuenca palustre de Sossís (Eoceno superior, Prepirineo de Lérida): ejemplo de la influencia de su actividad de abanicos aluviales en el desarrollo de una cuenca lacustre asociada. *Publicaciones del departamento de estratigrafía de la UAB. Tomo homenaje a Luis Sánchez de la Torre* 20, 223–267.
- Roca, E., Sans, M., Koyi, H.A., 2006. Polyphase deformation of diapiric areas in models and in the eastern Prebetics (Spain). *AAPG Bulletin* 90, 1, 115–136. <https://doi.org/10.1306/07260504096>
- Roigé, M., Gómez-Gras, D., Remacha, E., Boya, S., Viaplana-Muzas, M., Teixell, A., 2017. Recycling an uplifted early foreland basin fill: An example from the Jaca basin (Southern Pyrenees, Spain). *Sedimentary Geology* 360, 1–21. <https://doi.org/10.1016/j.sedgeo.2017.08.007>
- Roma, M., Ferrer, O., McClay, K.R., Muñoz, J.A., Roca, E., Gratacos, O., Cabello, P., 2018. Weld kinematics of syn-rift salt during basement-involved extension and subsequent inversion : Results from analog models. *Geologica Acta* 16, December, 391–410. <https://doi.org/10.1344/GeologicaActa2018.16.4.4>
- Rosell, J., Gómez-Gras, D., Luterbacher, H., Llompart, C., 1994. Memoria del mapa geológico de la hoja nº252/33-11 (Tresp). 1:50.000 Segunda Serie (MAGNA). Primera edición. IGME.
- Rosell, J., Gómez-Gras, D., Luterbacher, H., Llompart, C., Gabaldón, V., 1994. Mapa geológico de la hoja nº252 (Tresp), in: 1:50.000 Segunda Serie (MAGNA). Primera Edición. IGME.
- Rosell, J., Mutti, E., Allen, G., Fonnesu, F., Sgavetti, M., 1985. The Eocene Baronia tide dominated delta-self system in the Ager Basin, in: 6th European Regional Meeting. International Association of Sedimentologists. Excursion Guidebook. pp. 577–600.
- Rosell, J., Riba, O., 1966. Nota sobre la disposición sedimentaria de los conglomerados de la Pobla de Segur (Provincia de Lérida). Instituto de Estudios Pirenaicos, Zaragoza 1–16.
- Roure, F., Choukroune, P., Berástegui, X., Muñoz, J.A., Villien, A., Matheron, P., Bareyt, M., Séguret, M., Cámara, P., Deramond, J., 1989. Eors deep seismic data and

- balanced cross sections: Geometric constraints on the evolution of the Pyrenees. *Tectonics* 8, 1, 41–50. <https://doi.org/10.1029/TC008i001p00041>
- Rowan, M.G., Vendeville, B.C., 2006. Foldbelts with early salt withdrawal and diapirism: Physical model and examples from the northern Gulf of Mexico and the Flinders Ranges, Australia. *Marine and Petroleum Geology* 23, 9–10, 871–891. <https://doi.org/10.1016/j.marpetgeo.2006.08.003>
- Ruh, J.B., Kaus, B.J.P., Burg, J.P., 2012. Numerical investigation of deformation mechanics in fold-and-thrust belts: Influence of rheology of single and multiple décollements. *Tectonics* 31, 3, 1–23. <https://doi.org/10.1029/2011TC003047>
- Salvany, J.M., 1999. Diapirismo Triásico antiguo y reciente en el anticlinal de Canelles, Sierras Marginales catalanas (Zona Surpirenaica central). *Rev. Geol. Soc. España* 12, 2, 149–163.
- Salvany, J.M., Bastida, J., 2004. Análisis litoestratigráfico del keuper surpirenaico central. *Revista de la Sociedad Geológica de España* 17, 3–26.
- Sans, M., Vergés, J., 1995. Fold development related to contractional salt tectonics: southeastern Pyrenean thrust front, Spain, in: *Salt Tectonics: A Global Perspective*, AAPG Memoir 65. pp. 369–378.
- Santolaria, P., 2015. Salt and thrust tectonics in the south central Pyrenees. PhD thesis, Universidad de Zaragoza.
- Santolaria, P., Casas-Sainz, A.M., Soto, R., Casas, A., 2017. Gravity modelling to assess salt tectonics in the western end of the South Pyrenean Central Unit. *Journal of the Geological Society* 174, 2, 269–288.
- Santolaria, P., Casas-Sainz, A.M., Soto, R., Casas, A., 2014. The Naval diapir (Southern Pyrenees): Geometry of a salt wall associated with thrusting at an oblique ramp. *Tectonophysics* 637, November, 30–44. <https://doi.org/10.1016/j.tecto.2014.09.008>
- Saura, E., 2004. Anàlisi estructural de la zona de les Nogueres Pirineus Centrals. Tesi de la Universitat Autònoma de Barcelona.
- Saura, E., Ardèvol, L., Teixell, A., Vergés, J., 2016. Rising and falling diapirs, shifting depocenters, and flap overturning in the Cretaceous Sopeira and Sant Gervàs subbasins (Ribagorça Basin, southern Pyrenees). *Tectonics* 35, 3, 638–662. <https://doi.org/10.1002/2015TC004001>
- Saura, E., Teixell, A., 2006. Inversion of small basins: effects on structural variations at the leading edge of the Axial Zone antiformal stack (Southern Pyrenees, Spain). *Journal of Structural Geology* 28, 11, 1909–1920. <https://doi.org/10.1016/j.jsg.2006.06.005>
- Saura, E., Vergés, J., Martín-Martín, J.D., Messenger, G., Moragas, M., Razin, P., Grélaud, C., Joussiaume, R., Malaval, M., Homke, S., Hunt, D.W., 2014. Syn- to post-rift diapirism and minibasins of the Central High Atlas (Morocco): The changing face of a mountain belt. *Journal of the Geological Society of London* 171, 97–105. <https://doi.org/10.1144/jgs2013-079>

- Schmalholz, S.M., Podladchikov, Y.Y., Burg, J.-P., 2002. Control of folding by gravity and matrix thickness: Implications for large-scale folding. *Journal of Geophysical Research* 107, B1, ETG 1-1-ETG 1-16. <https://doi.org/10.1029/2001jb000355>
- Scotese, C.R., Schettino, A., 2017. Late Permian-Early Jurassic paleogeography of western Tethys and the world, Permo-Triassic Salt Provinces of Europe, North Africa and the Atlantic Margins. Elsevier. <https://doi.org/10.1016/B978-0-12-809417-4.00004-5>
- Séguret, M., 1972. Etude tectonique des nappes et séries décollées de la partie centrale du versant sud des Pyrénées. Caractère synsédimentaire, rôle de la compression et de la gravité. PhD thesis, Univ. de Montpellier.
- Séguret, M., 1970. Étude tectonique des nappes et séries décollées de la partie centrale du versant sud des Pyrénées. Montpellier Université des Sciences et Techniques Publications, Serie Geologie Structurale 2.
- Selzer, G., 1934. Geologie der südpyrenäischen Sierrren in Oberaragonien. *Neues Jahrbuch für Mineralogie, Paläontologie und Geologie* 71 (B), 270–406.
- Serrano, A., Martínez del Olmo, W., Cámara, P., 1989. Diapirismo del Trías salino en el dominio Cántabro-Navarro, in: *Libro Homenaje a Rafael Soler*. pp. 115–121.
- Sherkati, S., Letouzey, J., Frizon de Lamotte, D., 2006. Central Zagros fold-thrust belt (Iran): New insights from seismic data, field observation, and sandbox modeling. *Tectonics* 25, 4, 1–27. <https://doi.org/10.1029/2004TC001766>
- Simó, A., 1993. Cretaceous carbonate platforms and stratigraphic sequences; south-central Pyrenees; Spain., in: *Cretaceous Carbonate Platforms: AAPG Memoir 56*. pp. 325–342. <https://doi.org/10.1306/M56578C1>
- Simó, A., 1986. Carbonate platform depositional sequences, Upper Cretaceous, south-central Pyrenees (Spain). *Tectonophysics* 129, 205–231.
- Simpson, G.D.H., 2006. Modelling interactions between fold-thrust belt deformation, foreland flexure and surface mass transport. *Basin Research* 18, 2, 125–143. <https://doi.org/10.1111/j.1365-2117.2006.00287.x>
- Sinclair, H.D., Gibson, M., Naylor, M., Morris, R.G., 2005. Asymmetric growth of the Pyrenees revealed through measurement and modeling of orogenic fluxes. *American Journal of Science* 305, 369–406. <https://doi.org/10.2475/ajs.305.5.369>
- Soto, J.I., Flinch, J.F., Tari, G., 2017. Permo-Triassic Basins and Tectonics in Europe, North Africa and the Atlantic Margins, in: *Permo-Triassic Salt Provinces of Europe, North Africa and the Atlantic Margins*. Elsevier, pp. 3–41. <https://doi.org/10.1016/b978-0-12-809417-4.00038-0>
- Soto, R., Casas, a. M., Storti, F., Faccenna, C., 2002. Role of lateral thickness variations on the development of oblique structures at the Western end of the South Pyrenean Central Unit. *Tectonophysics* 350, 3, 215–235. [https://doi.org/10.1016/S0040-1951\(02\)00116-6](https://doi.org/10.1016/S0040-1951(02)00116-6)
- Soto, R., Pocoví, A., Santolaria, P., 2015. El sistema de pliegues y cabalgamientos

- oblicuos de St. Jordi – Sierra Boada (Sierras Marginales, Unidad Surpirenaica Central). *Geogaceta* 58, 91–94.
- Storti, F., Soto, R., Rossetti, F., Casas-Sainz, A.M., 2007. Evolution of experimental thrust wedges accreted from along-strike tapered, silicone-floored multilayers. *Journal of the Geological Society* 164, 1, 73–85. <https://doi.org/10.1144/0016-76492005-186>
- Teixell, A., Barnolas, A., 1996. Mapa geológico de la hoja nº327/32-13 (Os de Balaguer), in: Mapa Geológico de España E. 1:50.000. Segunda Serie (MAGNA). Primera Edición. IGME.
- Teixell, A., Barnolas, A., 1995. Significado de la discordancia de Mediano en relación con las estructuras adyacentes. *Geogaceta* 18, 34–37.
- Teixell, A., Barnolas, A., Rosales, I., Arboleya, M.L., 2017. Structural and facies architecture of a diapir-related carbonate minibasin (lower and middle Jurassic, High Atlas, Morocco). *Marine and Petroleum Geology* 81, 334–360. <https://doi.org/10.1016/j.marpetgeo.2017.01.003>
- Teixell, A., Labaume, P., Ayarza, P., Espurt, N., de Saint Blanquat, M., Lagabrielle, Y., 2018. Crustal structure and evolution of the Pyrenean-Cantabrian belt: A review and new interpretations from recent concepts and data. *Tectonophysics* 724–725, January, 146–170. <https://doi.org/10.1016/j.tecto.2018.01.009>
- Teixell, A., Leyva, F., Caus, E., Granados, L., Cabra, P., Barnolas, A., 1996. Memoria del mapa geológico de la hoja nº327/32-13 (Os de Balaguer). Mapa Geológico de España E. 1:50.000. Segunda Serie (MAGNA). Primera edición. IGME.
- Teixell, A., Muñoz, J.A., 2000. Evolución tectono-sedimentaria Pirineo meridional durante el terciario: Una síntesis basada en la transversal del río Noguera Ribagorçana. *Revista de la Sociedad Geológica de España* 13, 2, 251–264.
- Trocmé, V., Albouy, E., Callot, J.-P., Letouzey, J., Rolland, N., Goodarzi, H., Jahani, S., 2011. 3D structural modelling of the southern Zagros fold-and-thrust belt diapiric province. *Geological Magazine* 148, 879–900. <https://doi.org/10.1017/S0016756811000446>
- Vacherat, A., Mouthereau, F., Pik, R., Bellahsen, N., Gautheron, C., Bernet, M., Daudet, M., Balansa, J., Tibari, B., Jamme, R.P., Radal, J., 2016. Rift-to-collision transition recorded by tectono-thermal evolution of the northern Pyrenees. *Tectonics* 35, 4, 907–933. <https://doi.org/10.1002/2015TC004016>
- Vergés, J., 2003. Evolución de los sistemas de rampas oblicuas de los Pirineos meridionales: fallas del Segre y Pamplona. *Boletín Geológico y Minero* 114, 1, 87–101.
- Vergés, J., 1993. Estudi geològic del vessant sud del Pirineu oriental i central. Evolució cinemàtica en 3D. PhD thesis, Universitat de Barcelona.
- Vergés, J., Martínez, A., 1988. Corte compensado del Pirineo oriental: Geometría de las cuencas de antepís y edades de emplazamiento de los mantos de corrimiento. *Acta geologica hispanica* 23, 2, 95–105.

- Vergés, J., Muñoz, J.A., 1990. Thrust sequences in the southern central Pyrenees. *Bulletin de la Société Géologique de la France* 8, 265–271.
- Vidal-Royo, O., Koyi, H.A., Muñoz, J.A., 2009. Formation of orogen-perpendicular thrusts due to mechanical contrasts in the basal décollement in the Central External Sierras (Southern Pyrenees, Spain). *Journal of Structural Geology* 31, 5, 523–539. <https://doi.org/10.1016/j.jsg.2009.03.011>
- Vincent, S.J., 2001. The Sis palaeovalley : a record of proximal fluvial sedimentation and drainage basin development in response to Pyrenean mountain building. *Sedimentology* 48, 1235–1276.
- Warsitzka, M., Kley, J., Kukowski, N., 2015. Analogue experiments of salt flow and pillow growth due to basement faulting and differential loading. *Solid Earth* 6, 1, 9–31. <https://doi.org/10.5194/se-6-9-2015>
- Warsitzka, M., Kley, J., Kukowski, N., 2013. Salt diapirism driven by differential loading — Some insights from analogue modelling. *Tectonophysics* 591, 83–97. <https://doi.org/10.1016/j.tecto.2011.11.018>
- Whitchurch, A.L., Carter, A., Sinclair, H.D., Duller, R.A., Whittaker, A.C., Allen, P.A., 2011. Sediment routing system evolution within a diachronously uplifting orogen: Insights from detrital zircon thermochronological analyses from the South-Central pyrenees. *American Journal of Science* 311, 5, 442–482. <https://doi.org/10.2475/05.2011.03>
- Williams, G.D., Fischer, M.W., 1984. A balanced section across the Pyrenean Orogenic Belt. *Tectonics* 3, 7, 773–780. <https://doi.org/10.1029/TC003i007p00773>
- Yamato, P., Kaus, B.J.P., Mouthereau, F., Castelltort, S., 2011. Dynamic constraints on the crustal-scale rheology of the Zagros fold belt, Iran. *Geology* 39, 9, 815–818. <https://doi.org/10.1130/G32136.1>
- Yelland, A.J., 1991. Thermo-tectonics of the Pyrenees and Provence from fission track studies. PhD thesis from Birkbeck College, University of London.
- Zamorano, M., 1993. Los sistemas deltaicos del Ilerdiense superior-cuisciense de la cuenca de Ager (Fm. Ametlla). Prepirineo de Lleida. PhD thesis, Universitat Autònoma de Barcelona.
- Ziegler, P.A., 1990. Pangaea break-up: Jurassic–Early Cretaceous opening of Central and North Atlantic and Western Tethys, in: *Geological Atlas of Western and Central Europe*. Bath: Geological Society Publishing House, pp. 91–123.
- Zwart, H.J., 1979. The Geology of the Central Pyrenees. *Leidse Geologische Mededelingen* 1–74.

Acknowledgements

Agraïments

Acknowledgements

Em sento immensament afortunada d'haver pogut participar en un projecte que m'ha permès fer treball de camp en un lloc tan estimat per mi com és el Pirineu i alhora viatjar pel món. Tot això acompanyada d'amics i gent meravellosa que he conegut pel camí. Per a tots vosaltres, el meu més sincer agraïment.

Primer de tot, vull agrair al meu director de tesi, el Toni Teixell, l'oportunitat de participar en aquest projecte i la confiança dipositada en mi des del primer dia. Treballant amb tu he après moltíssim i sempre m'has donat la llibertat de decidir cap a on tirar. Quan no ho he tingut clar, m'has ajudat a pensar i a trobar la manera de continuar. Gràcies per ensenyar-me l'ofici de la geologia de camp. També per animar-me a anar a tants congressos, a discutir amb tothom, i fer-me veure la geologia com una feina col·lectiva. Gràcies per portar-me a l'Atlas, on vaig conèixer una geologia fantàstica. Però sobretot, et vull agrair que sempre trobis temps per parlar o revisar tot el que escric, i el teu suport constant, especialment aquest darrer any tan complicat.

Vull agrair als membres del departament de geologia haver-me acollit durant tots aquests anys, molt especialment a la María Luisa Arboleya i l'Albert Griera, amb qui he compartit dies de camp, congressos i assignatures del grau. Gràcies per tot el que he après amb vosaltres, pels bons consells i per fer-me sentir tan còmoda.

També vull donar les gràcies al David Gómez. M'ha encantat poder treballar amb tu i el Xavi en un estudi tan bonic com el dels conglomerats de la Pobla i Gulp. He après moltíssim de codolets, petro i procedència, cosa que ha enriquit la perspectiva d'aquesta tesi. El teu bon humor i suport m'han fet el final de la tesi molt més fàcil.

A les "secres" del departament, vull agrair-vos que sempre estigueu allà per solucionar qualsevol problema que a mi em sembla impossible. Gràcies per la vostra alegria.

I want to thank Mike Hudec the opportunity to spend five months in Austin working with the AGL group, which has provided so many results and discussion to this thesis. I also want to thank him the opportunity to present in the AGL annual meeting and the invitation to the Paradox basin fieldtrip, where I gained so much salt tectonics

background and visited the most beautiful outcrops. I also want to thank his implication in the Pyrenees study and the discussions on the first draft of my manuscript.

A Naiara Fernández quiero agradecerle haberme presentado el mundo de la modelización numérica y su implicación constante en este proyecto. Muchas gracias por todos los consejos, por leerme mis manuscritos y hacer siempre comentarios tan “on point”. Gracias por hacerme sentir como en casa en Austin. Ojalá podamos seguir trabajando con todas las ideas que han quedado pendientes!

I am very thankful also to all the members and collaborators of the AGL group for all the discussions and the encouragement during my visits to Austin. Special thanks go to Olly Duffy, Tim Dooley, Maria Nikolinakou, Gill Apps, Frank Peel, Chris Jackson and Juan Ignacio Soto. It has been a privilege to get to share my research with you.

Moltes gràcies també la meva família austinita. Vinyet Baqués, mira que haver-nos de conèixer a l'altre banda del mon! Gràcies per tots els momentazos i per cuidar-me.

Merci à toutes les personnes du projet Orogen pour l'opportunité de discuter de mes recherches avec tant de géologues pyrénéens et la possibilité de publier dans le volume spécial.

Merci à Pierre Labaume pour la discussion sur les manuscrits et son aide quand j'ai dû écrire en français.

Gràcies al Toni Barnolas per tot el que he après al camp a la Sierra de Guara i a l'Atlas.

Gràcies a tots els companys doctorands i ex-doctorands del departament que m'heu acompanyat en aquesta muntanya russa. Especialment vull agrair al Norbert Caldera, el Xavi Coll, el Camilo Ruiz i el Guillem Piris tots els moments viscuts al camp i a la uni, que ja els estic trobant a faltar. Gràcies al Gerard Casado, el Marc Guardia, la Gisela Leoz, la Carla Garrido i l'Esteban Mellado per les discussions a l'hora del cafè. A la Marta Roigé, el Salva Boya, l'Isaac Corral i la Lucía Struth els vull agrair la seva ajuda i els savis consells de qui ja ha passat per tot això.

Vull agrair als amics del grau de geologia que sempre esteu allà, des de fa quasi 10 anys. Especialment l'Andreu Vinyoles, el Pablo Rodríguez i el Tomàs Nassar, que encara teniu punxes a les botes de caminar pel Montsec i les Serres Marginals a ple sol.

Gràcies a l'Enric i la Tere d'Àger i al Jaume, la Carme i l'Oreig de Cal Maciarol per ajudar-me a arribar a cada racó del Montsec per terra i aigua, i per acollir-me a casa vostra.

Vull agrair el suport que he trobat en els amics que he fet lluitant contra la precarietat en la ciència. Maria, Dani, Laura, Alejandro, Guillem, Sara, Jara, i tants d'altres, seguim!

Dani, gracias por acompañarme durante este proyecto, por ayudarme a creer en mí y por revisar mi inglés del Vallès en los primeros manuscritos de los artículos.

Gracias a mis amigos de Cerdanyola, Manchester y Austin.

Olga y Nacho, gracias por todo el apoyo que me habéis dado en este último año de locos, escuchándome a cualquier hora, ayudándome a mirar para adelante y haciéndome reír. Gracias por cuidarme tantísimo.

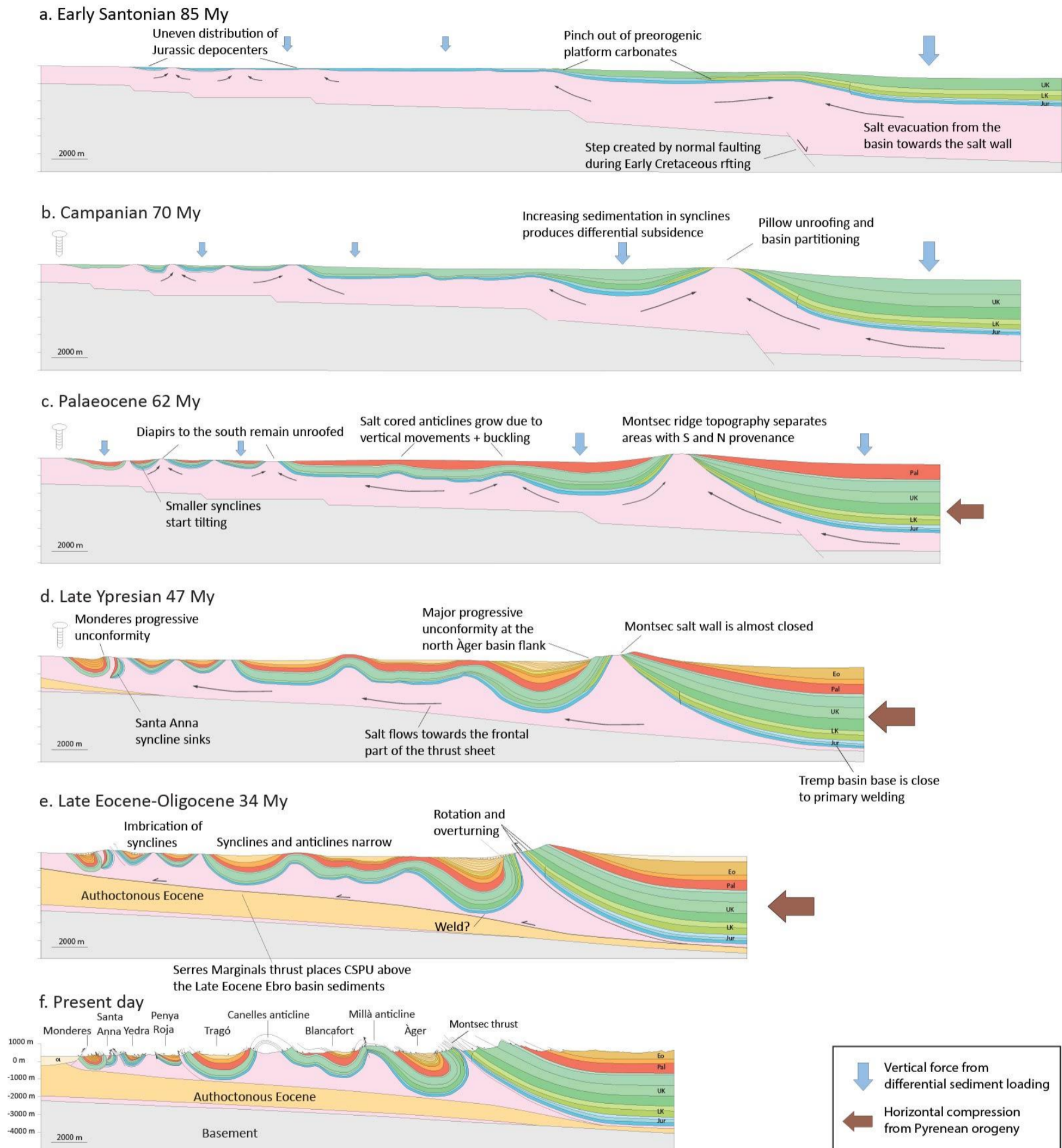
Finalmente, quiero dar las gracias a mi familia, a los que están y a los que ya no. A mis abuelos María, Francisco, Aurora y Virgilio, os quiero agradecer mis primeros recuerdos en las montañas y las meriendas al lado del río. A mis padres, Chelo y Virgili, os quiero agradecer todo lo que habéis hecho por mí, vuestro cariño, vuestro apoyo constante y toda la ayuda para que me siga dedicando a lo que más me gusta. Os quiero mucho.

Gracias a todos!

Appendix 1

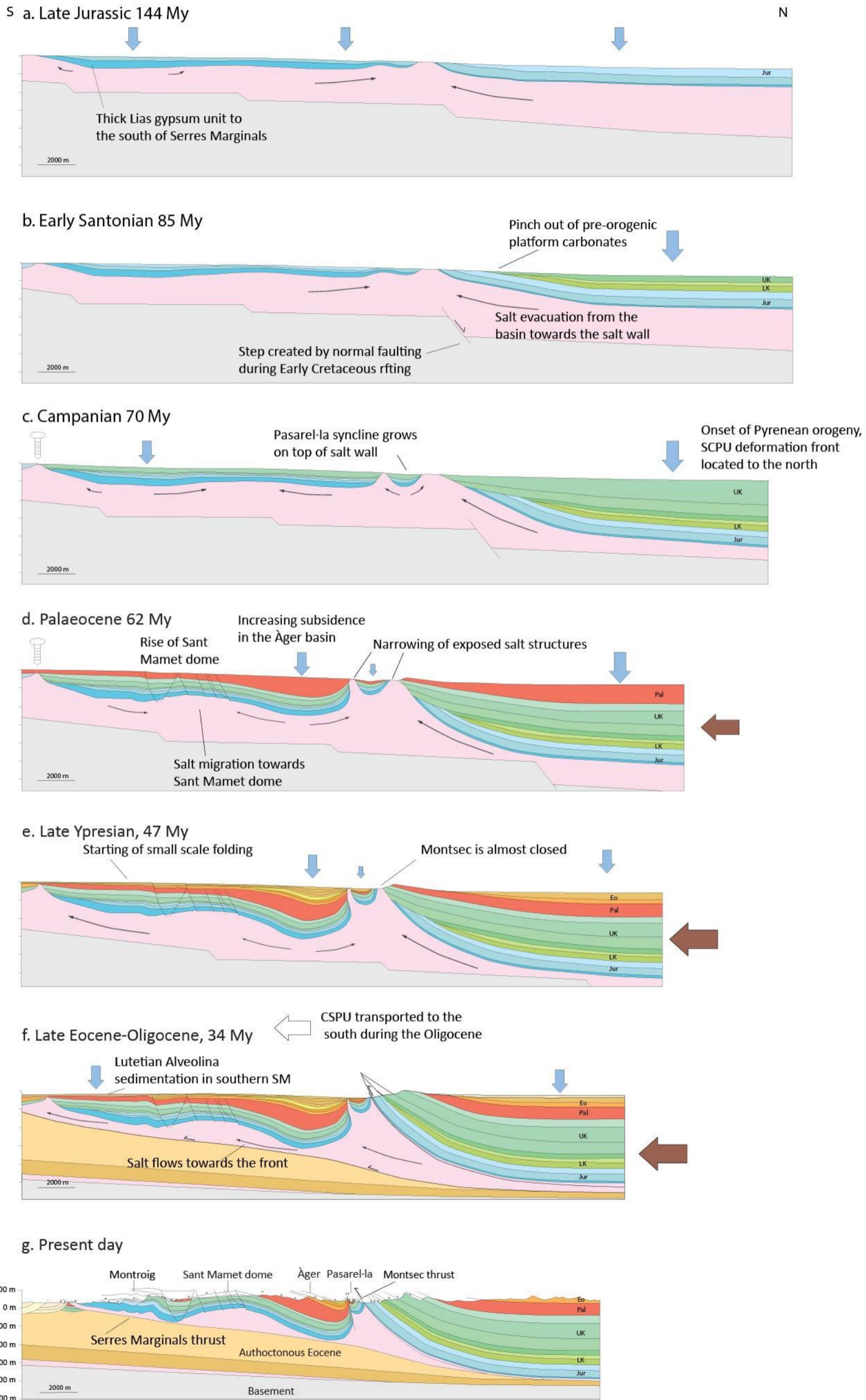
*Amplified versions of the restored
cross-sections in chapter 2*

Ribagorçana transect



Amplified version of **figure 2.10**, the restored cross-section of the Ribagorçana transect

Pallaresa transect



Amplified version of figure 2.11, the restored cross-section of the Pallaresa transect

Appendix 2

*Amplified versions of the numerical
models in chapter 4*

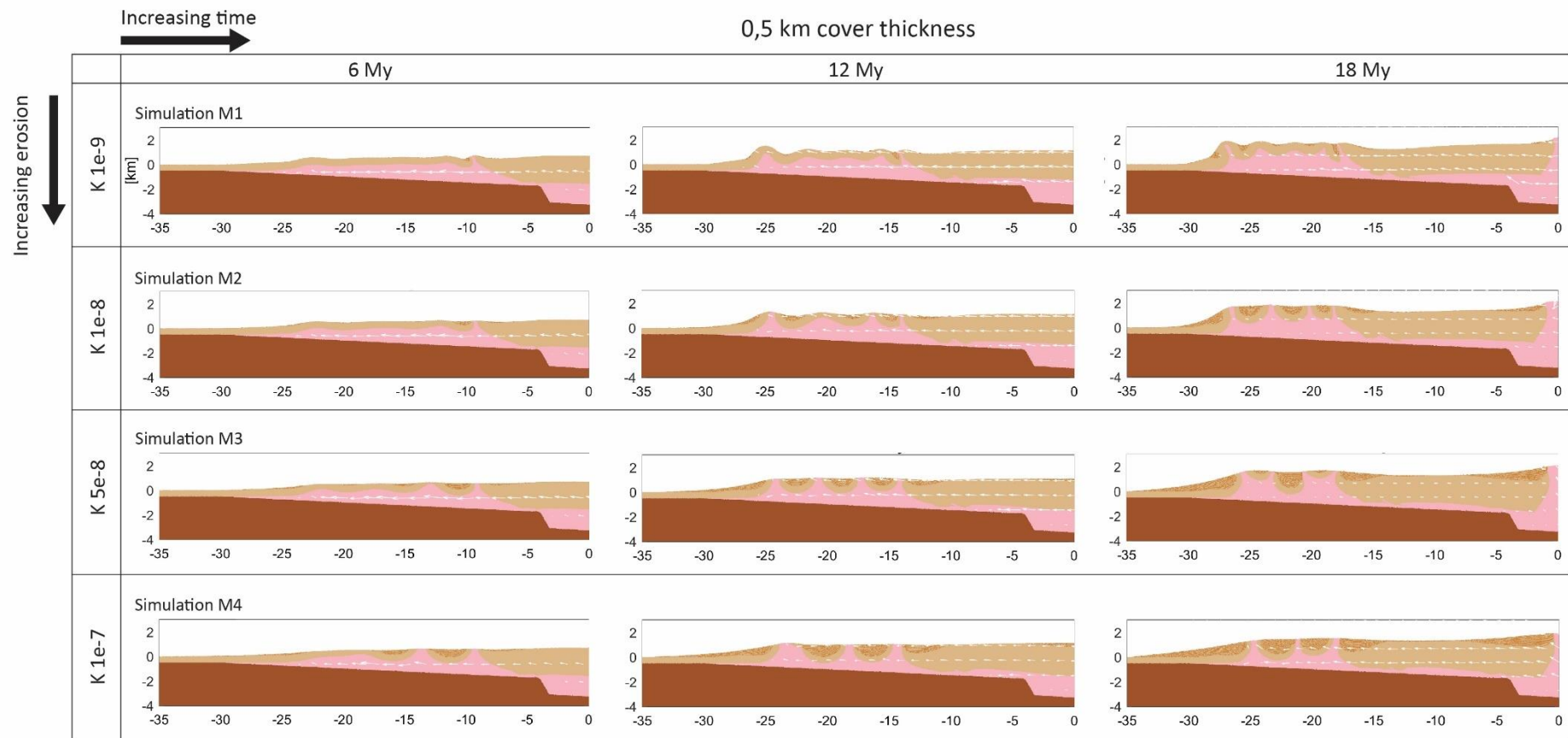


Figure 4.11. Results of the simulations with 0,5 km cover thickness of the systematic study on syntectonic sedimentation and erosion. Geometries after 6, 12 and 18 My.

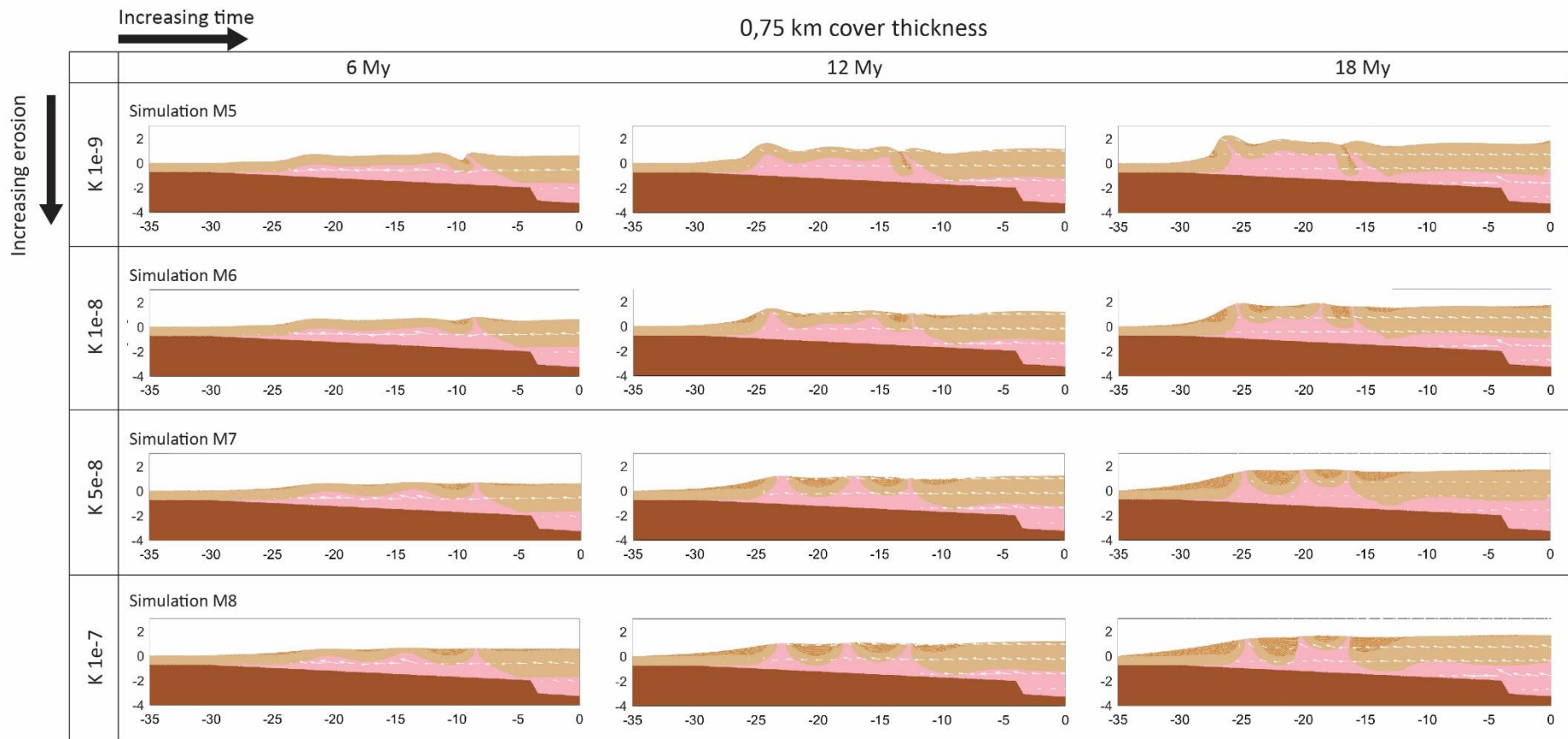


Figure 4.12. Results of the simulations with 0,75 km cover thickness of the systematic study on syntectonic sedimentation and erosion. Geometries after 6, 12 and 18 My

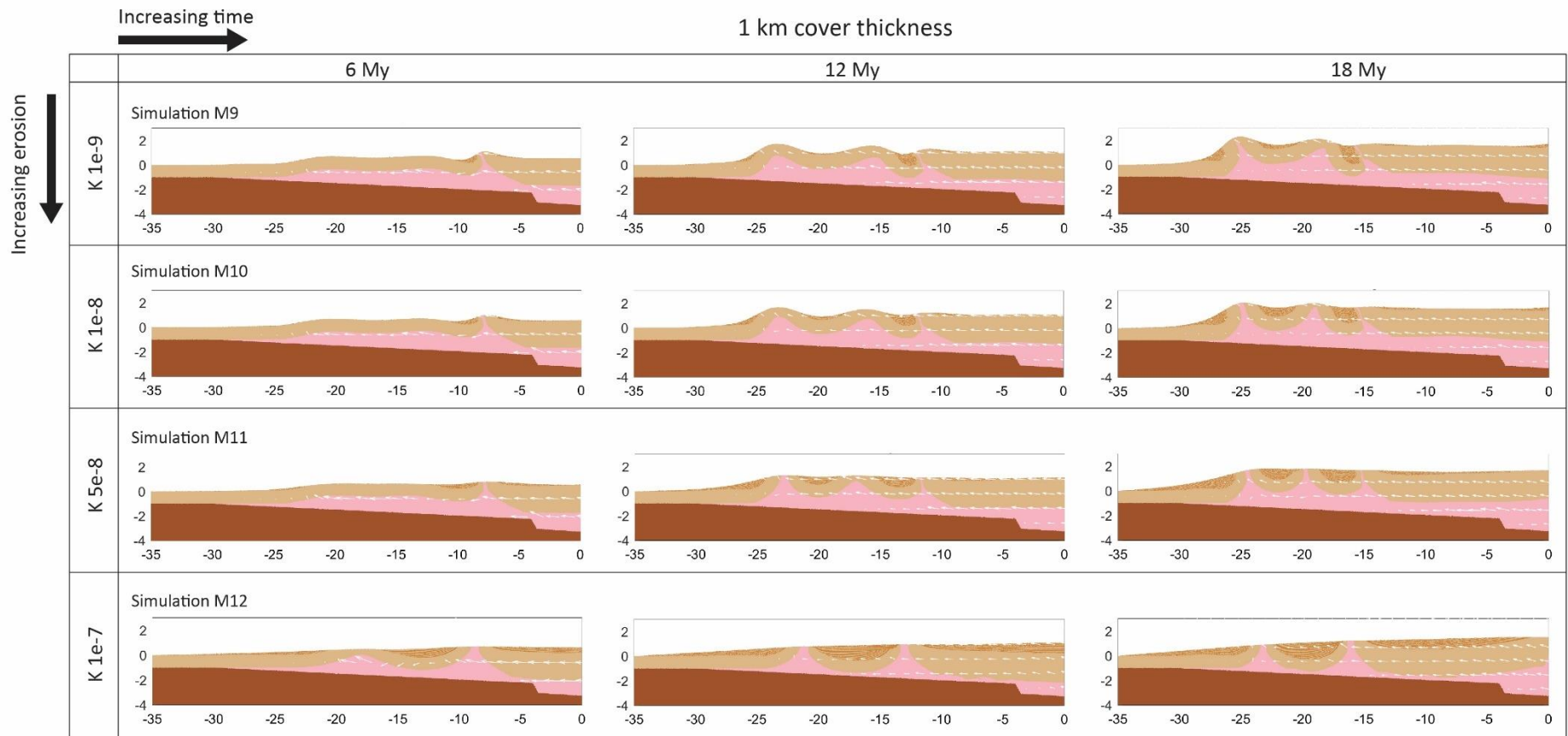


Figure 4.13. Results of the simulations with 1 km cover thickness of the systematic study on syntectonic sedimentation and erosion. Geometries after 6, 12 and 18 My

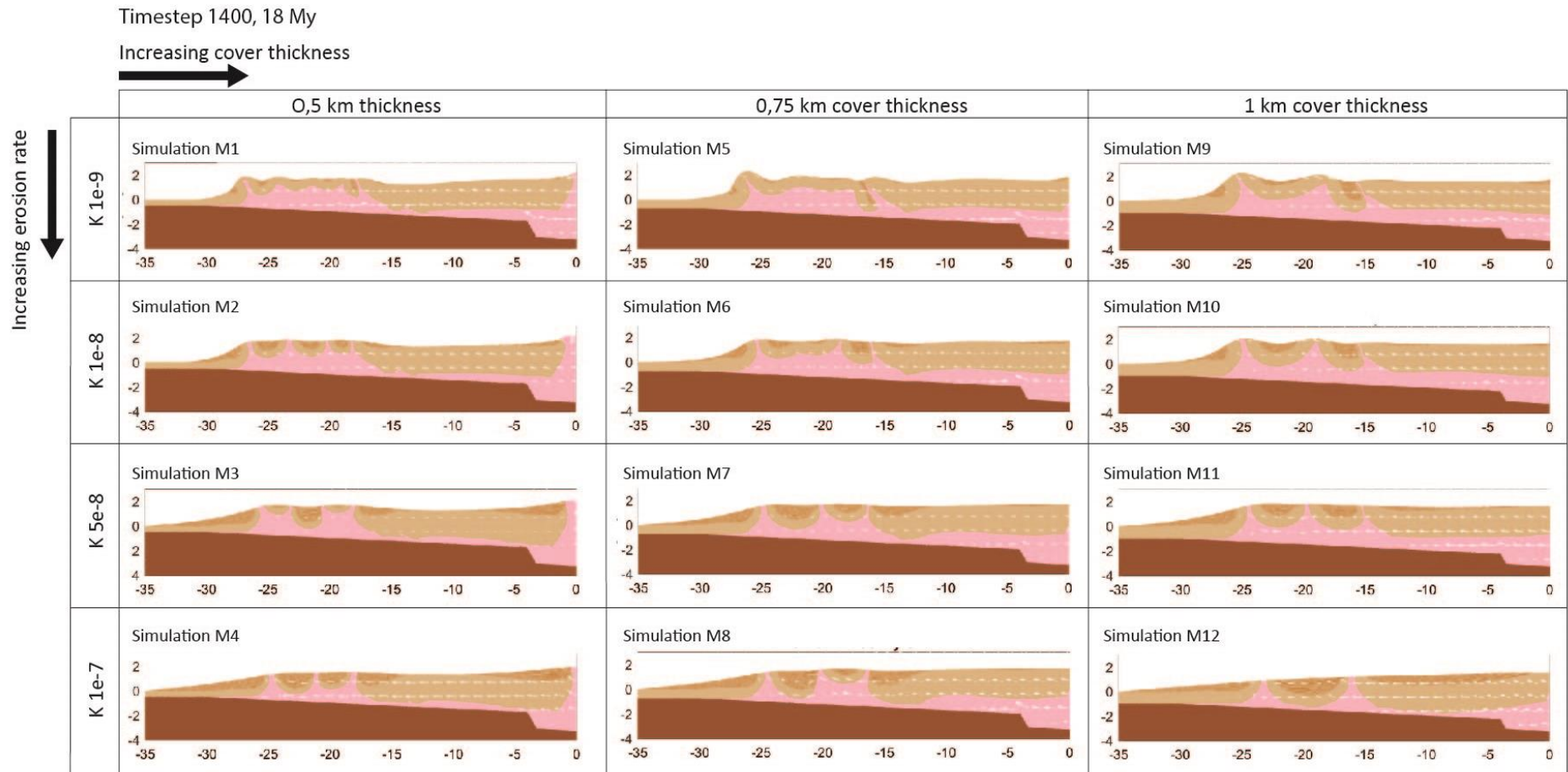


Figure 4.14. Geometries after 18 My of all the simulations of the study on syntectonic sedimentation and erosion.